HAL
open science

Sugar reduction in extruded cereal based products : impact of water content on the structure and molecular dynamics in such material

Supuksorn Masavang

▶ **To cite this version:**

Supuksorn Masavang. Sugar reduction in extruded cereal based products : impact of water content on the structure and molecular dynamics in such material. Food and Nutrition. Université Bourgogne Franche-Comté, 2019. English. NNT : 2019UBFCK025 . tel-02297490

HAL Id: tel-02297490
https://theses.hal.science/tel-02297490

Submitted on 26 Sep 2019

THESE DE DOCTORAT DE L'ETABLISSEMENT UNIVERSITE BOURGOGNE FRANCHE-COMTE

PREPAREE A UMR A 02. 102 Procédés Alimentaires et Microbiologiques» (UMR PAM)

Equipes Physico-Chimie de l'Aliment et du Vin (PCAV)

(AgroSup Dijon – Université de Bourgogne Franche-Comté)

Ecole doctorale n° 554

ED ES : Environnements santé

Doctorat de Biotechnologies agro-aliments

Par

Madame MASAVANG Supuksorn

Sugar reduction in extruded cereal based products: impact of water content on the structure and molecular dynamics in such material.

Thèse présentée et soutenue à the lecture Chosson – Amphithéâtre Chosson Bâtiment Grand Champ Dijon, site Déméter rue des Champs Prévois 2100 DIJON, le 29 aout 2019

Composition du Jury :

Pr. Thomas Karbowiak	Professor, UMR PAM-PCAV (UBFC-Agrosup Dijon), Dijon)	Président
Pr. Pawinee Chinachoti	President, Quest, Ltd., Thailand	Rapporteur
Pr. Job B. Unnink	Professor, California Polytechnic State University, California, USA	Rapporteur
Pr. Peter Lillford	University of Birmingham, United Kingdom	Examinateur
Dr. Edgar Chavez Montes	S&T group leader, Nestlé R&D Orbe, Switzerland	Examinateur
Pr. Dominique Champion	Professor, UMR PAM-PCAV (UBFC-Agrosup Dijon), Dijon	Directeur de thèse
Dr. Gaëlle Roudaut	Lecturer, UMR PAM-PCAV (UBFC-Agrosup Dijon), Dijon	Codirecteur de thèse
Pr. Yjrö Roos	University College of Cork, Ireland	Invité

Titre : Réduction du sucre dans les produits extrudés à base de céréales: impact de la teneur en eau sur la structure et la dynamique moléculaire de ces matériaux.

Mots-clés: Extrudat, Absorption d'eau, Réduction du sucre, Mobilité moléculaire, Vieillissement physique

Résumé: Les systèmes à base de biopolymères à faible teneur en humidité sont couramment rencontrés dans les aliments. Bien entendu, il est primordial de comprendre les bases physiques de leur qualité: texture, performances dans le temps ou en fonction de leur composition. Le vieillissement physique des systèmes composites rend les changements survenant dans le stockage des produits comestibles difficiles à prévoir. Les objectifs de ce travail étaient d'évaluer l'incidence de la présence de saccharose et de la teneur en eau de fabrication sur les propriétés physico-chimiques du produit fini. La stabilité physique de ces matériaux a été contrôlée grâce à une étude à différentes échelles moléculaires. Ensuite, les relations entre les données multi-échelles ont été examinées. L'effet du saccharose (0 à 20%) et de l'eau d'alimentation (10 et 15%) sur les mélanges d'extrusion a été étudié à l'aide d'un extrudeur double vis conduit dans les mêmes conditions. Les propriétés physiques et microstructurales des produits extrudés expansés ont été examinées sous diverses conditions d'humidité relative. La réduction des teneurs en sucre et en eau d'alimentation a fait augmenter la pression et l'énergie mécanique spécifique, ce qui a réduit la dégradation de l'amidon et augmenté la viscosité dans l'extrudeur en particulier à la teneur en eau la plus élevée. L'augmentation de la pression dans l'extrudeur a entraîné une expansion plus importante des extrudés. Par contre, la technique d'imagerie neutronique montré que le saccharose réduisait la taille des pores, et donc augmentait la densité apparente et ce qui était particulièrement évident en utilisant. Cette technique a été appliquée pour la première fois sur des produits extrudés. Les images de tomographie 2D ont indiqué des différences structurelles internes entre les extrudés à différentes teneurs en saccharose et stockés à humidité relative différente. Toutefois, l'analyse d'images 3D a montré que l'impact de ces facteurs sur la distribution de la taille des pores et le taux de porosité n'était pas significatif. En fin d'extrusion, les échantillons étaient à l'état amorphe à la suite de la gélatinisation de l'amidon et de la fonte du sucre. Leursrs propriétés thermiques ont été analysées par analyse enthalpique différentielle (AED) et les températures e transition vitreuse ont été étudiées. Les thermogrammess d'AED ont été minutieusement étudiés via une déconvolution de la dérivée première de la variation d'enthalpie. Cette approche a mis en évidence que les systèmes composites étudiés présentaient des phases multiples avec des transitions vitreuses distinctes. Ces dernières sont associées à une phase riche en polymère (amidon principalement) et / ou à une phase riche en plastifiant (sucre) dont le comportement dépendait de la teneur en eau de l'échantillon. Les isothermes de sorption ont montré qu'aux faibles Aw et pour une valeur donnée, a la teneur en eau des extrudés diminuait avec l'augmentation des teneurs en saccharose et que l'effet inverse était observé aux aw élevées. L'étude de la cinétique apparente de lala diffusion de l'eau a mis en évidence deux sites de sorption différents. Le premier est caractérisé par une cinétique quasi constante qui pourrait correspondre à un phénomène d'adsorption à la surface. Le second site présente d'abord un ralentissement initial de la cinétique de sorption, tandis qu'une forte augmentation est constatée lorsque la teneur en eau était plus élevée. Ce comportement peut être lié à un effondrement de la structure.

Une étude par RMN à cyclage de champ rapide à bass fréquence a montré que les temps de relaxation dépendaier de la teneur en saccharose et en eau.

Une carte de stabilité a été tracée pour modéliser le évolutions rhéologiques des matrices avec la teneur en ea en lien avec les transitions de phases des matériaux. Cette carte est un outil prédictif du comportement des produi amorphes de part et d'autre de la température de transitio vitreuse face à des variations de teneurs en eau ..

Title : Sugar reduction in extruded cereal based products: impact of water content on the structure and molecular dynamics in such material.

Keywords : Extrudate, Water uptake, Sugar reduction, Molecular mobility, Physical aging

Abstract: Low-moisture biopolymer-based systems are commonly encountered in food. Obviously, understanding the physical basis of their quality: *e.g* texture, or performance over time or as a function of their composition is of primary importance. Physical aging of composited systems makes the changes occurring on storage of edible products difficult to predict. The objectives of this work were to evaluate how the presence of sucrose and water content affects physico-chemical properties. The physical stability of these materials were monitored through an insight at different molecular scales. Then the relations between the multi-scale studies were investigated. The effect of sucrose (0–20%) and feed water (10 and 15%) on extrusion blends was studied using a co-rotating twin screw extruder under the same processing settings. The physical and microstructural properties of expanded extruded products were examined at various relative humidity. Reducing both sugar levels and feed water increased die pressure and specific mechanical energy, as a consequence, it reduced starch degradation and increased in viscosity. The effect was more pronounced with increasing feed water content. The increased die pressure resulted in higher expansion of the porous extrudates. Sucrose was shown to increase the bulk density and reduce the pore size, this was particularly evident by using neutron imaging technique. This technique was applied for the first time in extrudate. 2D tomography images indicated internal structural differences between extrudates containing different sucrose content and stored at low and high % RH, while 3D image analysis showed impact of these factors on pore size distribution and % porosity were not significant. At the end of the extrusion process, the samples were in the amorphous state as a result of starch gelatinization and sugar melting. Their thermal properties were analyzed with differential scanning calorimetry (DSC) and their glass transitions (T_g) were studied. The DSC thermograms were thoroughly studied through a Gaussian deconvolution of the first derivative of their heat low. This approach evidenced a multiple phase behavior with different glass transitions in composite systems. They were associated with either a polymer-rich phase and/or a plasticizer (sugar)-rich phase which behavior depended on the sample water content. Physical aging accompanied with an increase in rigidity at low a_w, resulted in an increased bulk density and more pronounced with increasing sucrose content. Sorption isotherms showed the water content of extrudates decreased when product contains high sucrose at low a_w range and the inverse effect was observed at high a_w. Apparent kinetics of water diffusion showed two different sorption sites, the first kinetics was almost constant and could be adsorption phenomena at the surface. The second one reflected first an initial slowing in dynamics whereas a sharp increase was found at higher water content. This behavior might be related to structure collapse. Addition of sucrose or water decreased both T_gs in extrudates. Young's modulus showed water acts as anti-plasticizer at low a_w, while it shows a plasticizing effect at high a_w. A stability map can explain the brittle-ductile transition occurred below T_g. Fast field cycling NMR study at low frequency highlighted that T_1 depended on sucrose and water content. T_1 and T_2 measured using Low field NMR decrease as a function of water content, while the impact pf sucrose were not significant. T_2 showing a minimum probably indicating the exchange of protons of water and macromolecules in composite system. The impact of sucrose content was not significant for T_1 and for T_2 at low water content. FFC NMR showed T_1 results consistent with the LF NMR measurement.

Université Bourgogne Franche-Comté
32, avenue de l'Observatoire
25000 Besancon

Abstract

Low-moisture biopolymer-based systems are commonly encountered in food. Obviously, understanding the physical basis of their quality: *e.g* texture, or performance over time or as a function of their composition is of primary importance. Physical aging of composited systems makes the changes occurring on storage of edible products difficult to predict. The objectives of this work were to evaluate how the presence of sucrose and water content affects physico-chemical properties. The physical stability of these materials were monitored through an insight at different molecular scales. Then the relations between the multi-scale studies were investigated. The effect of sucrose (0–20%) and feed water (10 and 15%) on extrusion blends was studied using a co-rotating twin screw extruder under the same processing settings. The physical and microstructural properties of expanded extruded products were examined at various relative humidity. Reducing both sugar levels and feed water increased die pressure and specific mechanical energy, as a consequence, it reduced starch degradation and increased in viscosity. The effect was more pronounced with increasing feed water content. The increased die pressure resulted in higher expansion of the porous extrudates. Sucrose was shown to increase the bulk density and reduce the pore size, this was particularly evident by using neutron imaging technique. This technique was applied for the first time in extrudate. 2D tomography images indicated internal structural differences between extrudates containing different sucrose content and stored at low and high % RH, while 3D image analysis showed impact of these factors on pore size distribution and % porosity were not significant. At the end of the extrusion process, the samples were in the amorphous state as a result of starch gelatinization and sugar melting. Their thermal properties were analyzed with differential scanning calorimetry (DSC) and their glass transitions (T_g) were studied. The DSC thermograms were thoroughly studied through a Gaussian deconvolution of the first derivative of their heat low. This approach evidenced a multiple phase behavior with different glass transitions in composite systems. They were associated with either a polymer-rich phase and/or a plasticizer (sugar)-rich phase which behavior depended on the sample water content. Physical aging accompanied with an increase in rigidity at low a_w, resulted in an increased bulk density and more pronounced with increasing sucrose content. Sorption isotherms showed the water content of extrudates decreased when product contains high sucrose at low a_w range and the inverse effect was observed at high a_w. Apparent kinetics of water diffusion showed two different sorption sites, the first kinetics was almost constant and could be adsorption phenomena at the surface. The second one reflected first an initial slowing in dynamics whereas a sharp increase was found at higher water content. This behavior might be related to structure collapse. Addition of sucrose or water decreased both T_gs in extrudates. Young's modulus showed water acts as anti-plasticizer at

low a_w, while it shows a plasticizing effect at high a_w. A stability map can explain the brittle-ductile transition occurred below T_g. Fast field cycling NMR study at low frequency highlighted that T_1 depended on sucrose and water content. T_1 and T_2 measured using Low field NMR decrease as a function of water content, while the impact pf sucrose were not significant. T_2 showing a minimum probably indicating the exchange of protons of water and macromolecules in composite system. The impact of sucrose content was not significant for T_1 and for T_2 at low water content. FFC NMR showed T_1 results consistent with the LF NMR measurement.

The study on different molecular scales for extrudates showed that the addition of sucrose required a modification of the extrusion operating conditions to produce extrudates with optimal textural and storage properties. In conclusion, physicochemical studies of the influence of water and sucrose content on glassy materials showed that the material properties can be investigated at different levels from the macro- to the microscopic scale and these results clearly presented the need for complementary techniques to probe the dynamics in the glassy state of heterogeneous food systems that could be facilitated to manage the stability during storage of this type of dry products.

Acknowledgements

Curriculum Vitae

Professional Experiences

2015-2019 (4 years)   **PhD student in Food Science**

Supervisors: Prof. Dominique Champion, Dr. Gaëlle Roudaut

2013-2013 (1 years)   **Quality control supervisor**, Northeastern Starch Co., Ltd. (Nakhonratchasima, Thailand)

2010-2012 (3 years)   **Quality assurance and Quality control supervisor / Quality Management Representative (QMR)**, Eiamheng Modified Starch Co., Ltd. (Nakhonratchasima, Thailand)

2008-2010 (2 years)   **Quality assurance specialist**, Cargill Siam Co., Ltd. (Mahasarakham, Thailand)

2005-2006 (1 years)   **Quality control supervisor**, Chaiyaphum Co., Ltd. (Chaiyaphum, Thailand)

2002-2005 (3 years)   **Quality control technician**, General Starch Co., Ltd. (Nakhonratchasima, Thailand)

Educational Experiences

2015-2019 (4 years)   **PhD student in Food Science**, Université Bourgogne - Franche-Comté (Dijon, France)

Research grants: Ministry of Science and Technology, Thailand

2006-2008 (2 years)   **M.S. in Science (Major: Food Technology)**, Khon Kaen University (Khon Kean, Thailand)

Research grants: The Thailand Research Fund (TRF) and Postharvest Technology Innovation Center

1998-2002 (4 years)   **B.S. in Science (Major: Biotechnology)**, Mahidol University (Bangkok, Thailand)

Theses

PhD   Sugar reduction in extruded cereal based products: impact of water content on the structure and molecular dynamics in such material (wrote in English).

Advisors: Prof. Dominique Champion, Dr. Gaëlle Roudaut.

Related scientific articles: 1 papers were published and 3 are planned to be submitted.

M.S.	Effect of salt and alkaline on cross-linking and acetylation of tapioca starch. (wrote in Thai).
	Advisors: Asst. Assoc. Prof. Voranuch Srijesdaruk.
B.S.	Gene transformation by Agrobacterium spp. and electroporation in rice and cucumber (wrote in Thai).
	Advisors: Asst. Assoc. Prof. Jarunya Narangajavana.

Languages

Thai	Native speaker
Lao	Native speaker
English	Fair knowledge of English and ability to communicate in English.
French	Learning

List of publications and communications

Articles

Masavang, S.; Roudaut, G.; Champion, D. (2019) Identification of complex glass transition phenomena by DSC in expanded cereal-based food extrudates: Impact of plasticization by water and sucrose. *Journal of Food Engineering*, 245, 43-52.

Oral communications

Masavang, S.; Roudaut, G.; Champion, D. Study of water uptake of extruded breakfast cereal models: Impact of sucrose and water content during processing. ISOPOW XIII. *International Symposium on the Properties of water*, Lausanne, Switzerland, 26-29 June 2016.

Masavang, S.; Champion, D.; Roudaut, G.; Loupiac, C.; Bidault, O.; Bodart, P. Water uptake in breakfast cereal models: Impact of sucrose and water content. *FJL 2017*, 23e Forum des Jeunes Chercheurs, Dijon, France, 15-16 June 2017.

Masavang, S.; Roudaut, G.; Champion, D. Water uptake ability of breakfast cereal model: Impact of sugar and water content. SLIM 2017, *8th Shelf Life International Meeting*, Bangkok, Thailand 1-3 November, 2017.

Poster communications

Masavang, S.; Champion, D.; Rachocki A.; Bodart, P. NMR Relaxometry in real and model food systems: Impact of sucrose and water content on the structure and molecular dynamics in cereal based-products. FFC RELAX, *11th Conference on Fast Field Cycling NMR Relaxometry*, Pisa, Italy, 5-7 June 2019.

List of Figures

List of Tables

List of abbreviations

2D	two-dimensional image
3D	three-dimensional image
τ	interpulse spacing time (msec)
$\emptyset$	Porosity (%)
ϵ_E	strain
σ_E	stress
μCT	X-ray microtomography
ΔC_p	step associates with the glass transition on the second heating scan on DSC thermogram $(J.g^{-1}.^oC^{-1})$
A_0	area under compression curve
A_1	proportional of the 1st exponential for the two kinetics exponential model
A_2	proportional of the 2nd exponential for the two kinetics exponential model
$A(t)$	NMR signal intensity at time t for the two-exponential fitting
a_w	water activity (p/p_0)
a_{wc}	critical water activity (p/p_0)
a	constant defining the polar-polar interactions in the rigid part for Abragam fitting
b	constant defining the polar-polar interactions in the rigid part for Abragam fitting
$b *$	constant describes the slope of transition of variable of Fermi equation
BET model	Brunauer-Emmet-Teller model
C	surface heat constant of the GAB constants
D	time constant of apparent water diffusion dependent on water activity for Fermi equation (min)
D_0	value of the time constant at aw ~ 0 for Fermi equation (min)
D_e	piece density (g/mm^3)
D_{eq}	equivalent pore diameter (mm)
D_r	residual magnitude of the property after the transition for Fermi equation (min)
D_{rap}	rapeseed density

DDI	dynamic dewpoint isotherms
DMSO	dimethylsulphoxide
DSC	differential scanning calorimetry
DVS	dynamic vapor sorption humidity generating instrument
EMC	equilibrium moisture content (g/ 100 g dry solid)
ER	expansion ratio
E_y	Young's modulus (Pa)
FFC NMR	Fast field cycling relaxometry
FID	Free induction decay signal
$F_{(t)}$	force as function of time (N/m)
FWHM	full widths at half maximum
GAB model	Guggenheim-Anderson-de Boer equation
G_i	derivative signals were fitted by Gaussian distribution functions
H_0	sample initial height (mm)
HPSEC	high-performance size exclusion chromatography
i	different phases of derivative signals
$I(t)$	intensity of the total relaxation signal for Abragam fitting
I_1	the amplitude of the rigid proton populations for Abragam fitting
I_2	the amplitude of the flexible proton populations for Abragam fitting
k	multilayer factor of the GAB constants
k^*	Fermi's constants
k_s	adjustable parameter of the Gordan-Taylor equation
L	the component with longer relaxation time constant
LF NMR	Low-field nuclear magnetic resonance spectroscopy
m	moisture content (g/100g dry solids)
m_0	monolayer moisture content (g/100g dry solids)
M_2	second moment ()
MDSC	modulated differential scanning calorimetry
m_i	experimental values for evaluation the goodness of the fit
m_{pi}	predicted values for evaluation the goodness of the fit
MRI	Magnetic resonance imaging

N	number of experimental data
NMR	nuclear magnetic resonance spectroscopy
NMRD	nuclear magnetic relaxation dispersion profiles
p values	goodness of the fit (%)
R_1	relaxation rate (s^{-1})
RH	relative humidity (%)
RHc	critical relative humidity
ROI	Region of interest for image analysis
RTg	corresponded temperature range of glass transition
RVA	Rapid viscosity analysis
SEI	cross-sectional expansion index
SL	specific length of extrudates
SME	specific mechanical energy
SSS	saturated salt solution method for Sorption isotherms experiment
t_0	initial time (min)
t_1	sorption kinetics time constant representing fast water sorption processes (min)
T_1	spin-lattice relaxation time constant (ms)
T_{1w1}	spin-lattice relaxation times measured in the time ranges window 1 (ms)
T_{1w2}	spin-lattice relaxation times measured in the time ranges window 2 (ms)
t_2	sorption kinetics time constant representing slow water sorption processes (min)
T_2	spin-spin relaxation time constant (msec)
T_{FWHM}	temperature at full widths at half maximum positions
T_g	glass transition temperature (^{o}C)
T_{gh}	glass transition at high temperature (2nd transition)
$T_{g,i}$	respective glass transitions to different phases (^{o}C)
T_{gl}	glass transition at low temperature (1st transition)
T_{gm}	glass transition temperature of mixture (K)
T_{gs}	glass transition temperature of anhydrous solids (K)
T_{gw}	glass transition temperature of water (K)

T_p	first threshold level for detection of pores
T_w	second threshold detection of sample without voids
T_{1W1}	relaxation times at time windows beginning at 0.016 ms (ms)
T_{1W2}	relaxation times at time windows beginning at 0.1 ms
V_{3D}	volume of pore in 3D (mm^3 or voxel)
V_e	equivalent volume of extrudate (mm^3 or voxel)
V_{pore}	total volume of pores (mm^3)
V_{total}	total volume of a sample studied (mm^3)
WAI	water absorption index
%wb	weight percent on dry basis (%)
W_c	critical water content (%)
W_e	weight of extrudate (g)
WSI	water solubility index
%wt	weight percent (%)
XRD	X-ray diffraction
x_s	mass fraction of solids (g/100g wet basis)
x_w	mass fraction of water (g/100g wet basis)
y	moisture content at infinite time of sample exposure of the sample at a constant RH (g/100g dry basis)
y_0	moisture content of the sample at time zero (g/100g dry basis)
Y_o	initial value of the analyzed result for Young's modulus
W_r	rapeseed weight (g)

Table of Contents

Chapter 1:

Introduction

Introduction

Cereal-based products are often produced by an extrusion-cooking process that allows fast mixing-cooking-drying of the ingredients under high mechanical pressure. This process generally induces melting in the barrel and material vitrification following fast water evaporation at the exit of the die. This freezing of the structure into a solid foam is due to both the pressure and temperature difference between the extruder and atmospheric conditions after the die (Bhandari and Howes 1999, Roos 2003). Although cereals are mainly composed of complex carbohydrates, they are also a source of low molecular weight sugars as a result of both process and recipe (Williams 2014). Therefore, even if breakfast cereals are mainly composed of complex carbohydrates, they also contain low molecular weight sugars now recognized as inappropriate for children and adults (Harris *et al,.* 2011, Williams 2014, Fayet-Moore *et al,.* 2017). Reducing the sucrose content and increasing the protein level in breakfast cereals could induce changes in texture and stability which should not be perceived by the consumers of these products (Farhat *et al,.* 2000, Mezreb *et al,.* 2006, Pitts *et al,.* 2014, Philipp *et al,.* 2017). Extruded foods are composed mainly of flour while salt and sugars are only minor constituents in the formulation. Each of these ingredients has physico-chemical properties playing a specific part in the processing characteristics and textural quality of the product (Pitts *et al,.* 2014).

The general objectives for this research project were to provide a better understanding of the ingredients impact on the extruded product macrostructure and stability in different storage conditions. Water and sucrose were varied in concentration and flour amount was used to compensate for the change of mass. This study of extruded products with various sucrose contents, appears very complex due to the hygroscopic nature of components affecting the overall water content and varying the water distribution between its main polymeric components and small hygroscopic molecules. The strategy used was:

1. To investigate the effect of sucrose content in a wheat blend formation and feed water content on the extrusion processing characteristics, production quality, expansion, density, water

absorption, water solubility, microstructure and textural properties of extruded products and identify **correlation between process properties of cereal with microstructure and physical attributes** of the final product.

2. To evaluate how **changes in plasticizer contents affect the mechanical properties** of the matrix and confirm if the changes in texture are related to phase transitions such as the glass transition of extrudates. Moreover, the effect of storage time was also studied.

3. To **assess the effect of sucrose content on sorption** (dynamic and at equilibrium) of extrudate when exposed to an environment with a high relative humidity, including the application of models to predict the water sorption behavior, water migration and the textural behavior of porous solid systems during storage.

4. To **study molecular dynamics over storage.** ^{1}H NMR relaxometry was used to follow the changes in relaxation times (T_1 and T_2) for extruded samples at different relative humidity, relating proton mobility to the motions of small and large molecular components.

In order to manage the possible evolution of a modified recipe of extruded cereal-based products, we aimed at better understanding the structural aspects and product stability affected by the change of recipe.

Firstly, bibliographic review was carried out and a summary is provided in the next section.

1.1 Impact of sugar addition

The modification of solid foam texture by the addition of sucrose is due to plasticization of macromolecules (mainly, starch, gluten) by sucrose, which induces effects on macrostructure. Plasticization of starch systems by small molecular weight constituents is a widely reported phenomenon (Shogren 1992, Slade and Levine 1995). The addition of sugars increases solid foam density and results in a reduction in expansion and pore size of corn or wheat based products (Barrett *et al,.* 1995, Carvalho and Mitchell 2000, Farhat *et al,.* 2003, Mezreb *et al,.* 2006). As a consequence, it

also affects the mechanical and sensory fracture properties by increasing the fracture force. Plasticization by sucrose results in an increase in the molecular mobility of polymers, a feature which is reflected in a number of properties. The effect of sugar as a starch plasticizer also has been studied by Kalichevsky *et al,.* (1993), who determined the depression of glass transition temperature (T_g) of amylopectin films by calorimetric and mechanical methods. (Fan *et al,.* 1996b, Fan *et al,.* 1996a) investigated the effect of sugar inclusion on the extrusion of maize grits. The observed reduction in sectional expansion and specific mechanical energy (SME) was considered to be a consequence of the decrease in T_g on replacement of starch by sugar. Although sugar concentration is known to affect the structure and texture of cereal based-extrudates, the effects of sucrose on extrudates prepared from different cereal type have varied. Carvalho and Mitchell (2001) reported that the extent of sugar plasticization was lower for wheat compared with corn and maize grit. It is suggested that this was because of the more amorphous character of the wheat extrudates. The smaller effect of sugar on the expansion of wheat flour compared with maize grits was proposed to be due to the greater degree of starch conversion in the latter system at all the sugar levels. Expansion was much lower for maize grits compared with the wheat flour, probably because of the lower elasticity in the less converted starch. These authors also noted that the replacement of maize by sucrose at constant water content reduced the specific mechanical energy and as a consequence, reduced the degree of starch conversion and sectional expansion. In contrast, replacing wheat flour by sucrose even at levels as high as 20% of the flour weight had little effect. This is possibly due to less efficient plasticization of wheat flour by sucrose compared with maize grits at low water contents, and a specific role for gluten and the larger particle size of maize grits compared with wheat flour. (Carvalho and Mitchell 2000). Mezreb *et al,.* (2006) related the difference effects of sucrose on corn and wheat extrudates by their composition. They showed that sucrose induced a reduction in product expansion, which was more pronounced for corn extrudates. Possible causes discussed were that within the wheat melt, competition should exist between the viscoelastic characteristics conferred by the gluten, and the drop in water availability.

They noted that independent of the flour type, an increase in sucrose leads to crisper products until an optimal content has been reached, beyond which crispness decreases..

1.2 Effect of water in amorphous foods

Water is considered to be the most effective plasticizer in food matrices, decreasing T_g and mechanical resistance (Slade and Levine 1991, Moraru *et al,.* 2002, Pittia and Sacchetti 2008). Water has solvent properties and promotes mobility of polymer chain (Lewicki *et al,.* 2004) and crisp, hard or tough materials become soft, extensible and flowable at high hydration levels. Water plasticization is a process of great importance mainly in low moisture, cellular or porous foods, such as seeds, breakfast cereals or snacks of cereal origin, whose original state are characterized by a crispy and brittle texture. This is relevant for their sensory acceptability and/or processing (Pittia and Sacchetti 2008). Despite its well-recognized and studied plasticizing effect, it has been observed that in some glassy polymer-plasticizer systems, at temperatures below T_g, the increase of plasticizer concentration leads to an increase in rigidity and firmness despite a T_g decrease. This behavior is called the anti-plasticization effect of water (Pittia and Sacchetti 2008) (Fig. 1.1). This effect has been observed in many food systems differing in nature, composition and production process: starch extrudate (Shogren 1992), breakfast cereal (Gondek and Lewicki 2006), cracker and corn-rye crisp bread (Lewicki *et al,.* 2004), flat extruded wheat and rye bread (Marzec and Lewicki 2006), complex meat-starch extrudate (Moraru *et al,.* 2002), white and extruded breads (Roudaut *et al,.* 1998), corn flakes (Farroni *et al,.* 2008).
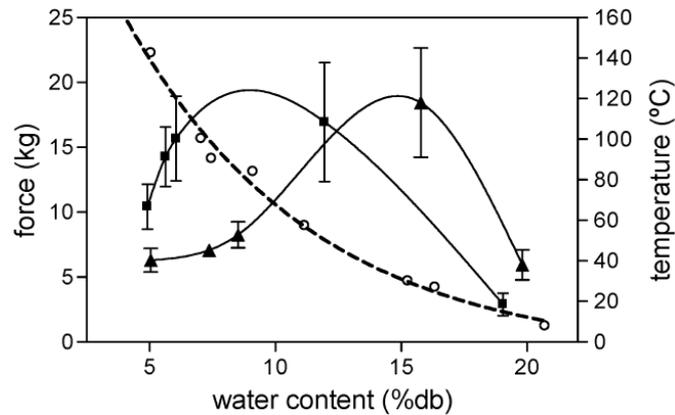
Fig. 1.1 Force at maximum deformation for common corn flakes (▲) and sugar-frosted corn flakes (■), and onset temperature of glass transition for common corn flakes (O) at different water content. Symbols represent experimental values. Solid lines are the results of spline fit indicating the tendency of data points. The error bars represent standard deviation (Farroni *et al,.* 2008).

The stability and textural properties of food products are closely related to their mechanical and thermal properties. If the moisture of products increases due to water sorption from the atmosphere or by mass transport from neighboring areas, the plasticizing effect of water severely reduces crispness (Farroni *et al,.* 2008). This loss of crispness has been shown to occur in the glassy state, implying the onset of molecular motion below the glass transition temperature (T_g) (Nicholls *et al,.* 1995). Decrease of mechanical resistance with increasing water content in cereal-based products emphasizes the plasticizing effect of water, reducing T_g (Roudaut *et al,.* 1998, Chaunier *et al,.* 2007) below consumption temperature. However, the prediction of crispness, on the basis of knowledge of the glass transition temperature alone, is not possible, because biopolymers can exhibit changes in fracture mechanisms in the glassy state. Molecular mobility can be considered from a structural and macromolecular level, and therefore, T_g can be a descriptive parameter of the physical state of macromolecules, which differs from the molecular mobility of smaller molecular such as water and sucrose (Barrett *et al,.* 1995). As polymers absorb water, their properties are not affected in the same manner, and in the low to intermediate humidity range, some mechanical properties such as the force at maximum deformation, or Young's modulus show a maximum or plateau region (Fig. 1) when

plotted versus water content while T_g continuously decreases (Roos *et al,.* 1998, Roudaut *et al,.* 1998, Lewicki *et al,.* 2004, Farroni *et al,.* 2008).

1.3 Glass transition identification

Water relationships are particularly relevant for amorphous, dry food systems. Such products are numerous as many processes (baking, dissolution/drying) lead to a loss of crystallinity, resulting in many foods showing polymeric material below or close to their T_g in storage conditions. The precise determination of the glass transitions of composite food matrices is not trivial, in particular when multiple glass transitions occur in close proximity due to the presence of different phases (Tedeschi *et al,.* 2016). Several methods may be employed for the analysis of the glass transitions in such situations such as the method based on the tangents to the heat flow curve. The onset and end of glass transitions are then determined as the temperatures at which the tangent at the inflection point intersects with the low-temperature baseline (T_g, onset) and the high temperature baseline (T_g, end), respectively. In addition, the midpoint glass transition temperature is defined as the temperature at which the inflection point occurs. Alternative methods for the determination of glass transition temperatures occurring in multiple amorphous phases include the analysis of the first derivative of the heat flow curve, the modeling of the heat flow curves by a suitable two-stage mathematical model, and the separation of the two glass transitions by DSC (Tedeschi *et al,.* 2016). Roudaut and Wallecan (2015) showed that the first derivative of the heat flow of low moisture baked product could be represented by a sum of two or three Gaussian functions suggesting that several glass transitions were present in flour-sucrose-water matrices (Fig. 1.2). This was of particular interest, as baked flour is a complex system containing starch and gluten, that has until now always been described as having a single glass transition (Pereira and Oliveira 2000, Carvalho and Mitchell 2001). The two T_g s were associated with either a polymer-rich phase and/or a plasticizer (sugar)-rich phase whose behavior depended on the

sample water content (Roudaut and Wallecan 2015). This approach evidenced a multiple phase

behavior with different glass transitions in composite systems.
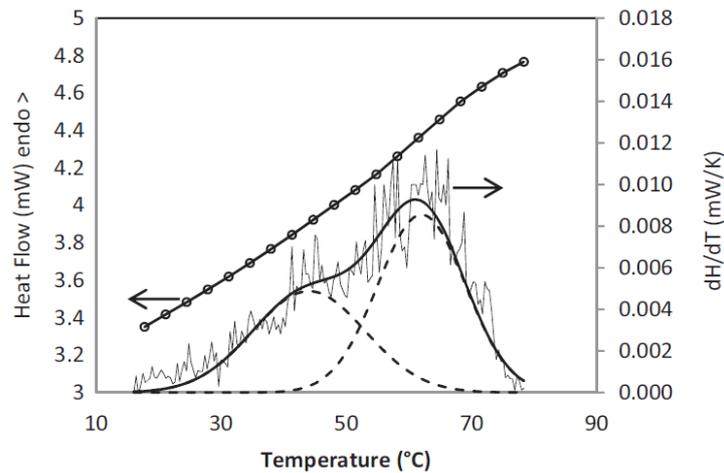
Fig. 1.2. Deconvolution of the DSC thermogram of baked flour-sucrose-water blend equilibrated at a_w

= 0.75. Heat flow: -o- (left Y axis); first derivative of the heat flow of second heating scan: (right Y axis);-

--- Gaussian functions fitting the signal; sum of Gaussian functions (Roudaut and Wallecan 2015).

Common methods for investigating glass transitions have focused on identifying

thermodynamic, mechanical, or dielectric changes versus temperature while scanning through T_g. This

testing is done at constant moisture content. However, increased plasticization of amorphous glassy

materials induces a glass transition even while temperature is kept constant. Because moisture is the

most common plasticizer in food materials, a critical moisture content, or a critical water activity can

be associated to the transition from a glass to a rubber at constant temperature. In theory, scanning

temperature and scanning plasticizer level should lead to the same equivalent glass transition event

(Fig. 1.3). However, what has not been fully explored is the use of water vapor sorption-based

experiments to directly determine the critical moisture content and relative vapor pressure associated

with the glassy to rubbery transition. Only a few researchers have investigated the use of water vapor

sorption-based experiments for determining the glass transition (Oksanen and Zografi 1990, Bell 1995,

Ubbink *et al,.* 2007). Ubbink *et al,.* (2007) used a theoretical approach to identify the location of the

glassy to rubbery transition in the sorption isotherm, whereas Oksanen and Zografi (1990) and Bell

(1995) used an empirical approach.
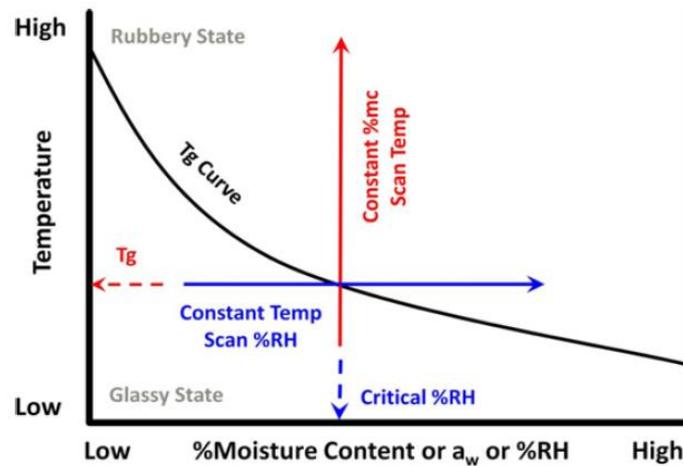
Fig. 1.3. Comparison between thermal methods that scan temperature while holding moisture content

(% moisture content) constant to determine the glass transition temperature (T_g) and sorption

isotherm methods that scan water activity to identify a critical water activity (RH_c) while holding

temperature constant. In theory, both methods should provide the same information (Yuan *et al,.*

2011).

The glass transition temperatures of dry or intermediate moisture food vary significantly from

temperatures below room temperature to very high values. In amorphous carbohydrates and proteins,

water acts as a plasticizer, i.e., associated with a replacement of polymer interaction by a polymer

solvent interaction resulting in a decrease in T_g. Therefore, changes in amorphous food properties may

result either from glass transition occurring because of increasing temperature (thermal plasticization)

or increasing water content (water plasticization) (Fig. 1.3). Several studies have used the Gordon-

Taylor (Roos and Karel 1991) or Couchman-Karasz (Kalichevsky *et al,.* 1993) relationships to predict the

water dependence of glass transition temperatures. The established diagrams show critical values for

water content and water activity that result in glass transition at storage temperatures (Fig. 1.4). The

critical water content and water activity diagrams together with state diagrams are important in

explaining changes in time-dependent mechanical and flow properties that are governed by glass

transition and water plasticization (Roos 1995). Roos *et al,.* (1998) fitted the Gordon-Taylor and the

Guggenheim-Anderson-de Boer (GAB) relationships to glass transition, water plasticization, and water

sorption data. The GAB model is well known to fit to the water sorption data of food materials at

various relative humidities (Roos 1995).
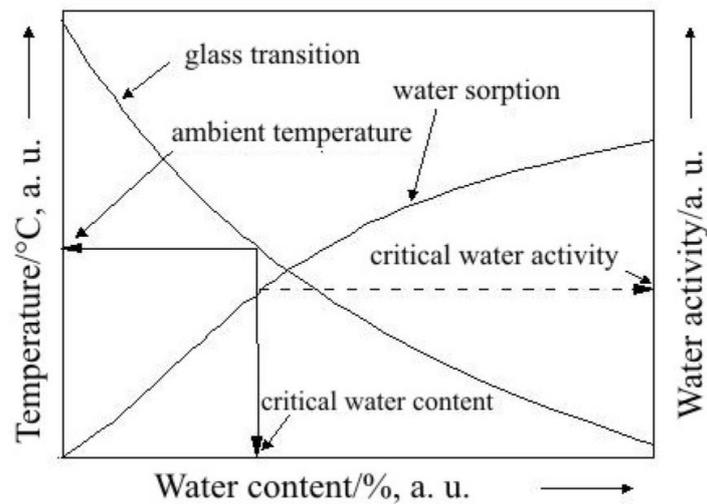
Fig. 1.4 Typical state diagram of amorphous biological materials based on the glass transition
temperature (Roos 2003).

1.4 Kinetics of water uptake during storage

Moisture migration is a common problem in many composite food systems where components

of high/low water activity are adjacent (Guillard *et al,.* 2003b). Water diffuses from high RH into the

low RH component leading to irreversible texture losses (Labuza and Hyman 1998). The transport and

equilibrium properties of water for each compartment are important factors needed for modelling and

predicting moisture transfer between components and, as a consequence, shelf life of the product

(Guillard *et al,.* 2003b). The characterization and quantification of vapor sorption and diffusion in a

material is of fundamental importance to the understanding and prediction of how the material will

function over time. Many studies are focused on characterizing the sorption and diffusion

characteristics of a vapor in a material to gain insight into the structure or chemical nature of the

material (Harley *et al,.* 2012). Owing to the complexity of food products, equilibrium hydration properties and water transport have been studied frequently in food model systems such as sponge-cake (Guillard *et al,.* 2003b); cereal based-biscuit (Bourlieu *et al,.* 2008). Several mathematical models have been used to predict moisture transfer in foods such as; a single exponential for bread crusts (Van Nieuwenhuijzen *et al,.* 2008); the empirical model based on Fick's second raw (Guillard *et al,.* 2003b, Guillard *et al,.* 2003a, Roca *et al,.* 2006, Bourlieu *et al,.* 2008). A maximum in the water uptake rate or effective diffusivity was found as a function of water content (Fig. 1.5). In addition, Karathanos *et al,.* (1990) and Guillard *et al,.* (2003b) found that moisture diffusivity within porous starch-based products increased gradually as the moisture content rose, reaching a maximum and sharply decreased. They attributed the changes in diffusivity to the changes in porosity of the starch material resulting from a collapse phenomenon and water transport occurring in the liquid phase within the swollen matrix. The difficulties generally encountered in determining accurate values of mass transfer coefficients and several interfering phenomena (swelling, different mechanisms of water transport) made the direct transposition of sorption kinetics values to moisture transfer difficult in composite foods. Nonetheless, identification of water uptake from water sorption kinetics seems a good means to assess diffusivity changes with moisture content and to provide a diffusivity model and initial parameters for modelling moisture transfer in a composite food. However this diffusivity model should still be quantitatively adjusted to apply to moisture migration experiments modelling (Guillard *et al,.* 2004). This maximum of diffusivity upon hydration has been related to the glass transition. Therefore, examining this behavior below or above the glass transition could contribute to a better understanding of the physical stability of the products.
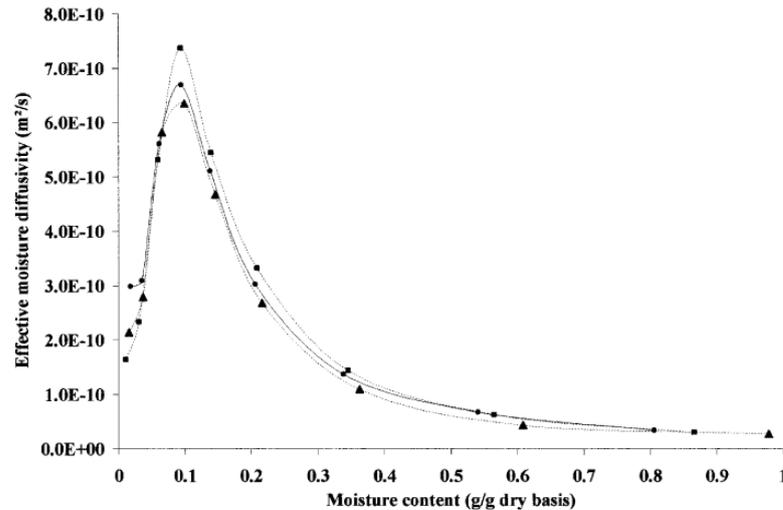
Fig. 1.5 Effective moisture diffusivity of sponge-cake at 20 °C as a function of moisture content (plotted moisture contents are arithmetic mean between initial and equilibrium moisture contents for the corresponding relative humidity range) (Guillard *et al,.* 2003b).

The transitions or endothermal changes occurring below the glass transition temperature that provide information on the mobility within glassy materials have been examined.. Proton nuclear magnetic resonance (^{1}H NMR) provides useful information on molecular mobility through relaxation times, such as the impact of water-solid interactions on molecular mobility and water populations (Kou *et al,.* 2000). This technique allows differences in molecular mobility of polymers and water to be measured via the change in spin-lattice (T_1) or spin-spin (T_2) relaxation time constants with temperature or water content. Low field NMR has been used by Farhat *et al,.* (1996) to investigate the mobility in maze-sucrose extrudate as a function of hydration level. Shorter T_2 values for the more mobile components of the signal recorded for the samples containing sugar were reported. As the water content was increased, the amplitude of the normalized NMR signal arising from the rigid component decreased for the samples containing sucrose, suggesting an increased mobility. Moreover, Roudaut *et al,.* (2009) studied proton mobility of the sugar starch systemsas a function of sucrose and water content, including the effect of storage temperature. They reported that T_2 increased with water content (up to 13% wb) at all temperatures. For a given water content, both rigid

and mobile protons exhibited a lower mobility in the presence of sucrose and that a temperature increase induced an increase in both rigid and mobile protons mobility. Curti *et al,.* (2011) studied bread stealing in white bread over 14 days of storage by using low field nuclear magnetic resonance (LF NMR) and Fast field cycling nuclear magnetic resonance FFC NMR). Proton T_2 relaxation time shifted toward shorter times, indicating a proton mobility reduction of the bread matrix during storage. Proton T_1 of bread was measured at variable frequencies (FFC NMR) and found to decrease in bread during storage. In the work reported here, the NMR relaxation parameters were employed to study the molecular mobility of various components in extruded system and attempted to examine water dynamic and molecular changes occurring during storage in glassy state.

1.5 3D analysis of microstructure

Imaging techniques have the ability to supplement analytical techniques by supplying information on the macro and microstructure of solid foams (porosity, wall thickness). Conventional imaging methods used when studying starch extrudates are light microscopy (Altan *et al,.* 2009) and electron microscopy (Lopez-Rubio *et al,.* 2008, Mahasukhonthachat *et al,.* 2010). However, these techniques are generally used to image cross-sections or surface structures of the material and are not used to provide images of hydrated products. 3D tomography is more and more applied in the medical and food industry, but most of studies have focused on using X-ray tomography to determine characteristics of porosity in a wide range of food items, such as fried potato chips (Yang *et al,.* 2017), fried nuggets (Adedeji and Ngadi 2009), baked goods (Esveld *et al,.* 2012), cereals (Chaunier *et al,.* 2007) and extrudates (Dalen *et al,.* 2007, Chevallier *et al,.* 2014, Pitts *et al,.* 2014, Philipp *et al,.* 2017).

Neutron imaging and tomography also allow the observation of large sample structures at the scale of a few micrometers. Neutron imaging experiments are performed by transmission of neutrons through the matter and exploit their high sensitivity towards hydrogen (Tanoi *et al,.* 2009). Neutron tomography has been successfully deployed in material science, geology, archeology, etc.,so it is not

surprising that it is an emerging technique to study food microstructure (Tanoi *et al,.* 2009, Lagorce-Tachon *et al,.* 2015, Aregawi *et al,.* 2013). For example, neutron radiography has been used to explore cork stoppers, and more precisely to study their quality through the quantification of their defects (Lagorce-Tachon *et al,.* 2015); the impact of cooking on beef meat (Scussat *et al,.* 2016); the moisture loss in fruit or fish dehydration (Tanoi *et al,.* 2009, Aregawi *et al,.* 2013, Defraeye *et al,.* 2013). The work reported here used neutron imaging technique (applied for the first time to extruded products) to observe the changes occurring during storage of products formed from different recipes.

1.6 Effect of storage time

The complex composition of extruded products may lead to phase separation of the ingredients which may make the characterization of phase transitions very complex. As a result,he usual DSC, and DMA techniques generally used for this purpose need careful analysis.

Physical aging is also a structural relaxation occurring in glassy materials. It is characterized by the movement of structural components toward their equilibrium states as a function of aging time (Chung and Lim 2006). Many cereal-based processed foods are manufactured through thermal processing with relatively limited moisture and form as glasses at the point of manufacture.. During their storage, these cereal-based products gradually undergo slow relaxation processes. These physical changes are often responsible for the deterioration of the product quality as well as chemical reactions which continue to occur during storage, due to the remaining mobility of molecules at a temperature below their glass transition. (Champion *et al,.* 2000). Aging induces the changes in both thermodynamic and mechanical properties of the products, including enthalpy, modulus, volume, and molecular diffusivity. Since the matrix material is predominantly starch, control of the physical aging phenomenon of starch is needed.. The physical aging of various glassy polymers has been characterized by using dilatometry and differential scanning calorimetry (DSC) (Lourdin *et al,.* 2002). Dielectric and dynamic mechanical measurements have also been performed on low moisture food such as white

bread and starches (Chung and Lim 2004, Roudaut *et al,.* 1999, Chung *et al,.* 2004). In addition to these two commonly used techniques, proton NMR relaxation techniques also have been used to detect dynamic mobility which also relates to a change in the state of material under investigation (Barrett *et al,.* 1995, Roudaut *et al,.* 2009).

Based on the state of art drawn from literature, three main questions remain and give orientation to this Ph.D. work:

1°) The solid foam studied contains mainly two plasticizers (water and sucrose) in bio-polymeric matrices: **how does the variation of their amount induce changes during processing?**

2°) **How do these two molecules modify the macro and microstructure of the foam?**

3°) A**re the effects of these two plasticizers on water sorption, and molecular mobility synergistic or antagonistic?**

4°) A**re techniques combination useful to study product stability?**

This PhD report is written as the first draft, preparing for scientific publication. Only material in the 5th Chapter has already been published. The work is divided in four main sections followed by conclusions and perspectives.

In the first part, the results of a direct comparison between the effects of added sucrose on the extrusion behavior of the solids produced at 10% and 15% feed water content are reported. The influence of sugar on the expansion parameters (sectional and longitudinal expansion indices), the physico-chemical properties (water solubility and absorption indices, viscosity) and molecular size distribution of wheat extrudates have been determined. A question of interest is whether the same general behavior is found for extrudate produced at different feed water content.

In the next section, the influence of water and sucrose on extrudate will be monitored at the microscopic scale. The neutron imaging technique is used on extrudates to provide a more complete

picture of microstructure of samples at different relative humidities. The 2-D and 3-D microstructure of extrudates were determined to have a better understanding of the impact of sucrose content on extrudate structure, and consequent water absortion.

The third part focuses mainly on the physical state change. The plasticizing effect of sucrose on the glass transition temperature (T_g) is discussed, using differential scanning calorimetry (DSC). This T_g value was obtained at different water and sucrose contents. Similarly to the sorption studies, phenomenological models used to predict T_g are presented and applied to the experimental data. It is well recognized that adding sugar also has an effect on the mechanical properties of these materials. The Young's modulus was also evaluated using the compression method for samples at various water and sucrose content. State diagrams were established to assess the effect of T_g on the mechanical properties of these systems, including critical water content and water activity were provided.

Finally, water dynamics will be considered. In the last section, the experimental work includes water sorption studies of extruded products. The sorption kinetics for each equilibrating relative humidity were determined and in order to improve the understanding of sorption and diffusion behavior, phenomenological models were used. Work was undertaken to study the effect of sucrose and relative humidity on water dynamics and the molecular changes occurring during storage, by means of ^1H NMR relaxometry.

The study is genuinely multi-scale (from macrostructure to molecular scale) with a particular insight for the structural properties and molecular mobility of glasses in extruded products. Thus the efforts to link product properties through an insight at different length scales will be shown to contribute to a better understanding of the physical stability of these materials.

References

Adedeji, A. A. & Ngadi, M. O. (2009). 3-D Imaging of deep-fat fried chicken nuggets breading coating using X-ray micro-CT. *International Journal of Food Engineering,* **5,** Article 11.

Altan, A., McCarthy, K. L. & Maskan, M. (2009). Effect of Extrusion Cooking on Functional Properties and in vitro Starch Digestibility of Barley-Based Extrudates from Fruit and Vegetable By-Products. *Journal of Food Science,* **74,** E77-E86.

Aregawi, W., Defraeye, T., Saneinejad, S., Vontobel, P., Lehmann, E., Carmeliet, J., Derome, D., Verboven, P. & Nicolai, B. (2013). Dehydration of apple tissue: Intercomparison of neutron tomography with numerical modelling. *International Journal of Heat and Mass Transfer,* **67,** 173-182.

Barrett, A., Kaletunç, G., Rosenburg, S. & Breslauer, K. (1995). Effect of sucrose on the structure, mechanical strength and thermal properties of corn extrudates. *Carbohydrate Polymers,* **26,** 261-269.

Bell, L. N. (1995). Investigations Regarding the Determination of Glass Transition Temperatures from Moisture Sorption Isotherms. *Drug Development and Industrial Pharmacy,* **21,** 1649-1659.

Bhandari, B. & Howes, T. (1999). Implication of glass transition for the drying and stability of dried foods. *Journal of Food Engineering,* **40,** 71-79.

Bourlieu, C., Guillard, V., Powell, H., Vallès-Pàmies, B., Guilbert, S. & Gontard, N. (2008). Modelling and control of moisture transfers in high, intermediate and low aw composite food. *Food Chemistry,* **106,** 1350-1358.

Carvalho, C. W. P. & Mitchell, J. R. (2000). Effect of sugar on the extrusion of maize grits and wheat flour. *International Journal of Food Science & Technology,* **35,** 569-576.

Carvalho, C. W. P. & Mitchell, J. R. (2001). Effect of Sucrose on Starch Conversion and Glass Transition of Nonexpanded Maize and Wheat Extrudates. *Cereal Chemistry Journal,* **78,** 342-348.

Champion, D., Le Meste, M. & Simatos, D. (2000). Towards an improved understanding of glass transition and relaxations in foods: molecular mobility in the glass transition range. *Trends in Food Science & Technology,* **11,** 41-55.

Chaunier, L., Della Valle, G. & Lourdin, D. (2007). Relationships between texture, mechanical properties and structure of cornflakes. *Food Research International,* **40,** 493-503.

Chevallier, S., Réguerre, A.-L., Le-Bail, A. & Della Valle, G. (2014). Determining the Cellular Structure of Two Cereal Food Foams by X-ray Micro-Tomography. **9,** 219-228.

Chung, H.-J., Chang, H.-I. & Lim, S.-T. (2004). Physical aging of glassy normal and waxy rice starches: Effect of crystallinity on glass transition and enthalpy relaxation. *Carbohydrate Polymers,* **58,** 101-107.

Chung, H.-J. & Lim, S.-T. (2004). Physical aging of glassy normal and waxy rice starches: thermal and mechanical characterization. *Carbohydrate Polymers,* **57,** 15-21.

Chung, H.-J. & Lim, S.-T. (2006). Physical Aging of Amorphous Starches (A Review). *Starch - Stärke,* **58,** 599-610.

Curti, E., Bubici, S., Carini, E., Baroni, S. & Vittadini, E. (2011). Water molecular dynamics during bread staling by Nuclear Magnetic Resonance. *LWT - Food Science and Technology,* **44,** 854-859.

Dalen, G., Peter, N., Van Vliet, L., Voortman, L. & Esveld, D. C. (2007). 3D Imaging and analysis of porous cereal products using X-ray microtomography. **26,** 169-177.

Defraeye, T., Aregawi, W., Saneinejad, S., Vontobel, P., Lehmann, E., Carmeliet, J., Verboven, P., Derome, D. & Nicolaï, B. (2013). Novel Application of Neutron Radiography to Forced Convective Drying of Fruit Tissue. *Food and Bioprocess Technology,* **6,** 3353-3367.

Esveld, D. C., van der Sman, R. G. M., van Dalen, G., van Duynhoven, J. P. M. & Meinders, M. B. J. (2012). Effect of morphology on water sorption in cellular solid foods. Part I: Pore scale network model. *Journal of Food Engineering,* **109,** 301-310.

Fan, J., Mitchell, J. R. & Blanshard, J. M. V. (1996a). The effect of sugars on the extrusion of maize grits: I. The role of the glass transition in determining product density and shape. *International Journal of Food Science & Technology,* **31,** 55-65.

Fan, J., Mitchell, J. R. & Blanshard, J. M. V. (1996b). The effect of sugars on the extrusion of maize grits: II. Starch conversion. *International Journal of Food Science & Technology,* **31,** 67-76.

Farhat, I. A., Blanshard, J. M. V., Descamps, M. & Mitchell, J. R. (2000). Effect of Sugars on Retrogradation of Waxy Maize Starch-Sugar Extrudates. *Cereal Chemistry Journal,* **77,** 202-208.

Farhat, I. A., Mitchell, J. R., Blanshard, J. M. V. & Derbyshire, W. (1996). A pulsed 1H NMR study of the hydration properties of extruded maize-sucrose mixtures. *Carbohydrate Polymers,* **30,** 219-227.

Farhat, I. A., Mousia, Z. & Mitchell, J. R. (2003). Structure and thermomechanical properties of extruded amylopectin–sucrose systems. *Carbohydrate Polymers,* **52,** 29-37.

Farroni, A. E., Matiacevich, S. B., Guerrero, S., Alzamora, S. & del Pilar Buera, M. (2008). Multi-Level Approach for the Analysis of Water Effects in Corn Flakes. *Journal of Agricultural and Food Chemistry,* **56,** 6447-6453.

Fayet-Moore, F., McConnell, A., Tuck, K. & Petocz, P. (2017). Breakfast and Breakfast Cereal Choice and Its Impact on Nutrient and Sugar Intakes and Anthropometric Measures among a Nationally Representative Sample of Australian Children and Adolescents. *Nutrients,* **9,** 1045.

Gondek, E. & Lewicki, P. P. (2006). Antiplasticization of cereal-based products by water. Part II: Breakfast cereals. *Journal of Food Engineering,* **77,** 644-652.

Guillard, V., Broyart, B., Bonazzi, C., Guilbert, S. & Gontard, N. (2003a). Evolution of Moisture Distribution During Storage in a Composite Food Modelling and Simulation. *Journal of Food Science,* **68,** 958-966.

Guillard, V., Broyart, B., Bonazzi, C., Guilbert, S. & Gontard, N. (2003b). Modelling of Moisture Transfer in a Composite Food: Dynamic Water Properties in an Intermediate aw Porous

Product in Contact with High aw Filling. *Chemical Engineering Research and Design,* **81,** 1090-1098.

Guillard, V., Broyart, B., Guilbert, S., Bonazzi, C. & Gontard, N. (2004). Moisture diffusivity and transfer modelling in dry biscuit. *Journal of Food Engineering,* **64,** 81-87.

Harley, S. J., Glascoe, E. A. & Maxwell, R. S. (2012). Thermodynamic Study on Dynamic Water Vapor Sorption in Sylgard-184. *The Journal of Physical Chemistry B,* **116,** 14183-14190.

Harris, J. L., Schwartz, M. B., Ustjanauskas, A., Ohri-Vachaspati, P. & Brownell, K. D. (2011). Effects of Serving High-Sugar Cereals on Children's Breakfast-Eating Behavior. *Pediatrics,* **127,** 71-76.

Kalichevsky, M. T., Blanshard, J. M. V. & Tokargzuk, P. F. (1993). Effect of water content and sugars on the glass transition of casein and sodium caseinate. *International Journal of Food Science & Technology,* **28,** 139-151.

Karathanos, V. T., Villalobos, G. & Saravacos, G. D. (1990). Comparison of Two Methods of Estimation of the Effective Moisture Diffusivity from Drying Data. *Journal of Food Science,* **55,** 218-223.

Kou, Y., Dickinson, L. C. & Chinachoti, P. (2000). Mobility Characterization of Waxy Corn Starch Using Wide-Line 1H Nuclear Magnetic Resonance. *Journal of Agricultural and Food Chemistry,* **48,** 5489-5495.

Labuza, T. P. & Hyman, C. R. (1998). Moisture migration and control in multi-domain foods. *Trends in Food Science & Technology,* **9,** 47-55.

Lagorce-Tachon, A., Karbowiak, T., Loupiac, C., Gaudry, A., Ott, F., Alba-Simionesco, C., Gougeon, R. D., Alcantara, V., Mannes, D., Kaestner, A., Lehmann, E. & Bellat, J.-P. (2015). The cork viewed from the inside. *Journal of Food Engineering,* **149,** 214-221.

Lewicki, P. P., Jakubczyk, E., Marzec, A., Cabral, M. C. & Pereira, P. M. (2004). Effect of water activity on mechanical properties of dry cereal products. **4,** 381-391.

Lopez-Rubio, A., Flanagan, B. M., Shrestha, A. K., Gidley, M. J. & Gilbert, E. P. (2008). Molecular Rearrangement Of Starch During In Vitro Digestion: Toward A Better Understanding Of Enzyme Resistant Starch Formation In Processed Starches. *Biomacromolecules,* **9,** 1951-1958.

Lourdin, D., Colonna, P., Brownsey, G. J., Noel, T. R. & Ring, S. G. (2002). Structural relaxation and physical ageing of starchy materials. *Carbohydrate Research,* **337,** 827-833.

Mahasukhonthachat, K., Sopade, P. A. & Gidley, M. J. (2010). Kinetics of starch digestion and functional properties of twin-screw extruded sorghum. *Journal of Cereal Science,* **51,** 392-401.

Marzec, A. & Lewicki, P. P. (2006). Antiplasticization of cereal-based products by water. Part I. Extruded flat bread. *Journal of Food Engineering,* **73,** 1-8.

Mezreb, K., Goullieux, A., Ralainirina, R. & Queneudec, M. (2006). Effect of sucrose on the textural properties of corn and wheat extrudates. *Carbohydrate Polymers,* **64,** 1-8.

Moraru, C. I., Lee, T. C., Karwe, M. V. & Kokini, J. L. (2002). Plasticizing and Antiplasticizing Effects of Water and Polyols on a Meat-Starch Extruded Matri. *Journal of Food Science,* **67,** 3396-3401.

Nicholls, R. J., Appelqvist, I. A. M., Davies, A. P., Ingman, S. J. & Lillford, P. J. (1995). Glass transitions and the fracture behaviour of gluten and starches within the glassy state. *Journal of Cereal Science,* **21,** 25-36.

Oksanen, C. A. & Zografi, G. (1990). The Relationship Between the Glass Transition Temperature and Water Vapor Absorption by Poly(vinylpyrrolidone). *Pharmaceutical Research,* **7,** 654-657.

Pereira, P. M. & Oliveira, J. C. (2000). Measurement of glass transition in native wheat flour by dynamic mechanical thermal analysis (DMTA). *International Journal of Food Science & Technology,* **35,** 183-192.

Philipp, C., Oey, I., Silcock, P., Beck, S. M. & Buckow, R. (2017). Impact of protein content on physical and microstructural properties of extruded rice starch-pea protein snacks. *Journal of Food Engineering,* **212,** 165-173.

Pittia, P. & Sacchetti, G. (2008). Antiplasticization effect of water in amorphous foods. A review. *Food Chemistry,* **106,** 1417-1427.

Pitts, K. F., Favaro, J., Austin, P. & Day, L. (2014). Co-effect of salt and sugar on extrusion processing, rheology, structure and fracture mechanical properties of wheat–corn blend. *Journal of Food Engineering,* **127,** 58-66.

Roca, E., Guillard, V., Guilbert, S. & Gontard, N. (2006). Moisture migration in a cereal composite food at high water activity: Effects of initial porosity and fat content. *Journal of Cereal Science,* **43,** 144-151.

Roos, Y. & Karel, M. (1991). Amorphous state and delayed ice formation in sucrose solutions. *International Journal of Food Science & Technology,* **26,** 553-566.

Roos, Y. H. (1995). Characterization of food polymers using state diagrams. *Journal of Food Engineering,* **24,** 339-360.

Roos, Y. H. (2003). Thermal analysis, state transitions and food quality. *Journal of Thermal Analysis and Calorimetry,* **71,** 197-203.

Roos, Y. H., Roininen, K., Jouppila, K. & Tuorila, H. (1998). Glass transition and water plasticization effects on crispness of a snack food extrudate. *International Journal of Food Properties,* **1,** 163-180.

Roudaut, G., Dacremont, C. & Meste, M. L. (1998). Influence of water on the crispness of cereals-based foods: Acoustic, Mechanical, and sensory studies. *Journal of Texture Studies,* **29,** 199-213.

Roudaut, G., Farhat, I., Poirier-Brulez, F. & Champion, D. (2009). Influence of water, temperature and sucrose on dynamics in glassy starch-based products studied by low field 1H NMR. *Carbohydrate Polymers,* **77,** 489-495.

Roudaut, G., Maglione, M., Van Dusschoten, D. & Le Meste, M. (1999). Molecular Mobility in Glassy Bread: A Multispectroscopy Approach. *Cereal Chemistry Journal,* **76,** 70-77.

Roudaut, G. & Wallecan, J. (2015). New insights on the thermal analysis of low moisture composite foods. *Carbohydrate Polymers,* **115,** 10-15.

Scussat, S., Ott, F., Hélary, A., Desert, S., Cayot, P. & Loupiac, C. (2016). Neutron Imaging of Meat during Cooking. *Food Biophysics,* **11,** 207-212.

Shogren, R. L. (1992). Effect of moisture content on the melting and subsequent physical aging of cornstarch. *Carbohydrate Polymers,* **19,** 83-90.

Slade, L. & Levine, H. (1991). Beyond water activity: Recent advances based on an alternative approach to the assessment of food quality and safety. *Critical Reviews in Food Science and Nutrition,* **30,** 115-360.

Slade, L. & Levine, H. (1995). Water and the glass transition — Dependence of the glass transition on composition and chemical structure: Special implications for flour functionality in cookie baking. *Journal of Food Engineering,* **24,** 431-509.

Tanoi, K., Hamada, Y., Seyama, S., Saito, T., Iikura, H. & Nakanishi, T. M. (2009). Dehydration process of fish analyzed by neutron beam imaging. *Nuclear Instruments and Methods in Physics Research Section A: Accelerators, Spectrometers, Detectors and Associated Equipment,* **605,** 179-184.

Tedeschi, C., Leuenberger, B. & Ubbink, J. (2016). Amorphous–amorphous phase separation in hydrophobically-modified starch–sucrose blends I. Phase behavior and thermodynamic characterization. *Food Hydrocolloids,* **58,** 75-88.

Ubbink, J., Giardiello, M.-I. & Limbach, H.-J. (2007). Sorption of Water by Bidisperse Mixtures of Carbohydrates in Glassy and Rubbery States. *Biomacromolecules,* **8,** 2862-2873.

Van Nieuwenhuijzen, N. H., Meinders, M. B. J., Tromp, R. H., Hamer, R. J. & van Vliet, T. (2008). Water Uptake Mechanism in Crispy Bread Crust. *Journal of Agricultural and Food Chemistry,* **56,** 6439-6446.

Williams, P. G. (2014). The Benefits of Breakfast Cereal Consumption: A Systematic Review of the Evidence Base. *Advances in Nutrition,* **5,** 636S-673S.

Yang, J., Martin, A., Richardson, S. & Wu, C.-H. (2017). Microstructure investigation and its effects on moisture sorption in fried potato chips. *Journal of Food Engineering,* **214,** 117-128.

Yuan, X., Carter, B. P. & Schmidt, S. J. (2011). Determining the Critical Relative Humidity at which the Glassy to Rubbery Transition Occurs in Polydextrose Using an Automatic Water Vapor Sorption Instrument. *Journal of Food Science,* **76,** 78-89.

Chapter 2:

Macromolecular changes in extruded cereal based-products plasticized with sucrose and water.

Supuksorn Masavang, Gaëlle Roudaut, Dominique Champion*
Université Bourgogne Franche-Comté, AgroSup Dijon, UMR PAM, 1 Esplanade Erasme, 21000 Dijon, France

*Corresponding author: Dominique Champion
Tel: (+33) 038 0774055
E-mail address: dominique.champion@agrosupdijon.fr

Abstract

The effect of sucrose content (0–20%), and of water amount (10–15%) used during extrusion process using co-rotating twin screw extruder, on macrostructure of expanded cereal-based extrudates were studied. An increase in feed water contents resulted in lower specific mechanical energy (SME), die pressure, expansion ratio and water solubility index (WSI), water absorption index (WAI) and higher bulk density. Higher sucrose levels led to increased values of WSI and to reduced values of SME, bulk density and WAI, the large molecules of extrudates were less degraded as sucrose content increased, while expectedly more degraded than their native starch counterparts. HPSEC of extrudates showed less extensive degradation of amylopectin fraction with increasing sucrose contents. However, HPSEC did not show obvious effects of sucrose content on starch molecules when extruded at the highest feed water.

Keywords: Expanded extrudate, Sucrose, Water, Extrusion, Viscosity, Molecular size distribution

1. **Introduction**

Breakfast cereal based-products have currently become an important source of energy in human nutrition, since their high carbohydrate, bran, mineral and vitamins content, together with a low fat amount, makes them suitable for a healthy breakfast (Bertrais *et al,.* 2000). Extrusion technology has been extensively applied to produce many novel starch- or protein-based foods. During twin-screw extrusion, the powdered ingredient mixture and feed water are introduced into the heated screw barrel of the extruder, heated, transported, compressed by the rotating screw, and pumped through the die at high temperature and pressure. The combination of shearing, temperature, hydration and pressure creates many opportunities for molecular changes such as starch gelatinization, protein denaturation , enzyme (in)activation and color changes (Wen *et al,.* 1990), and the product extent of which depend on the conditions of extrusion (temperature, initial moisture content, and screw speed) (Martínez *et al,.* 2014a). Extrusion cooking also changes the extent of molecular associations between components, e.g. the amylose-lipid complex and starch conversion which is dependent on the treatment intensity and feed composition(Fan *et al,.* 1996b, Martínez *et al,.* 2014a, Martínez *et al,.* 2014b, Sun *et al,.* 2014). Those changes at the constituents' level modify the rheological behavior of flour (Hagenimana *et al,.* 2006).

Water is an essential reaction partner in gelatinization and plays one of the major roles in controlling extrudate attributes. Water addition is required for proper extrusion, improving blend flow, hydration of macromolecules (starch, gluten) and viscosity development, and extrudate cellular formation. When producing extruded snack products, there are many variables affecting the characteristics of the final product. Among these variables, however, feed water is one of the most important aspects in manipulating the physical characteristics of extruded products because it can substantially influence the temperature of melt, viscosity, and shear stress experienced by the material inside the extrusion barrel (Sumargo *et al,.* 2016). Different levels of water during extrusion have been studied on corn starch (Barrett *et al,.* 1995, Thymi *et al,.* 2005, Stojceska *et al,.* 2009), wheat flour rice and pea grits (Singh *et al,.* (2007), and on regular and waxy barley flours (Baik *et al,.* (2004). They found

that higher water feed level during extrusion decreased the radial expansion (Singh *et al,.* 2007),volumetric expansion (Ryu *et al,.* 1993a), the mean cell size, and the fracturability of extrudates (Barrett *et al,.* 1995) whereas it increased bulk density and hardness of extrudates. After extrusion, water absorption index increased with a more pronounced effect when extruded with low feed water (Fan *et al,.* 1996a, McPherson *et al,.* 2000). Extrusion conditions showed large effects on the molecular weight of the extruded starches. Indeed increasing feed water content reduced both the specific mechanical energy (Barrett *et al,.* 1995) and resulting amylopectin degradation (McPherson and Jane 2000). A question of interest is whether the same general behavior is found for extruded samples with different sucrose content.

Sugars are the second major component, after flour, in the formulation of pre-sweetened cereals. In directly expanded products, the total concentration of sugar can be added during extrusion up to 50% by weight (Hsieh *et al,.* 1990). Sugars are added to ready to eat cereals principally for taste. However, sugars also contribute to the color, structure, and texture of extruded products. The effects of sugar on extrusion processing and extrudate quality parameters have been investigated extensively. The addition of sugars increases product density and result in a reduction in expansion and pore size of corn or wheat based products (Moore *et al,.* 1990, Ryu *et al,.* 1993a, Sopade and Le Grys 1991, Jin *et al,.* 1994, Barrett *et al,.* 1995). As a consequence, it also affects the mechanical fracture properties of extrudates and their sensory properties. Mezreb *et al,.* (2006) revealed that the internal structure of the extrudates evaluated by image analysis showed a reduction of cell size with the sucrose addition in corn and wheat extrudates. This resulted in a reduction in overall product expansion and the change in extrudates physical structure strongly influenced the fracturability characteristics and sensory texture. In addition, Pitts *et al,.* (2014) noticed that reducing salt and sucrose level of wheat-corn extrudates increased torque, die pressure and specific mechanical energy resulting in higher expansion of extrudate i.e. with a more porous structure. It is believed that the presence of sugar in the extrusion melt alters the viscosity and/or glass transition temperature (T_g) of starchy based materials, thus influences the processing temperature required to convert materials from glassy state to rubbery

molten flow, resulting in changes in the expansion properties (Chinnaswamy 1993). Many researchers have reported, a raise of starch gelatinization temperature and a resulting increase in viscosity. Moreover, the gelatinization phenomenon has been seen to increase with sugar concentration (Zhou *et al,.* 2011, Funami *et al,.* 2005, Mezreb *et al,.* 2006). Carvalho and Mitchell (2000) reported that, the viscosity peak generally associated with the swelling of highly converted (hydrolyzed into sugars) starch conversion at low sugar content was not seen in extrudates with 20% sugar, suggesting a lower degradation at high sugar content due to an increase in the temperature of the melt and thus a reduction in the mechanical energy. Carvalho and Mitchell (2001) suggested that starch conversion decreased with increasing sugar content. In this work, the response to added sucrose at different feed water content on the extrusion behavior are reported.

Sucrose and water synergistic effects on extrudates physical properties have been reported. Sucrose together with feed water were found to progressively facilitate corn extrudates collapse and reduce expansion (Sopade and Le Grys 1991). Barrett *et al,.* (1995) reported that for samples produced at 20% feed content, sucrose progressively reduced cell size and increased density, starting at 2% concentration. However, in samples produced at 15% feed water content, low levels of sucrose cause only negligible structural changes resulting in an increase in density and a reduction in mean cell size occur at sucrose contents of 8% or higher. The phenomenon is believed to be due to the co-solute effect of sugar to competing for water with starch. However, these results implied that for the lowest feed water, the synergistic effects were moderate and only obvious at the highest sucrose levels. By contrast, for the high extrusion moisture samples for which viscosity was already reduced by the higher hydration, the effect was comparatively more pronounced and obvious even from 2% sucrose levels. Similar effects of sucrose on the structure of wheat flour extrudates have been reported by Ryu *et al,.* (1993a) at 5 and 10% sucrose levels and 30% feed water. Ortiz *et al,.* (2010) also reported that water and sucrose content have a synergistic effect on cassava flour extrudates. The results indicated a decreased in SME and water solubility index (WSI), while water absorption index (WAI) and viscosities were more influenced by water content than sugar. The different effects of sugar indicated that this

plasticizer acted differently in determining the structure during extrusion depending on the sugar concentration and extrusion parameters. Both water and sucrose play an important role in the structure and final texture of an extruded product and may have a major effect on the consumer acceptability of the finished product.

The reactions in the extruder depend on a large number of machine variables and raw material parameters. The effects of the extrusion process on extrudates structures have been studied (Barrett *et al,.* 1995, Fan *et al,.* 1996a, Carvalho and Mitchell 2000, Stojceska *et al,.* 2009, Alam *et al,.* 2013, Yeung and Rein 2015, Alam *et al,.* 2016). The specific mechanical energy (SME) is responsible for fragmentation of starch molecules (Lai and Kokini 1991, Fan *et al,.* 1996b, Gropper *et al,.* 2002). As a result of the applied shear forces, amylopectin molecules are broken. This phenomenon has been attributed to the decrease in the shear forces applied to molecules (Davidson *et al,.* 1984).

The Rapid Visco Analyser (RVA) have been reported to directly measure the transformation of starch in products made by twin-screw extrusion (Becker *et al,.* 2001) and to provide a quick analytical tool for characterising extruded products due to their sensitivity to changes of processing parameters (Whalen *et al,.* 1997). Products extruded in different conditions have been reported to display different viscosity profiles: i) the higher the feed moisture content during extrusion the higher the viscosity at 25°C on the RVA analysis, d final starch viscosities, ii) the greater the extrusion temperature and the shear the lower the viscosities in the early stage (25 °C) of the RVA measurement (McPherson *et al,.* 2000). More detailed descriptions of starch breakdown during extrusion have evolved through the use of intrinsic viscosity, which can be correlated with molecular weight (Millard *et al,.* 1997). Viscosity by RVA depend very strongly on the dry matter concentration. Slight changes in the amount of water or sample may introduce error in the final viscosity. For this purpose, in this study, the sample suspension will be stirred at 25oC to disperse uniformly the sample and to remove sample lumps until reaching a constant viscosity, after which all the lumps will break down and fully dissolve into a homogeneous and viscous slurry.

The degradation of starch in extruders also revealed that the highly branched large polymer like amylopectin is more prone susceptible to breakdown during extrusion than the linear polymer, amylose (Della Valle *et al,.* 1996). As specific mechanical energy and resulting starch breakdown are usually affected more by the feed moisture content than by extruder temperature. It has often been seen that lower feed moisture leads to increased breakdown or dextrinization, which may be due to the higher melt viscosity associated with that hydration level (van den Einde *et al,.* 2004, van den Einde *et al,.* 2005). Amongst the popular common techniques for molecular studies, size exclusion chromatography (SEC) is also an efficient method for monitoring starch breakdown and from such studies, it has been concluded that amylopectin, is more affected than amylose by extrusion processing, likely due to amylopectin being unable to align in a high shear environment (Davidson *et al,.* 1984, Kowalski *et al,.* 2018). Additionally, size exclusion chromatography has shown that amylopectin tends to break apart towards the inner region of the molecule (Li *et al,.* 2014, Kowalski *et al,.* 2018, Liu *et al,.* 2010). This work explores the degradation mechanism of extrudate with various sucrose content, to see if the degradation process has any selectivity toward structural features of the polymer molecule and changes in the size distributions.

Although it is well documented that extrusion cooking can change the structure of starch at every level (from molecules to granules) it is of great interest to know the dissimilarities in physical properties of extrudate processed at various sucrose and feed water contents. The effect of sugars and water on the extrusion processing of starches has already been studied by some authors (Hsieh *et al,.* 1990, Ryu *et al,.* 1993a, Barrett *et al,.* 1995, Carvalho and Mitchell 2000, Mezreb *et al,.* 2006). In this study, the results of a comparison beween the effect of added sucrose on extrusion behaviour at different feed water (10 and 15%) are reported. In addition, the dispersion time during RVA measurement and a comparison of viscosities beween blend and extrudate will be discussed. Moreover, the HPSEC technique was used to study the molecular properties of extrudates after processing. The influence of SME and molecular degradation on the pasting properties, water

absorption index, and water solubility index of extrudates during extrusion process were analyzed for complex formulations of breakfast cereals models.

2. Experimental

2.1 Preparation of the extruded samples

Wheat flour, wheat starch, gluten, sucrose and salt (water content:14.4%, 12.5%, 7.4%, 0.39% and 0.22% based on dry basis, respectively); of commercial grade were supplied by ADM CHAMTOR (Les Sohettes, France) or bought in local supermarket (salt and sucrose). The ingredient blends contained 0, 5, 10, 15, and 20% (w/w) sucrose with wheat flour (53-73%, w/w), wheat starch 16% w/w, gluten 16% w/w and salt 1% w/w. Their extrusion cooking was conducted on a Clextral BC-45 intermeshing twin-screws extruder with a 1.5 m long barrel using 10 and 15 % w/w initial moisture contents. The barrel heating zones were at 80 °C, 130 °C and 160 °C (±2 °C), and a 6.0 mm circular die was fitted to the end of the barrel. The screw speed was 150 rpm. The solid feed rate was 34 and 36 kg/ h, and water was added 6 and 4 l/h, resulting in a water content of ~10 and 15% wb in the final extruded samples, respectively. After removal of the die, samples were allowed to cool down to ambient temperature on a conveyer belt and were finally dried at 105 °C for 5 minutes to bring the final product to a moisture content of approximately at 3-4 %. After cooling, samples were hermetically sealed inhermetic bags and stored at ambient temperature.

2.2 Bulk density

The piece density (D_e) was determined as the weight of extrudate (W_e) divided by the equivalent volume of solid foam (V_e). The volume (V_e) was determined by substituting rapeseed weight (W_r) for extrudate volume and dividing it by rapeseed density (D_r); measurements were carried out 5 times and average were calculated (Eq. 2.1).

$$D_e = W_e \times \frac{D_r}{W_r} \qquad\qquad\qquad \text{Eq. 2.1}$$

2.3 Specific mechanical energy (SME)

The specific mechanical energy was calculated with Eq. 1.2 (Hu et al., 1993).

$$SME \ (kJ.kg^{-1}) = \frac{Screw\ speed\ (r.p.m) \times Motor\ power\ (kW) \times Torque\ (N.m)}{Max.screw\ speed\ (r.p.m) \times Throughout\ (kg.s^{-1}) \times 100} \qquad \text{Eq. 2.2}$$

2.4 Expansion

The cross-sectional expansion ratio (ER) was determined as the diameter of extrudates divided by the diameter of the die exit (6.0 mm). Each value was an average of 10 measurements measured just after extrusion (after leaving the die).

2.5 Rapid Viscosity Analysis (RVA)

The extruded samples were ground to a fine powder using an agate pestle and mortar. Moisture contents of the ground samples were determined by the air oven method of (AOAC 2005). A Rapid Viscosity Analyser (Model 3-CR, NewPort Scientific Pty. Ltd., Sydney, Australia) was used to measure the apparent viscosity of samples as a function of temperature. 2.5 g of ground sample (mass adjusted to have equivalent to 14% water on a dry basis for all powders) were added to 25 g of distilled water. A plastic paddle was inserted into the canister and it was rotated to disperse the material without any lumps. The sample temperature was equilibrated to 25 $^{\circ}$C for 110 min to stabilize the temperature and ensure maximum dissolution and powder dispersion, the sample was then heated to 55 $^{\circ}$C at 6 $^{\circ}$C/min subsequently held at 10 min at 55°C and then cooled to 25 $^{\circ}$C, at 6 $^{\circ}$C/min and held there for 30 min. Then, it was heated up to 95 $^{\circ}$C, at 6 $^{\circ}$C/min, held at that temperature for 5 min and then cooled down to 25 $^{\circ}$C at the same rate and held for 30 min (Fig. 2.5).

2.6 *Water absorption index (WAI) and water solubility index (WSI)*

The WAI and WSI were determined in triplicate according to the method described by (Anderson *et al,.* 1970) with modifications. Briefly, known weights (2.5 g) of sample powder were added to 30 mL of distilled water. The resulting slurries were then stirred for 3 hr. The suspension was

then centrifuged at 3000 g for 20 min (Thermo IEC model CL3-R, Waltham, MA USA). The supernatant was decanted into an aluminum dish of known weight and the sample dried at 105 °C until constant mass of dried matter. The remaining sediment in centrifuge tube was weighed and the WAI calculated (Eq. 2.3).

$$WAI \; (g/g) = \frac{Weight \; of \; sediment}{Weight \; of \; dry \; solid}$$
Eq. 2.3

The weight of solids in the supernatant was used to calculate the WSI as a percentage of dry weight of extrudate (Eq. 2.4).

$$WSI \; (\%) = \frac{Dry \; weight \; of \; dissolved \; solids \; in \; supernatant}{Weight \; of \; dry \; solids} \times 100$$
Eq. 2.4

2.7 High-performance size exclusion chromatography (HPSEC)

The sample (1 g) was first dissolved in 95% dimethylsulphoxide (DMSO) (20 mL) with magnetic stirring for 3 days at room temperature. The sample was then precipitated with 60 mL of pure ethanol and stored overnight at 4 °C. The precipitate was filtered over a glass filter and washed successively with acetone (10 mL) and diethylether (10 mL). The precipitate was air-dried under a hood for few hours to eliminate the solvents, and finally dried in oven at 45 °C for 18–20 h. An aliquot of dried sample (150 mg) was solubilized in 20 mL deionized water and stirred with a magnetic stirrer in a boiling water for 30 min. Solutions were cooled down in ice bath for 30 min and then centrifuged at 12,000 g for 20 min at 15 °C. The supernatant solution was filtered using a 0.5 μm syringe filter. The filtrate was injected (100 mL) in an HPSEC system (LaChrom Elite HPLC Systems (Hitachi High Technologies Co., Tokyo, Japan)). The system consisted of a Hitachi pump L-2130 and a differential refractive index detector (Model Spectra SYSTEM RI-150, Thermo Separation Products). The size-exclusion system comprised a TSK gel G5000-PWXL size-exclusion analytical column (7.8 x 300 mm (Tosoh, Japan) HPSEC columns connected and kept at 20 °C. The mobile phase was Millipore water passed through the system at a flow rate of 0.7 mL/min. A deconvolution technique developed to find the peak function using OriginPro 2017 (OriginLab, Northamton, USA), typically a Bi-Gaussian was

applied to convert the SEC data in terms of elution time. The relative percentages of amylopectin and amylose were obtained as the areas under the first and second deconvoluted curves, respectively.

Results and discussion

3.1 Specific mechanical energy (SME) and die pressure

Specific mechanical energy (SME) values may be defined as the energy input transmitted to the material being extruded by the screws, which characterizes the extruder operations and is often correlated to product quality, this can be also correlated to the degradation of starch in the system. Indeed, SME value indicates the extent of molecule breakdown or degradation that mechanical force undergoes during extrusion process, so this value is an important parameter influencing final product characteristics such as solubility, expansion index, etc. (Carvalho and Mitchell 2000, Zhu *et al,.* 2010). When blend mixtures were extruded with low feed water content, extruded samples exhibited higher SME than samples with a higher feed water (Fig. 2.1a).Increased feed water content resulted in an heat transfer increase from the extruder to the feed material and consequently decreased viscosity, shear, and friction during extrusion. In fact, the higher water content, the lowered both torque and SME because of the reduction of force required to push wet mass through the die strictly linked to water plasticizing effect (Chen *et al,.* 2010).

As it can be seen in Fig. 2.1a, the incorporation of sucrose above 10% induced lower SME values compared to those for samples without sugar, presumably due to a torque decrease with increasing sugar content. Previous studies also showed that addition of sugar content in a wheat-corn flour blend caused a significant decrease in both die pressure and torque (Barrett *et al,.* 1995, Pitts *et al,.* 2014). In the present work, the SME values for 15% feed water batches are substantially lower than those for the 10% feed water batch. The effect on both SME and die pressure of increasing sucrose content is much less apparent, in the higher moisture samples (Fig. 2.1a, b), probably because the so high level of hydration in extruder gives a too low viscosity than it is not possible to identify the sucrose effect

on it. Ortiz *et al,.* (2010) reported also that water content is more effective in reducing SME, hence water, dissipates more energy than sugar.(Ryu *et al,.* 1993a, Barrett *et al,.* 1995).

SME is usually directly related to the expansion of extrudates: high SME inducing highly expanded extrudates. High values of SME were also measured by other authors (Carvalho and Mitchell 2001, Bindzus *et al,.* 2002, Pitts *et al,.* 2014, Pitts *et al,.* 2016) for extrusion of maize and wheat starches under low water content condition and the effects of sugar addition on SME were also found to decrease in die pressure (Fig. 2.1b) and expansion on maize and wheat starches (Carvalho and Mitchell 2000), and for sucrose and fructose (up to 20%) on maize grits (Fan *et al,.* 1996a).

3.2 Extrudate expansion and bulk density

Increasing feed water from 10 to 15% decreased the product diameter and cross-sectional expansion ratio (ER) and thus increased the bulk density of the extrudates. (Fig. 2.2a-c). Lower SME leads to lower melt temperature at the die and thus a lower driving force for expansion. At both feed water levels, the highest bulk density and the lowest expansion ratio were observed at 20% sucrose content. Bulk density of extrudates decreased as sucrose level increased, while the bulk density for samples extruded at 15% water showed no significant trend between 0 and 20% sucrose content, probably because of the high level of density reached for this product. Jin et al. (1994) also observed increased bulk density and decreased both axial and radial expansions with addition of sucrose. Lower driving force (SME) together with a greater collapse due to the plasticizing effect of sucrose (Sopade and Le Grys 1991) were probably the primary factors responsible for decrease in expansion with increase in sucrose level.

The expansion of extruded cereals or starch-based materials is dependent on the degree of gelatinization, which in turn was determined by processing temperature, shear rate, and moisture contents of the feed material (Guy and Horne 1988). The presence of sugar and salt is know to increase gelatinization temperature because they tend to reduce the availability of water for all ingredient hydration (Moore *et al,.* 1990), sugar and/or salt molecules may absorb more water from the corn

meal than starch does. Mezreb *et al,.* (2006) reported that a sugar content increase would effectively cause competition for the limited moisture available in the system for gelatinization. This inhibitory effect of sugars on starch gelatinization has been attributed to the decreased in the water activity values thereby impeding the penetration of water into the granule (Beleia *et al,.* 1996). Spies and Hoseney (1982) suggested that sugar molecules interact with the amorphous regions of starch into granules through the formation of bridges between sugar molecules and starch chains. Thus, more energy was required to melt the starch granules. Moreover, Hirashima *et al,.* (2005) observed that a lower content of sugar enchanced the swelling of starch granules.

Similarly, increasing the feed water resulted in decreased expansion ratio (Fig. 2.2b). Launay and Lisch (1983) proposed that the longitudinal and sectional expansions are dependent on the melt vicosity and elasticity. The increased temperature due to the decreasing feed water would yield a lower melt viscosity and increased longitudinal expansion, and cause a decrease in sectional expansion. The presence of sucrose inhibits the ability of the extrudates to expand and/or facilitates collapse of the structure after expansion, possibly by reducing melt viscosity and elasticity (Barrett *et al,.* 1995). The impact of sucrose addition on specific lenght, SL (length of sample divide by weight of sample) was not significant, while more showed higher SL when samples extruadte at higher feed water (data not show). The sectional indices decreased with the addition of sucrose, thereby leading to a less expanded product. Mezreb *et al,.* (2006) and Fan *et al,.* (1996a) suggested that a drop in expansion could be considered as a consequence of the decrease in the melt glass transition temperature with sucrose addition. However, sucrose addition did not affect the SL of extrudate processed at 15% feed water. The high feed water content may have reduced both the viscosity and the melt temperature resulting in low SME, consequently the feed material got insufficiently sheared and a irregular shape of extrudate was observed. This may have affected the determination of the samples dimentsions (e.g. SL)

The effect of sucrose on the bulk density of extrudates produced at 15% extrusion water was more scattered than that of extrudates produced at 10% (Fig. 2.2c). However, the slope of the linear

reagression are probably similar. The density determination of extrudate colud be affected due to the difficulty with accurated dimensions measuring of the irregularly shaped samples containing sucrose for extrudates produced at 15% sucrose. The effects of sucrose and feed water content on the shape of extrudates are visible on the photographs of extrudates containing various sucrose levels and obtained under different feed water (10% and 15%) shown in Fig. 2.3. The extrudates processed at 15% feed water and with 0 and 5% sucrose had the form of a straight rod-like thread, while the extrudates with 10, 15 and 20% sucrose had a rod-like cross section twisted into the form of a spiral. The most striking observation was that, depending on processing water level, the aspect of extrudates changed from a smooth cylinder at 10% feed water to a twisted, screw marked cylinder at 15% (especially from 10% sucrose). When sucrose increased from 0 to 20% for a 10% feed water, expansion decreased as reflected in the diameter decrease. The occurrence of irregularly shaped extrudates has been associated with situations where the processing temperatures were low, or the feed material insufficiently sheared or where there was little filler or processing aid present. In addition, Lue *et al,.* (1991) reported regular, ridged surface distortion (sharkskin) in corn meal extrudates with 30% fiber and extruded at a screw speed of 300 rpm. They suggested that this phenomenon depended primarily on either the linear extrusion speed or temperature. El Kissi *et al,.* (1997) explained that the roughness or sharkskin appears due to the relaxation of tensile stress downstream of the exit section. Indeed, during the formation of cracks, the melt sticks against the wall, forming a ring where it leaves the die. As the ring develops, the melt continues to flow, producing a screated rod that produces a rough surface with the appearance of sharkskin.

The results also showed that the higher the SME, the lower the bulk density (Fig. 2.2c). The release of evaporating water and the cooling of the resulting porous starch matrix led to the expansion of starch when it came out of the extruder die into the atmosphere. Indeed when the sample exits the die, the pressure drops to atmospheric pressure, which leads to a sudden expansion of the sample due to the release of water vapour. Water vapour expansion causes bubbles to grow and the viscosity of the bubble wall becomes a major factor in the final size of the gas cells. Low viscosity of the bubble

wall allows greater bubble growth but the resulting structure can collapse if hygroscopic properties of ingredients delay the dehydration of the matrix which collaspes before drying. Viscosities will be a function of the molecular size and shape of the polymers. If the water vapour is no longer inflating the bubbles; then the bubbles may collapse if their walls are not sufficiently rigid (as exemple for the samples with higher moisture content). This viscosity will depend on temperature, particularly in the region of the glass transition temperature. If the walls are still in the rubbery state then bubble collapse is likely to happen (Majzoobi and Farahnaky 2010). Just after the die, there are kinetics effects between expansion due to water evaporation under pressure differential and vitrification due to a fast drying of the matrix.

3.3 Water absorption index (WAI) and water solubility index (WSI)

WSI and WAI are two important measurements of physico-chemical changes in starch as a result of extrusion processing (Fig. 2.4). The water solubility index of wheat flour, wheat starch, and extrudates took into account starch and soluble component. Both indices increased with SME (data not shown). Shear energies are known to increase the breakdown of both starch granules and macromolecules and subsequentely the starch granules absorbed water at room temperature and swelled much more than flour and natives ones, causing an increase in viscosity (7.48 and 0.62%, respectively). Silva *et al,.* (2009) suggested that the starch granules should undergo a certain degree of conversion to initiate water absorption. Native starch can only absorb a minimum amount of water (Guha *et al,.* 1997). Higher WAI indicates the presence of larger granule fragments, while higher WSI implies that starch was depolymerized (Kristiawan *et al,.* 2018, de Mesa *et al,.* 2009).

High WAI is an vitro indicator of good starch digestibility as it implies the extent of gelatinization and dextrinization (Guha *et al,.* 1997). The WAI measures the amout of water absorbed by starch and can be used as an index of gelatinization (Anderson *et al,.* 1970, Kirby *et al,.* 1988). It may be expected that as the the starch granule structure is disrupted, more water gets bound to the starch molecule resulting in higher WAI values (Ding *et al,.* 2006), which explains that WAI increased

with feed water increase and sucrose content decrease (Hagenimana *et al,.* 2006). WAI depends on the availability of hydrophilic groups and on the capacity of gel formation of the macromolecule (Gomez and Aguilera 1983).Regardless of the sucrose level in the mix, the WAI showed a reduction in this parameter value with a sucrose content increase, which extrudates may decrease their capacity to form a gel with an increasing of sucrose content. Mezreb *et al,.* (2006) and Sopade and Le Grys (1991) WAI decreased with an increase in sucrose content for maize extudates showed, indicating that the presence of sucrose could have reduced any detrimental effect on water binding sites of the gelatinized starch and inhibited degradation of starch molecules bringing about higher WAI.

WSI, often used as an indicator of degradation of molecular components, slightly increaseed with increasing sucrose content (Fig. 2.4b). The quantity of water-soluble fractions in extruded samples increased with sucrose content due to the higher amount of sucrose in the sample and decreased with feed water probably due to a lower macromolecule degradation. An increase in WSI was observed with decreasing amounts of water, which is consistent with the result reported by Ding *et al,.* (2005) and Silva *et al,.* (2009). Extrusion at low water contents would cause an increase in the amount of water soluble molecules.

3.4 Viscosity of blends and resuspended extrudates

Native flour and blend before extrusion demonstrated a typical RVA profile, showing a peak viscosity during heating at 95 °C, but this peak was not observed at 55 °C heating phase because the temperature was too low for gelatinization (Fig. 2.5 and 2.6). It was noticed that blends took both a longer pasting time and higher temperature to swell and gelatinize the starch granules than the native flour did. Native starch granules are insoluble in water due to the strong hydrogen bonds holding the starch polymers together; but, when the aqueous suspension is heated, the granules begin to swell when sufficient heat energy is present to overcome the hydrogen-bonding forces. Viscosity shows a maximum corresponding to both granule swelling and burst, making amylose and amylopectin soluble. The increase in viscosity during cooling is induced by temperature effect and the rearrangement of

leached out amylose, which then forms a thin amylose gel layer (Jane et al., 1999) as well interactions in this new organisation between lipids, protein and complex carbohydrates (Kaur *et al,.* 2009, Jane *et al,.* 1999).

In order to further understand the effect of sucrose and extrusion water on material behaviour and melt rheology of wheat flour blends, the dry samples extruded with 10% sucrose were grounded and resuspended. Extrusion processing usually involves breakdown of the starch granules and interactions with the other ingredients of the blend such as here: protein, sucrose. Rapid Visco Analyser (RVA) can monitor the degree of gelatinization for blend with native starch but also viscosity evolution as a function of temperature treatment for extruded products (Ryu *et al,.* 1993b, Zhu *et al,.* 2016, Guo *et al,.* 2018). Starch gelatinization is a process of breaking down the starch intermolecular bonds in the presence of water and heat, allowing the hydrogen bonding sites to engage more water. It corresponds both to the melting of the crystalline parts of native starch granules, and the glass transition of the amorphous ones: gelatinization of starch makes amylose and amylopectine soluble in water at 'high" temperature. The viscosity of a blend depends to a large extent on the degree of gelatinization of the starch granules (Carvalho *et al,.* 2010). RVA profiles (Fig. 2.5) of grounded sample with 10% sucrose extruded at 10% feed water were studied at 25°C during 110 min in order to obtain a stable viscosity: it correponds to the particle swelling and dissolution of all soluble components. A temperature treatment at 55°C was carried out to help for extrudates complete dispersion and/or dissolution.

Compared with that of native wheat flour and native (before extrusion) blend with 10% sucrose (Fig. 2.5) the initial viscosity of extrudates was much higher than that of native flour and blends because extruded samples were already gelatinized in extruder and an another temperature treatment at 95°C in RVA did not change the measured viscosity at 25°C, showing a full melting of starch during the extrusion process. However, the viscosity after the 95°C treatment was much lower for powders from extrudates than for native flour and blends powder: this clearly suggests that the extrusion process caused macromolecule disruption. When extruded samples were processed with 15% water,

the dissolution/dispersion phenomena in RVA can, be more difficult due to the higher density of the products : it appears more difficult to have a stable viscosity and this viscosity is higher than for samples processed with 10% water: 1.67 Pa.s for the sample containing 10% sucrose processed with 10% feed water against 2.74 Pa.s for the one processed with 15% water after a temperature treatment at 55°C helping for dispersion/dissolution. It is important to notice that only the temperature treatment done at 95°C induced a decrease of viscosty for 15% feed water samples, giving viscosity values in the same order of magnitude as samples proceeded with 10% water (Fig 2.6 and Table. 2.1). A higher amount of water during the process appears to induce less macromolecular disruption: either starch is not fully gelatinized and amylopectin and amylose were not well dispersed or protein molecules were not fully denaturated.

RVA plots of extrudates with various sucrose levels and extruded at 10% and 15% feed water (Fig. 2.6a, b respectively) show a decrease in viscosity with an increase in sucrose content. In fact, a higher amount of damaged starch, resulting from increased shearing forces (higher SME) is observed with lower plasticization during extrusion (Whalen *et al,.* 1997, Ortiz *et al,.* 2010). The lowest viscosities values for extrudate containing 20% sucrose at both 10% and 15% feed water content (Fig. 2.6) seemed to have a direct and inverse relationship to SME values.

Due to low feed water content, starch were likely gelatinied to a greater extent and the resistance against the flow could increase with generating more shearing forces. Thus the starch molecules could be depolymerized due to the effect of mechanical shearing forces along with degradative effect temperature (Fallahi *et al,.* 2016). It has been well documented that lower viscosity values for extruded starch are influnced by molecular degradation which occurs during extrusion (Ozcan and Jackson 2005). Blanche and Sun (2004) also observed that higher feed water and lower screw speed each caused an increase in the viscosity values of corn starch extrudates due to the presence of starch granules remaining ungelatinized upon extrusion cooking.

3.5 HPSEC of extrudate

Based on the previously described results, it was hypothesised that molecular degradation occurred through extrusion. The extrudates were analysed with HPSEC for their molecular sizes distribution and relative percentage changes of large and small macromolecules along with native wheat starch as a reference. HPSEC profiles (Fig. 2.7) provide insight into this phenomenon since elution time is related to the molecular weight. The extruded samples and native wheat starch showed two peaks. The first one around 7.5-10.5 min was associated with large molecules and the second one around 10.5-16.0 min elution time is associated with small molecules. The peaks were better individualised for native starch than for the extrudates for which the second peak became wider, in agreement with previous works (Wen *et al,.* 1990, McPherson and Jane 2000, Van Lengerich 1990). In addition, the first and main peak was slightly shifted towards higher elution times for extrudates. Indeed, extrusion of starch caused the degradation of amylopectin molecules, most probably through the cleavage of outer linear chains, resulting in a broadening of the second peak, reflecting increased amylose-like fractions (Chinnaswamy and Hanna 1990, Chinnaswamy and Hanna 1991, Pushpadass *et al,.* 2009).

Extrusion of blends at 10% feed water and addition of sucrose increased the intensity for large molecule fraction and elution volume range slightly shifted to lower values, probably due to a lower degradation in presence of sucrose. Indeed maximum starch degradation occurred for extruded sample without sucrose (Fig. 1.8). Starch depolymerization upon extrusion has been shown before, for cereals starches (Della Valle *et al,.* 1995, McPherson and Jane 2000, McPherson *et al,.* 2000), but the extent of degradation for extrudates with various sucrose content have rarely been reported and it seems that sucrose addition seem to limits the starch degradation (Fig. 2.8).

For extruded samples, the small and large molecule regions overlapped, and thus normalization was done to set the integral of the curve equal to unity to follow any change in the distribution of elution time upon process. For extruded sample produced at 10% feed water, a

reductions in the relative percentages of large molecules was accompanied by a corresponding increase in small molecules (Fig. 2.8), while there was no obvious difference for extrudates produced at 15% water. The relative percentages of large and small molecules in native starch were 54 and 46%, respectively, which changed in extrudates with various sucrose content to 38-56.2% and 43.7-62.2%, respectively, in the extrudates. Compared to native starch, the longer elution times of the small molecule fraction in extruded samples implied that the degraded large molecules fraction, then resembling that of smaller molecules, might have eluted along with the amylose fraction. In addition, Van Lengerich (1990) suggested that glycosidic bonds between glucose units in starch molecules were broken by the extrusion process. In particular, amylopectin molecules could be affected by this molecular depolymerization, while breakdown of amylose molecules is either negligibly small or would not take place during wheat molecules extrusion. Amylopectin depolymerised into both large and small fragments. The larger fragments were intermediate in size between amylopectin and amylose. However, the smaller fragments were the same or nearly the same size as the amylose molecules and thus caused an increase in the amylose peak. Percentage of amylose and amylopectin which corresponds to small and large molecules in native wheat starch using HPSEC and extracted by KOH-urea solution reported by Grant *et al,*. (2002), showing the amounts of amylose and amylopectin are 23-27% and 73-77%, respectively while the percentage of small and large molecules for the extrudates of the present study are different from these amounts, possibly due to the presence of residaul protein in the extracted and injected samples. Sample prepration and extraction sould be taken into account before performing HPSEC measurements. The extent of fragmentation in the large and small molecules did not show obvious the effects of feed water. Therefore, the different effects of moisture and sucrose indicated that these plasticizers acted differently in determining the fragmentation of starch molecules during extrusion processing. In addition, more detailed knowledge of macromolecular branching structure and degradation chemistry needs to be understood in explaining the degradation processes.

4. Conclusion

The properties of extrudates depend on sucrose content in blend and feed water during extrusion. Increasing the sucrose and feed water contents decreased the SME input, die pressure, product diameter, expansion index, specific length, hence reduced starch degradation in the extruder. However, the bulk density increased as the sucrose content increased for samples extruded at 10% feed water, while no obvious difference was shown for samples extruded at 15% feed water, probably due to the proeminent effect of water amount during shearing. The SME, expansion ratio, viscosities of extrudates decreased with increasing sucrose content. Higher feed water contents decreased the melt viscosity, and then the expansion ratio of the extrudates, resulting in a higher density. HPSEC showed that both amylopectin and amylose macromolecules were fragmented during extrusion, resulting in reductions in the relative percentages of amylopectin. However, this technique did not show obvious effects of sucrose content on starch molecules when extruded at high feed water. Our results demonstrated that specific mechanical energy plays a critical role in the degradation of starch in wheat flour in a twin-screw extruder. It was also shown that sucrose content and feed water acted as plasticizers and impacted molecular size distribution of extrudates. This knowledge can help manufacturers to better control process conditions within an extruder to yield products with predictable and consistent characteristics.

the facilities of the Jules Guyot Wine and Vine Institute, Université de Bourgogne sponsored by

Bourgogne Franche Comté region.

References

Alam, M. S., Kaur, J., Khaira, H. & Gupta, K. (2016). Extrusion and Extruded Products: Changes in Quality Attributes as Affected by Extrusion Process Parameters: A Review. *Critical Reviews in Food Science and Nutrition,* **56,** 445-473.

Alam, S. A., Järvinen, J., Kirjoranta, S., Jouppila, K., Poutanen, K. & Sozer, N. (2013). Influence of Particle Size Reduction on Structural and Mechanical Properties of Extruded Rye Bran. *Food and Bioprocess Technology,* **7,** 2121-2133.

Anderson, R. A., Conway, H. F. & Peplinski, A. J. (1970). Gelatinization of Corn Grits by Roll Cooking, Extrusion Cooking and Steaming. *Starch - Stärke,* **22,** 130-135.

AOAC (2005). Official Methods of Analysis. 18th edn. Association of Official Analytical Chemists. *Arlington, VA, USA*.

Baik, B.-K., Powers, J. & Nguyen, L. T. (2004). Extrusion of Regular and Waxy Barley Flours for Production of Expanded Cereals. *Cereal Chemistry,* **81,** 94-99.

Barrett, A., Kaletunç, G., Rosenburg, S. & Breslauer, K. (1995). Effect of sucrose on the structure, mechanical strength and thermal properties of corn extrudates. *Carbohydrate Polymers,* **26,** 261-269.

Becker, A., Hill, S. E. & Mitchell, J. R. (2001). Relevance of Amylose-Lipid Complexes to the Behaviour of Thermally Processed Starches. *Starch - Stärke,* **53,** 121-130.

Beleia, A., Miller, R. A. & Hoseney, R. C. (1996). Starch Gelatinization in Sugar Solutions. *Starch - Stärke,* **48,** 259-262.

Bertrais, S., Polo Luque, M. L., Preziosi, P., Fieux, B., Torra de Flot, M., Galan, P. & Hercberg, S. (2000). Contribution of Ready-to-Eat Cereals to Nutrition Intakes in French Adults and Relations with Corpulence. *Annals of Nutrition and Metabolism,* **44,** 249-255.

Bindzus, W., Livings, S. J., Gloria-Hernandez, H., Fayard, G., van Lengerich, B. & Meuser, F. (2002). Glass Transition of Extruded Wheat, Corn and Rice Starch. *Starch - Stärke,* **54,** 393-400.

Blanche, S. & Sun, X. (2004). Physical characterization of starch extrudates as a function of melting transitions and extrusion conditions. *Advances in Polymer Technology,* **23,** 277-290.

Carvalho, C. W. P. & Mitchell, J. R. (2000). Effect of sugar on the extrusion of maize grits and wheat flour. *International Journal of Food Science & Technology,* **35,** 569-576.

Carvalho, C. W. P. & Mitchell, J. R. (2001). Effect of Sucrose on Starch Conversion and Glass Transition of Nonexpanded Maize and Wheat Extrudates. *Cereal Chemistry Journal,* **78,** 342-348.

Carvalho, C. W. P., Takeiti, C. Y., Onwulata, C. I. & Pordesimo, L. O. (2010). Relative effect of particle size on the physical properties of corn meal extrudates: Effect of particle size on the extrusion of corn meal. *Journal of Food Engineering,* **98,** 103-109.

Chen, F. L., Wei, Y. M., Zhang, B. & Ojokoh, A. O. (2010). System parameters and product properties response of soybean protein extruded at wide moisture range. *Journal of Food Engineering,* **96,** 208-213.

Chinnaswamy, R. (1993). Basis of cereal starch expansion. *Carbohydrate Polymers,* **21,** 157-167.

Chinnaswamy, R. & Hanna, M. A. (1990). Macromolecular and Functional Properties of Native and Extrusion-Cooked Corn Starch. *Cereal Chemistry,* **67,** 490-499.

Chinnaswamy, R. & Hanna, M. A. (1991). Physicochemical and Macromolecular Properties of Starch-Cellulose Fiber Extrudates. *Journal of Food Structure, 10,* 229-239.

Davidson, V. J., Paton, D., Diosady, L. L. & Rubin, L. J. (1984). A Model for Mechanical Degradation of Wheat Starch in a Single-Screw Extruder. *Journal of Food Science, 49,* 1154-1157.

de Mesa, N. J. E., Alavi, S., Singh, N., Shi, Y.-C., Dogan, H. & Sang, Y. (2009). Soy protein-fortified expanded extrudates: Baseline study using normal corn starch. *Journal of Food Engineering, 90,* 262-270.

Della Valle, G., Boché, Y., Colonna, P. & Vergnes, B. (1995). The extrusion behaviour of potato starch. *Carbohydrate Polymers, 28,* 255-264.

Della Valle, G., Colonna, P., Patria, A. & Vergnes, B. (1996). Influence of amylose content on the viscous behavior of low hydrated molten starches. *Journal of Rheology, 40,* 347-362.

Ding, Q.-B., Ainsworth, P., Plunkett, A., Tucker, G. & Marson, H. (2006). The effect of extrusion conditions on the functional and physical properties of wheat-based expanded snacks. *Journal of Food Engineering, 73,* 142-148.

Ding, Q.-B., Ainsworth, P., Tucker, G. & Marson, H. (2005). The effect of extrusion conditions on the physicochemical properties and sensory characteristics of rice-based expanded snacks. *Journal of Food Engineering, 66,* 283-289.

El Kissi, N., Piau, J. M. & Toussaint, F. (1997). Sharkskin and cracking of polymer melt extrudates. *Journal of Non-Newtonian Fluid Mechanics, 68,* 271-290.

Fallahi, P., Muthukumarappan, K. & Rosentrater, K. A. (2016). Functional and Structural Properties of Corn, Potato, and Cassava Starches as Affected by a Single-Screw Extruder. *International Journal of Food Properties, 19,* 768-788.

Fan, J., Mitchell, J. R. & Blanshard, J. M. V. (1996a). The effect of sugars on the extrusion of maize grits: I. The role of the glass transition in determining product density and shape. *International Journal of Food Science & Technology, 31,* 55-65.

Fan, J., Mitchell, J. R. & Blanshard, J. M. V. (1996b). The effect of sugars on the extrusion of maize grits: II. Starch conversion. *International Journal of Food Science & Technology, 31,* 67-76.

Funami, T., Kataoka, Y., Omoto, T., Goto, Y., Asai, I. & Nishinari, K. (2005). Effects of non-ionic polysaccharides on the gelatinization and retrogradation behavior of wheat starch☆. *Food Hydrocolloids, 19,* 1-13.

Gomez, M. H. & Aguilera, J. M. (1983). Changes in the starch fraction during extrusion-cooking of corn. *Journal of Food Science, 48,* 378-381.

Grant, L. A., Ostenson, A. M. & Rayas-Duarte, P. (2002). Determination of Amylose and Amylopectin of Wheat Starch Using High Performance Size-Exclusion Chromatography (HPSEC). *Cereal Chemistry, 79,* 771-773.

Gropper, M., Moraru, C. I. & Kokini, J. L. (2002). Effect of Specific Mechanical Energy on Properties of Extruded Protein-Starch Mixtures. *Cereal Chemistry, 79,* 429-433.

Guha, M., Ali, S. Z. & Bhattacharya, S. (1997). Twin-screw extrusion of rice flour without a die: Effect of barrel temperature and screw speed on extrusion and extrudate characteristics. *Journal of Food Engineering, 32,* 251-267.

Guo, P., Yu, J., Copeland, L., Wang, S. & Wang, S. (2018). Mechanisms of starch gelatinization during heating of wheat flour and its effect on in vitro starch digestibility. *Food Hydrocolloids, 82,* 370-378.

Guy, R. C. E. & Horne, A. W. (1988). Extrusion and Co-extrusion of Cereals. In: Blanshard, J.M.V., Mitchell, J.R. (Eds.), Food structure 1st Edition : Its creation and evaluation. *Butterworth-Heinemann, London, England*, 331-350.

Hagenimana, A., Ding, X. & Fang, T. (2006). Evaluation of rice flour modified by extrusion cooking. *Journal of Cereal Science, 43,* 38-46.

Hirashima, M., Takahashi, R. & Nishinari, K. (2005). Changes in the viscoelasticity of maize starch pastes by adding sucrose at different stages. *Food Hydrocolloids, 19,* 777-784.

Hsieh, F., Peng, I. C. & Huff, H. E. (1990). Effects of Salt, Sugar and Screw Speed on Processing and Product Variables of Corn Meal Extruded with a Twin-Screw Extruder. *Journal of Food Science, 55,* 224-227.

Jane, J., Chen, Y. Y., Lee, L. F., McPherson, A. E., Wong, K. S., Radosavljevic, M. & T., K. (1999). Effects of amylopectin branch chain length and amylose content on the gelatinization and pasting roperties of starch. *Cereal Chemistry, 76,* 629-637.

Jin, Z., Hsieh, F. & Huff, H. E. (1994). Extrusion Cooking of Corn Meal with Soy Fiber, Salt, and Sugar. *Cereal Chemistry, 71,* 227-234.

Kaur, S., Singh, N., Sodhi, N. S. & Rana, J. C. (2009). Diversity in properties of seed and flour of kidney bean germplasm. *Food Chemistry, 117,* 282-289.

Kirby, A. R., Ollett, A. L., Parker, R. & Smith, A. C. (1988). An experimental study of screw configuration effects in the twin-screw extrusion-cooking of maize grits. *Journal of Food Engineering, 8,* 247-272.

Kowalski, R. J., Hause, J. P., Joyner, H. & Ganjyal, G. M. (2018). Waxy flour degradation – Impact of screw geometry and specific mechanical energy in a co-rotating twin screw extruder. *Food Chemistry, 239,* 688-696.

Kristiawan, M., Micard, V., Maladira, P., Alchamieh, C., Maigret, J. E., Réguerre, A. L., Emin, M. A. & Della Valle, G. (2018). Multi-scale structural changes of starch and proteins during pea flour extrusion. *Food Research International, 108,* 203-215.

Lai, L. S. & Kokini, J. L. (1991). Physicochemical changes and rheological properties of starch during extrusion. (A review). *Biotechnology Progress, 7,* 251-266.

Launay, B. & Lisch, J. M. (1983). Twin-screw extrusion cooking of starches: Flow behaviour of starch pastes, expansion and mechanical properties of extrudates. *Journal of Food Engineering, 2,* 259-280.

Li, M., Hasjim, J., Xie, F., Halley, P. J. & Gilbert, R. G. (2014). Shear degradation of molecular, crystalline, and granular structures of starch during extrusion. *Starch - Stärke, 66,* 595-605.

Liu, W.-C., Halley, P. J. & Gilbert, R. G. (2010). Mechanism of Degradation of Starch, a Highly Branched Polymer, during Extrusion. *Macromolecules, 43,* 2855-2864.

Lue, S., Hsieh, F. & Huff, H. E. (1991). Extrusion Cooking of Corn Meal and Sugar Beet Fiber: Effects on Expansion Properties, Starch Gelatinization, and Dietary Fiber Content. *Cereal Chemistry, 68,* 227-234.

Majzoobi, M. & Farahnaky, A. (2010). Comparison of the effects of extrusion cooking on some cereal starches. *International Journal of Food Engineering, 6,* Article 2.

Martínez, M. M., Calviño, A., Rosell, C. M. & Gómez, M. (2014a). Effect of Different Extrusion Treatments and Particle Size Distribution on the Physicochemical Properties of Rice Flour. *Food and Bioprocess Technology, 7,* 2657-2665.

Martínez, M. M., Rosell, C. M. & Gómez, M. (2014b). Modification of wheat flour functionality and digestibility through different extrusion conditions. *Journal of Food Engineering,* **143,** 74-79.

McPherson, A. E., Bailey, T. B. & Jane, J. (2000). Extrusion of Cross-Linked Hydroxypropylated Corn Starches I. Pasting Properties. *Cereal Chemistry Journal,* **77,** 320-325.

McPherson, A. E. & Jane, J. (2000). Extrusion of Cross-Linked Hydroxypropylated Corn Starches II. Morphological and Molecular Characterization. *Cereal Chemistry Journal,* **77,** 326-332.

Mezreb, K., Goullieux, A., Ralainirina, R. & Queneudec, M. (2006). Effect of sucrose on the textural properties of corn and wheat extrudates. *Carbohydrate Polymers,* **64,** 1-8.

Millard, M. M., Dintzis, F. R., Willett, J. L. & Klavons, J. A. (1997). Light-Scattering Molecular Weights and Intrinsic Viscosities of Processed Waxy Maize Starches in 90% Dimethyl Sulfoxide and H2O. *Cereal Chemistry,* **74,** 687-691.

Moore, D., Sanei, A., Van Hecke, E. & Bouvier, J. M. (1990). Effect of Ingredients on Physical/Structural Properties of Extrudates. *Journal of Food Science,* **55,** 1383-1387.

Ortiz, J. A. R., Carvalho, C. W. P. d., Ascheri, D. P. R., Ascheri, J. L. R. & Andrade, C. T. d. (2010). Effect of sugar and water contents on non-expanded cassava flour extrudates. *Food Science and Technology,* **30,** 205-212.

Ozcan, S. & Jackson, D. S. (2005). Functionality Behavior of Raw and Extruded Corn Starch Mixtures. *Cereal Chemistry Journal,* **82,** 223-227.

Pitts, K. F., Favaro, J., Austin, P. & Day, L. (2014). Co-effect of salt and sugar on extrusion processing, rheology, structure and fracture mechanical properties of wheat–corn blend. *Journal of Food Engineering,* **127,** 58-66.

Pitts, K. F., McCann, T. H., Mayo, S., Favaro, J. & Day, L. (2016). Effect of the Sugar Replacement by Citrus Fibre on the Physical and Structural Properties of Wheat-Corn Based Extrudates. *Food and Bioprocess Technology,* **9,** 1803-1811.

Pushpadass, H. A., Kumar, A., Jackson, D. S., Wehling, R. L., Dumais, J. J. & Hanna, M. A. (2009). Macromolecular Changes in Extruded Starch-Films Plasticized with Glycerol, Water and Stearic Acid. *Starch - Stärke,* **61,** 256-266.

Ryu, Neumann P. E. & E., W. C. (1993a). Effects of Some Baking Ingredients on Physical and Structural Properties of Wheat Flour Extrudates. *Cereal Chemistry,* **70,** 291-297.

Ryu, G. H., Neumann, P. E. & Walker, C. E. (1993b). Pasting of Wheat Flour Extrudates Containing Conventional Baking Ingredients. *Journal of Food Science,* **58,** 567-573.

Silva, M. C. d., Carvalho, C. W. P. d. & Andrade, C. T. (2009). The effects of water and sucrose contents on the physicochemical properties of non-directly expanded rice flour extrudates. *Food Science and Technology,* **29,** 661-666.

Singh, B., Sekhon, K. S. & Singh, N. (2007). Effects of moisture, temperature and level of pea grits on extrusion behaviour and product characteristics of rice. *Food Chemistry,* **100,** 198-202.

Sopade, P. A. & Le Grys, G. A. (1991). Effect of added sucrose on extrusion cooking of maize starch. *Food Control,* **2,** 103-109.

Spies, R. D. & Hoseney, R. C. (1982). Effect of Sugars on Starch Gelatinization. *Cereal Chemistry,* **59,** 128-131.

Stojceska, V., Ainsworth, P., Plunkett, A. & İbanoğlu, Ş. (2009). The effect of extrusion cooking using different water feed rates on the quality of ready-to-eat snacks made from food by-products. *Food Chemistry,* **114,** 226-232.

Sumargo, F., Gulati, P., Weier, S. A., Clarke, J. & Rose, D. J. (2016). Effects of processing moisture on the physical properties and in vitro digestibility of starch and protein in extruded brown rice and pinto bean composite flours. *Food Chemistry,* **211,** 726-733.

Sun, Q., Han, Z., Wang, L. & Xiong, L. (2014). Physicochemical differences between sorghum starch and sorghum flour modified by heat-moisture treatment. *Food Chemistry,* **145,** 756-764.

Thymi, S., Krokida, M. K., Pappa, A. & Maroulis, Z. B. (2005). Structural properties of extruded corn starch. *Journal of Food Engineering,* **68,** 519-526.

van den Einde, R. M., Akkermans, C., van der Goot, A. J. & Boom, R. M. (2004). Molecular breakdown of corn starch by thermal and mechanical effects. *Carbohydrate Polymers,* **56,** 415-422.

van den Einde, R. M., van der Veen, M. E., Bosman, H., van der Goot, A. J. & Boom, R. M. (2005). Modeling macromolecular degradation of corn starch in a twin screw extruder. *Journal of Food Engineering,* **66,** 147-154.

Van Lengerich, B. (1990). Influence of Extrusion Processing on In-Line Rheological Behavior, Structure, and Function of Wheat Starch. *In: Faridi H., Faubion J.M. (eds) Dough Rheology and Baked Product Texture. Springer, Boston, MA***,** 421-471.

Wen, L.-F., Rodis, P. & Wasserman, B. P. (1990). Starch Fragmentation and Protein Insolubilization During Twin-Screw Extrusion of Corn Meal. *Cereal Chemistry,* **67,** 268-275.

Whalen, P. J., Bason, M. L., Booth, R. I., Walker, C. E. & Williams, P. J. (1997). Measurement of extrusion effects by viscosity profile using the Rapid Visco Analyser. *Cereal Foods World,* **42,** 469-475.

Yeung, C.-W. & Rein, H. (2015). Hot-melt extrusion of sugar-starch-pellets. *International Journal of Pharmaceutics,* **493,** 390-403.

Zhou, H., Wang, J., Li, J., Fang, X. & Sun, Y. (2011). Pasting properties of Angelica dahurica starches in the presence of NaCl, Na2CO3, NaOH, glucose, fructose and sucrose. *Starch - Stärke,* **63,** 323-332.

Zhu, L.-J., Shukri, R., de Mesa-Stonestreet, N. J., Alavi, S., Dogan, H. & Shi, Y.-C. (2010). Mechanical and microstructural properties of soy protein – high amylose corn starch extrudates in relation to physiochemical changes of starch during extrusion. *Journal of Food Engineering,* **100,** 232-238.

Zhu, L., Lewis, L., Stark, C. R., Guo, Q., Alavi, S. & Jones, C. (2016). An evaluation of total starch and starch gelatinization methodologies in pelleted animal feed1. *Journal of Animal Science,* **94,** 1501-1507.
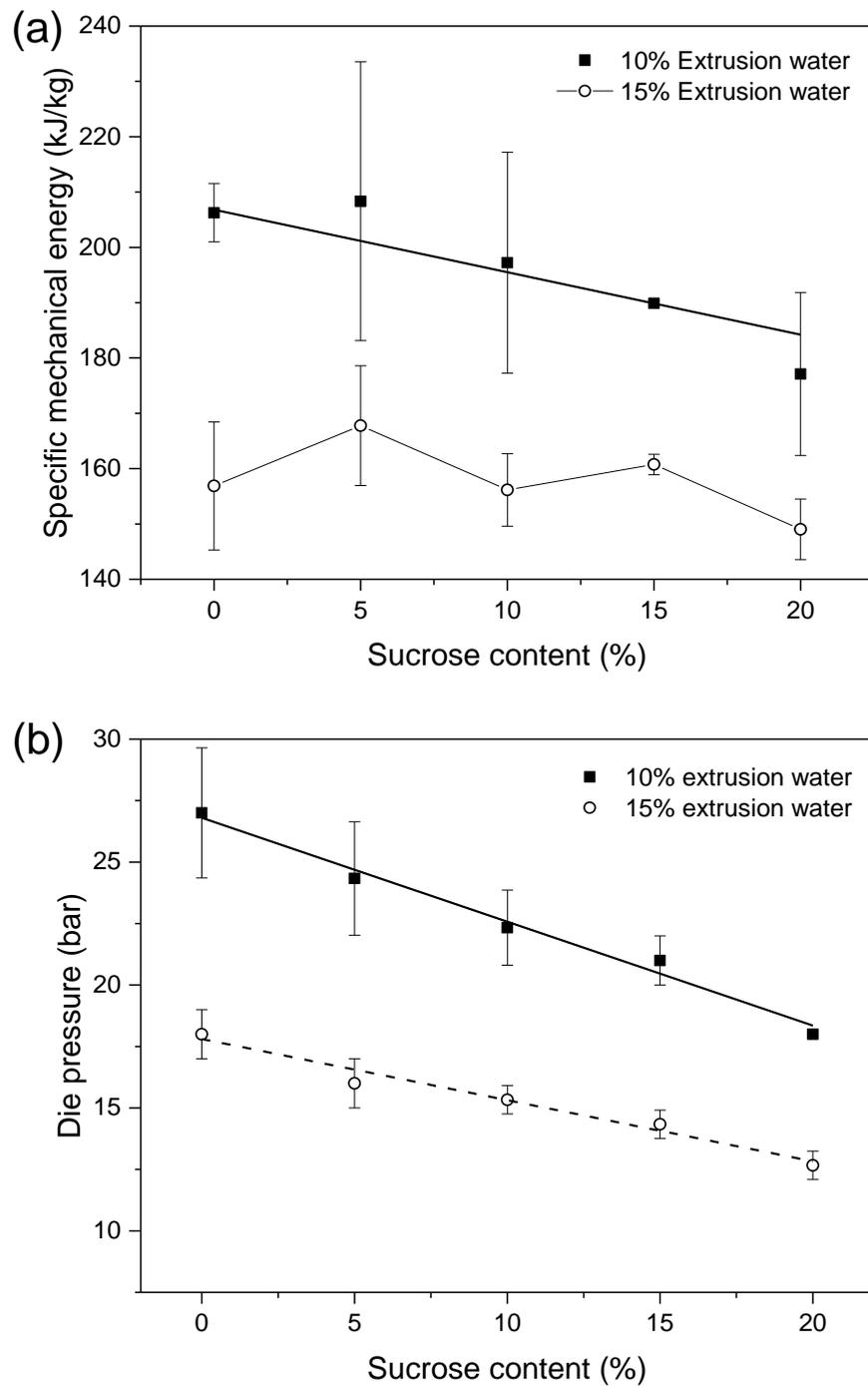
Fig. 2.1 Effect of sucrose content and extrusion water on specific mechanical energy (SME) (a) and die pressure (b) during extrusion process for extruded samples. Symbols and lines represent experimental data and linear fitting, respectively. Samples extruded at 10% extrusion water (■, solid line) and 15% extrusion water (○, dash line).
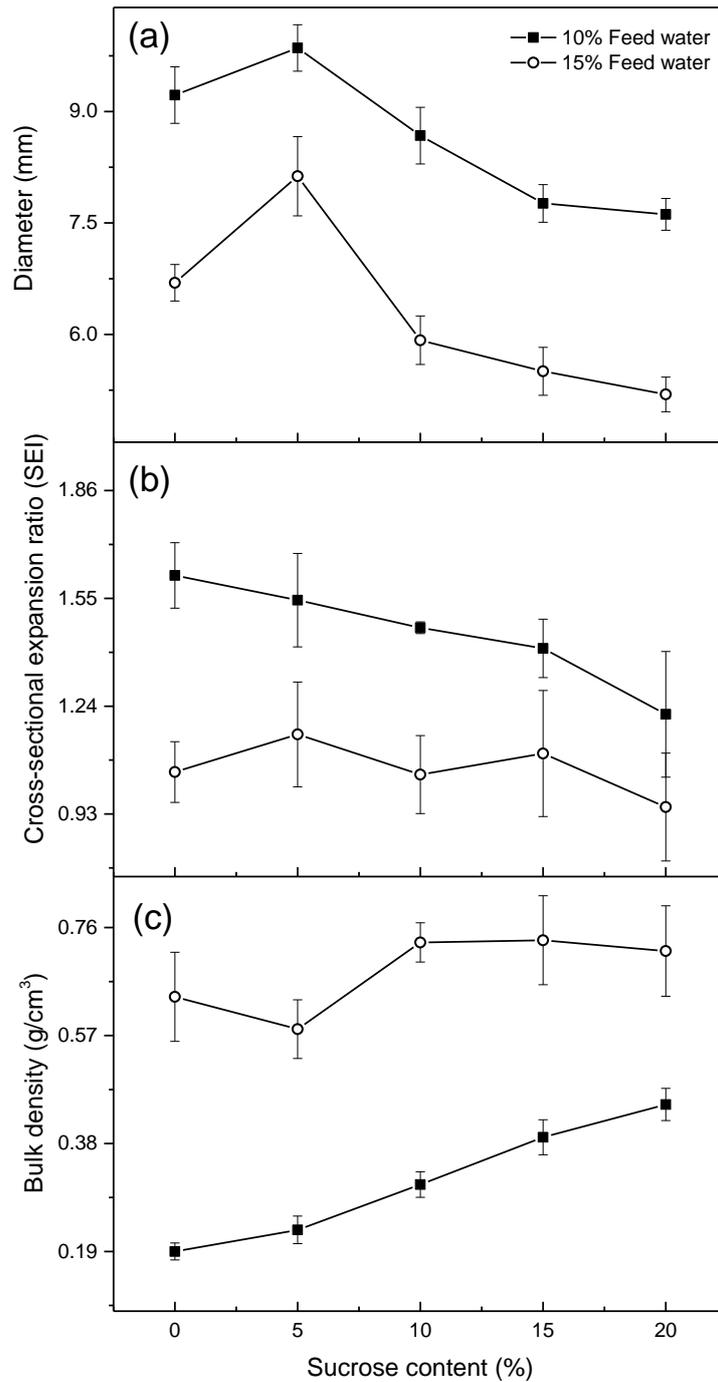
Fig. 2.2 Effect of sucrose content and extrusion water on extrudate diameter (a), cross-sectional expansion index (b), and bulk density (c). Symbols and lines represent experimental data and linear fitting, respectively. Samples extruded at 10% extrusion water (■) and 15% extrusion water (○).
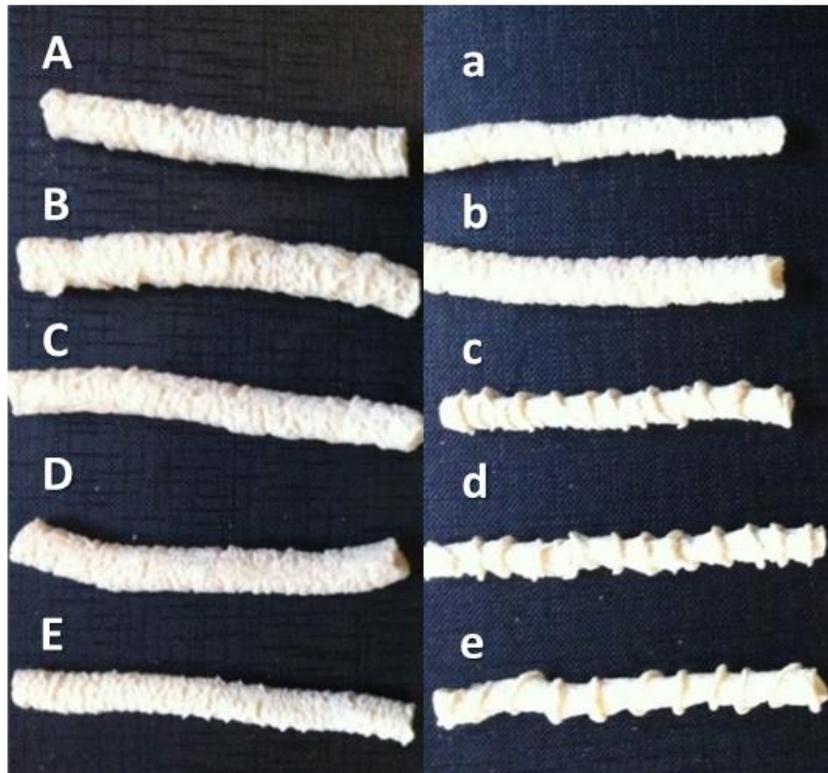
Fig. 2.3 Photographs of extrudates with 0, 5, 10, 15 and 20% sucrose and processed at 10% (A,B,C,D, and E, respectively) and 15% extrusion water (a,b,c,d, and e, respectively).

(a)

y = 5.54 - 0.03x

y = 4.80 - 0.05x

(b)

y = 32.7 + 0.61x

y = 17.9 +0.66x
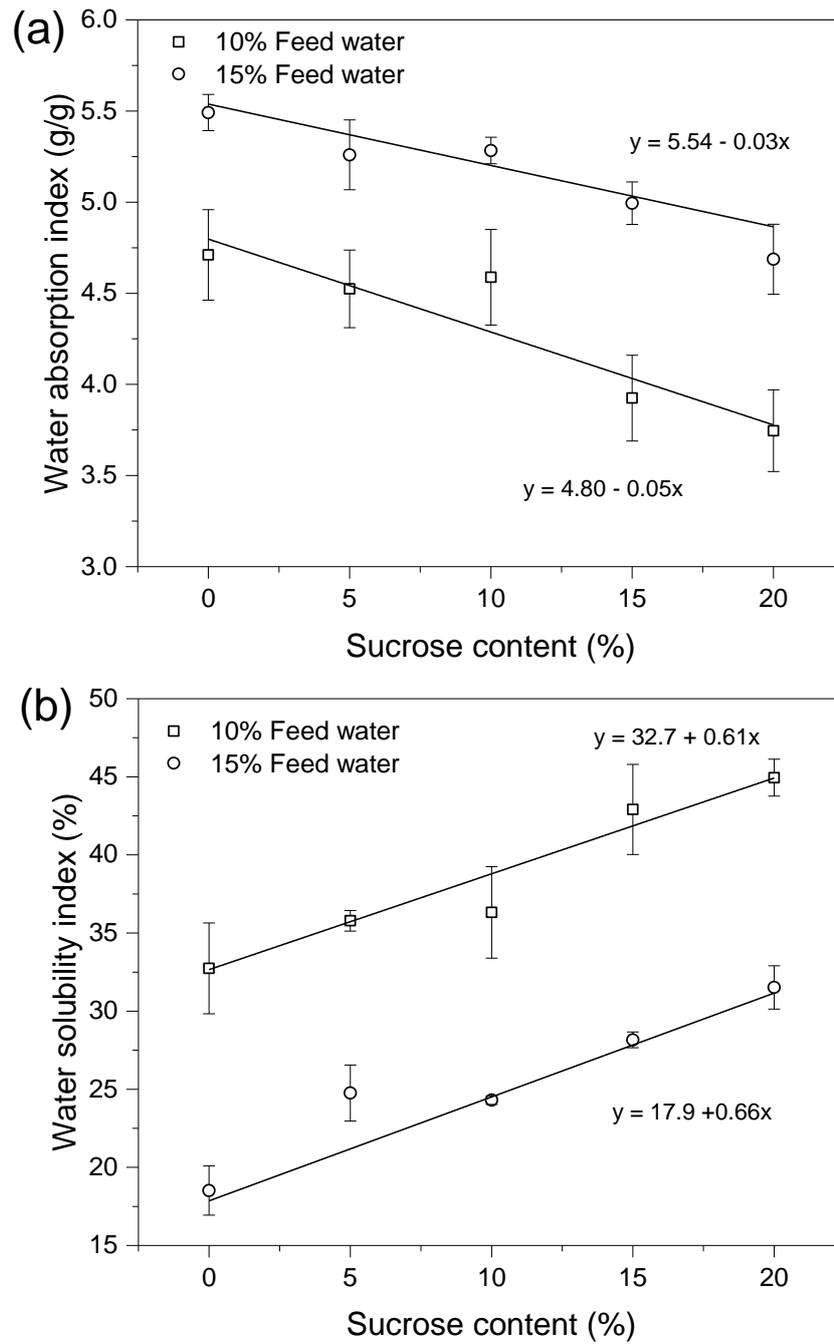
Fig. 2.4 Effect of feed water and sucrose contents on the water absorption (WAI) and water solubility indices (WSI) for extruded products produced at 10% (□) and 15% (O) feed water.
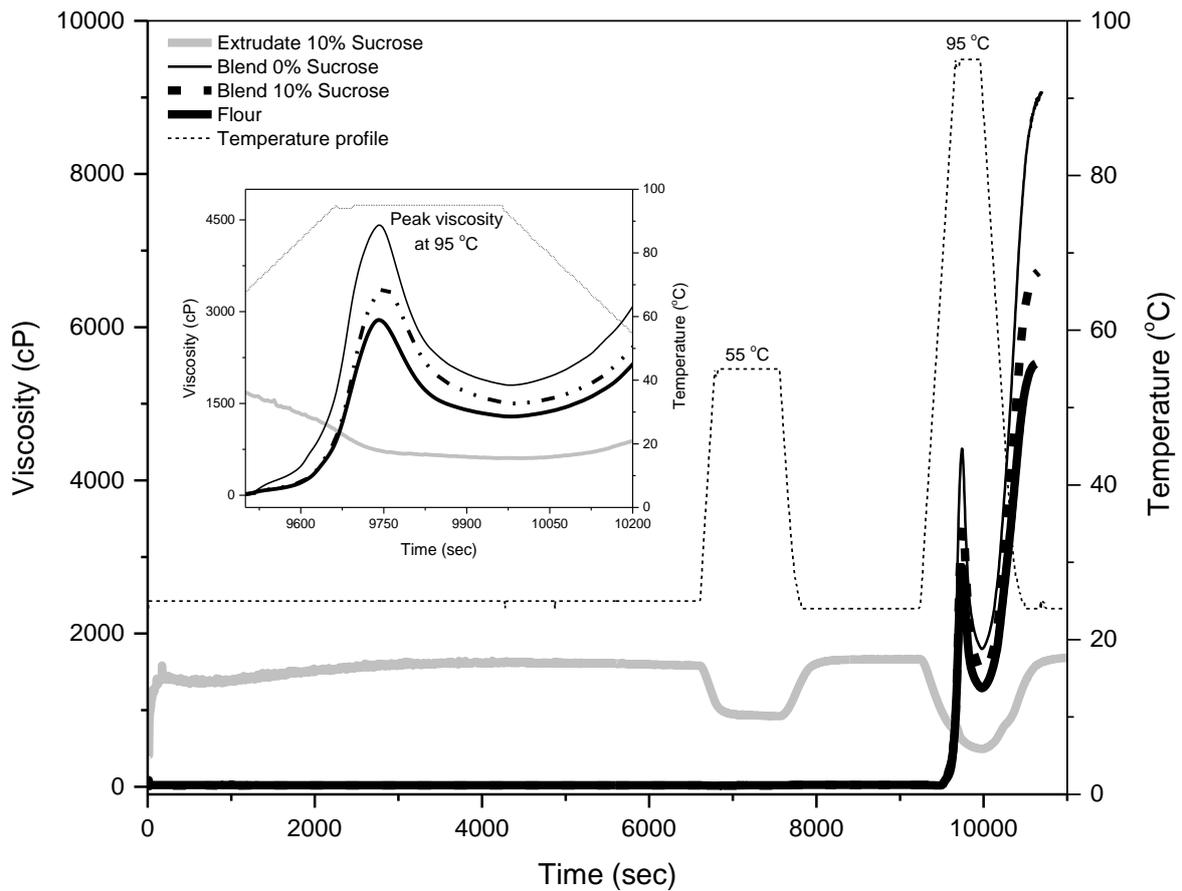
Fig. 2.5 Rapid Visco Analyser pasting profiles of native wheat flour (bold black line), blend with 0% and 10% sucrose before extrusion (thin black line and bold dashed black line) and extrudate with 10% sucrose content (clear grey line) processed at 10% extrusion water. Temperature profile (thin dashed line).
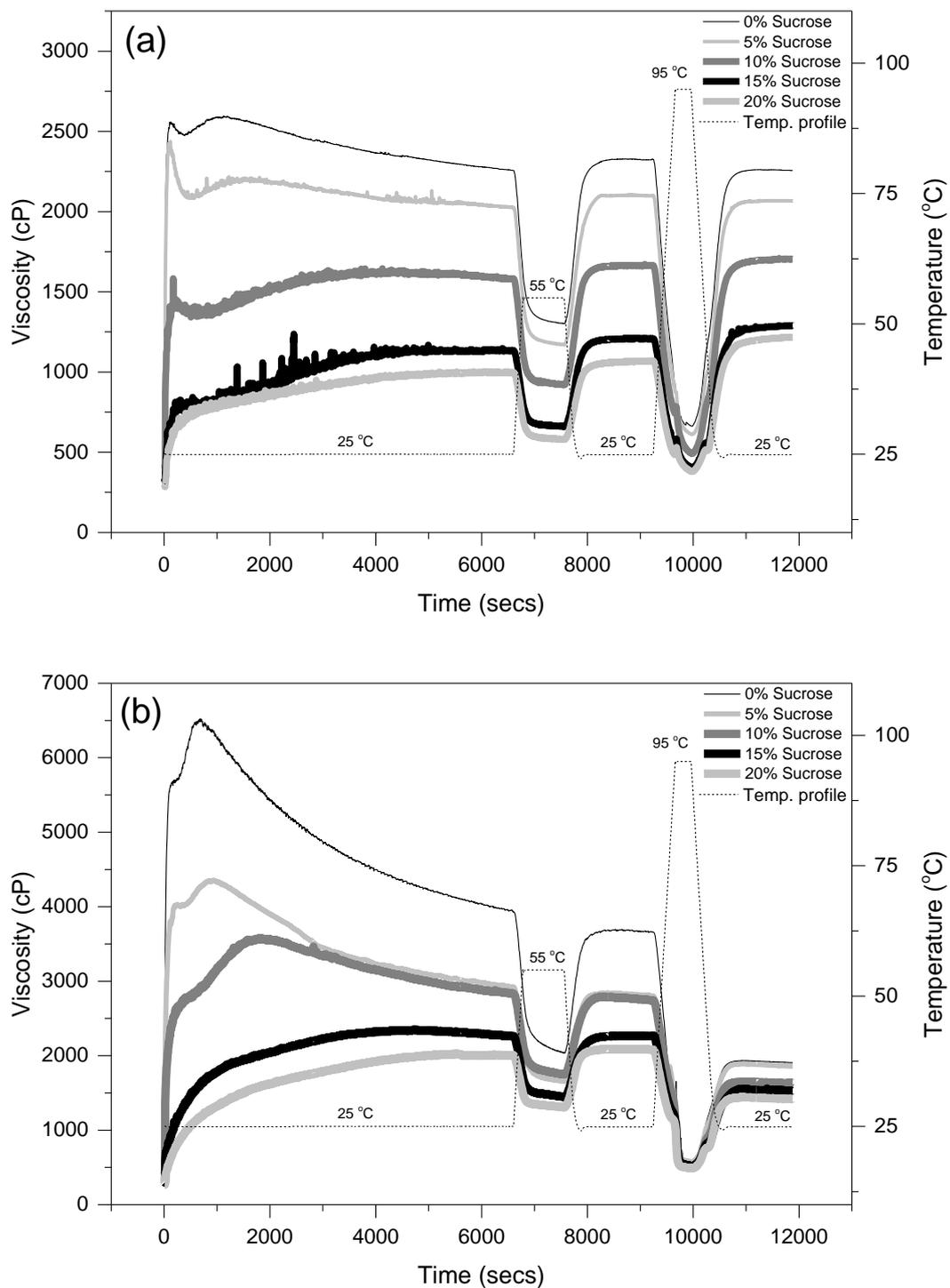
Fig. 2.6 Effect of sucrose content on the viscosity profile (RVA) of extrudates processed at 10% (a) and 15(%) extrusion water content in feed. 0% sucrose (thin black line), 5% sucrose (thin clear grey line), 10% sucrose (bold dark grey line), 15% sucrose (bold black line), 20% (bold clear grey line) and temperature profile (dashed line).
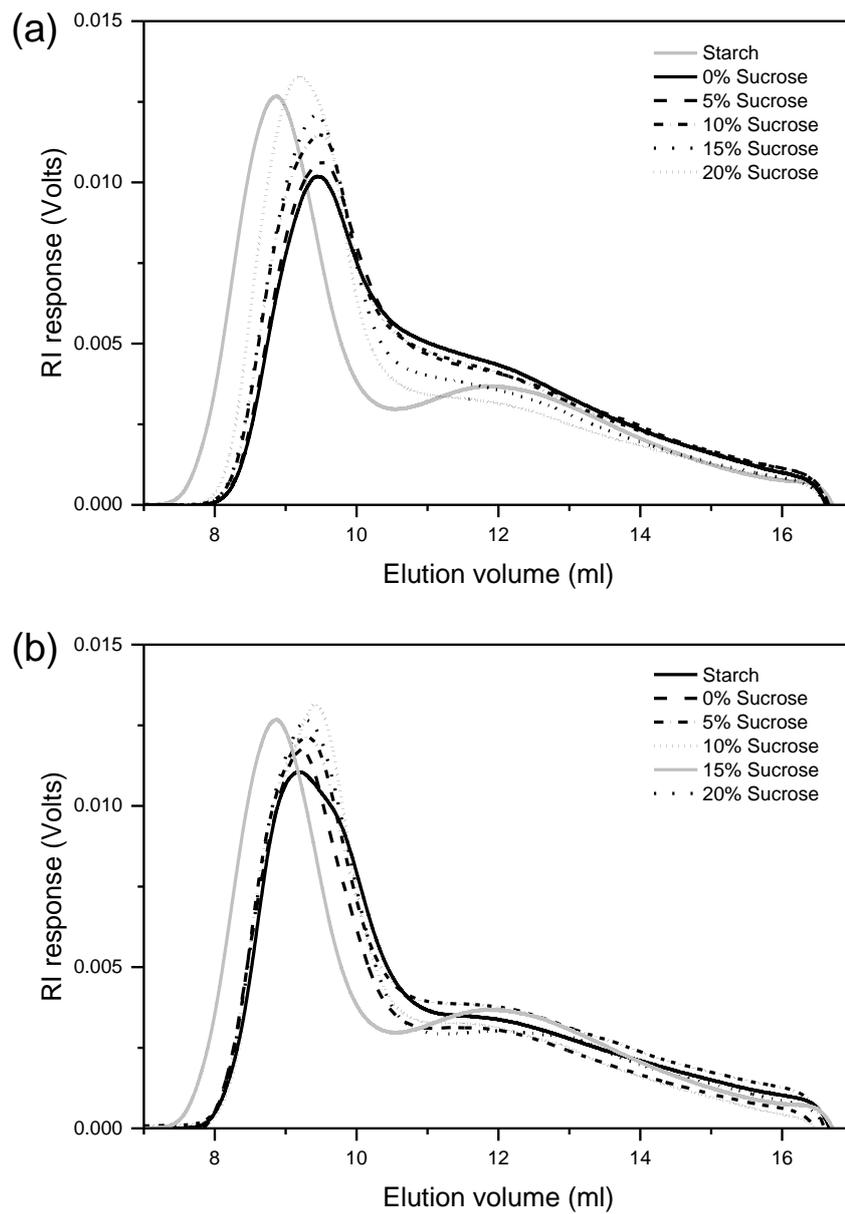
Fig. 2.7 Size exclusion chromatograms of extrudates containing 0, 5, 10, 15, and 20% sucrose content and processed at 10% (a) and 15% (b) water content.
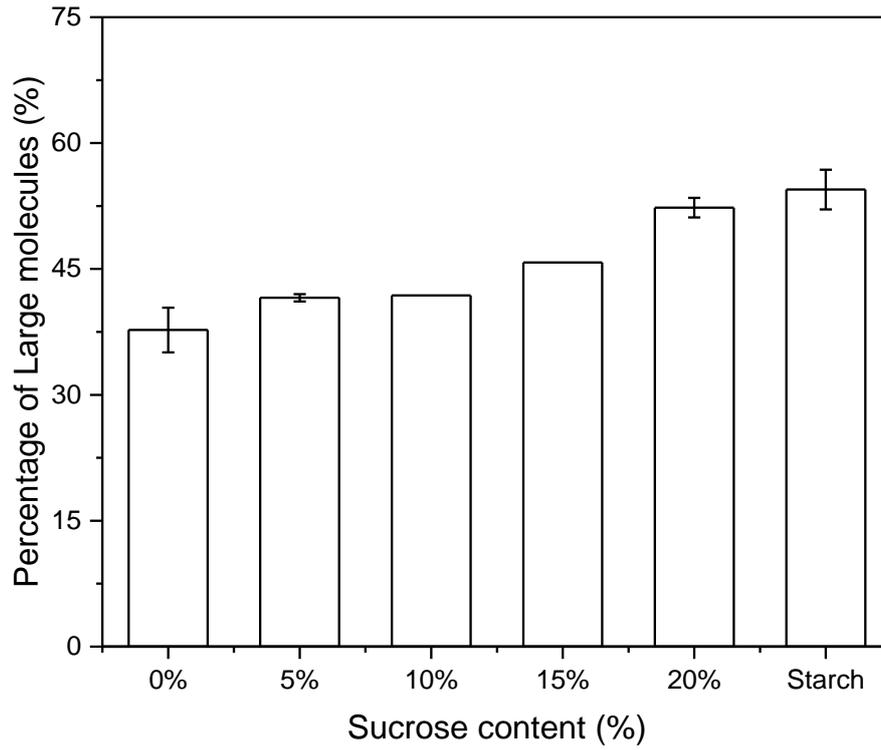
Fig. 2.8 Effect of sucrose content on large and small molecular fractions determined using HPSEC for extrudates processed at 10% feed water.

Table. 2.1 Viscosities of raw flour, blends and extrudates. (data extracted from the RVA profile, Fig. 5.5-5.6 .)

Sample	Feed water content (%)	Sucrose content (%)	Viscosity at 25 °C for 110 min (cP)	Viscosity after heating at 55 °C (cP)	Viscosity after heating at 95 °C (cP)
Raw flour	-	-	18	24	4572
Blend	-	0	19	27	7386
Blend	-	10	17	21	5578
Extrudate	10	0	2328 [b,c]	2337 [b]	2275 [a]
Extrudate	10	5	2094 [b,c]	2143 [b]	2090 [a]
Extrudate	10	10	1639 [d]	1599 [b,c]	1745 [a]
Extrudate	10	15	1162 [d,e]	1241 [c]	1255 [b]
Extrudate	10	20	851 [e]	913 [c,d]	1026 [c]
Extrudate	15	0	4094 [a]	3789 [a]	1988 [a]
Extrudate	15	5	2949 [b,c]	2861 [b]	1844 [a]
Extrudate	15	10	3299 [b]	2636 [b]	1729 [a]
Extrudate	15	15	2492 [b,c]	2488 [b]	1690 [a]
Extrudate	15	20	1920 [b,c]	2028 [b]	1530 [a]

Chapter 3:

Impact of composition: sucrose and water content and storage conditions on microstructural properties of extruded cereal-based products studied by neutron tomography.

Supuksorn Masavang*, Philippe Bodart, Camille Loupiac, Dominique Champion.
Université Bourgogne Franche-Comté, Agrosup Dijon, UMR PAM, 1 Esplanade Erasme, 21000 Dijon, France

*Corresponding author: Supuksorn Masavang
Tel:
E-mail address:

Abstract

Cereal based products with different sucrose content were processed using co-rotating twin screw extruder under the same processing settings but at different water content into extruder (extrusion water:10–15%) in order to obtain different macrostructure for the obtained solid foam. Neutron tomography was used to study these solid foams microstructure and its relationship to composition, and 3D image analysis showed a decrease in both pore size distribution median and porosity (% hole volume/total product volume) of solid foam with the addition of sucrose. The impact of sucrose content and relative humidity is not significant on pore size distribution and %porosity. An increase in the number of visible pores while median of pore size distribution are similar. The obtained results demonstrate the potential of neutron tomography for extracting structural information which can be used to aid understanding of physical change depending on storage conditions and its recipe for extruded products.

Keywords: Solid foam, extrusion, Sucrose, Microstructure, Porosity, Neutron Tomography.

1. Introduction

As the number of extruded products expands in the food industry, there is need for a better understanding of the changes occurring in these products during storage since they may lead to loss of quality. Typically, extruded products are studied using analytical methods, such as differential scanning calorimetry to determine the glass transition temperature (T_g), and sorption isotherm to measure the amount of water as a function of the storage relative humidity. However, analytical methods lack the ability to provide information about the structural organization and its potential changes after storage at different RH. To aid understanding the physicochemical properties as well as physical change behavior of foods, dedicated techniques for exploration the phenomena occurring at small scales or microstructure level are required. Imaging methods are not widely used on extruded starch products. The conventional imaging measurement of these types of materials include light microscopy in extruded black beans (Berrios *et al,.* 2004); polarized light microscopy for barley-based extrudates (Altan *et al,.* 2009) or for corn-based extrudates (Karkle *et al,.* 2012); stereoscopic microscopy in rice, bean and corn starch extrudates (Jafari *et al,.* 2017), and electron microscopy in starch-guar gum extrudates (von Borries-Medrano *et al,.* 2016), and sorghum flour extrudates (Jafari *et al,.* 2017). However, these techniques are generally used to images cross-sections or surface structure of material and do not provide images according to hydrogen contrast as neutrons do. In addition, MRI imaging and X-ray tomography have been used to study structural change due to the change of moisture on maize starch extrudates (Castlejohn 2012). X-ray tomography has been applied by several authors to study the structure of dry food products such as bread, extrudate starches (Babin *et al,.* 2007, Pitts *et al,.* 2014, Pitts *et al,.* 2016), cornflakes (Chaunier *et al,.* 2007), extruded insect-rich snack (Azzollini *et al,.* 2018), extruded rice starch-pea protein snacks (Philipp *et al,.* 2017), fried potato chips (Alam and Takhar 2016, Yang *et al,.* 2017). These methods have demonstrated their usefulness, but each of them has its own set of limitations. X-ray interaction with matter occurs with the electrons in the atomic shells of materials. Therefore, the interaction probability is directly proportional to the number of electrons, namely the atomic number. Light elements (such as hydrogen) have little chance to absorb X-ray and are nearly invisible, whereas heavy elements absorb a lot and result in high transmission through thick layer of heavy metals

(Grünzweig *et al,.* 2013). They may differ with respect to their spatial and temporal resolution, their capability to detect water qualitatively (dynamic range, i.e. number of contrast levels) and quantitatively (absolute water content), their accessibility as well as their ease of use (Defraeye et al., 2012a). Neutron imaging method can be applied to overcome these limitations and provide a more complete picture of the structure of food materials. In addition, none of these imaging methods were used to observe the effects of composition (sucrose and water content) under storage at different relative humidities in extruded cereal-based products.

Neutron tomography is one of the nondestructive techniques that enable one to visualize and characterize the heterogeneity of internal structural architecture, porosity, cell wall thickness and cell diameter of food samples with a field of view around 10 to 10 cm at a resolution of 100 micrometers. Cellular solid foods samples such as bread, extruded snacks, biscuits and cakes can be processed. Neutron tomography is similar to corresponding x-ray technique but is most cases the mechanisms of neutron interaction with matter provide an image contrast that is complementary to that of x-rays. Neutrons only interact with the atomic nuclei of the tested material. Most of the relevant materials scatter neutrons at the nuclei (Grünzweig *et al,.* 2013). Most metals are transparent to neutrons, while a lighter element such as hydrogen is very sensitive to neutrons with high attenuation. More scattering than in X-ray imaging may be present, particularly with hydrogen. When both the water content and sample thickness are high, the scanned object may be opaque for neutrons. Still, in small samples presenting a water content gradient, neutron imaging can be readily applied with a better sensitivity for water than X-ray imaging or MRI (Bilheux *et al,.* 2009), which makes it excellent to look at the effects of moisture content changes, such as during drying or hygroscopic loading (Verboven *et al,.* 2018). Neutron have been applied to food in order to visualize and quantify water content changes in products such as fruit during hydration (Defraeye *et al,.* 2016, Aregawi *et al,.* 2013), dry fish during drying (Tanoi *et al,.* 2009) and meat during cooking (Scussat *et al,.* 2017, Scussat *et al,.* 2016).

Although 2D image analysis is fast and relatively easy technique compared to 3D image analysis, image analysis of cereal solid foams needs third orthogonal dimension to produce high-quality 3D images

representing proper structure of air cells and thus likely to represent original size and shape of the cellular structure including cell size distribution, average cell wall thickness, average cell diameter and finally connectivity of cells through the quantitate analysis of projection data (Sozer *et al,.* 2011). The interconnected pores can be segmented by watershed algorithm in order to accurately evaluate the pore sizes and shapes (Plews Andrew *et al,.* 2009). This technique can be used to analyze samples with inhomogeneous porosity where pore size was based on volume fraction. The algorithm itself is an efficient tool to determine the open cell numbers and to obtain pore size distributions. Apparent pore size distribution can be obtained from 3D analysis, although it is challenging to get accurate information on pore connectivity; 3D analyses give thorough characterization of the porous food structure, provided that they have sufficient density difference throughout the matrix.

It is well known that the cellular structure of solid cereal foams such as bread, cake, extruded snacks and biscuits, has an effect on textural properties such as hardness, chewiness or crispness based on product category. Sensory quality of baked and extruded cereal foods are strongly dependent on the structural architectures such as air cell size, shape and their distribution within the food matrix; therefore, it is important to evaluate these structural parameters to aid product design and optimize processing conditions (Sozer *et al,.* 2011).

Cooking extrusion delivers aerated texture, leading to the formation of a solid foam with specific structural characteristics (pore wall size and thickness, porosity, density) and mechanical properties (Azzollini *et al,.* 2018). These properties are driven by the degree of aeration and microstructure of the cellular structure. The expanded structures can be quantified by imaging technique such as microcomputer X-ray tomography combined with 3D image analysis which allows quantifying the porous structure through a variety of attributes such as e.g. porosity, cells size, walls thickness or number of cells.

The sugar addition in the formulation for extrusion processing is also known to affect the processing conditions and final product quality. Sucrose addition induced an increase in the bulk density and a decrease in expansion and pore size of corn or wheat-based products (Moore *et al,.* 1990, Barrett *et al,.* 1995). Microstructure changes in the solid foam resulted in change of both the mechanical fracture properties and

sensory attributes of extrudates (Mezreb *et al,.* 2006). Fan *et al,.* (1996) found that the addition of sugar in maize grit blend formulation decreased SME (specific mechanical Energy in extruder), which resulted in a reduction starch conversion and promoted bubble rupture at lower extension. Similar result was demonstrated by (Pitts *et al,.* 2014) when reduction of sugar content in a wheat-corn blend formulation increased screw torque value, die pressure and specific mechanical energy (SME), which resulted in a higher expansion and more porous structure of product. In addition, Pitts *et al,.* (2016) found that replacing 5 % sugar with an equal quantity of fiber resulted in an increase in die pressure, torque and specific mechanical energy (SME), and consequently the expansion ratio increased. A further increase in fiber content to 10 % as sugar is 0 %, had a little effect on the extrusion processing parameter. The microstructure of extrudates examined by X-ray computed tomography shows that the porosity of the extrudates increased with increasing fiber content. However, conflicting results have also been report. Hsieh *et al,.* (1990) found that a 0 to 4% addition of sugar in the feed decreased the die pressure, % torque and specific energy, while at 6 and 8%, sugar increased the three processing parameters which enhanced extrudate radial and axial expansions, but reduced product bulk density and breaking strength.

More insight of the microstructure and further understanding of its relation to water mobility which arises in a sample when it is exposed to an environment with a higher relative humidity is necessary to develop stable products. Crispness is one of the most features in term of consumer acceptation of dry porous cereal-based products (Esveld *et al,.* 2012). It is lost in storage due to a change in water content, change in water distribution or change in mobility of water (Dalen *et al,.* 2007). Therefore, it is likely that different concentrations of sucrose and storage relative humidities of extruded cereal-based products will change the expansion, microstructure and therefore, texture of product in this work. The effects of these factors are quantified and visualized through the 3D internal structure of foods using the imaging technique.

Imaging techniques and tomography allow the observation of large sample structures at the scale of a few micrometers. Typical image studies of these types of materials include magnetic resonance imaging (MRI) and X-ray microtomography (μCT). MRI allows the real time visualization of the effect of hydration in term of transportation/diffusion rate and spatial distribution of structural change (Dalen *et al,.* 2005). μCT

on the other hand has allowed high resolution 3D visualization and characterization of non-hydrated material before and after certain duration of hydration, such as porous biscuits (Dalen *et al,.* 2007), fried potato disks (Alam and Takhar 2016), fried potato chips (Yang *et al,.* 2017), and extruded rice starch-pea protein snacks (Philipp *et al,.* 2017).

We have previously studied the glass transition and textural properties of extrudates (Masavang *et al,.* 2019) and showed that there is heterogeneous water distribution into the matrix microstructure which is highlighted by the presence of two glass transition temperatures depending on their formulation and storage humidity. Another aim of this study is to gain more insight between the structural characteristics (porosity, pore size distribution) and water uptake arising in a sample exposed to an environment with high relative humidity (75 % RH relative humidity).

2. Experimental

2.1 Preparation of the extruded samples

Wheat flour, wheat starch and gluten of commercial grade was supplied by CHAMTOR (Les Sohettes, France); sucrose of commercial grade was bought in supermarket. The ingredient blends containing 0, 10, and 15% wt sucrose with wheat flour (53-73%, wt, wheat starch 16% wt, gluten 16% wt and salt 1% wt were conducted on a Clextral BC-45 intermeshing twin-screws extruder with a 1.5 m long barrel using 10 and 15% wt initial moisture contents for the blend. The barrel heating zones were at 80 °C, 130 °C and 160 °C (±2 °C), and a 6.0 mm circular die was fitted to the end of the barrel. The screw speed was 150 rpm. The solid feed rate was 34 and 36 kg/h, and water was added in order to obtain a final water content of 6 and 4 l/h, respectively. After removal of the die, samples were allowed to cool to ambient temperature on a conveyer belt and dried at 105 °C for 5 minutes to bring the final product to a moisture content of approximately at 3-4%. The extruded ribbons were sealed in plastic bags under vacuum and stored at ambient temperature.

2.2 Neutron tomography

The experiments were performed at the Laboratoire Léon Brillouin (CEA Saclay- France). The neutron imaging station, Imagine (Ott *et al,.* 2015), is located in the neutron guide hall on a cold neutron guide. The guide

cross section is 25 mm × 50 mm. The available neutron spectrum extends from 3 Å to 20 Å. We used the classical configuration of the instrument (field of view 80 × 80mm^2, pinhole source diameter of 20 mm, distance between the source pinhole to detector length of 4 m) resulting in 2 x 10^7 neutrons/s/cm^2 flux on the sample. A multi-megapixel camera (model Neo 5.5 sCMOS, ANDOR), equipped with a detector (size of 16.6 × 14.0 mm^2, 2560 × 2160 pixels, so 5.5 Mpx sCMOS) was used. The size of one camera pixel is 6.5 × 6.5 µm^2, and to reduce noise, the camera was cooled down to −30 °C. Images were recorded in 16 bit in "*.fits" format. The camera is coupled with a 100 µm thickness lithium scintillator was used for data acquisition. For these experiments, an aluminum tube (diameter of 1 cm) was used as a sample holder to reduce neutron absorption. The sample holder was positioned 5 cm away from the scintillator on a rotating table allowing a rotating of the sample over 180°. 181 images were collected in increments of 1°. At each rotation, samples were exposed for 120 s to the neutron beam. For normalization, 10 images of flat-field were recorded before and after the sample imaging.

2.3 Image processing

The image processing was performed with a computer able to analyze 3D graphics. The computer was equipped with Intel i5-quad core microprocessor, 3.40 GHz; 32 GB ram; discrete GPU, NVIDIA GeForce GTX970; SSD memory. In the first step, every collected image was initially analyzed by ImageJ 1.48 (Abramoff *et al,.* 2004) to remove noise ("despeckle" command), and white points due to gamma rays ("remove outliers" command, radius of 2 pixels). The resulting images were saved as stacks of 16-bit tiff-format images. In the second step, this dataset was reconstructed by Octopus 8.7 software (Octopus Imaging, Inside Matters, Belgium) after image cropping, normalization with the flat-fields image by the electronic noise and open beam, filtering to remove rings due to scattering phenomena, and correction of the tilt angle of the rotation axis and building sinograms. The resulting volume datasets were exported as stacks of 32-bit tiff-format images, each of which represents a tomographic cross section of the sample at successive points along the vertical axis. In a third step, Avizo Fire 9.2 (FEI, Hillsboro, Oregon USA) software was used for image and porosity analysis.

2.4 Region of interest (ROI)

A typical sample studied is presented in Fig. 3.1a with radial and axial reconstructed slices of the sample (Fig. 3.1b and c, respectively). Bright pixels are associated with regions where the neutron adsorption is significant they correspond to hydrogen-rich sample areas i.e. the solid matrix of the sample. Grey zones correspond to pores. As a consequence of the flux of the drought in the die, the axial length of the pore appears greater than the radial dimension. The samples studied have a cylinder shape but vary in size (from 1 to 2 cm height and 1.5 to 0.8 cm width). The first parameter to handle is the definition of a common size for the region of interest (ROI). The ROI has been chosen as rectangular parallelepiped and as example, figure 3.1(a) shows the cumulative histogram of the 2D-projection recorded for sample without sucrose and produced at 10% feed water for three ROIs of 27 mm^2 square base with distinct heights (2.6, 5.25, and 9.6 mm). Histograms count each grey level occurrence, and very comparable distributions were obtained for all the ROIs. In the following, all the image processings have been performed with the same ROI of 27 mm2 x 9.6 mm-height.

2.5 Thresholding

Image segmentation is a critical pre-processing step for differencing objects (e.g. porosity from the matrix). It is based on grey-scaled thresholding of the histograms. All the studied samples present identical histogram similarities to those of Fig. 3.1(d): on the left, a sharp distribution corresponds to dark pixel resulting from no or little absorption of the neutron beam by the sample (they correspond to holes in the sample). On the right the broader distribution is associated with clear pixels corresponding to the solid matrix, where the neutron adsorption occurs. Histograms have a clear bimodal distribution with unfortunately a strong overlapping which is certainly one of the main limiting factors of the analyses. The valley gives a reasonable threshold value for the matrix/hole separation, but it may not be the optimum value (Wang and Ward 2007). To ascertain our choice of the threshold level, we systematically vary the threshold value and check the stability of the calculated parameters defining the porosity.

2.6 %Porosity

Figure 3.2 details the steps of the porosity analysis: (1) ROI selection by cropping the stack of 2D images, excluding edges which may be affected by physical cutting of the sample and eliminating the difference due to size-fluctuations of the samples. (2) Binarization of the images: after an automatic brightness and contrast enhancement of the images, pixels corresponding to pores were selected by inputting threshold level (T). All pixels with a grey level value below T were assigned a unity values associated with holes and all pixels above T were set to zero and are related with the solid matrix (pore walls). (3) A watershed segmentation (Beucher 1991) was used to improve non-connected-holes identification. The software output a 3D-image showing colored pores (all connected pores have the same color) and produced a table reporting pores volumes. Porous properties, such as the number of pores, equivalent diameter, pore volume, and pore size distribution were analyzed using Origin Pro (Version 2017, OriginLab, Northampton, MA). Equivalent pore diameter (D_{eq}) was calculated from the pore volume (V_{3D}):

$$D_{eq} = \sqrt[3]{\frac{6 \times V_{3D}}{\pi}}$$
<div align="right">Eq. 3.1</div>

Porosity ($\emptyset$) is defined as:

$$\emptyset = \frac{V_{pore}}{V_{total}}$$
<div align="right">Eq. 3.2</div>

where, V_{pore} represents the total volume of pores, and V_{total} represents the total volume of a sample.

2.7 Expansion

The cross-sectional expansion ratio (ER) was determined as the diameter of extrudates divided by the diameter of the die exit (6.0 mm). Each value was an average of 10 measurements measured just after extrusion.

Results and discussion

3.1 Effect of composition (sucrose and water content) on microstructure

Fig. 3.3 shows typical 2D cross-section gray scale images obtained after 3D reconstruction of extrudates containing 0, 10 and 15% sucrose and stored at 11 and 75% relative humidity. Images showed

differences in internal structure. At the two relative humidities chosen for samples equilibration, the size of the pore and the diameter of the extrudate decreased as the sugar content increased. Sucrose adding had a more pronounced effect. Relatively big internal air voids were found in extrudate without sucrose, while extrudates containing 10 and 15% sucrose had smaller pores distributed more randomly though the sample. The microstructure of extrudates appeared denser as sucrose content increased, resulting in higher bulk density (data not shown). The cross-sectional expansion index (SEI) defined as the diameter of extrudates over the diameter of the die exit (6.0 mm). This parameters allowed to quantify this observation, whatever the sucrose content, the SEI was reduced by 25% when formulation sucrose content varied from 0 to 20% (Fig. 3.4). Similar observations have been reported: with a reduction in mean cell size in corn extrudates (Barrett *et al,.* 1995) and volumetric expansion in wheat flour extrudates (Ryu *et al,.* 1993) as sucrose content increased, resulting in a decrease in SEI. Moreover, a negative correlation between radial expansion of extrudates and moisture content were reported (Barrett and Ross 1990, Barrett *et al,.* 1995).

As evidenced by the microstructure, 0% sucrose contained more pores than 10 and 15% sucrose, which was mainly due to the sucrose in their formulation. Similar results were reported by Mezreb *et al,.* (2006) in corn and wheat extrudates. They noticed that the internal structure of the extrudates evaluated by image analysis showed a reduction of the cell size with sucrose addition. In addition, regarding the relationships between porous structure of extruded starchy products and their mechanical properties, Babin *et al,.* (2007) showed that for the same relative density, lower mechanical resistance was obtained for products displaying a wide range of cell size and wall thickness. If relative density is key for mechanical resistance, the internal structure of porous extruded cereals has also an impact.

The relationship between sucrose content, pore diameter, total porosity percentages, determined by imaging technique, was assessed. Quantitative analysis of 3D images of extruded samples showed that the cellular structure of extruded samples varied with average pore size of 0.04-2.52 mm. Generally, all samples consisted of several small pores and the pore size distribution was bimodal with pore sizes ranging between equivalent diameter range of 0.02 and 0.2 mm, while the bigger pores were between 0.2 and 1.0 mm (Fig. 3.5). Similar behaviour was observed in supercritical fluid extrusion samples with practically a non-

porous outside layer, the large of small cells towards the surface, a small number of large cells towards the center due to a free expansion of the bubbles, whereas the nuclei were restricted at surface by the die. Besides, nuclei located towards the center had more time to expand (Gueven and Hicsamaez 2013). The amount of the bigger pores mainly contributed to the porous structure, thus this work mainly focus on the second population of pore. Fig 3.6 shows the equivalent diameter distribution curves for extrudates at 0, 10 and 15% sucrose and with equivalent diameter greater than 0.2 mm. All curves showed non-normal pore size distribution. The extrudates without sucrose were found to have the widest range of pore size distribution followed by 10% sucrose and 15% sucrose, which suggested that the pore size in the extrudates was relatively small in the presence of sugar. The percentage of pores was also highly dependent on sucrose content and density, with low density products having the highest count (Fig. 3.6). The pore size distribution of extrudate with 15% sucrose shifted towards smaller pore sizes and resulted in more ? uniform-size pores than extrudate without 10% sucrose. Barrett *et al,.* (1995) reported that in samples produced at 20% moisture content, sucrose progressively reduced cell size and increased density. In both batches, sucrose eventually inhibited the ability of the samples to expand and/or facilitated collapse of the structure, possibly by reducing melt viscosity and elasticity. Similar effects of sucrose on the structure of wheat flour extrudates have been reported by Ryu *et al,.* (1993). These authors observed that sucrose significantly reduced the volumetric expansion of extrudates at a 10% sucrose concentration level, while the extrudate bulk density and the number of cells per unit area increased with increasing sucrose. An increase in the number of cells per unit area, accompanied by a decrease in the sectional expansion index, correlated well with our observation of a reduction in cell size as the sucrose content increased.

Figure 3.8 shows 3D tomography of extrudates containing 0, 10 and 15% sucrose, equilibrated at 11 and 75% RH. Previous observation of pore size evolution were confirmed, (as sucrose and water content increased, the pore size decreased), but the tomography further highlighted a concomitant increase of the matrix thickness (the width of the pore walls) but porosity is the ratio of pure volume to apparent volume of the porous medium. Changes in porosity and the cellular structure of extrudates during storage are believed to influence on product stability and thus the product quality. The % porosity for extrudates were in range of

46.0-48.7%. There was no visible difference in the % porosity of extrudates containing different sucrose content. In this work, the image anlysis was done by the same manner in order to compare the effect of product formulation. We expected to detect the different % porosity, as we observed an obvious bubble in the 2D-image of extrudates without sucrose (Fig. 3.3). The reason we failed to calculate % porosity might come from the way of image analysis such as thresholding by AvizoFire softwear. Moreover, the large range of pore sizes resulted in large variations for quantitative results. Images of 2D slices of extrudates showed that the pores are elongated in the longitudinal direction, whereas they are spherical in the radial direction (Cho and Rizvi 2010). It probably occured due to the orientation of the shear field as the screw pushed the material through the barrel towards the die and out of die to ambient resulting in elastic recovery (Moraru and Kokini 2003). These pores cloud effect on the quantitative results due to only pores in range of 0.2-0.7 mm were used for % porosity calculation, resulting in the difference in % porosity depending on sucrose content. The accuracy of the image analysis depended on image resolution, brightness/ contrast, and type of segmentation approach followed (Guarino *et al,.* 2010). The image acquisition and the proper thresholding also might be considered. In generally, low porosity of the extrudates containing high sucrose content indicated that starch granules were more distrupted and tended to expand less compared to extrudate without sucrose (Pitts *et al,.* 2014, Pitts *et al,.* 2016). A good correlation was found between macro- and microstructral properties, where positive correlation was found between expansion and porosity. Bulk density was negatively correlated. This correlation indicates that the increase in expansion gave increased porosity and decreased bulk density and is in agreement with previous work reported by Singkhornart *et al,.* (2014), Robin *et al,.* (2012) and Alam *et al,.* (2013) . At this point, it is difficult to state any significant trend of % porosity due to the lack quality of the data quantitative analysis. However, it is clear that the extrusion at various sucrose content could cause the variation of porosity.

3.2 Impact of storage at different relative humidities

The shelf life of low moisture food depends on water content, water migration, and moisture uptake during storage. The major external parameters affecting the rate of water diffusion are the relative humidity of storage (Guillard *et al,.* 2003a, Guillard *et al,.* 2003b, Guillard *et al,.* 2004, Roca *et al,.* 2007, Bourlieu *et al,.*

2008). In this work, the moisture was transported into extrudates by diffusion through the vapor phase and the local diffusive penetration in the solid will be taken into account. The product was not in direct contact with water. The distribution of the pores of extrudates containing 0% and 15% sucrose and stored at 11% and 75% were plotted in in semi-log scale as shown in Fig. 3.7. There was no obvious difference in the distribution of the pores for all samples at both 11% and 75% RH. On the other hand, Yang *et al,.* (2017) showed that a higher percentage of porosity was followed by higher moisture content in the potato chips. Porosity in particular influences the water diffusion rate. We hypothesize that moisture redistribution throughout the porous structure relocated the water contributing to the change in microstructure during storage. Mechanical property (such as hardness, rigidity) of extrudate is also related to moisture redistribution from outside to inside. Thus, controlling the moisture migration from outside to inside matrix can slow the physical change.

Extrudates did not show significant difference in % porosity upon storage relative humidity. As discussed above, the image analysis plays an important role on quantitative data. Neutron imaging technique allowed to investigate extruded cereal-based products for the first time to study their microstructure. This technique showed the potential to apply in low-moisture food and suggested new insight: considering the parameters during performing and image processing could contribute to a better quantitative data. The changes observed in the pores showed some basic structural changes occuring during storage that would be unobservable using other methods. DSC and mechanical properties suggested that physical changes occurred even below the glass transition, the changes in pore characteristics also confirmed that some physical aging mechanism was at work during storage. There is a possibility that the changes observed in pore network were due to moisture migration instituing minute textural changes via swelling or plasticization. Generally, these findings could provide some guidance in improving product design, process optimization, texture, and shelf life of extruded products.

4. Conclusion

In conclusion, this study has shown the use of a combined neutron microtomography technique and 3D image analyses to illustrate the effect of microstructural properties on extruded products. A correlation between the SEI, median of pore size, and percentage of porosity was found. The pore size and pore size distributions together with different sucrose content provided detailed information on the porous structure of the extruded samples. The microstructure of extrudate affected its physical properties and, subsequently, its behavior in its surrounding environment. 2D neutron cross-section images displayed a highly porous microstructure in extrudate with sucrose and appeared to have thinner walls and larger pores than the other. However, the impact of sucrose content and relative humidity on pore distribution and %Porosity were not significant due to the lack quality image analysis. For a better understanding and control of water migration in extruded products, futher experiments need to probe the water distribution changes in porous structure during storage by quantitative neutron imaging. Neutron imaging allowed to investigate microstructure for a first time in extrudate and showed potential to apply in low-moisture food but to the improve the quality of quantitative results the image processing and image analysis could be considered. 3D image analyses of high-quality processed images can also be used in the food industry as a reliable and accurate control of heterogeneous food structure, which can be further used to understand the relationship between physico-chemical properties of porous solid foods and food morphology.

References

Abramoff, M. D., Magalhães, P. J. & Ram, S. J. (2004). Image processing with ImageJ. *Biophotonics international,* **11,** 36-42.

Alam, S. A., Järvinen, J., Kirjoranta, S., Jouppila, K., Poutanen, K. & Sozer, N. (2013). Influence of Particle Size Reduction on Structural and Mechanical Properties of Extruded Rye Bran. *Food and Bioprocess Technology, 7,* 2121-2133.

Alam, T. & Takhar, P. S. (2016). Microstructural Characterization of Fried Potato Disks Using X-Ray Micro Computed Tomography. *Journal of Food Science, 81,* E651-E664.

Altan, A., McCarthy, K. L. & Maskan, M. (2009). Effect of Extrusion Cooking on Functional Properties and in vitro Starch Digestibility of Barley-Based Extrudates from Fruit and Vegetable By-Products. *Journal of Food Science, 74,* E77-E86.

Aregawi, W., Defraeye, T., Saneinejad, S., Vontobel, P., Lehmann, E., Carmeliet, J., Derome, D., Verboven, P. & Nicolai, B. (2013). Dehydration of apple tissue: Intercomparison of neutron tomography with numerical modelling. *International Journal of Heat and Mass Transfer, 67,* 173-182.

Azzollini, D., Derossi, A., Fogliano, V., Lakemond, C. M. M. & Severini, C. (2018). Effects of formulation and process conditions on microstructure, texture and digestibility of extruded insect-riched snacks. *Innovative Food Science & Emerging Technologies, 45,* 344-353.

Babin, P., Della Valle, G., Dendievel, R., Lourdin, D. & Salvo, L. (2007). X-ray tomography study of the cellular structure of extruded starches and its relations with expansion phenomenon and foam mechanical properties. *Carbohydrate Polymers, 68,* 329-340.

Barrett, A., Kaletunç, G., Rosenburg, S. & Breslauer, K. (1995). Effect of sucrose on the structure, mechanical strength and thermal properties of corn extrudates. *Carbohydrate Polymers, 26,* 261-269.

Barrett, A. H. & Ross, E. W. (1990). Correlation of Extrudate Infusibility with Bulk Properties using Image Analysis. *Journal of Food Science, 55,* 1378-1382.

Berrios, J. D. J., Wood, D. F., Whitehand, L. & Pan, J. (2004). SODIUM BICARBONATE AND THE MICROSTRUCTURE, EXPANSION AND COLOR OF EXTRUDED BLACK BEANS. *Journal of Food Processing and Preservation, 28,* 321-335.

Beucher, S. (1991). Mathmatique, C.D.M. The Watershed Transformation Applied To Image Segmentation. *Scanning microscopy. Supplement, 6,* 299-314.

Bilheux, H. Z., McGreevy, R. & Anderson, I. S. (2009). Neutron imaging and applications. *Springer US, Boston, MA*.

Bourlieu, C., Guillard, V., Powell, H., Vallès-Pàmies, B., Guilbert, S. & Gontard, N. (2008). Modelling and control of moisture transfers in high, intermediate and low aw composite food. *Food Chemistry, 106,* 1350-1358.

Castlejohn, C. A. (2012). Analysis of changes in structure and moisture in starch extrudates during storage using micro-CT and MRI imaging techniques. *Ph.D. Thesis. UGA Electronic Theses and Dissertations*.

Chaunier, L., Della Valle, G. & Lourdin, D. (2007). Relationships between texture, mechanical properties and structure of cornflakes. *Food Research International, 40,* 493-503.

Cho, K. Y. & Rizvi, S. S. H. (2010). New generation of healthy snack food by supercritical fluid extrusion. *Journal of Food Processing and Preservation,* **34,** 192-218.

Dalen, G., Duynhoven, J., Blonk, J. C. G., Mohorič, A., Ramos-Cabrer, P. & van den Doel, R. (2005). Multi dimensional imaging of foods using magnetic resonance imaging. *GIT. Imaging & Microscopy,* **7,** 42-44.

Dalen, G., Peter, N., Van Vliet, L., Voortman, L. & Esveld, D. C. (2007). 3D Imaging and analysis of porous cereal products using X-ray microtomography. **26,** 169-177.

Defraeye, T., Nicolaï, B., Mannes, D., Aregawi, W., Verboven, P. & Derome, D. (2016). Probing inside fruit slices during convective drying by quantitative neutron imaging. *Journal of Food Engineering,* **178,** 198-202.

Esveld, D. C., van der Sman, R. G. M., van Dalen, G., van Duynhoven, J. P. M. & Meinders, M. B. J. (2012). Effect of morphology on water sorption in cellular solid foods. Part I: Pore scale network model. *Journal of Food Engineering,* **109,** 301-310.

Fan, J., Mitchell, J. R. & Blanshard, J. M. V. (1996). The effect of sugars on the extrusion of maize grits: I. The role of the glass transition in determining product density and shape. *International Journal of Food Science & Technology,* **31,** 55-65.

Grünzweig, C., Mannes, D., Kaestner, A., Schmid, F., Vontobel, P., Hovind, J., Hartmann, S., Peetermans, S. & Lehmann, E. (2013). Progress in Industrial Applications using Modern Neutron Imaging Techniques. *Physics Procedia,* **43,** 231-242.

Guarino, V., Guaccio, A., Netti, P. A. & Ambrosio, L. (2010). Image processing and fractal box counting: user-assisted method for multi-scale porous scaffold characterization. *Journal of Materials Science: Materials in Medicine,* **21,** 3109-3118.

Gueven, A. & Hicsamaez, Z. (2013). Quantitative measurement of the Pore stricter, In: Pore Structure in Food: Simulation, Measurement and Applications.

Guillard, V., Broyart, B., Bonazzi, C., Guilbert, S. & Gontard, N. (2003a). Evolution of Moisture Distribution During Storage in a Composite Food Modelling and Simulation. *Journal of Food Science,* **68,** 958-966.

Guillard, V., Broyart, B., Bonazzi, C., Guilbert, S. & Gontard, N. (2003b). Modelling of Moisture Transfer in a Composite Food: Dynamic Water Properties in an Intermediate aw Porous Product in Contact with High aw Filling. *Chemical Engineering Research and Design,* **81,** 1090-1098.

Guillard, V., Broyart, B., Guilbert, S., Bonazzi, C. & Gontard, N. (2004). Moisture diffusivity and transfer modelling in dry biscuit. *Journal of Food Engineering,* **64,** 81-87.

Hsieh, F., Peng, I. C. & Huff, H. E. (1990). Effects of Salt, Sugar and Screw Speed on Processing and Product Variables of Corn Meal Extruded with a Twin-Screw Extruder. *Journal of Food Science,* **55,** 224-227.

Jafari, M., Koocheki, A. & Milani, E. (2017). Effect of extrusion cooking on chemical structure, morphology, crystallinity and thermal properties of sorghum flour extrudates. *Journal of Cereal Science,* **75,** 324-331.

Karkle, E. L., Keller, L., Dogan, H. & Alavi, S. (2012). Matrix transformation in fiber-added extruded products: Impact of different hydration regimens on texture, microstructure and digestibility. *Journal of Food Engineering,* **108,** 171-182.

Masavang, S., Roudaut, G. & Champion, D. (2019). Identification of complex glass transition phenomena by DSC in expanded cereal-based food extrudates: Impact of plasticization by water and sucrose. *Journal of Food Engineering,* **245,** 43-52.

Mezreb, K., Goullieux, A., Ralainirina, R. & Queneudec, M. (2006). Effect of sucrose on the textural properties of corn and wheat extrudates. *Carbohydrate Polymers,* **64,** 1-8.

Moore, D., Sanei, A., Van Hecke, E. & Bouvier, J. M. (1990). Effect of Ingredients on Physical/Structural Properties of Extrudates. *Journal of Food Science,* **55,** 1383-1387.

Moraru, C. I. & Kokini, J. L. (2003). Nucleation and Expansion During Extrusion and Microwave Heating of Cereal Foods. *Comprehensive Reviews in Food Science and Food Safety,* **2,** 147-165.

Ott, F., Loupiac, C., Désert, S., Hélary, A. & Lavie, P. (2015). IMAGINE: A Cold Neutron Imaging Station at the Laboratoire Léon Brillouin. *Physics Procedia,* **69,** 67-70.

Philipp, C., Oey, I., Silcock, P., Beck, S. M. & Buckow, R. (2017). Impact of protein content on physical and microstructural properties of extruded rice starch-pea protein snacks. *Journal of Food Engineering,* **212,** 165-173.

Pitts, K. F., Favaro, J., Austin, P. & Day, L. (2014). Co-effect of salt and sugar on extrusion processing, rheology, structure and fracture mechanical properties of wheat–corn blend. *Journal of Food Engineering,* **127,** 58-66.

Pitts, K. F., McCann, T. H., Mayo, S., Favaro, J. & Day, L. (2016). Effect of the Sugar Replacement by Citrus Fibre on the Physical and Structural Properties of Wheat-Corn Based Extrudates. *Food and Bioprocess Technology,* **9,** 1803-1811.

Plews Andrew, G., Atkinson, A. & McGrane, S. (2009). Discriminating Structural Characteristics of Starch Extrudates through X-ray Micro-tomography using a 3-D Watershed Algorithm. In: International Journal of Food Engineering.

Robin, F., Dubois, C., Pineau, N., Labat, E., Théoduloz, C. & Curti, D. (2012). Process, structure and texture of extruded whole wheat. *Journal of Cereal Science,* **56,** 358-366.

Roca, E., Broyart, B., Guillard, V., Guilbert, S. & Gontard, N. (2007). Controlling moisture transport in a cereal porous product by modification of structural or formulation parameters. *Food Research International,* **40,** 461-469.

Ryu, Neumann P. E. & E., W. C. (1993). Effects of Some Baking Ingredients on Physical and Structural Properties of Wheat Flour Extrudates. *Cereal Chemistry,* **70,** 291-297.

Scussat, S., Ott, F., Hélary, A., Desert, S., Cayot, P. & Loupiac, C. (2016). Neutron Imaging of Meat during Cooking. *Food Biophysics,* **11,** 207-212.

Scussat, S., Vaulot, C., Ott, F., Cayot, P., Delmotte, L. & Loupiac, C. (2017). The impact of cooking on meat microstructure studied by low field NMR and Neutron Tomography. *Food Structure*.

Singkhornart, S., Edou-ondo, S. & Ryu, G.-H. (2014). Influence of germination and extrusion with CO2 injection on physicochemical properties of wheat extrudates. *Food Chemistry,* **143,** 122-131.

Sozer, N., Dogan, H. & Kokini, J. L. (2011). Textural Properties and Their Correlation to Cell Structure in Porous Food Materials. *Journal of Agricultural and Food Chemistry,* **59,** 1498-1507.

Tanoi, K., Hamada, Y., Seyama, S., Saito, T., Iikura, H. & Nakanishi, T. M. (2009). Dehydration process of fish analyzed by neutron beam imaging. *Nuclear Instruments and Methods in Physics Research Section A: Accelerators, Spectrometers, Detectors and Associated Equipment,* **605,** 179-184.

Verboven, P., Defraeye, T. & Nicolai, B. (2018). 1 - Measurement and visualization of food microstructure: Fundamentals and recent advances A2 - Devahastin, Sakamon. In: Food Microstructure and Its Relationship with Quality and Stability. Pp. 3-28. Woodhead Publishing.

von Borries-Medrano, E., Jaime-Fonseca, M. R. & Aguilar-Méndez, M. A. (2016). Starch–guar gum extrudates: Microstructure, physicochemical properties and in-vitro digestion. *Food Chemistry,* **194,** 891-899.

Wang, Q. & Ward, R. K. (2007). Fast Image/Video Contrast Enhancement Based on Weighted Thresholded Histogram Equalization. *IEEE Transactions on Consumer Electronics,* **53,** 757-764.

Yang, J., Martin, A., Richardson, S. & Wu, C.-H. (2017). Microstructure investigation and its effects on moisture sorption in fried potato chips. *Journal of Food Engineering,* **214,** 117-128.
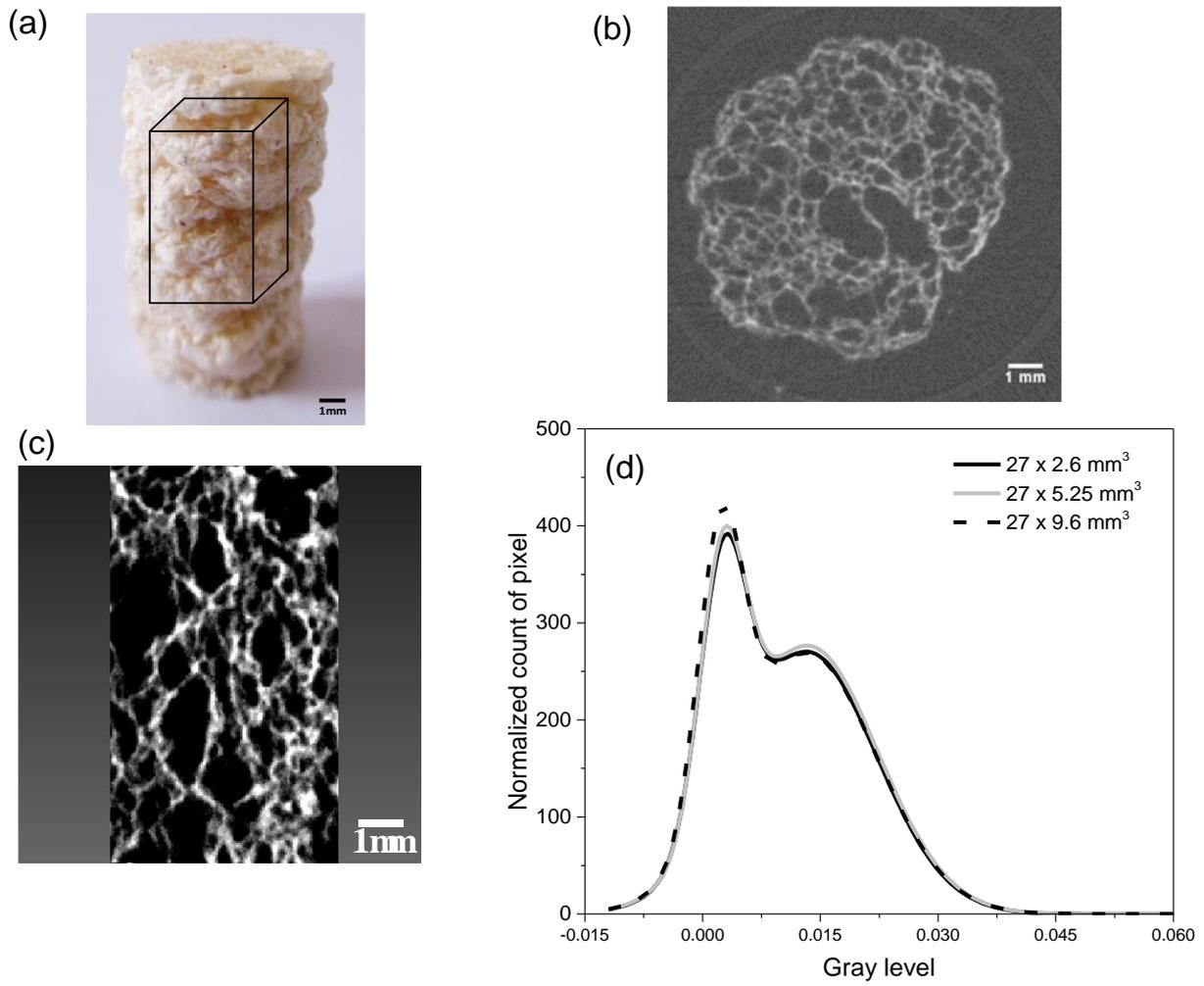
Fig. 3.1 (a) photos of extrudates with an illustration of ROI; (b) grey image of a reconstructed radial slice) (c) grey image of a reconstructed axial slice (d) histogram of a sample with different ROI.
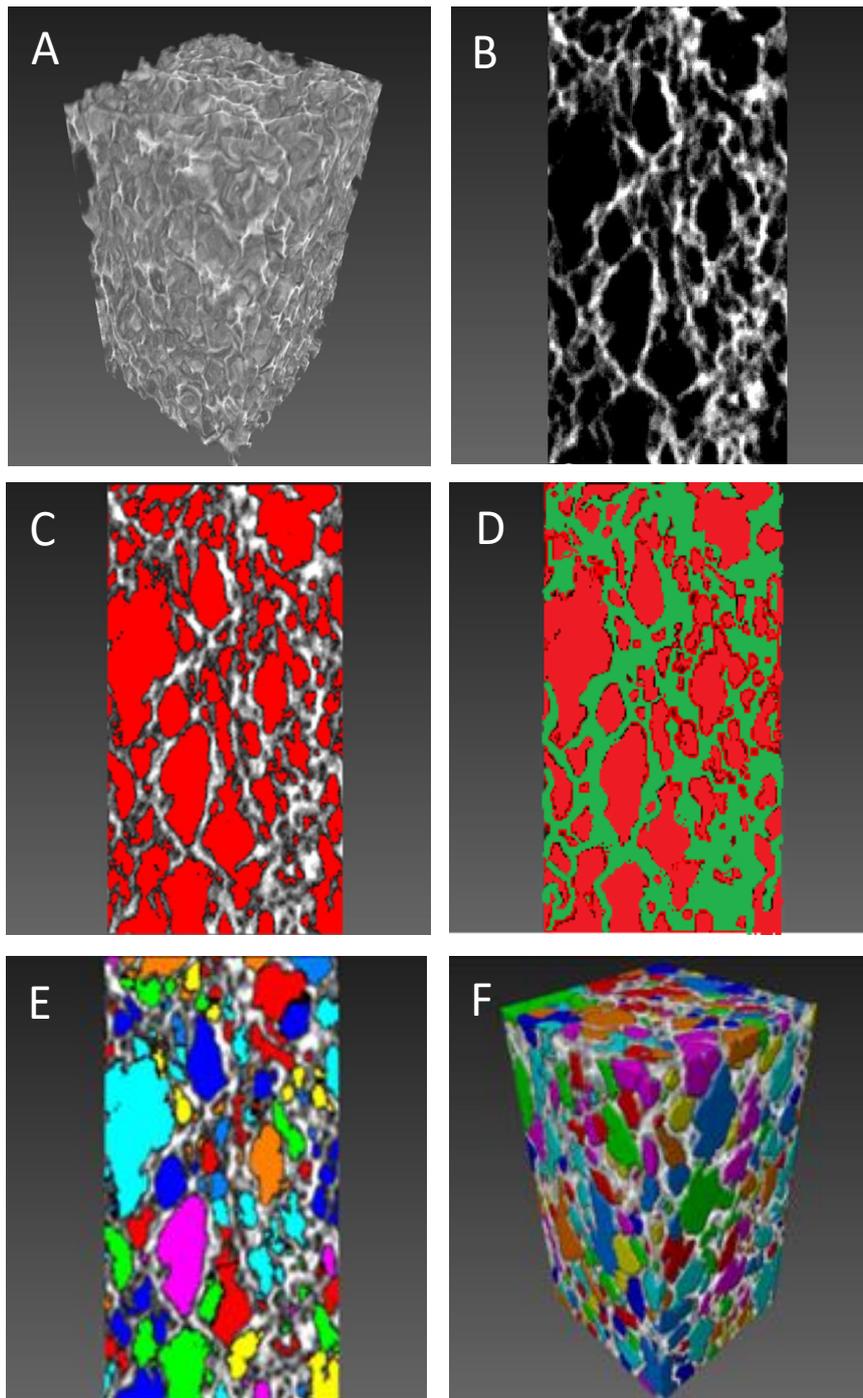
Fig. 3.2 Image processing steps of extrudate with 10% sucrose. (A) 3D rendering structure produced by Avizo. (B) extracted slice (2D-grayscale image) of A . (C) pore segmentation of the image (red) ,(D) matrix sehmentation (green), (E) Pores labeling (connected set of pores are labeled with same color). (F) reconstructed 3D-labelled tomography.

Relative humidity (%)	0% Sucrose	10% Sucrose	15% Sucrose
11%			
75%			
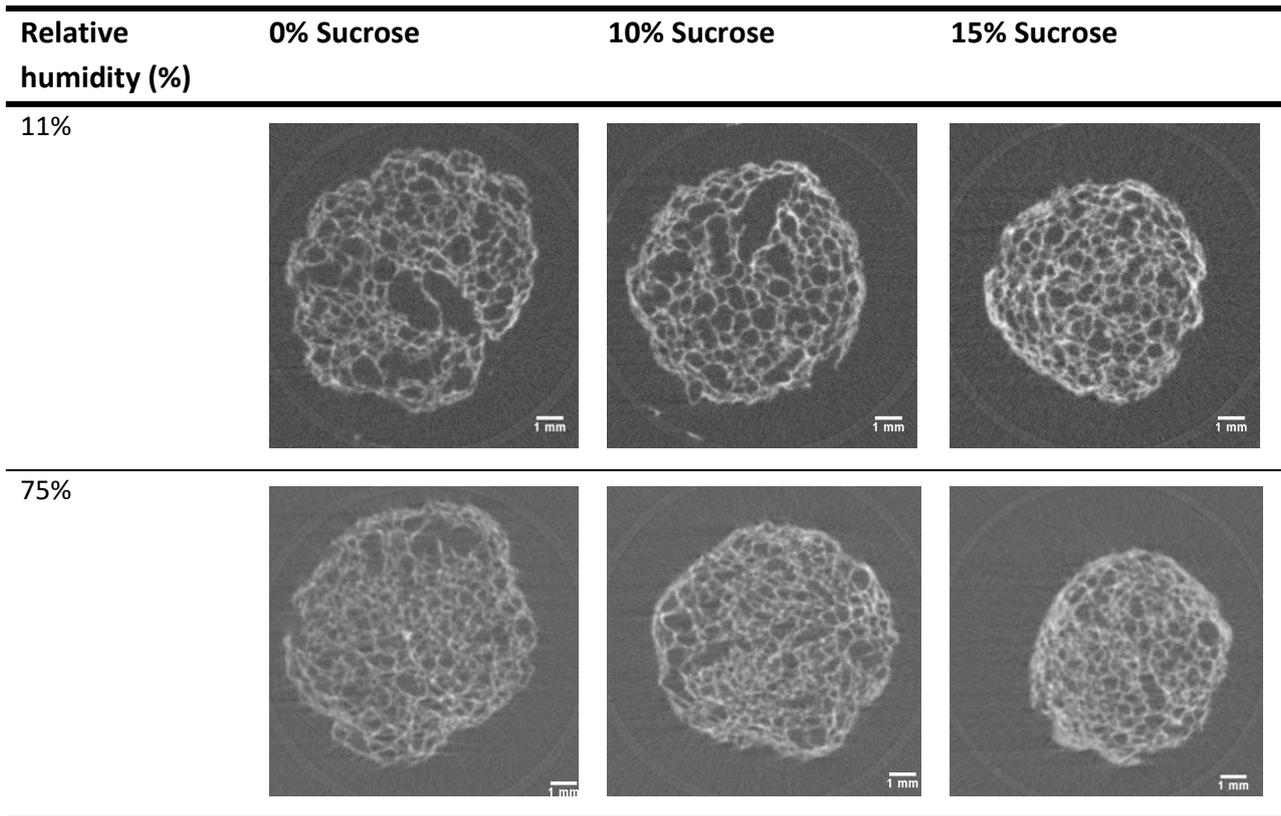
Fig. 3.3 2D horizontal cross-sections through 3D neutron tomography images for extrudate containing sucrose 0, 10 and 15% sucrose, processing with 10 and 15% feed water and storing at 11 and 75% RH.
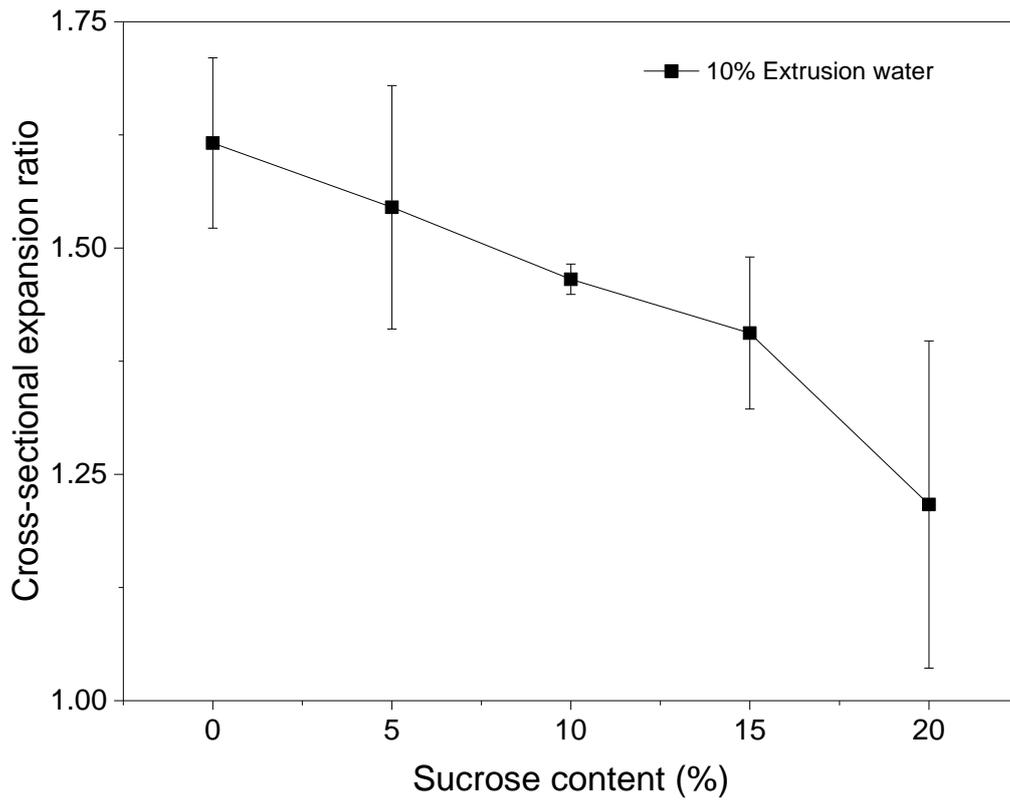
Fig. 3.4 The effect of sucrose content and extrusion water on SEI of extrudates contained various sucrose content and produced at 10% feed water.
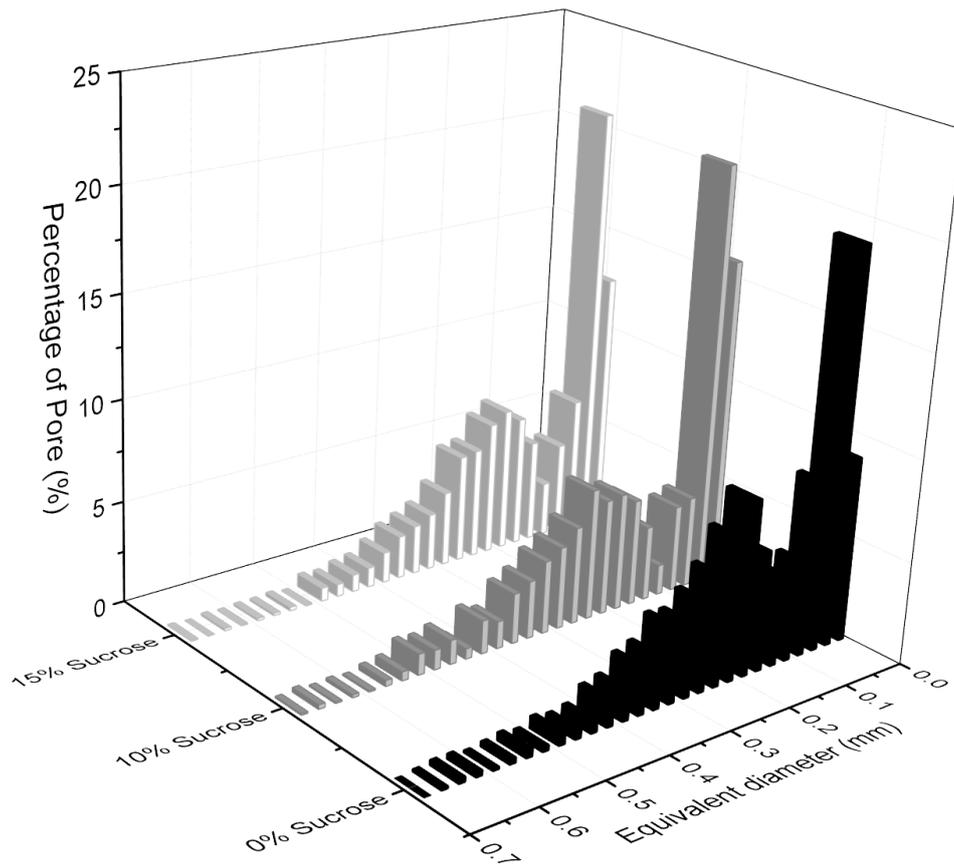
Fig. 3.5 Histogram showing the percentage of pores in a certain location of matrix of extrudates contain 0, 10 and 15% sucrose with dimension 5.26 x 5.26 x 9.6 mm^3 voxel for sample stored at 11% RH.
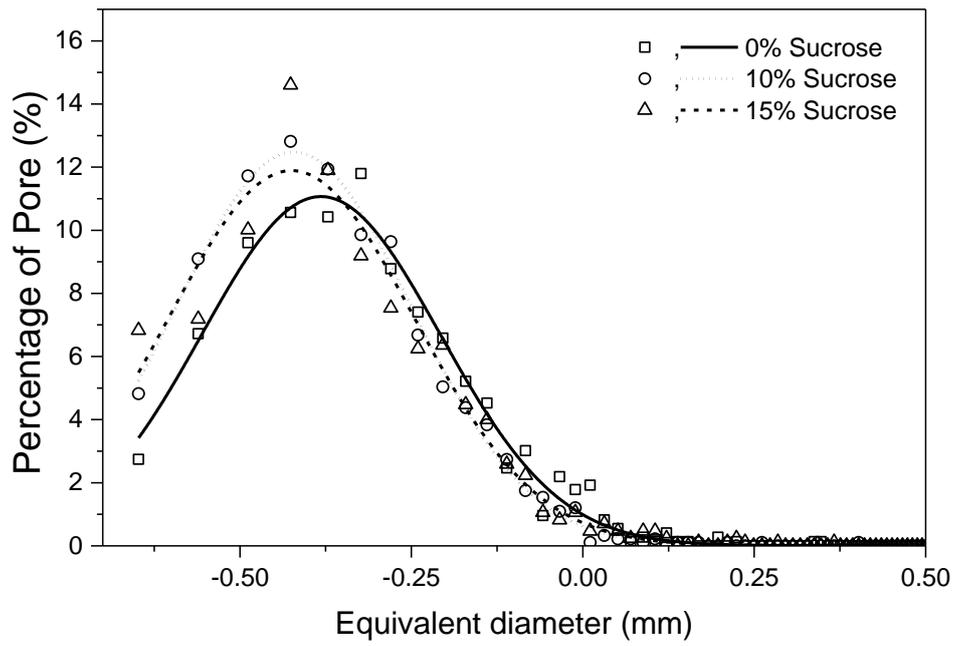
Fig. 3.6 Comparison pore distribution generated from the microstructure created in AvizoFire for extrudate with different sucrose content and stored at 11% RH.
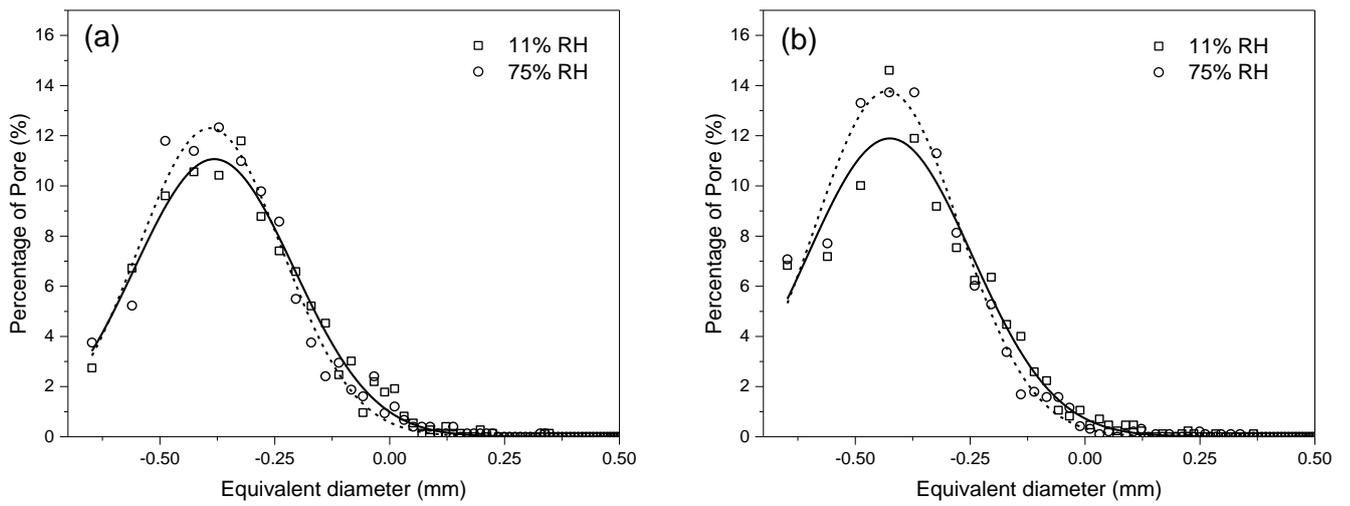
Fig. 3.7 Comparison pore distribution generated from the microstructure created in AvizoFire for extrudates contained 0% (a) and 15% (b) sucrose and stored at 11% and 75% RH.
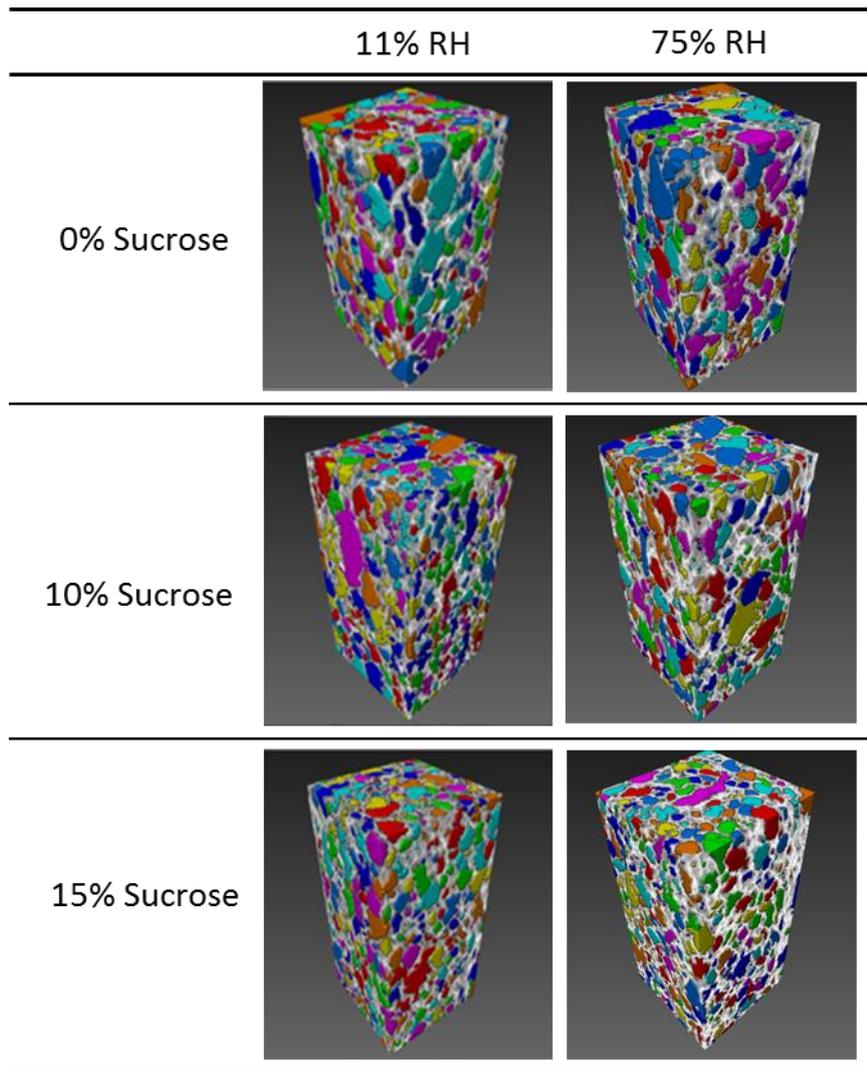
Fig. 3.8 3D visualization with labelled image of pores for extrudate contained sucrose 0, 10 and 15% sucrose, produced at 10% feed water and stored at 11 and 75% RH.

Chapter 4:

Study of water sorption for expanded cereal-based extrudates and the effect of physical aging.

Supuksorn Masavang, Gaëlle Roudaut Dominique Champion,
University of Bourgogne Franche-Comté, AgroSup Dijon, PAM UMR A 02.102, F-21000 Dijon, France

*Corresponding author: Dominique Champion
E-mail address: dominique.champion@agrosupdijon.fr

Abstract

The effect of sucrose content (0–10%), extrusion water (10–15%) and physical aging on the water uptake ability of expanded cereal-based extrudates were studied using co-rotating twin screw extruder under the same processing settings. The sorption isotherms obtained using dynamic vapor sorption instrument were applied with BET, GAB, Peleg and Freundlich model. Peleg's model gave the best fitting. GAB monolayer values showed different trends depending upon modelling range. Hysteresis decreased in magnitude with increasing sucrose and physical aging caused by water sorption history affected hysteresis. Apparent kinetics of water diffusion showed two different sorption sites, the first kinetic was almost constant and could be adsorption phenomena at the surface. The second one reflected first an initial slowing in dynamics whereas a sharp increase was found at higher water content. This behavior may be related to structure collapse. Sucrose, physical aging and sorption history could induce physical changes and impact water sorption behaviors.

Keywords: Extruded cereal-based products, Sugars, Sorption isotherm, Water uptake, Physical aging.

1. Introduction

Most of extruded cereal-based snack foods have a characteristic, porous, crispy texture. Their sugar content influences their taste and texture, but they are being disregarded due to the contribution of their high sugar content to a high glycemic index (Aston *et al,.* 2008). Sugar reduction in extruded products is one of the important goals for food manufacturers to produce healthier foods. Exposure of such food materials to high relative humidity (RH) often results in a detrimental increase in water content (Roos *et al,.* 1998) and change of texture. Katz and Labuza (1981) showed that many snack foods lost their crispness due to the plasticization by water of materials stored at a RH higher than a material-dependent critical value. The moisture sorption isotherm can be used to study storage stability and predict the possible changes that might affect the stability and quality of dried food. Breakfast cereals contain a variety of ingredients. The heterogeneity of such complex matrix can make sorption isotherm study of breakfast cereals challenging. There are two main factors influencing the amount and rate of moisture sorption: water activity equilibrium (*i.e* thermodynamics) and factors affecting the apparent diffusion rate of water (*i.e.* dynamics of mass transfer) (Labuza and Hyman 1998). A number of models have been suggested to describe moisture sorption isotherms (Guillard *et al,.* (2003) including kinetic models based on multilayer (BET and GAB models), semi-empirical (Ferro-Fontan, Henderson and Halsey models) and empirical models (Peleg, Smith and Oswin models). The GAB model is considered to be the most versatile sorption model available in the literature. Roca *et al,.* (2008) described a model of moisture transfer in a composite food consisting of a sponge cake in contact with a fresh wet filling using a mathematical model based on Fick's 2nd law. These models have also been extended to predict moisture content variations during fruits and grains drying (Mercier *et al,.* 2014, Li *et al,.* 2016), or soaking (Machado *et al,.* 1998, Sacchetti *et al,.* 2003, Sacchetti *et al,.* 2005).

However little published information exists in the literature regarding the kinetics of the sorption process for breakfast cereal as both a function of sucrose content and storage. Among these rare studies, Risbo (2003) developed a model to predict moisture transfer in breakfast cereal-resin system. Esveld *et al,.* (2012) discussed and simulated dynamics of moisture sorption into crackers with a pore scale network model. The application of predictive models to assess moisture transfer in a wide range of food products are

indeed valuable data for the food industry and help meeting the challenges associated with marketing innovative, long shelf life and nutritionally acceptable products.

The extrusion-cooking process of native starch destroys the crystallinity of the amylopectin component, leading to a mostly amorphous extrudate with relatively limited moisture, thus consumed in the glassy state. Dual glass transitions have been observed on differential scanning calorimetry (DSC) thermograms for extruded cereal-based products suggesting that the amorphous regions are heterogeneous (Masavang *et al,.* 2019). Such glassy, out of thermodynamical equilibrium, materials are known to possibly exhibit a structural relaxation over time to approach their thermodynamical equilibrium. Certain macroscopic properties such as density, mechanical properties, and vapor permeability, are accompanied by a time-dependent relaxation in amorphous glassy polymeric materials, including foods (Anzai *et al,.* 2011). Until now the relationship between storage in the glassy state (*i.e*. physical aging) and water sorption behavior has rarely been discussed (Kim et al. 2001) in detail. Among the few existing references on the matter, Kim *et al,.* (2001) indicated that the water sorption ability of glassy starch decreased simultaneously with the enthalpy relaxation associated with physical aging.

In addition to control the sorption properties of foods, it is also necessary to control the threshold temperature and humidity conditions to prevent a glass transition upon storage of powder products (Bhandari and Hartel 2005). The water activity value at which T_g becomes lower than room temperature has been identified as the critical relative humidity (RH_c) (Roos 2002, Sablani *et al,.* 2007, Sillick and Gregson 2010). Several studies have demonstrated that the RH_c value determined using automatic water vapor sorption instruments, could be used to identify the glassy to rubbery transition, in agreement with the DSC method (Burnett *et al,.* 2004, Li and Schmidt 2011). The high data resolution resulting from dynamic water sorption methods makes it possible to observe distinct inflection points in the curve representing the changes in sorption properties accompanying the glass transition (Carter and Schmidt 2012). Yuan *et al,.* (2010) and Yuan *et al,.* (2011) investigated the relationship between polydextrose T_gs values as a function of % RH, using thermal methods DSC and modulated differential scanning calorimetry (MDSC), and the RH_c values of polydextrose as a function of temperature (15–40 °C), using dynamic dewpoint isotherms (DDI). At

25 °C, the RH_c value was 49.7% RH, whereas the RH value associated with the MDSC midpoint T_g equal to 25°C was 44.6%. The authors attributed the differences between the two data sets to the time dependency of the DDI obtained RH_c values. Li and Schmidt (2011) applied two instrumental (DVS ramping and equilibrium) methods and the traditional salt slurry method to determine the RH_c values for amorphous polydextrose. The RH_c determined from the DVS equilibrium method was closer to the calculated DSC T_g onset RH_c value than the RH_c determined with the ramping method.

Although many studies have been conducted on physical aging of starch, few studies have been done on composite food. The relationship between physical aging and water sorption behavior of extruded products has not been studied in detail. In the present study, the effect of sucrose content on water uptake ability and that of physical aging (through storage in the glassy state) on water sorption has been investigated to control the physical changes induced by aging during ambient storage conditions.

2. Experimental

2.1 Sample composition and extrusion

Wheat flour, wheat starch, gluten and sucrose commercial grade were supplied by ADM CHAMTOR (Les Sohettes, France). The extrusion of the ingredient blends containing 0, 5, 10, 15 and 20% wt sucrose with wheat flour 53-73% wt, wheat starch 16% wt, gluten 16% wt and sodium chloride 1% wt was carried out in a Clextral BC-45 intermeshing twin-screws extruder with a 1.5 m long barrel using 10% wt initial moisture content (dry basis). The barrel heating zones were at 80 °C, 130 °C and 160 °C (±2 °C). A 6.0 mm circular die was fitted to the end of the barrel and used to produce the cylinder-shaped extrudates. The screw speed was 150 rpm. Feed rates were controlled: the solid feed at 36 kg/hr and water input of 4 L/hr, giving a water content of 19.5-24.5% wb of molten material in barrel depending on blend formulation and ~10% wb in the final extruded samples. After extrusion, samples were oven dried during 5 min at 150 °C and they were hermetically sealed in bag after cooling, and further kept at ambient temperature.

2.2 Moisture Sorption Isotherm–DVS Method

Samples (15±1 mg) stored over phosphorus oxide (P_2O_5) for 7 days were loaded onto pans and placed and sealed into the DVS sample chamber (Dynamic Vapor Sorption DVS-2000, Surface Measurement Systems, London, U.K.). The sample was placed in the DVS at 30 °C, a_w = 0.01 for 240 min with a dry nitrogen gas flow (100cm^3/min) to complete desiccation of the sample. The sample was then exposed at 25 °C to increasing relative humidity from 0% RH to 90% RH and then back down to 0% RH for adsorption and desorption processes following 10% increments, respectively. The relative mass change as function of time (dm/dt) criterion was set at 0.002%/min for 5 consecutive min and the maximum time at each %RH was set at 1500 min. Once the mass change was below 0.002%/min, the RH was set to the next programmed humidity stage. The balance was calibrated at 25 °C with a 100 mg weight.

2.3 Modeling methodology

2.3.1 Determination of water content of sorption kinetics (y_0)

The analysis of sorption kinetics was performed using a two exponential kinetics model (Eq. 4.1). Kinetics curves of each sample were obtained by plotting mass gain (%) or mass loss (%) against time. For the evaluation of the sorption kinetics each humidity level was treated separately. The time record and related weight change were transformed by setting the initial time, $t_0 = 0$ and the sample mass change, y_0 at time zero considering t$_0$ as the point where an RH step change occurred. Non-Linear curve fitting was fitted to the adsorption and desorption data curves of the extruded products using OriginPro2017 software (Origin Lab. Corporation USA).

$$y = y_0 + A_1.\exp\left(-\frac{x-x_0}{t_1}\right) + A_2.\exp\left(-\frac{x-x_0}{t_2}\right) \qquad\qquad \text{Eq. 4.1}$$

where y is the moisture content at infinite time of sample exposure at a constant RH and y_0 is the moisture content of the sample at time zero. The sorption kinetics curve is composed of two exponential terms representing fast and slow processes with characteristic times t_1 and t_2 respectively. A_1 and A_2 are constants. Extensive statistical procedures are available to test the results.

2.3.2 Modelling sorption isotherm

The data obtained corresponding to a_w and water content were adjusted to BET (Eq.2) (Brunauer *et al,.* 1938), GAB (Eq.3) (van den Berg 1985), Peleg (Eq.4) (Peleg 1993), and Freundlich (Eq.5) (Freundlich 1906) equations in order to determine the best fit for our extrudate samples. The model parameter estimations were carried out using the SOLVER module from Excel software (Microsoft Excel 2010).

The equations can be expressed as Equations 4.2-5:

$$y_0 = \frac{m_0 C a_w}{(1-a_w)(1-a_w+C\cdot a_w)} \qquad\qquad \text{Eq. 4.2}$$

$$y_0 = \frac{m_0 C k a_w}{(1-k\cdot a_w)(1-k\cdot a_w+C\cdot k\cdot a_w)} \qquad\qquad \text{Eq. 4.3}$$

$$y_0 = k_1 a_{w1}^n + k_1 a_{w2}^n \qquad\qquad \text{Eq. 4.4}$$

$$y_0 = k_F a_w^{1/n} \qquad\qquad \text{Eq. 4.5}$$

The y_0 and a_w are equilibrium moisture content and water activity, respectively. The other symbols are the model constants.

Fermi's equation (Eq. 4.6) was used to describe the changes in kinetics of water transfer with the environmental relative humidity at a constant temperature.

$$t_i = \frac{(t_0 - t_r + k)}{\left\{1 + exp\left[\frac{(a_w - a_{wc})}{b}\right]\right\}} + t_r \qquad\qquad \text{Eq. 4.6}$$

Where t_i is the time constant of apparent water diffusion dependent on water activity; t_o is the value of the time constant at $a_w \sim 0$; t_r is the residual magnitude of the property after the transition; a_w is the water activity; a_{wc} is the critical water activity where $t_i = t_o/2$ (and where a drastic change in time constant takes place); k is a constant corresponding to the slope of the increasing region before the peak and b a constant describing the slope of transition of the analyzed variable (Arimi *et al,.* 2010).

To evaluate the goodness of the fit by each equation of the experimentally determined isotherms, the mean absolute percentage error modules (p) was calculated using the following equation:

$$p\,\% = \frac{100}{N}\sum_{i=1}^{N}\frac{m_i - m_{pi}}{m_i} \qquad\qquad \text{Eq. 4.7}$$

where N is the number of experimental data; m_i are experimental values and m_{pi} are predicted values. It is generally assumed that a good fit is obtained when $p < 10\%$.

2.4 X-ray diffraction (XRD).

The extrudate powders were kept in sealed containers containing saturated solutions of lithium chloride and potassium chloride, which produced relative humidities of 11% and 84% respectively at 25 °C. Before analysis, the samples were all equilibrated to specific water activities for at least 2 weeks. Vacuum was used to accelerate equilibrium. The crystalline structure of powdered extrudates was studied with a X-Rays Diffractometer (Siemens D5000, Germany). The X-ray generator supplied CuKα radiation at 0.154 nm wavelength (λ = 1.5406 °A) and an INEL CPS 120 curved detector. X-ray patterns were recorded in the 2θ range 5–100° at an angular interval of 0.5°min^{-1}.

3. Results and discussion

3.1 Water sorption isotherms

The water sorption and desorption of extruded sample at 10% sucrose content are shown in Fig 4.1. Figures 4.1b-c illustrates the sorption and desorption of the same sample in the range 50-60 % RH. The sorption kinetics for each humidity step were described with a two exponential equation (Eq. 4.1) and estimated equilibrium moisture values (y_0) were obtained. The results of the model suggested the existence of two distinct sorption processes with different accessibilities for water vapor, according to the different characteristic times. BET, GAB, Peleg, and Freundlich models were applied to fit sorption isotherm data (Eq. 4.2-4) and the sorption description by these models (Table 4.1) showed different fit goodness

The most successful four parameter model is the Peleg model because of its number of parameters to adjust. The highest p values (40.08%) were observed for Freundlich equation for all types of extrudates studied indicating a poor fitting.

Equilibrium moisture content (EMC) increased slowly in the a_w range (0 to 0.6), followed by a steep rise at a_w 0.7 for both extrudates produced at 10 and 15% extrusion water (Fig. 4.2a,b). At low water activities, the physical state of sugars may have an effect on the sorption properties. Amorphous sugars are known to adsorb more water than crystalline materials (Chinachoti and Steinberg 1986a). At higher a_w (> 0.7), an exudation (leaching of sugars) was observed.

Survey of literature has shown that the GAB and Peleg models could give very reliable approximation of the full range of water vapor sorption data for many raw and processed food materials (Shittu *et al,.* 2015). The GAB constants M_o, C and K were computed from linear regression of water content versus a_w. In the case of BET, the data was modelled up to a relative humidity of 50%, as suggested by literature. The GAB model was fitted either to the whole data range (0-90% RH) or up to 50% RH only. The value of the monolayer moisture content (m_0) is of particular interest since it indicates the amount of water strongly adsorbed to specific sites at substrate surface and is considered as the optimal value to ensure stability of material (Rao 2015). Below m_0, rate of deteriorative changes is kept minimum. The m_0 values of extrudates produced at 10 and 15% extrusion water at various sucrose content estimated by GAB and BET are shown in Fig 4.3. For the GAB monolayer modelled up to 90% RH, m_0 appears to increase when the sucrose content is increase but in opposite, with the same GAB model, if RH is considered below 50% only for fitting, m_0 appears to decrease with the amount of sucrose (Table 4.2). It seems that at low RH, sucrose decreased the availability of active sorption sites for water on biopolymers, hence reducing the surface area available for water molecules. The fitted values for m_0 is consistent with the shape of isotherm curves (Fig. 4.2): showing a lower water content at equilibrium with an increase of sucrose content for low RH, but also a reverse effect for high RH. In fact, the water vapor adsorption isotherms had the shape of Brunauer's type II isotherm characteristic for products with a high sugar content. At low water activities (below ~ 0.6), the amount of adsorbed water increased gradually. This reflected water sorption by the starch-based components of extrudate made from composite flour mixture. At water activities exceeding 0.6, there is a steep rise in the isotherm due to water is in the free state and condensed into the pores of the material, gaps and capillaries (Rakshit *et al,.* 2014). However, the sugar component in the extrudate influenced the sorption behavior, increasing the equilibrium water uptake at RH higher than 60%. (Panjagari *et al,.* 2015). This step suggests changes in the product quality, when the soluble materials of the products began to dissolve in the condensed water (Chetana *et al,.* 2005). A crossover point between the various sucrose of isotherm was clearly observed at a water activity of 0.60-0.75. The isotherm crossover behavior in presence of plasticizers (glycerol and sugar) or temperature has been widely observed in -carbohydrate rich foods such as dried

fruits, barley malt, bovine gelatin films, cold water fish gelatin films, soy protein-sugar systems and rice and waxy maize extrudate (Tsami *et al,.* 1990, Enrione *et al,.* 2007b, Díaz *et al,.* 2011, Hazaveh *et al,.* 2015). Labuza (1984) and Gogus *et al,.* (1998) suggested that the crossing of isotherms could be caused by the dissolution of sugars or crystalline substances. As sucrose content increased, the dissolution of sugars could increase and result in a greater amount of water sorption by the extrudates. In agreement with Laaksonen and Labuza (2001). Kilburn *et al,.* (2005) stated that the higher water sorption resulted from an increased hydrogen bonding as the structure of the material became more flexible. As a consequence, amorphous sucrose in sample may recrystallize above all for the highest sucrose contents (20%) if exposures at high relative humidity. Similar results have been obtained for various dry foods: for example in dry biscuits (Bourlieu *et al,.* 2008), and in various cookies and corn snacks (Palou *et al,.* 1997). According to Falade and Aworh (2004), at low a_w it is possible to have a local dissolution of vitreous sugar, a swelling of proteins and appearance of new active sites. In the intermediate a_w range, sorption take place at less active sites and, from this point of view, amorphous sugars are known to adsorb more water than the crystalline materials (Chinachoti and Steinberg 1986b).These authors reported this behavior and attributed the crossover point to the endothermic dissolution of sugars at high water activity. Enrione *et al,.* (2007b) suggested the OH groups of plasticizer and biopolymer acting as an adsorbent at low RH may explain these results. At low vapor pressure hydrogen bonding is the main force involved in the adsorption mechanism, suggesting the predominance of plasticizer over water. Inversion behavior was detected for RH > 70%, where sucrose facilitated water sorption.

The sorption isotherm curves of products at sucrose content lower than 20%, produced at 15 % feed water during extrusion showed equilibrium moisture for each RH that is not significantly different than for sample produced at 10 % water processing (Fig 4.4). This result indicated that the macroscopic structure of the samples may be really different in porosity but because they have the same solid composition, they show the same sorption/desorption isotherm at equilibrium. For sample at 20% sucrose and processed with 15% feed water, the observed behavior is probably due to a partially sucrose crystallisation during the cooling just after extrusion.

At a certain RH (RH_c), water sorption lowered the glass transition temperature (T_g) of extrudate to the experimental temperature of isotherm determination. It is known that glass corresponds to an out of equilibrium physical state, but the rubber material above T_g is in equilibrium. From one glass, we may have one rubbery material, but from one rubber, you may several glassy materials depending on the cooling or dehydration kinetic. The points where sorption and desorption curves merged were called the "merging point" in this study (Fig. 4.4), and above this specific point, sorption/desorption curves gave the same values for equilibrium water content for a given RH. Below, the merging point, the water amount may differ as function of RH if sorption or desorption is considered. This merging point can be considered as the RH_c, the relative humidity that give a glass transition at temperature equal to the sorption/desorption temperature.

The effect of sample history on the sorption isotherm of extrudates with 10% sucrose was investigated (Fig 4.5) through the application of multiple sorption/desorption cycles. The second sorption curve exhibited a lower magnitude hysteresis than the first sorption. Interestingly there are differences in sorption curves recorded upon the 2 identical step cycles (0-90-0% RH) while the desorption curves followed nearly the same path (Fig 4.6b). Ramping cycles seemed to have less effect on sorption curves. This behavior remains yet to be understood; but it could be associated with an aging process occurring during the steps below RH_c (so below T_g). This highlights the effect of sample history upon its sorption properties.

3.2 Critical relative humidity RH_c and water content (W_c)

RH_c values can be used to detect the glassy to rubbery transition by a ramping method developing by Burnett *et al,.* (2004). Dynamic vapor sorption (DVS) instrument was used to identify the RH_c value inducing the glass transition at a specified temperature. The RH_c value that induced the glass transition at the experimental temperature was measured at the linear extrapolated intersection between surface adsorption of water vapor and absorption of water vapor into the bulk structure. Sorption isotherms often exhibit a critical turning point where the isotherm curve deviates from the initial flat region and begins to take up more water, when water uptake changes from surface adsorption to bulk absorption (Burnett *et al,.*

2004). Traditionally, the turning point/inflexion point is determined by fitting two straight lines before and after the critical points and determining their intersection point.

Fig. 4.7a displays the result for sorption experiments run at 2, 6 and 10% RH/h ramping rate for extrudate with 10% sucrose and Fig 4.7b for 0% sucrose sample. The net change in mass is plotted versus the sample RH(%) to highlight the effects of changing ramping rates. All features remain stable over the entire range of ramping rates and change in mass increased with decreasing ramping rate. The glass transition relative humidity (RH_g) was measured at the slope change in the curve (denoted by intersection of dashed lines in Fig.6b). However, RH_c was not easy to determine due to the multiple intersection points that could be chosen. To try to be more precise, first derivative of sorption isotherm was used to measure RH_c after a smoothing of the data using OriginPro 2017 software (Origin Lab. Corporation USA) (Fig 4.7c). The large change in slope was observed around 30% RH and >75% RH and the result was not clear to identify RH_c for extruded samples.

Several authors have coupled sorption isotherms data with those of glass transition temperatures, in order to obtain the critical condition for food storage (Karel *et al,.* 1994, Roos 1995, Ostrowska-Ligęza *et al,.* 2014). Our previous study showed two transition events in DSC thermograms assigned to a low glass transition temperature (T_{gl}) and a high glass transition temperature (T_{gh}). Both T_{gl} and T_{gh} were used to establish this stability map as shown in Fig. 4.8. First, W_{Tg} the critical water content was noticed for T_{gl} = 25°C and were compared with value W_{isot} at merging points of sorption/desorption isotherms measured at 25 °C (Fig. 4.8). A good agreement was found between the two ways to measure W_c the critical water content when T_{gl} is considered (Fig. 4.9). So with product showing heterogeneous phase characterized with the presence of several glass transitions, the lowest transition will the one which manage stability in the sample and may contribute to a better homogeneity.

3.3 Kinetic of water migration

The water sorption behavior of extrudate is complicated due to the complex internal geometry of porous structure. Van Nieuwenhuijzen *et al,.* (2010) have demonstrated that the water vapor sorption behavior of dry solid food products such as crispy rolls can be described using an exponential model. In this work, two

exponential models have been used for fitting the experimental mass change curves at each sorption level. It revealed two distinct mechanisms with slow and fast characteristics in the moisture uptake behavior (Fig. 4.10) with respectively a low (t_1) and high kinetic time constant (t_2). This could reflect amorphous regions with distinct sorption behaviors. Previous DSC studies (Masavang *et al,.* 2019) suggested the presence of multiple amorphous phases characterized by two glass transition temperatures. Figure 4.10 showed the kinetic time constant for the slow sorption process (t_2) as a function of moisture content, which reflect water migration into the material. These t_2 values for samples without sucrose were almost constant and independent from the humidity level, while extrudates with more than 10% sucrose exhibited a maximum in range of 0.3-0.6 a_w (Fig. 4.10). During primary stage, hydration of macromolecules was simultaneous with the saturation of pores with water, starting with the external surfaces, which were first in contact the water (Lucas *et al,.* 2007). The higher time constant for water uptake was observed into high sugar extrudates and it may be attributed to the interactions between biopolymers and sucrose molecule that reduced the kinetic of water migration. Fermi equation was applied to t_2 data (Fig. 4.10). In fact, t_2 were substantially increased at low water activity, then followed by a progressive increase of sorption rate when the product goes through its glass transition. It is most likely due to a progressive water plasticization of the structures. Hydration of macromolecules can be accompanied by swelling, which in turn the porous structure could also increase. This volume increase was slow with an average increase in length or diameter (Lucas *et al,.* 2007). The results can be noted that the surface adsorption of water is much smaller than the absorption of water by the bulk of material.

Bourlieu *et al,.* (2008) observed an increase of moisture effective diffusivity in biscuit starting at 20%, value at which dissolution of sugar could occur, and a decrease at higher moisture content which can be linked to both the closure of porosity starting above 0.75 a_w associated with the collapse of the cereal matrix. Similar results were obtained on breakfast cereal during soaking in milk by Sacchetti *et al,.* (2003). Moreover, Guillard *et al,.* (2004) described a model based on Fick's second law for predicting moisture diffusivity and transfer in biscuit. These authors presented that the diffusivity estimated from sorption kinetics increased up to a moisture content close to the monolayer value, and then, decreased at higher moisture content.

After a sharp decrease in t_2, the kinetic time constants were almost constant and close to the t_1 values at high water content. It likely results from the plasticizing effect of sucrose and water above the glass transition at 25 $^\circ$C. From the above results, there are two hypotheses to explain the sharp decrease in apparent water diffusion kinetics at high relative humidity: 1) structure collapse, 2) crystallization of sugar.

X-ray diffraction (XRD) experiments were performed to complete the investigation of structural change such as sucrose crystallization possibly occurring during the storage/dehydration cycles. X-rays diffractograms were recorded on 0, 10 and 20 % sucrose extruded sample equilibrated at different relative humidity in order to assess the crystalline order of the starch and of the sugar (Fig. 4.11a). The X-ray diffraction patterns of extrudates showed that the usual A-pattern of native cereal starches (Zobel *et al,.* 1988) had completely disappeared as a result of the extrusion, but that "V-pattern" was present for all samples. The A-type pattern characteristic of native cereal starches may have gradually transformed in presence of lipids during extrusion cooking, into the so called V-pattern, characteristic of amylose-lipid complex crystalline structure. The X-ray pattern developed was characteristic of an amylose/lipid complex (Mercier *et al,.* 1980). Fan *et al,.* (1996) have presented that an addition of sugars led to changes in the packing of amylose–lipid complexes in the extrudate of maize grits from an E-type to V-type. It is postulated that the complexes initially pack in the least stable E-form and then rearrange into the most stable V-form, a process which is accelerated by the addition of sugars because of the enhanced molecular mobility resulting from the reduced glass transition temperature. This rearrangement is also seen when extrudates containing no sugar are equilibrated at ambient temperature. Farhat *et al,.* (1996) suggested that the starch crystalline order was generally very limited in the extrudates. They calculated crystallinity indices using the method described by Hermans and Weidinger (1948) based on the relative area under the characteristic sharp peaks. These values were less than 2 to 4% in the extruded samples compared to 15-25% in the native material as the water content increased from 5 to 25% (w/w dry basis). No sharp peaks characteristic of crystalline sugars were observed in any of the x-ray diffactograms of extruded starch-sucrose samples, implying the absence of crystalline sucrose over the entire range of moisture contents investigated. Samples with 0, 10 and 20% sucrose content equilibrated at ambient temperature at 11 %RH exhibited 2 peaks with

the main one between 13 and 18° (2θ). In no cases was there any X-ray evidence for sugar crystals within the extrudates processed with 10% feed water. In all cases the X-ray pattern was dominated by E or V-response, as a result of the presence of amylose lipid complexes. Increasing plasticizer in the form of either water or sugar has been reported to increase the magnitude of the most stable V pattern (Fan *et al,.* 1996, Carvalho and Mitchell 2000). Besides, when samples were equilibrated at 84% RH, extrudates gave the V-type pattern with a second peaks at approximately 19.5° (2θ). The diffractograms acquired on the extrudates were typical of amorphous systems exhibiting a broad pattern regardless of their sucrose content (Fig. 4.11a). The feature centered at approximately 2θ = 12-13° resulted from the contribution of amorphous sucrose and the contribution of this peak to the total spectrum increased with increasing sucrose content in agreement with (Farhat *et al,.* 2003). On the one hand, the X-ray pattern of the sample containing sucrose equilibrated at 11 %RH showed a marked peak at 18.2° (2θ) with no sensitivity to sucrose content, while the X-ray pattern of the same samples equilibrated at 84 %RH exhibited a shift of this peak to higher 2θ values. This indicated a change in crystalline structure of extrudates after high hydration exposure with more V-type packing of amylose/lipid complex (Fan *et al,.* 1996). On the other hand, the effect of dehydration on crystallinity was studied by equilibrating the 10% sucrose sample previously equilibrated at 84 %RH and then dehydrating it to 11 %RH with storage over the appropriate saturated salt solution. The samples retained their amorphous character after dehydration (Fig. 4.11b), but the observed peak did not shift back to its original value before the sample hydration. Li *et al,.* (2014) suggested that the amorphous structure resulting from extrusion may only recrystallise upon retrogradation and that most of the residual crystalline structure in the extrudates originated from native crystalline structure, rather than from retrogradation. In the present study, the drying of extrudates could contribute to reduce the retrogradation. The result of X-ray diffraction proved that no sugar crystallization could explain the different sorption isotherm shape for extrudates at different sucrose content (Fig. 4.4). A notable feature was that no sharp peaks characteristic of crystalline sucrose were observed in any of the X-ray diffractograms of the extruded samples compared with a control sample containing 1% of crystalline sucrose, implying the absence of crystalline sucrose over the entire range of moisture contents investigated.

4. Conclusions

The moisture sorption and desorption isotherms of breakfast cereal model were determined for samples at different sucrose content and processed at different water levels. The equilibrium moisture content decreased with decreasing sugar content at constant water activity and the reverse effect of sugar content was observed at high water activity. Sucrose content, physical aging and water sorption history affected hysteresis behavior between sorption and desorption. The fitting model with a bi- exponential equation suggested a water migration process in two steps as function of time: the first kinetic with the shorter time constant was almost constant and could be adsorption phenomena at the surface. The second one, longer than the previous, may represent the apparent migration of water into the product. This time constant represents the apparent diffusivity in samples and shows a bell-shape as function of water content. This behavior is probably due to a change of sample size during hydration, a first step corresponding to the swelling of the sample, increasing the path for water migration, then lowering the apparent mass transfer; and a second step with an increase of water transfer kinetic (shorter time constant) for higher water content. To relate the hydration-induced changes in extrudates microstructure during storage, imaging technique can be applied for an assessment of the fine structure of the non-hydrated samples in order to correlate hydration properties with the possibles changes in porous structure (i.e. pore size and pore wall thickness) of extrudates (i.e. swelling and collapsing) occurring in the cereals upon hydration.

References

Anzai, M., Hagiwara, T., Watanabe, M., Komiyama, J. & Suzuki, T. (2011). Relationship between enthalpy relaxation and water sorption of ball-milled potato starch. *Journal of Food Engineering, 104,* 43-48.

Arimi, J. M., Duggan, E., O'Sullivan, M., Lyng, J. G. & O'Riordan, E. D. (2010). Effect of water activity on the crispiness of a biscuit (Crackerbread): Mechanical and acoustic evaluation. *Food Research International, 43,* 1650-1655.

Aston, L. M., Gambell, J. M., Lee, D. M., Bryant, S. P. & Jebb, S. A. (2008). Determination of the glycaemic index of various staple carbohydrate-rich foods in the UK diet. *European journal of clinical nutrition, 62,* 279-285.

Bhandari, B. R. & Hartel, R. W. (2005). Phase transitions during food powder production and powder stability. In: In Encapsulated, Powdered, Foods. Taylor and Francis, New York. Pp. 261-291 (Chapter 11).

Boente, G., González, H. H. L., Martínez, E., Pollio, M. L. & Resnik, S. L. (1996). Sorption isotherms of corn—Study of mathematical models. *Journal of Food Engineering, 29,* 115-128.

Bourlieu, C., Guillard, V., Powell, H., Vallès-Pàmies, B., Guilbert, S. & Gontard, N. (2008). Modelling and control of moisture transfers in high, intermediate and low aw composite food. *Food Chemistry, 106,* 1350-1358.

Brunauer, S., Emmett, P. H. & Teller, E. (1938). Adsorption of Gases in Multimolecular Layers. *Journal of the American Chemical Society, 60,* 309-319.

Burnett, D. J., Thielmann, F. & Booth, J. (2004). Determining the critical relative humidity for moisture-induced phase transitions. *International Journal of Pharmaceutics, 287,* 123-133.

Carter, B. P. & Schmidt, S. J. (2012). Developments in glass transition determination in foods using moisture sorption isotherms. *Food Chemistry, 132,* 1693-1698.

Carvalho, C. W. P. & Mitchell, J. R. (2000). Effect of sugar on the extrusion of maize grits and wheat flour. *International Journal of Food Science & Technology, 35,* 569-576.

Chetana, R., Srinivasa, P. C. & Yella Reddy, S. R. (2005). Moisture sorption characteristics of milk burfi, an traditional Indian sweet, using sugar substitutes. *European Food Research and Technology, 220,* 136-141.

Chinachoti, P. & Steinberg, M. P. (1986a). Crystallinity of Sucrose by X-ray Diffraction as Influenced by Absorption versus Desorption, Waxy Maize Starch Content, and Water Activity. *Journal of Food Science, 51,* 456-459.

Chinachoti, P. & Steinberg, M. P. (1986b). Moisture Hysteresis is Due to Amorphous Sugar. *Journal of Food Science, 51,* 453-455.

Díaz, P., Arratia, C., Vásquez, C., Osorio, F. & Enrione, J. (2011). Effect of glycerol on water sorption of bovine gelatin films in the glassy state. *Procedia Food Science, 1,* 267-274.

Enrione, J. I., Hill, S. E. & Mitchell, J. R. (2007a). Sorption and Diffusional Studies of Extruded Waxy Maize Starch-Glycerol Systems. *Starch - Stärke, 59,* 1-9.

Enrione, J. I., Hill, S. E. & Mitchell, J. R. (2007b). Sorption Behavior of Mixtures of Glycerol and Starch. *Journal of Agricultural and Food Chemistry, 55,* 2956-2963.

Esveld, D. C., van der Sman, R. G. M., Witek, M. M., Windt, C. W., van As, H., van Duynhoven, J. P. M. & Meinders, M. B. J. (2012). Effect of morphology on water sorption in cellular solid foods. Part II: Sorption in cereal crackers. *Journal of Food Engineering, 109,* 311-320.

Falade, K. O. & Aworh, O. C. (2004). Adsorption isotherms of osmo-oven dried african star apple (Chrysophyllum albidum) and african mango (Irvingia gabonensis) slices. *European Food Research and Technology, 218,* 278-283.

Fan, J., Mitchell, J. R. & Blanshard, J. M. V. (1996). The effect of sugars on the extrusion of maize grits: II. Starch conversion. *International Journal of Food Science & Technology, 31,* 67-76.

Farhat, I. A., Mitchell, J. R., Blanshard, J. M. V. & Derbyshire, W. (1996). A pulsed 1H NMR study of the hydration properties of extruded maize-sucrose mixtures. *Carbohydrate Polymers, 30,* 219-227.

Farhat, I. A., Mousia, Z. & Mitchell, J. R. (2003). Structure and thermomechanical properties of extruded amylopectin–sucrose systems. *Carbohydrate Polymers, 52,* 29-37.

Freundlich, H. M. F. (1906). Over the adsorption in solution. *The Journal of Physical Chemistry C,* **57,** 385-471.

Gogus, F., Maskan, M. & Kaya, A. (1998). Sorption isotherms of turkish delight. *Journal of Food Processing and Preservation,* **22,** 345-357.

Guillard, V., Broyart, B., Bonazzi, C., Guilbert, S. & Gontard, N. (2003). Moisture Diffusivity in Sponge Cake as Related to Porous Structure Evaluation and Moisture Content. *Journal of Food Science,* **68,** 555-562.

Guillard, V., Broyart, B., Guilbert, S., Bonazzi, C. & Gontard, N. (2004). Moisture diffusivity and transfer modelling in dry biscuit. *Journal of Food Engineering,* **64,** 81-87.

Hazaveh, P., Mohammadi Nafchi, A. & Abbaspour, H. (2015). The effects of sugars on moisture sorption isotherm and functional properties of cold water fish gelatin films. *International Journal of Biological Macromolecules,* **79,** 370-376.

Hermans, P. H. & Weidinger, A. (1948). Quantitative X-Ray Investigations on the Crystallinity of Cellulose Fibers. A Background Analysis. *Journal of Applied Physics,* **19,** 491-506.

Karel, M., Anglea, S., Buera, P., Karmas, R., Levi, G. & Roos, Y. (1994). Stability-related transitions of amorphous foods. *Thermochimica Acta,* **246,** 249-269.

Katz, E. E. & Labuza, T. P. (1981). Effect of Water Activity on the Sensory Crispness and Mechanical Deformation of Snack Food Products. *Journal of Food Science,* **46,** 403-409.

Kilburn, D., Claude, J., Schweizer, T., Alam, A. & Ubbink, J. (2005). Carbohydrate Polymers in Amorphous States: An Integrated Thermodynamic and Nanostructural Investigation. *Biomacromolecules,* **6,** 864-879.

Kim, Y. J., Suzuki, T., Hagiwara, T., Yamaji, I. & Takai, R. (2001). Enthalpy relaxation and glass to rubber transition of amorphous potato starch formed by ball-milling. *Carbohydrate Polymers,* **46,** 1-6.

Laaksonen, T. J. & Labuza, T. P. (2001). EFFECTS OF MOISTURE, SUCROSE, NaCl, AND ARABINOXYLAN ON RELAXATION IN WHEAT DOUGH AS MEASURED BY DMTA. *International Journal of Food Properties,* **4,** 311-325.

Labuza, T. P. (1984). Moisture sorption: Practical Aspects of Isotherm Measurement and use. . *American Association of Cereal Chemists, St. Paul, MN.*

Labuza, T. P. & Hyman, C. R. (1998). Moisture migration and control in multi-domain foods. *Trends in Food Science & Technology,* **9,** 47-55.

Lazou, A. & Krokida, M. (2011). Thermal characterisation of corn–lentil extruded snacks. *Food Chemistry,* **127,** 1625-1633.

Li, M., Hasjim, J., Xie, F., Halley, P. J. & Gilbert, R. G. (2014). Shear degradation of molecular, crystalline, and granular structures of starch during extrusion. *Starch - Stärke,* **66,** 595-605.

Li, Q. E. & Schmidt, S. J. (2011). Use of Ramping and Equilibrium Water Vapor Sorption Methods to Determine the Critical Relative Humidity at which the Glassy to Rubbery Transition Occurs in Polydextrose. *Journal of Food Science,* **76,** E149-E157.

Li, X.-j., Wang, X., Li, Y., Jiang, P. & Lu, H. (2016). Changes in moisture effective diffusivity and glass transition temperature of paddy during drying. *Computers and Electronics in Agriculture,* **128,** 112-119.

Lucas, T., Le Ray, D. & Mariette, F. (2007). Kinetics of water absorption and solute leaching during soaking of breakfast cereals. *Journal of Food Engineering,* **80,** 377-384.

Machado, M. d. F. t., Oliveira, F. A. R., Gekas, V. & Singh, R. P. (1998). Kinetics of moisture uptake and soluble-solids loss by puffed breakfast cereals immersed in water. *International Journal of Food Science & Technology,* **33,** 225-237.

Masavang, S., Roudaut, G. & Champion, D. (2019). Identification of complex glass transition phenomena by DSC in expanded cereal-based food extrudates: Impact of plasticization by water and sucrose. *Journal of Food Engineering,* **245,** 43-52.

Mercier, C., Charbonniere, R., Grebaut, J. & F., d. l. G. J. (1980). Formation of amylose-lipid complexes by twin-screw extrusion cooking of manioc starch. *Cereal Chemistry,* **57,** 4-9.

Mercier, S., Marcos, B., Moresoli, C., Mondor, M. & Villeneuve, S. (2014). Modeling of internal moisture transport during durum wheat pasta drying. *Journal of Food Engineering,* **124,** 19-27.

Ostrowska-Ligęza, E., Jakubczyk, E., Górska, A., Wirkowska, M. & Bryś, J. (2014). The use of moisture sorption isotherms and glass transition temperature to assess the stability of powdered baby formulas. *Journal of Thermal Analysis and Calorimetry,* **118,** 911-918.

Pallavi, B. V., Chetana, R., Ravi, R. & Reddy, S. Y. (2015). Moisture sorption curves of fruit and nut cereal bar prepared with sugar and sugar substitutes. *Journal of Food Science and Technology,* **52,** 1663-1669.

Palou, E., López-Malo, A. & Argaiz, A. (1997). Effect of temperature on the moisture sorption isotherms of some cookies and corn snacks. *Journal of Food Engineering,* **31,** 85-93.

Panjagari, N. R., Singh, A. K., Ganguly, S. & Indumati, K. P. (2015). Beta-glucan rich composite flour biscuits: modelling of moisture sorption isotherms and determination of sorption heat. *Journal of Food Science and Technology,* **52,** 5497-5509.

Peleg, M. (1993). Assessment of a semi-empirical four parameter general model for sigmoid moisture sorption. *Journal of Food Process Engineering,* **16,** 21-37.

Rakshit, M., Moktan, B., Hossain, S. A. & Sarkar, P. K. (2014). Moisture sorption characteristics of wadi, a legume-based traditional condiment. *Journal of Food Science and Technology,* **51,** 301-307.

Rao, C. G. (2015). Chapter 40 Water activity and shelf life, In : Engineering for storage of Friuts and Vegetables. Kidlington, Oxford, UK.

Risbo, J. (2003). The dynamics of moisture migration in packaged multi-component food systems I: shelf life predictions for a cereal–raisin system. *Journal of Food Engineering,* **58,** 239-246.

Roca, E., Broyart, B., Guillard, V., Guilbert, S. & Gontard, N. (2008). Predicting moisture transfer and shelf-life of multidomain food products. *Journal of Food Engineering,* **86,** 74-83.

Roos, Y. H. (1995). Characterization of food polymers using state diagrams. *Journal of Food Engineering,* **24,** 339-360.

Roos, Y. H. (2002). Importance of glass transition and water activity to spray drying and stability of dairy powders. *Lait,* **82,** 475-484.

Roos, Y. H., Roininen, K., Jouppila, K. & Tuorila, H. (1998). Glass transition and water plasticization effects on crispness of a snack food extrudate. *International Journal of Food Properties,* **1,** 163-180.

Sablani, S. S., Kasapis, S. & Rahman, M. S. (2007). Evaluating water activity and glass transition concepts for food stability. *Journal of Food Engineering,* **78,** 266-271.

Sacchetti, G., Pittia, P., Biserni, M., Pinnavaia, G. G. & Della Rosa, M. (2003). Kinetic modelling of textural changes in ready-to-eat breakfast cereals during soaking in semi-skimmed milk. *International Journal of Food Science & Technology,* **38,** 135-143.

Sacchetti, G., Pittia, P. & Pinnavaia, G. G. (2005). The effect of extrusion temperature and drying-tempering on both the kinetics of hydration and the textural changes in extruded ready-to-eat breakfast cereals during soaking in semi-skimmed milk. *International Journal of Food Science & Technology,* **40,** 655-663.

Shittu, T. A., Idowu-Adebayo, F., Adedokun, I. I. & Alade, O. (2015). Water vapor adsorption characteristics of starch–albumen powder and rheological behavior of its paste. *Nigerian Food Journal,* **33,** 90-96.

Shivhare, U. S., Arora, S., Ahmed, J. & Raghavan, G. S. V. (2004). Moisture adsorption isotherms for mushroom. *LWT - Food Science and Technology,* **37,** 133-137.

Sillick, M. & Gregson, C. M. (2010). Critical water activity of disaccharide/maltodextrin blends. *Carbohydrate Polymers,* **79,** 1028-1033.

Tsami, E., Marinos-Kouris, D. & Maroulis, Z. B. (1990). Water Sorption Isotherms of Raisins, Currants, Figs, Prunes and Apricots. *Journal of Food Science,* **55,** 1594-1597.

van den Berg, C. (1985). Development of B.E.T.-Like Models for Sorption of Water on Foods, Theory and Relevance. In: Properties of Water in Foods: in Relation to Quality and Stability (edited by SIMATOS, D. & MULTON, J. L.). Pp. 119-131. Dordrecht: Springer Netherlands.

Van Nieuwenhuijzen, N. H., Tromp, R., Mitchell, J. R., Primo-Martín, C., Hamer, R. & van Vliet, T. (2010). Relations between sensorial crispness and molecular mobility of model bread crust and its main components as measured by PTA, DSC and NMR. *Food Research International,* **43,** 342-349.

Yuan, X., Carter, B. P. & Schmidt, S. J. (2010). Determining the Critical Relative Humidity at which the Glassy to Rubbery Transition Occurs in Polydextrose Using an Automatic Water Vapor Sorption Instrument. *Journal of Food Science,* **76,** E78-E89.

Yuan, X., Carter, B. P. & Schmidt, S. J. (2011). Determining the Critical Relative Humidity at which the Glassy to Rubbery Transition Occurs in Polydextrose Using an Automatic Water Vapor Sorption Instrument. *Journal of Food Science,* **76,** 78-89.

Zobel, H. F., Young, S. N. & Rocca., L. A. (1988). Starch Gelatinization: An X-ray Diffraction Study. *Cereal Chemistry,* **65,** 443-446.

Table 4.1. Selected isotherm equation for experimental data fitting.

Model	Equation		Model parameters	Reference	Product
Peleg	$M = k_1 a_{w1}^n + k_1 a_{w2}^n$	Eq. 1	M – equilibrium moisture content (g/100 g dry solids) a_w – water activity (p/p$_0$) k_1,k_2,n_1,n_2 – empirical constants $n_1 < 1$ and $n_2 > 1$	(Palou et al., 1997)	- Cookies and corn snacks
GAB	$M = \dfrac{m_0 C k a_w}{(1 - k \cdot a_w)(1 - k \cdot a_w + C \cdot k \cdot a_w)}$	Eq. 2	M – equilibrium moisture content (g/100 g dry solids) a_w – water activity (p/p$_0$) C – dimensionless parameter, related to heat of sorption of monolayer region k – dimensionless parameter, related to heat of sorption of monolayer region m_0 –monolayer moisture content (g /100 g dry solids)	(Pallavi et al., 2015) (Lazou and Krokida, 2011)	- Nut cereal bars - Corn-lentil extruded snacks
BET	$M = \dfrac{m_0 C k a_w}{(1 - a_w)(1 - a_w + C \cdot a_w)}$	Eq. 3	M – equilibrium moisture content (g/100 g dry solids) a_w – water activity (p/p$_0$) C – dimensionless parameter, related to heat of sorption of monolayer region m_0 –monolayer moisture content (g /100 g dry solids)	(Enrione et al., 2007a, b)	- Extruded Waxy Maize Starch-Glycerol Systems - Mixtures of Glycerol and Starch
Freundlich	$M = k_F a_w^{1/n}$	Eq. 4	M – equilibrium moisture content (g/100 g dry solids) a_w – water activity (p/p$_0$) n – Freundlich adsorption constant, indicated adsorption intensity k_F – Freundlich adsorption constant, indicated adsorption capacity	(Boente et al., 1996) (Shivhare et al., 2004)	- Maize grains - Dried mushroom

Table 4.2 Estimated parameters of the sorption models for extruded products.

Model /Sucrose content (%)		10% extrusion water					15% extrusion water				
		0	5	10	15	20	0	5	10	15	20
Peleg (model up to 90% RH)	k_1	13.71	12.86	13.44	13.55	20.17	13.04	14.42	14.00	14.05	14.83
	a_{w1}	0.60	0.67	0.91	1.08	1.43	0.59	0.76	0.87	0.87	0.84
	k_2	35.10	41.96	43.86	47.11	51.05	33.96	46.38	43.94	51.60	52.37
	a_{w2}	7.83	7.58	7.43	7.34	8.95	7.31	9.63	7.39	7.29	7.54
	p value	3.36	3.51	5.21	7.50	6.00	1.02	2.04	2.76	5.15	2.18
GAB (model up to 90% RH)	k	0.91	0.95	0.95	0.95	0.94	0.92	0.95	0.95	0.95	0.95
	C	23.86	14.38	4.43	2.19	1.75	21.57	14.60	5.08	4.27	5.44
	m_0	5.03	4.62	4.95	5.40	6.44	4.95	4.53	5.08	5.37	5.45
	p value	4.21	4.19	4.82	7.80	9.29	2.66	7.39	5.12	4.62	2.31
GAB (model up to 50% RH)	k	0.80	0.93	0.98	1.19	1.29	0.78	0.90	1.06	1.12	0.84
	C	13.88	13.74	7.16	7.13	3.78	13.29	9.89	7.98	9.86	5.60
	m_0	6.07	4.72	4.13	2.82	3.04	6.063	5.14	4.03	3.72	5.98
	p value	4.22	4.85	4.06	2.98	9.13	0.38	5.94	0.84	1.73	1.33
BET (model up to 50% RH)	C	19.84	18.03	6.03	5.59	1.58	19.15	6.92	7.11	7.60	7.51
	m_0	4.91	4.26	4.33	3.57	6.42	4.80	5.06	4.37	4.36	4.78
	p value	5.03	4.78	4.01	2.05	10.81	3.12	9.13	7.47	1.98	2.85
Freundlich (model up to 40% RH)	k_F	12.87	11.15	11.04	9.52	13.18	12.63	15.19	11.75	10.96	13.50
	n	1.79	1.74	1.33	1.25	0.94	1.77	1.26	1.33	1.45	1.30
	p value	4.15	3.79	3.32	1.56	7.66	0.82	2.80	3.31	0.83	1.16
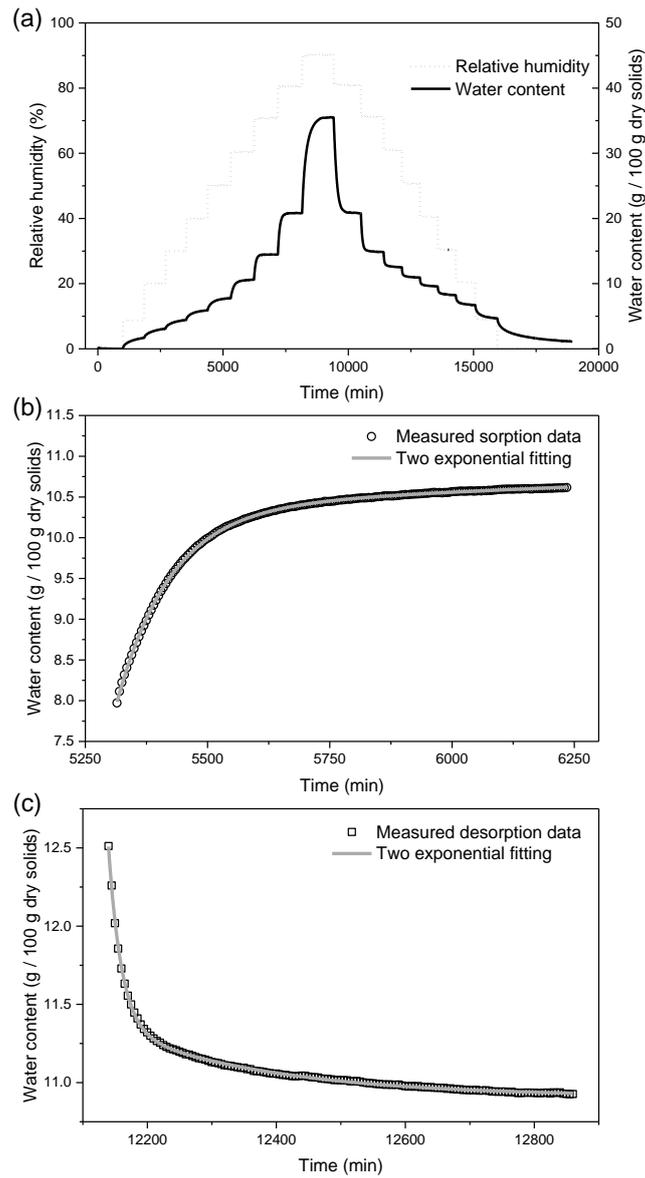
Fig. 4.1 Example of a sorption experiment using dynamic vapor sorption instrument. Step-by-step increase and decrease of relative humudity and related change of water content for extrudate with 10% sucrose (a). The circles indicate the kinetic curves evaluated sorption step 50-60% RH (b) and sorption step 60-50% RH (c).
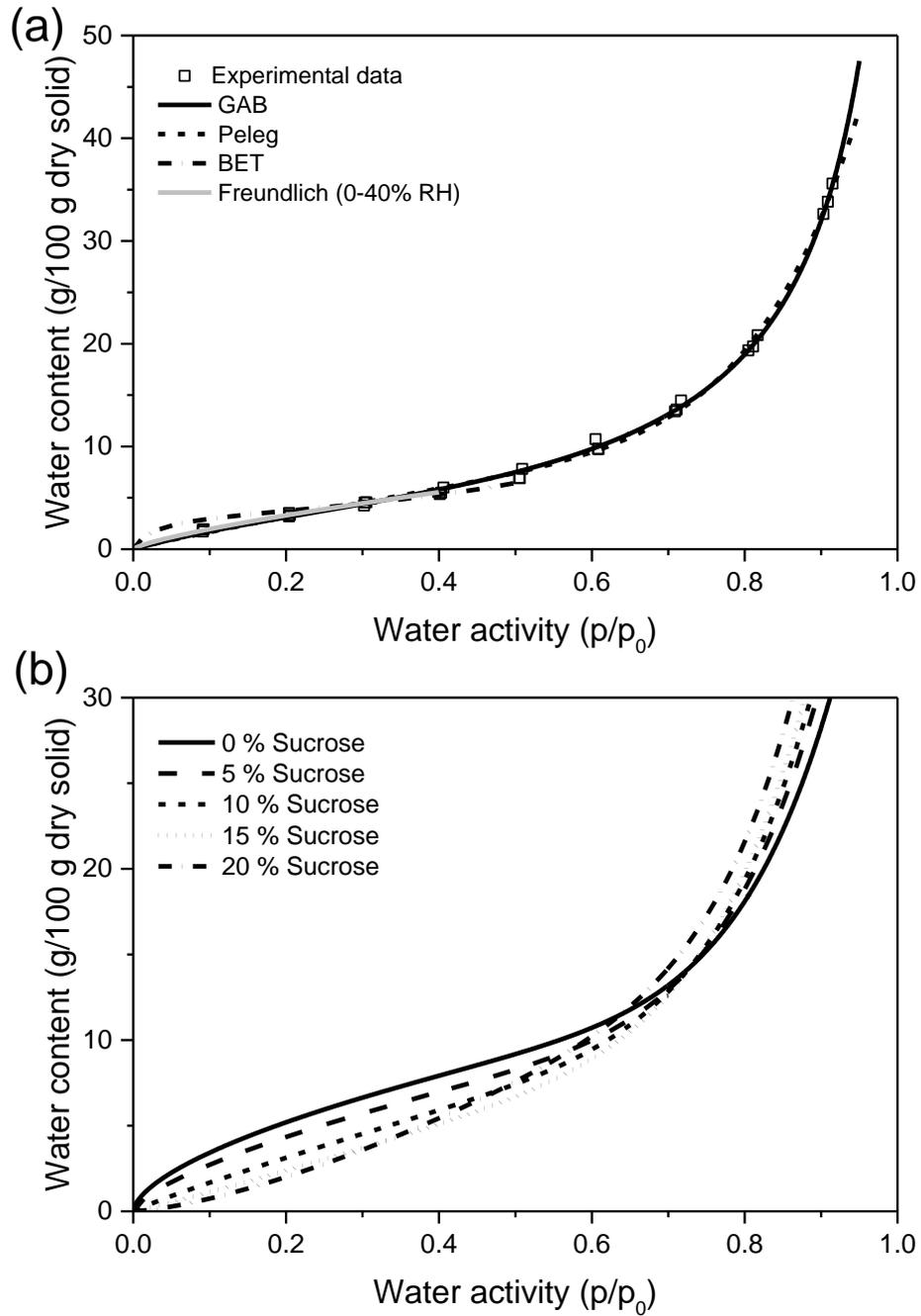
Fig. 4.2 Comparison between the normalized GAB, Peleg, (0-40% RH) and BET (0-50% RH) sorption isotherm for extrudate contains 10% sucrose (a) and the effect of sucrose on sortion isotherm curve of extrudates exposed at 0-90% RH at 25 °C using the DVS instrument (b).
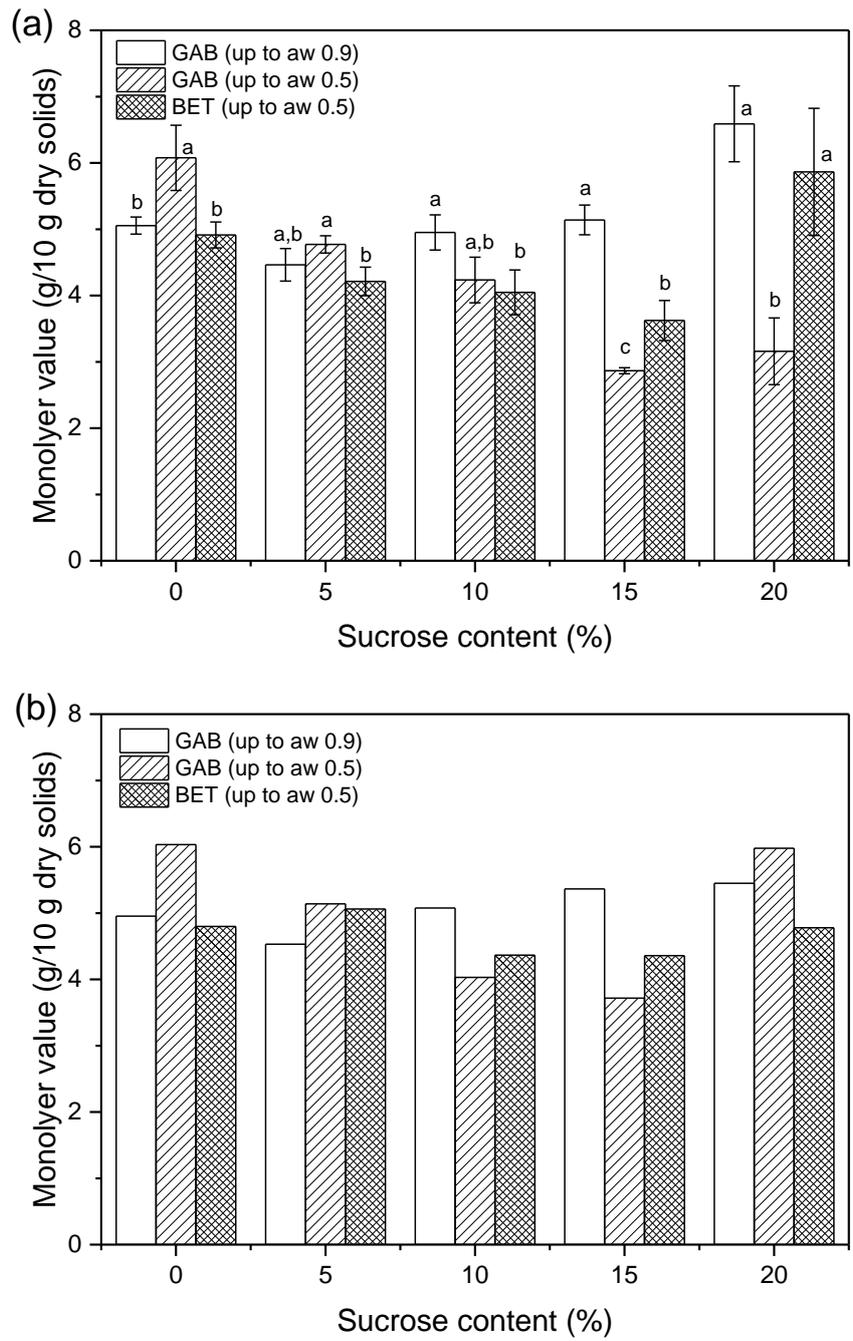
Fig 4.3. Effect of sucrose content on monolayer water content for extrudate produced at 10 (a) and 15 (b) % extrusion water.
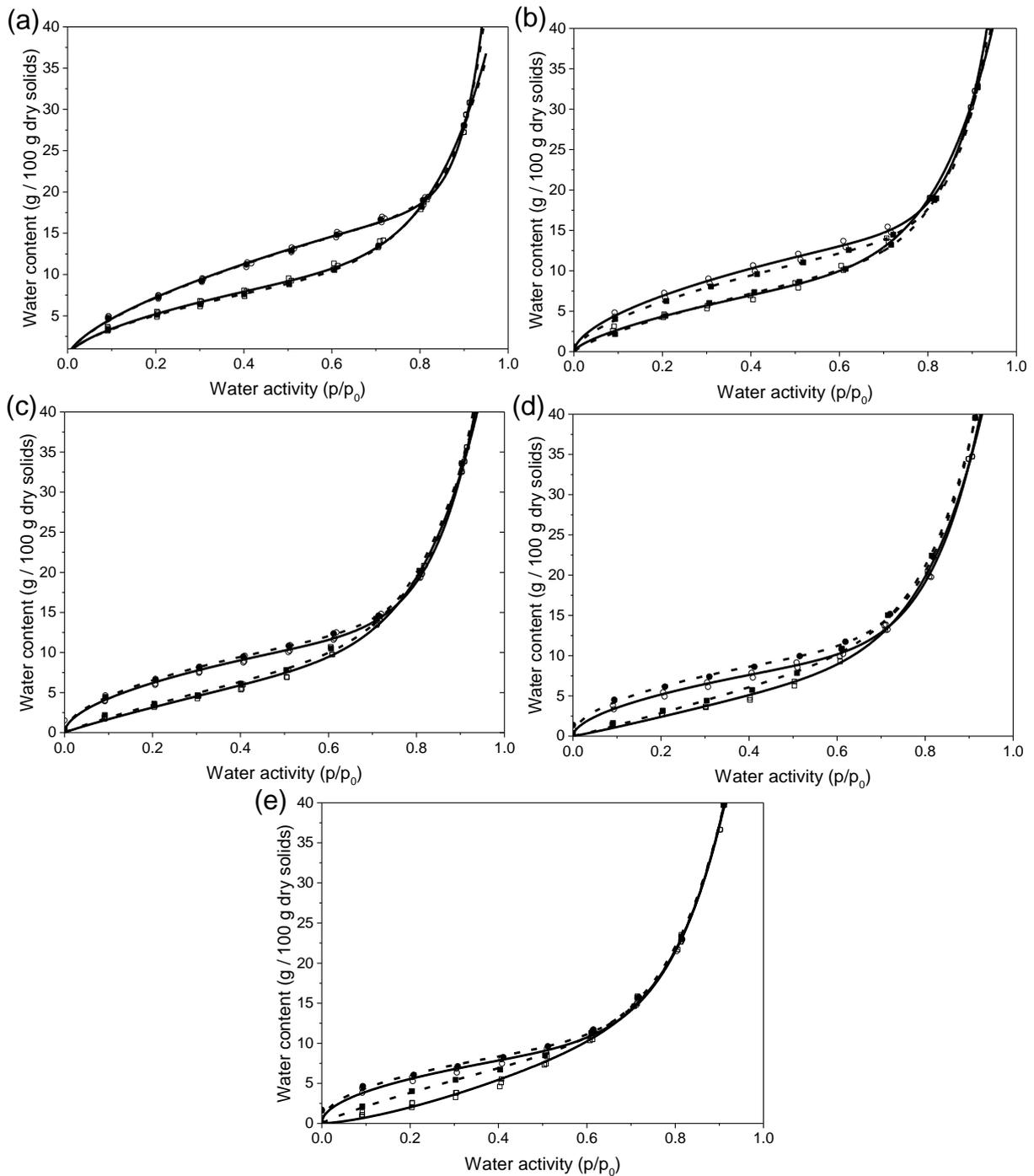
Fig 4.4. Water sorption isotherm of extrudates showing the effect of sucrose content on hysteresis of samples where a,b,c,d, and e are extrudates contain 0, 5, 10, 15, and 20% sucrose content, respectively. Markers are experimental data for sorption (rectangle) and desorption (circle). Lines represent Peleg fitting for sample produced with 10% (open symbol with solid line) and 15% (filled symbol with dashed line) extrusion water.
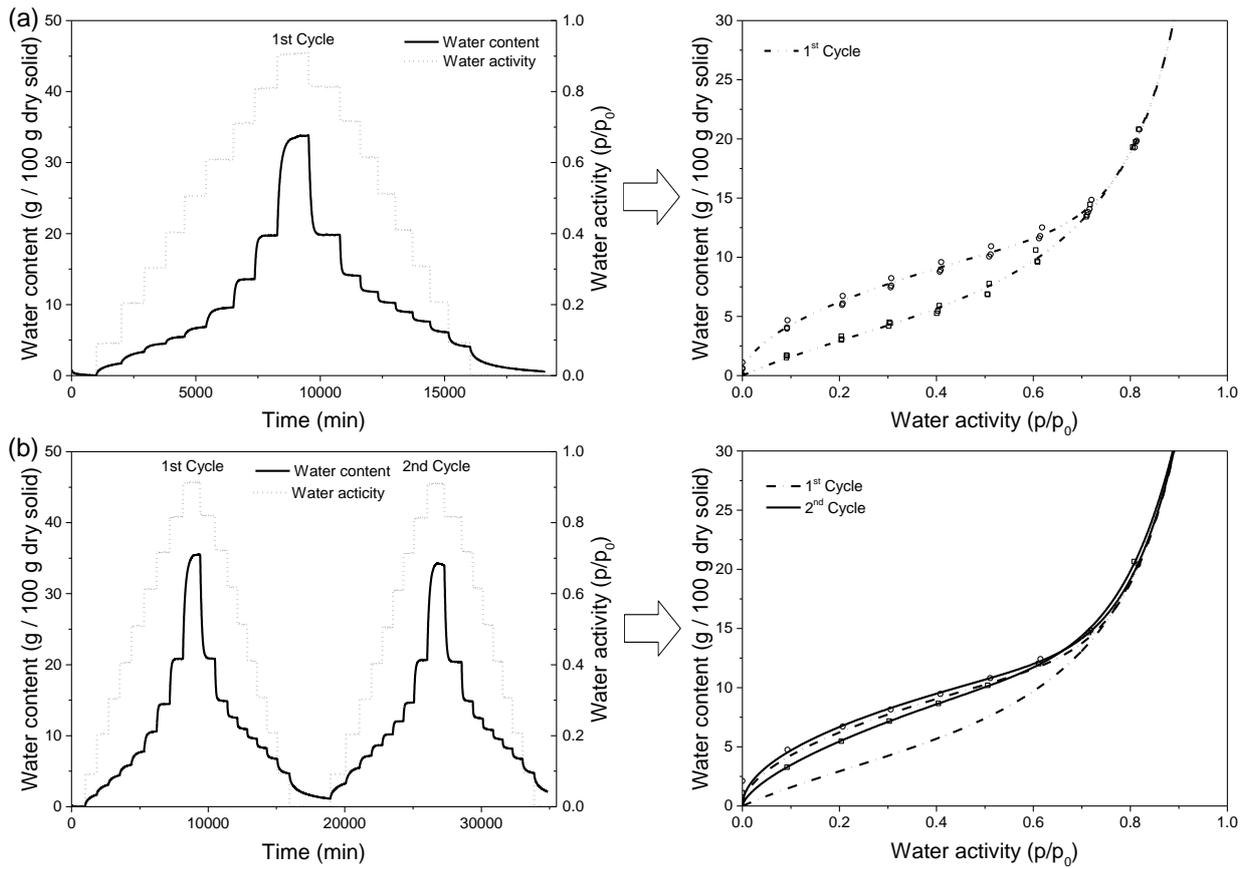
Fig 4.5. Effect of sorption-desorption cycle on sorption isotherm curve for extrudate with 10% sucrose content produced at 10% extrusion water. (a) and (b) are kinetic water sorptions and sorption isothrems for 1 cycle and 2 cycles, respectively.
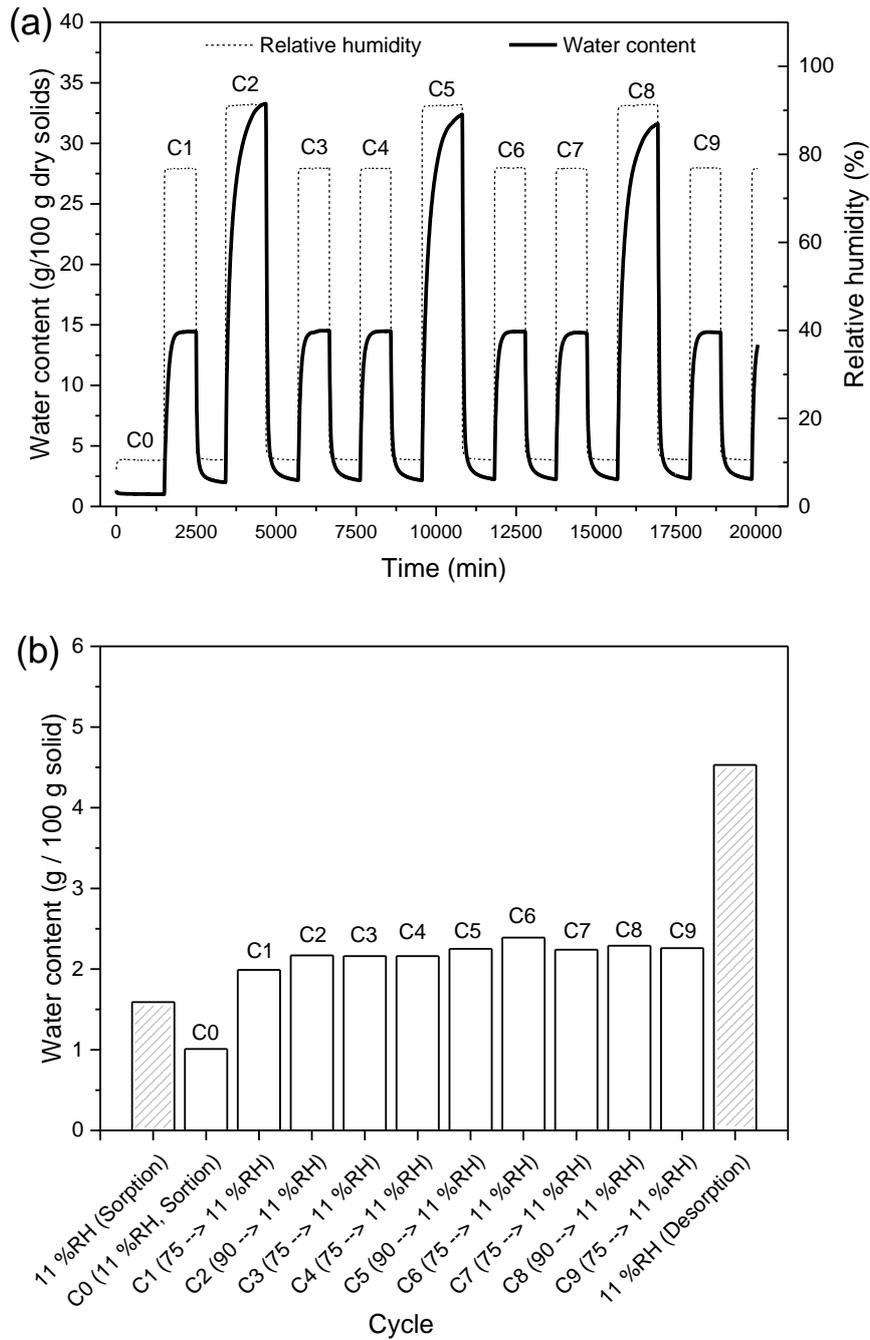
Fig. 4.6 Effect of hydration-dehydration multi-cycle on water vapor sorption of extrudate with 10% sucrose; (a) is kinetic curve evaluated using DVS and (b) is the plot of water contents for each desorption steps.
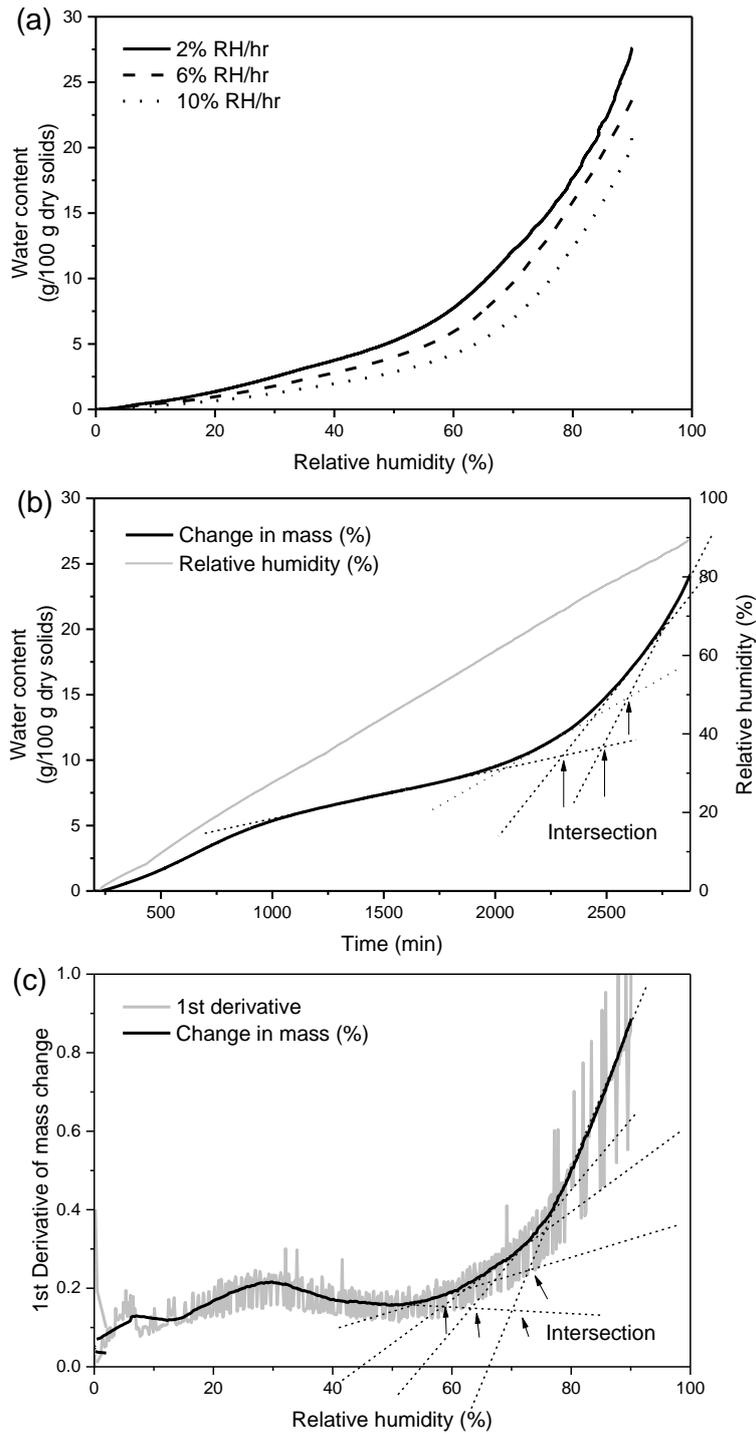
Fig 4.7 Relative humidity ramping experiment for a range of relative humidity ramping rates for extrudate with 10% sucrose content at 25 °C (a); net change in mass or water content as a function of time for extrudate with 0, 10, and 20% sucrose content at 2% RH/hr (b); 1st derivative of mass change for 0, 10, and 20% sucrose content at 10% RH/h as a function of %RH (c).
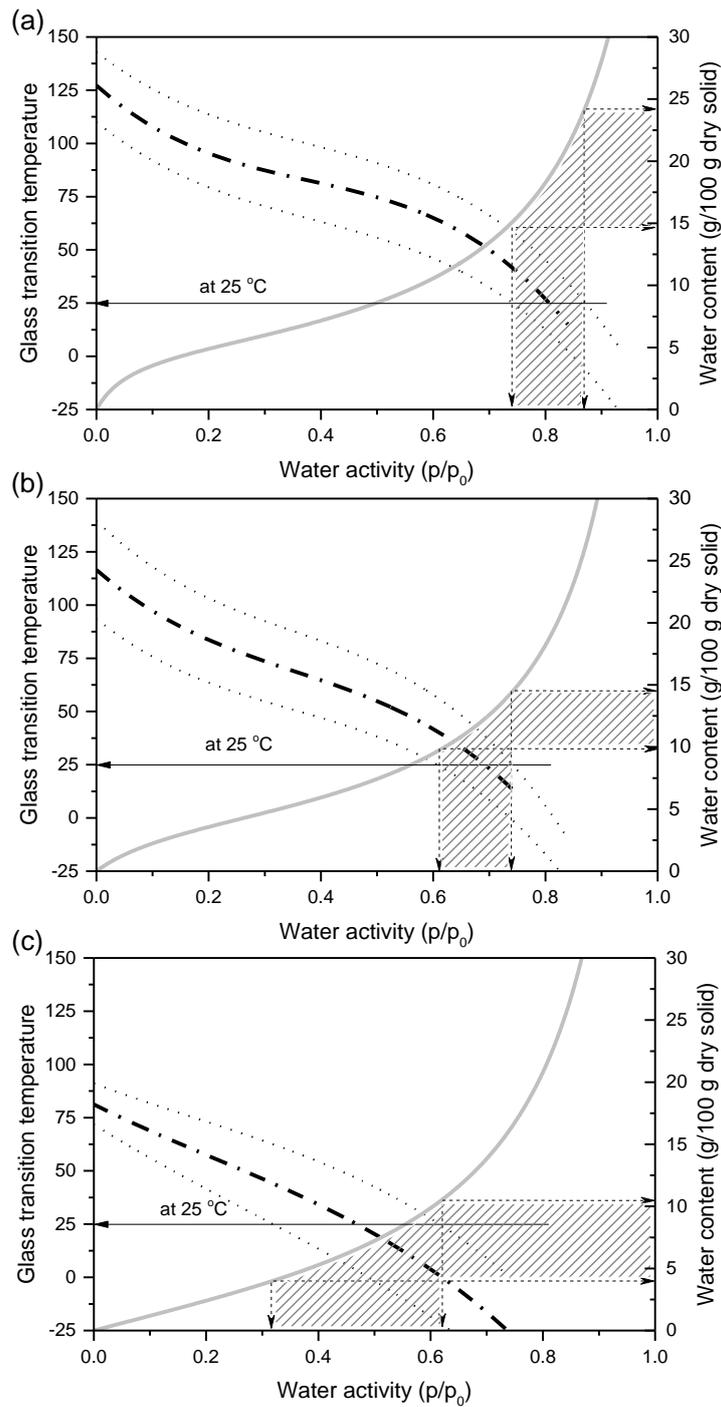
Fig. 4.8 Schematic view, as a function of water activity, of water contents (──), low glass transition temperature Tgl (━·━) and its range (···) for extrudates containing 0% (a), 10% (b) and 20% (c) sucrose. The hatched areas correspond to the zones of critical water activity and and glass transition at 25 °C.
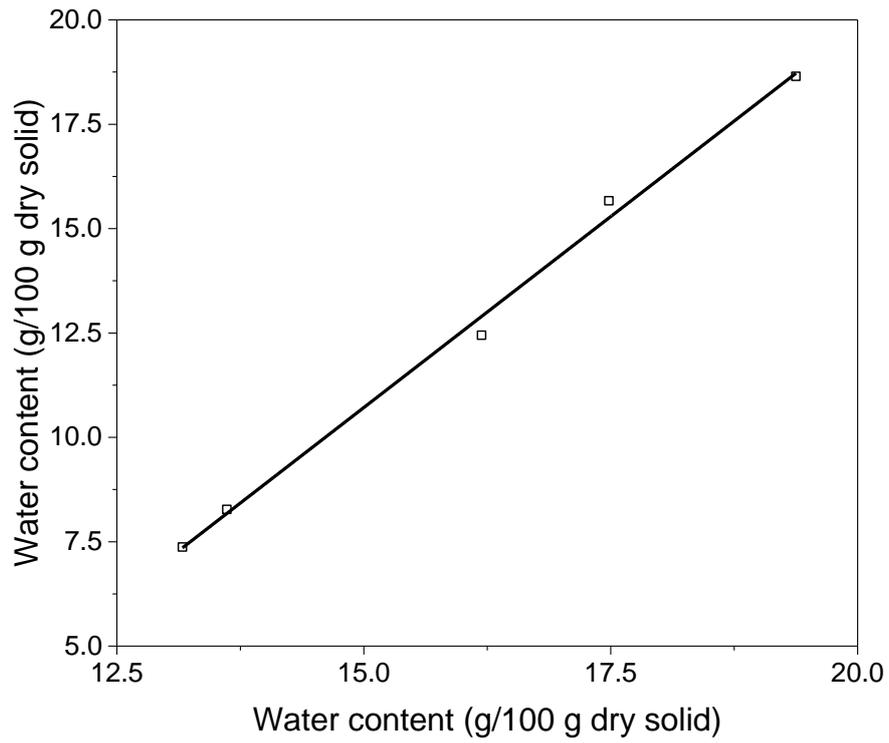
Fig. 4.9 The correlation between water content and water activity at merging of sorption isotherm and critical water content for extrudates with various sucrose content.
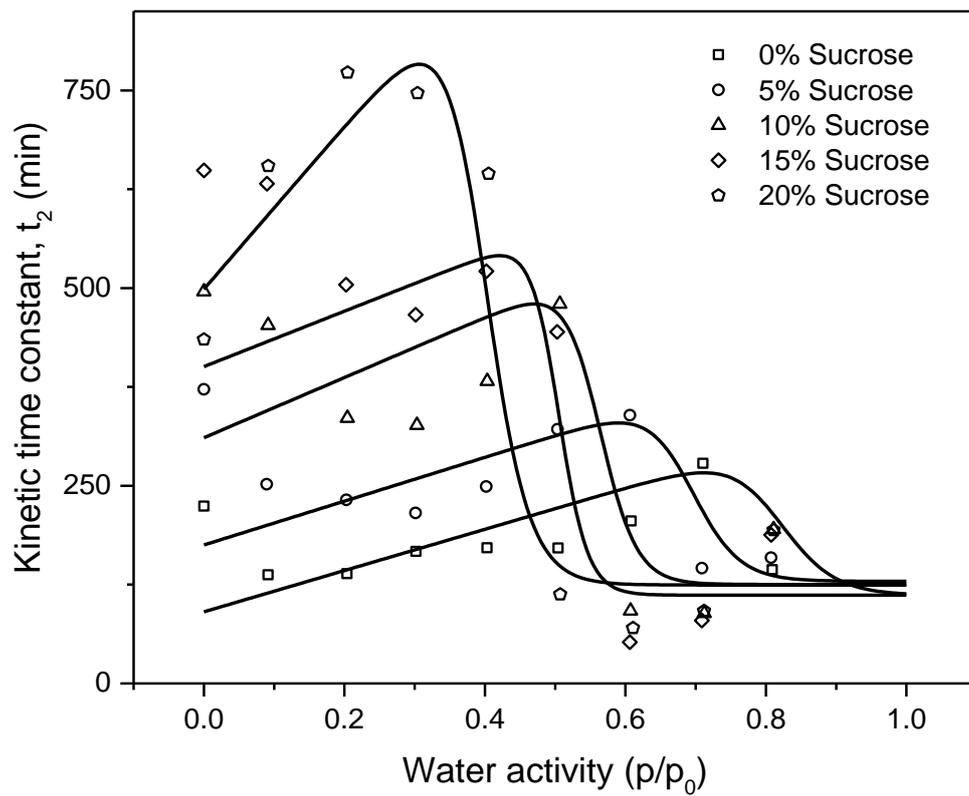
Fig. 4.10 Effect of sucrose content on kinetic time constants t_2 of water diffusion for extrudates. (lines represented Fermi fitting).
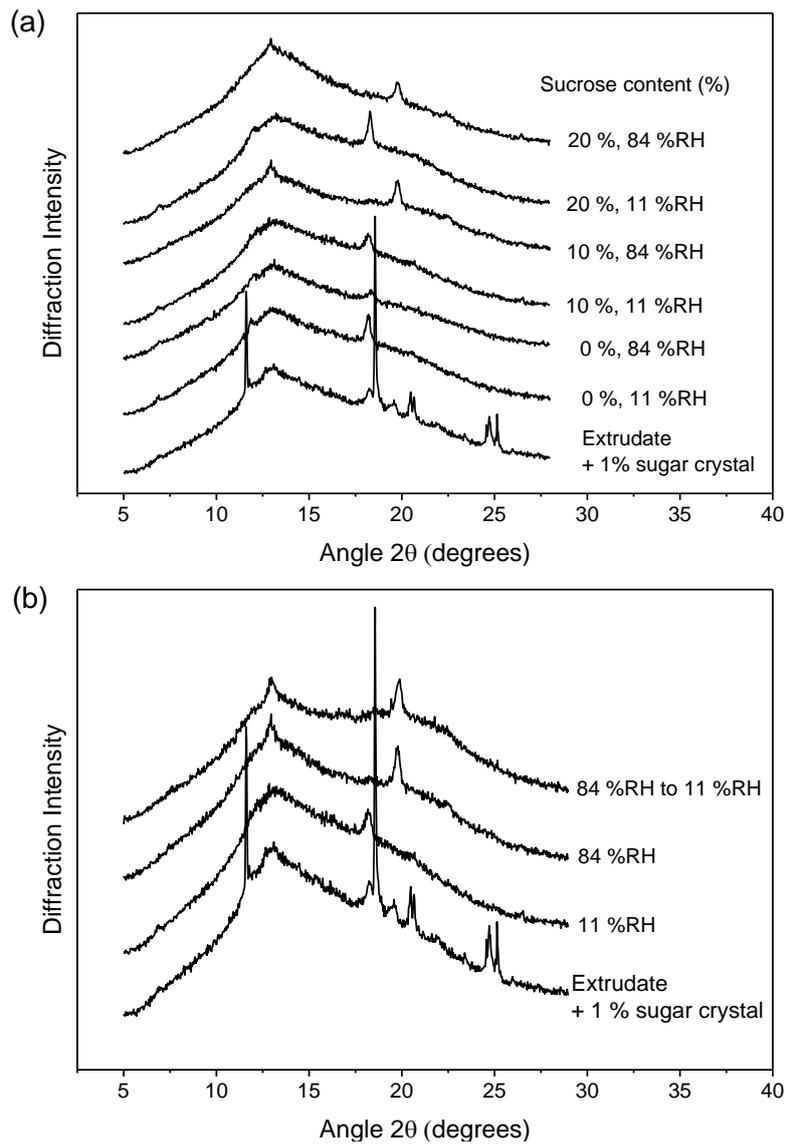
Fig 4.11. X-ray diffraction patterns of extrudates produced at 10% extrusion water with 0, 10, and 20% sucrose equilibrated at 11 and 84% RH (a) and the extrudate with 10% sucrose content equilibrated at 11 and 84 % Rh compared with dehydrated sample (b).

Chapter 5:

Identification of complex glass transition phenomena by DSC in expanded cereal-based food extrudates: impact of plasticization by water and sucrose.

Supuksorn Masavang, Gaëlle Roudaut, Dominique Champion*
University of Bourgogne Franche-Comté, AgroSup Dijon, PAM UMR A 02.102, F-21000 Dijon, France

*Corresponding author: Dominique Champion
E-mail address: dominique.champion@agrosupdijon.fr

Abstract

The physical state and mechanical properties of extruded cereal based products were studied as a function of sucrose content and relative humidity (RH) to evaluate how the presence of sucrose affects glass transition temperature (T_g), sorption isotherm, and texture parameters. Extrudates were prepared with different sucrose content (0 – 20 %wt). Sorption isotherm showed the water content of extrudates decreased when product contains high sucrose at low water activity (a_w) range and the inverse effect was observed at high a_w. T_g s were determined using differential scanning calorimetry (DSC) and two transitions were detected on the heat flow first derivative curve. Addition of sucrose or water decreased both T_g s in extrudates. Young's modulus showed water acts as anti-plasticizer at low a_w, while shows plasticizing effect at high a_w. A stability map can explain the brittle-ductile transition occurred while it was below T_g.

Keywords: Extrudate cereal based-products, sugars, texture, thermal properties, heterogeneity, stability map.

1. Introduction

Although cereals are mainly composed of complex carbohydrates, they are also a source of low molecular weight sugars as a result of both process and recipe. (Williams 2014). However, even if breakfast cereals are mainly composed of complex carbohydrates, they also contain a ratio of low molecular weight sugars now recognized as inappropriate for children and adults (Harris *et al,.* 2011, Williams 2014, Fayet-Moore *et al,.* 2017). Reducing the sucrose content and increasing the protein level in breakfast cereals could induce changes in texture and stability which should not appear to the consumers of these products (Farhat *et al,.* 2000, Barrett *et al,.* 1995, Mezreb *et al,.* 2006, Pitts *et al,.* 2014, Philipp *et al,.* 2017). In order to manage the possible evolution of a modified recipe of extruded cereal-based products, we aimed at better understanding the structural aspects affected by the change of recipe.

Cereal-based products are often produced by extrusion-cooking process that allows a fast mixing-cooking-drying of the ingredients under high mechanical pressure. This process induces melting in the barrel and vitrification of the material at the end with fast water evaporation; this freezing of the structure into a solid foam is due to both the pressure and temperature difference between the extruder and atmospheric conditions after the die. So after extrusion, the obtained material is an amorphous solid structure and glassy material in a non-equilibrium state, which can be changed either by removing water or following rapid super-cooling (Bhandari and Howes 1999, Roos 2003).

Extruded foods are composed mainly of flour opposed to the other minor components, while salt and sugars are only minor constituents in the formulation. Each of these ingredients has physico-chemical properties playing a specific part in the processing characteristics and textural quality of the product (Pitts *et al,.* 2014). In fact, textural properties of low moisture cereal foods are key drivers for their acceptability and their sensory quality depends mainly on crispness. It has been shown that the sucrose exhibits a crispness protecting action against hydration, shifting for sucrose-rich extruded starch the critical hydration towards higher values than for pure extruded starch (Valles Pamies *et al,.* 2000, Roudaut *et al,.* 2002). Indeed, residual water in breakfast cereals appears as the most important ingredient affecting texture through its effect on the glass transition temperature which is widely used to assess stability (Roos and Drusch 2016). The glass

transition temperature (T_g) is specifically the temperature at which an amorphous material changes from a glassy solid structure to a "rubbery" state. The glass transition occurs over a temperature range, although it is often referred to a single temperature value. Pure food components, such as amorphous sugars, often show a single, clear glass transition that can be observed following dielectric, mechanical or thermal properties (Roos 2003). However, in many real food systems, components may be only partially amorphous (carbohydrates, e.g., starch and sugars; proteins) or many food components may only be partially miscible or immiscible at all with each other, forming single or several phases at microstructure scale (Roos 2003). More recently several authors (Roudaut and Wallecan 2015, Tedeschi *et al,.* 2016) evidenced that composite materials may present the thermal signature of two glass transitions in differential scanning calorimetry, reflecting the possible inhomogeneity of the structure with different areas more or less rich in plasticizing molecules.

If the glass transition contributes to the softening of glassy material at high water content, there are also other processes, such as physical aging, that affect textural properties in the glassy state. Results of previous work indicated that compression force showed a maximum and crispness perception decreased as a function of water content while the samples were still at ambient temperature below their T_g (Farroni *et al,.* 2010). Since these glassy products are not in thermodynamic equilibrium at temperatures below their glass transition temperature, they may undergo physical changes when their thermodynamic properties (e.g. enthalpy, free volume) decrease to reach a lower energy state. Such evolution is associated with a physical aging process occurring during storage (Simatos *et al,.* 1996). The structural state of glass depends on thermal history of the glass upon its processing and storage below T_g (Tonchev and Kasap 2002).

Although the phase transition of complex products has been thoroughly studied such as in waffle (Roudaut and Wallecan 2015), starch and sucrose mixture (Roudaut and Champion 2011, Tedeschi *et al,.* 2016), or in extruded products (Roos *et al,.* 1998, Roudaut and Champion 2011), very few studies have investigated the contribution of sucrose to the thermal transition attributed to the glass transition of sugar-containing materials. The objective of this study was to characterize the effects of water uptake and sucrose content on the thermal events occurring at glass transition temperature and product stability in extruded

cereal-based products and to determine the relationship between the temperature of these events and texture properties as observed by mechanical analysis. This objective should provide a general view of the samples stability versus moisture taking into account different behaviours: thermal phase behaviour, and mechanical behaviour in material containing several types of biopolymers and several plasticizers. More specifically, an alternative technique for the determination of multiple glass transitions in composite food, which is the analysis of the DSC heat flow curve derivative was used. In this paper, we report in the first part of our study, a focus on an approach on overlapping endotherms in samples by using Gaussian fitting of the derivative. In the next part, the physicochemical aspects of phase separation in the matrix were analyzed in relation to the glass transition concepts. The results obtained by this multi-analytical approach were combined to better understand the role of water status and sucrose in formulation of extrudates in the determination of plasticization effect and more specifically to highlight heterogeneities in this type of complex materials.

2. Materials and methods

2.1 Sample composition and extrusion

Wheat flour, wheat starch, gluten and sucrose commercial grade were supplied by ADM CHAMTOR (Les Sohettes, France). The extrusion of the ingredient blends containing 0, 5, 10, 15 and 20% wt sucrose with wheat flour 53-73% wt, wheat starch 16% wt, gluten 16% wt and sodium chloride 1% wt was carried out in a Clextral BC-45 intermeshing twin-screws extruder with a 1.5 m long barrel using 10% wt initial moisture content (dry basis). The barrel heating zones were at 80 °C, 130 °C and 160 °C (±2 °C). A 6.0 mm circular die was fitted to the end of the barrel and used to produce the cylinder-shaped extrudates. The screw speed was 150 rpm. Feed rates were controlled: the solid feed at 36 kg/hr and water input of 4 L/hr, giving a water content of 19.5-24.5% wb of molten material in barrel depending on blend formulation and ~10% wb in the final extruded samples. After extrusion, samples were oven dry during 5 min at 150 °C and after cooling, they were hermetically sealed in bag to be kept at ambient temperature.

2.2. Sorption isotherms

The common methods of generating equilibrium moisture sorption isotherms are compared. In this work, the saturated salt solution (SSS) method and humidity generating instruments such as dynamic Vapor Sorption (DVS) instrument were used for determining the hygroscopic behavior of extruded samples.

2.2.1 Salt saturated solutions (SSS)

The samples (water content in range of 2.8-5.2% depending on sucrose content) were equilibrated at different relative humidities in hermetic containers containing P_2O_5 or various saturated salt solutions. P_2O_5 and the saturated solutions of different salts (LiCl, $KC_2H_3O_2$, $MgCl_2$, K_2CO_3, NaBr, NaCl and KCl) and were used to stabilize relative humidity (RH) at respectively 0, 11, 23, 32, 43, 59, 75, and 84% RH for samples needed for experiments, and for determining the sorption isotherms (water content versus water activity) at 25 °C. For storage experiment, the samples were stored at ambient temperature in hermetically sealed polyethylene bags for 24 months. After process their relative humidity was on average 30% RH. When we used the samples, they were equilibrated over saturation salt solution in hermetic boxes at ambient temperature at least 4 weeks and water activity was checked before sample analysis. Constant mass of powders was reached after 4 weeks storage and water content was quantified by the standard oven dehydration method (105 °C/24 h).

2.2.2 Dynamic vapor sorption (DVS method)

Sorption isotherms were determined by a humidity generating instrument: dynamic vapor sorption instrument (DVS-2000, Surface Measurement Systems, London, United Kingdom) that allows the recording of sample mass while exposed to different RH. An approximately 15 mg sample piece was stored over P_2O_5 at room temperature, put into a vacuum desiccator for 1 day, then loaded onto glass DVS pan to be introduced into the sample chamber. A dry nitrogen flow (100 cm^3/min) was used during 1000 min to maximally dry the sample in the chamber: the sample final mass after this step was considered as its dry matter. The equipment kept the same RH in the atmosphere around the sample until a stable mass (dm/dt below 0.002%) for 5 consecutive minutes at 25 °C. The value of the water content for each RH step was determined by fitting, with the asymptotic value of the sample mass evolution curve.

DVS equipment and saturated salt solution experiments were both used to generate the water sorption isotherms. The data were fitted to the GAB model (Eq. 5.1) using SOLVER module from the Excel software (Microsoft Excel 2010):

$$\frac{m}{m_0} = \frac{Cka_w}{[(1-ka_w)(1-ka_w+Cka_w)]}$$

Eq. 5.1

Where, m is the predicted moisture content (g/100g dry solids), a_w is the related water activity, m_0 is the monolayer moisture content (g/100g dry solids), and C and k are GAB constants.

2.3. Differential scanning calorimetry

The glass transition temperature of equilibrated samples was determined using a differential scanning calorimetry (DSC), using Q20 calorimeter (TA instrument, Inc., New Castle, DE, United states) under a nitrogen atmosphere at a flow-rate of 25 mL/min. Experiments were carried out with approximately 5-10 mg of sample hermetically sealed in a medium-pressure aluminum pan (Tzero pan with Tzero Hermetic Lid). An empty pan was used as a reference. The instrument was calibrated at 10 °C/min for temperature and energy with azobenzol and indium. Samples were scanned at 10 °C/min for both cooling and heating in the temperature range of -50 to 170 °C (Figure 2). Two heating scans were done: the first one to erase the thermal history and the possible overshoot associated with enthalpy relaxation (physical aging) and the second one to analyze the reversible contribution of the phase transition (Roudaut and Wallecan 2015). A peak analyzer wizard (OriginPro 2017, OriginLab, Northampton, USA) was used to fit the heat flow first derivative signal of the second DSC heating. The derivative signals (G_i) were fitted by Gaussian distribution functions (Eq. 5.2) and it was possible to identify several T_g (s) by fitting. Full widths at half maximum (FWHM) were determined by peak analyzer option in the software.

$$G_i = \frac{\Delta C_{p,i}}{\Delta T_{g,i}(\pi/2)^{1/2}} exp\left(-\frac{2(T-T_{g,i})^2}{(\Delta T_{g,i})^2}\right)$$

Eq. 5.2

The presence of different phases (i) with their respective glass transitions ($T_{g,i}$) was deduced from the deconvolution of the signal in multiple Gaussians, $\Delta T_{g,i}$ corresponding to the full width at half maximum (FWHM) for a Gaussian. This method is based on the notion that the dH/dT versus temperature signal of a

pure polymer or polymer fraction can be described by one Gaussian function at the glass transition (Roudaut and Wallecan 2015, Hourston *et al,.* 1999).

2.4 Prediction of T_g of mixtures

Gordon-Taylor equation (Gordon and Taylor 1952) is applied to predict the influence of moisture content on the glass transition temperature (Eq. 5.3); initially used for binary systems, the T_g of the overall dry matter was calculated with the same equation:

$$T_{gm} = \frac{x_s \cdot T_{gs} + k_s \cdot x_w \cdot T_{gw}}{x_s + k_s \cdot x_w}$$

Eq. 5.3

Where T_{gm}, T_{gs}, T_{gw} are glass transition temperature (K) of mixture, anhydrous solids and water, respectively; x_s and x_w the mass fraction of solids and water (g/100g wet basis), respectively, and k_s is a constant proportional to the plasticizing effect of the water. The data was fitted to the Gordon Taylor equation using Microsoft Excel 2016, using 138 K as the T_{gw} value for water (Blond and Simatos, 1991).

2.5 Texture analysis

Extrudates were submitted to uniaxial compression test using texture analyzer (TA HD plus, Texture Technologies, Hamilton, MA, USA) with a 100 kg load cell. Compression tests were performed with an aluminum cylinder probe (25 mm, P/25, Stable Microsystems, UK) at room conditions. Force calibration and sensitivity were checked with a 2 kg weight and probe position calibrations were performed before the test. The tests were performed with constant crosshead speed of 0.5 mm/s. Samples were compressed up to 30% strain but only the reversible domain was considered. Strain–stress curves were analyzed and Young's modulus (E_y) was calculated from the slope in the elastic region. Extrudates were pre-equilibrated at different RH before measurements. From 5 to 10 replicates depending on the availability of the equilibrated samples at different RH, were performed to reduce the variation introduced by the heterogeneity of extruded samples. Force vs. distance data were transformed into stress (σ_E) vs. strain (ε_E) using Eqs. (5.4) and (5.5) (Fontanet *et al,.* 1997):

$$\sigma_E = \frac{F_{(t)}}{A_0}$$

Eq. 5.4

$$\varepsilon_E = \frac{H_{(t)}}{H_0}$$

Eq. 5.5

where $F_{(t)}$ is force as function of time, H_0 is sample initial height, H_t is sample height as a function of time, and A_0 is the area under compression curve. Young's modulus, E_y was calculated as the slope of σ_E vs. ε_E curves in the lineal region (Eq. 5.6) (Farroni *et al,.* 2015):

$$E_y(Pa) = \frac{\sigma_{E(t)}}{\varepsilon_{E(t)}}$$

Eq. 5.6

where stress and strain were measured in the reversible domain and calculated taking into account the geometry of the sample (height and section).

The relationship between E_y and water activity was modelled using the Fermi equation (Eq. 5.7) to describe the sigmoid curve obtained from plotting parameters (Peleg 1994, Roudaut *et al,.* 1998, Pittia and Sacchetti 2008, Arimi *et al,.* 2010).

$$Ey = \frac{(Y_0 - Y_r + ka_w)}{\left\{1 + exp\left[\frac{(a_w - a_{wc})}{b}\right]\right\}} + Y_r$$

Eq.5.7

Where E_y is the Young's modulus values dependent on water activity; Y_o is the initial value of the analyzed result (in this study values corresponding to the values at $a_w \sim 0$); a_w is the water activity; a_{wc} is the critical water activity where $Ey = Y_o/2$ a drastic textural change takes place; k is a constant corresponding to the slope of the increasing region and b is a constant describing the slope of transition of analyzed variable (Arimi *et al,.* 2010).

3. Results and discussion

3.1 Water sorption isotherms

The water sorption isotherm of food is obtained from the equilibrium moisture contents determined at several a_w values at constant temperature. Sorption isotherms are used for a number of purposes in food research such as food processing, packing and storage (Labuza and Hyman 1998). The saturated salt slurry method can be used to generate isotherm but it takes a rather long time (4 weeks) for the product to achieve equilibrium and requires large sample mass to obtain a measurement with good accuracy for water content determination. In order to overcome these disadvantages, DVS was also used to generate sorption isotherms in a relatively shorter period of time due to sample size and nitrogen flow controller; this technique is designed to accurately measure the sample weight change at given RH for a constant temperature.

The extruded sample isotherm data at 25 °C (Fig. 5.1) obtained using both SSS and DVS methods, showed slight difference in the range of a_w 0.10-0.40; no significant difference was found at the higher a_w values according to the standard deviation for the water content determinations. The difference measured at low RH may be attributed to difficulties in water content determination by oven dehydration that induces chemical reactions (i.e. non- enzymatic browning, polymerization) where water molecules are involved or produced. Once the a_w is high enough ($a_w > 0.4$), water is able to diffuse into the extruded matrix more rapidly and both methods come into agreement probably because mass stability is easier to reach. (Schmidt and Lee 2012) explained that below a_w 0.40, it is hypothesized that water is mainly adsorbed (adsorption section of the working isotherm) or desorbed (desorption section of the working isotherm) from the surface of the cornflakes, following Fickian diffusion in each of the working isotherm methods, resulting in very little difference in moisture content. As a_w increase above 0.40, permeability of the laminate surface becomes sufficient for increased adsorption of moisture if given sufficient time (the time required being dependent on permeability and hence, a_w).

Experimental sorption data were fitted to GAB (Guggenheim-Anderson-de Boer) which has been used to describe the isothermal sorption behavior of many foods and biological materials (Fabra *et al,.* 2009, Andrade and Pérez 2011). The experimental and predicted water content values using the GAB equation for

extruded samples were determined at 25 °C (Fig. 5.1) with different sugar content (Fig. 5.1b). Similar type of curves for isotherms was observed by many researchers for extruded samples (Wani and Kumar 2016, Lazou and Krokida 2011). At low a_w, the slope of the curve was low and increased rapidly with further increase in a_w.

For all samples in the RH range of < 0.75, the higher the sucrose concentration in the sample, the lower is its water content after mass equilibrium in a given RH. This observation may be attributed to the preferentially cross-linking of biopolymer matrix by sugars when the availability of water is low (Hazaveh *et al,.* 2015). For a_w > 0.75, the accessibility of the hydroxyl groups to water molecules increases due to the swelling of the biopolymer, so there is a rise in accessibility of the polar groups to the water molecules. The observed behavior was typical of products with high-sugar content, which absorb relatively small amounts of water at low-water activities but exhibit a sharp increase in sorbed water at higher water activities. This could be due to the effect of solute-solvent interactions associated to sucrose instead of the previous prevailing effect of sucrose-biopolymer interactions hindering interactions with water molecules (Tsami *et al,.* 1990, Fabra *et al,.* 2009). This behavior is similar to that observed in literature for dry biscuits (Guillard *et al,.* 2004, Bourlieu *et al,.* 2008), for sponge cakes (Guillard *et al,.* 2003), for cookies and corn snacks (Palou *et al,.* 1997), for cereal bars (Pallavi *et al,.* 2015) and also for extruded snacks (Wani and Kumar 2016).

3.2. Differential scanning calorimetry study (DSC)

For all samples with or without added sucrose, the first DSC heating scan (Fig. 5.2) exhibited an endothermic peak ranging from 40 to 60 °C which is attributed to physical aging phenomenon that is only possible in the glassy state (Blond and Simatos 1991, Wungtanagorn and Schmidt 2001, Fan and Roos 2016). This enthalpy relaxation phenomenon was not immediately reversible after the first heating but may be recovered after several days of storage (data not shown). Physical aging refers to structural relaxation of glassy material and is accompanied by changes in several physical properties during storage such as loss of crispness resulting in a soggy and soft texture.

Thus, the presence or absence of this enthalpy recovery peak and its energy value are indicators as function of storage time of the relaxation ability of the material in the glassy state. Indeed, the enthalpy magnitude of the DSC endothermic peak is a measure of the extent of aging due to the residual mobility in amorphous solids. The denser the material was becoming during storage, the higher the measured enthalpy of de-aging in DSC is upon heating through the glass transition (Ho and Vu-Khanh 2003, Daly *et al,.* 2004).

The effect of aging of cereals-based extrudates below their glass transition temperature has been also studied by DSC methods by other authors (Roos *et al,.* 1998, Roudaut *et al,.* 1998, Roudaut *et al,.* 2002, Homer *et al,.* 2014). It is found that a pre-peak, as it is called, could be seen well below T_g depending on temperature and duration of storage time. In fact, the enthalpy energy of this endothermic event depends on the temperature difference between the storage temperature and glass transition temperature (T_g).

In this work for samples at RH below 84%, the aging peak is clearly identified on the first heating in DSC but not on the second one (Fig. 5.2). All samples were processed the same day and stored in the same conditions, but the higher the relative humidity (below 84 %RH) and sucrose content, the higher was the enthalpy of the structural relaxation. The aging ability of the material is facilitated by the possible molecular mobility in the glassy state which appears more important as the water or sucrose content is increased. For samples, stored at temperature above their T_g (samples at 84 %RH), no enthalpy relaxation could be seen on DSC curve.

DSC analyses were performed on samples with different hydration-dehydration history during storage. Extruded samples with 10% sucrose originally at a_w 0.33, stored for 24 months at room temperature within a sealed polythene bag underwent dehydration at low RH while equilibrating over P_2O_5 and then rehydration when stored at a_w 0.33. The first heating scan of the original samples showed an endothermic peak between 35 and 75 °C (Fig. 5.3). The hydration history affected the peak characteristics: the dehydrated sample exhibited a flattened enthalpy peak while the endothermic peak of the rehydrated sample showed an intermediate amplitude (greater than the dehydrated sample but almost the same as the initially equilibrated sample) over a broader temperature range than the initial sample. The 2nd heating scan showed a nearly flat thermogram for all samples (Fig. 5.3) as a result of the non-reversibility of the observed processes

and these two second scans are analogous, meaning that the sample recovered the same water content before and after dehydration/hydration process. (Appelqvist *et al,.* 1993) suggested that the endothermic event reflected the disruption of energetic association between water molecules and hydrophilic groups on the polysaccharide under conditions of restricted mobility. The peak due to enthalpy relaxation will show when there is sufficient mobility for the chains to move towards the equilibrium state. These relaxation processes before drying were not erased for samples studied after a storage under P_2O_5 RH but could not be seen on thermogram. Dehydration does not rejuvenate the sample although nothing is clearly seen on DSC. To go further, a fast rehydration of the sample (one week at 33%RH) allowed to recover almost the same relaxation enthalpy than the sample stored for several months. So the enthalpy endotherm seen after aging is clearly dependent on water content but does not reflect the densification of the sample which cannot de-age without water in DSC.

At constant water activity, the energy of the endothermic peak increased with increasing sucrose content, the peaks were wider and slightly shifted to lower temperature for samples with high sucrose content (Fig. 5.2c), probably because of the difference between the storage temperature and T_g the latter being expected to decrease with the sucrose amount in the sample. The relaxation enthalpy associated with the peak also increased with increasing a_w up to 0.58. Below this a_w, the T_g values of extruded samples were greater than 25 °C for all samples, allowing physical aging to occur over time as mentioned above. However, at higher hydration, the endothermic peak disappeared completely due to the increased chain mobility above T_g (Shogren 1992) (Fig. 5.2a, c).

The aging phenomena could interfere with the T_g determination since it is observed in the same temperature region and confirmed that samples went through their glass transition temperature in the temperature range considered (Fig. 5.2). However, it is not so obvious to see the ΔC_p (step) associated with the glass transition on the second heating scan (Fig. 5.2b), mainly because the material is a composite of several types of biopolymers (starch, gluten) and a low amount of sugars giving a wide temperature range for T_g, which may merge more or less in the baseline. Even if an increase in the sucrose content induced a better identification of the T_g range on the second heating scan, interpretation of the results can be

complicated by poor resolution of the events when plotted using heat flow signals of the second heating scan. Thermal events can be better analyzed using the first derivative of heat flow signal to identify glass transition (Sacha and Nail 2009). The first derivative calculated for the 2nd heating scan of extrudates displayed one or two endothermic events depending on the sample composition in sucrose and water. Due to the overlap of derivative peaks, more precise T_g values, associated with each peak, were determined by the fit of the derivative curve with one or two discrete Gaussian functions (Fig. 5.4). Peak fitting permits the deconvolution of the derivative DSC signal at different RH (Fig. 5.5); and the glass transition temperatures were determined with the maximum of each peak that mathematically corresponds to an inflection point in the heat flow curve.

For some samples, two Gaussian functions were used to fit the derivative curve: one at a low temperature designated by its maximum at T_{gl}, and another one, at a higher temperature, T_{gh} (Fig.4). Gaussian distribution showed a satisfactory fit with the experimental data. This identification of several glass transitions in complex food materials has been already done for waffle (Roudaut and Wallecan 2015) or starch-sucrose blends (Tedeschi *et al,.* 2016), and has been explained as phase separations between different plasticizer-rich areas at microscale level. Indeed, (Roudaut and Wallecan 2015) showed also two phases in baked waffle at $a_w > 0.2$ without added sugars and they attributed these two T_g to glass transitions of gluten-rich and starch-rich fractions. In our breakfast cereal samples stored below 23% RH, it was not possible to identify two glass transitions with the derivative curves, but it does not mean that they are not superimposed onto each other. At higher RH, T_{gl} and T_{gh} were clearly identified for samples with and without added sucrose.

The possible phase segregation appeared to be more related to the water content of the sample than to the sucrose concentration. Because our extruded samples are based on flour, wheat starch, sucrose, gluten, and salt, it may be hypothesized that the lower glass transition originated from small molecules or plasticizer rich fraction such as sucrose, while the higher temperature transition would result from the biopolymers, starch and/or protein fractions. However, to be visible on the DSC derivative, this phase separation required dynamics that could only be reached when the water content was sufficiently high. The

overlapping of the transition peaks suggests a non-unique composition for phases and distributions of microenvironments, *i.e* heterogeneities.

T_{gl} and T_{gh} are both shifted to lower temperatures with the increase in water or sucrose content in the sample, due to plasticizing effect of these small molecules for biopolymers (Fig. 5.5-6). As for glass transition, the reversible transformation of the solid to liquid-like behavior is expected to occur over a temperature "range" rather than at a constant temperature (Fan and Roos 2017). So instead of only considering the reference temperature with the inflection point T_{gl} and T_{gh} the width of the transitions was taken into account with the FWHM value of both fitted Gaussian functions. In fact, FWHM positions were used to define the corresponding temperature range of glass transition (RTg) which was calculated with Eq. 5.8.

$$RTg/2 = Tg \pm T_{FWHM}/2$$
Eq. 5.8

The glass transition T_{gl} and T_{gh} for sample with 10 % sucrose are shown in Fig.7. RTg for transitions characterized by T_{gl} spread on a 16 °C range for high amount of water, and of 47 °C for low amount, the range appeared narrower for T_{gh}. This observation may be opposite with the assumption of heterogeneities in the material with small molecules rich phases showing a lower T_g and with a richer phase of biopolymers characterized with higher T_g because it is expected that biopolymers go through the glass transition over a wider range of temperature. But we can assume 1) that the composition of the different phases, roughly the sucrose / biopolymers ratio, may be variable inducing a glass transition over a wide range of temperature or 2) that the width of the first transition is affected by structural relaxation during the second heating process in the DSC, because the kinetic of aging is faster for small molecules glasses than for polymeric material (Simatos *et al,.* 1996, Blond and Simatos 1991).

It can be observed that the width and height (Fig. 5.5) of the Gaussian peak is more affected by a_w than by the sucrose content of the samples, but it is difficult to conclude about the impact of water content

on heterogeneities in the material because it is also known that water content increases the ΔC_p step amplitude at T_g, making easier the visualization of expected peaks on derivative curves.

The influence of moisture content on the glass transition temperature of extruded samples was evaluated, the experimental T_{gl} and T_{gh} data were also subjected to a nonlinear least square regression analysis using Gordon-Taylor equation (Eq. 5.3) because the use of this model provides a convenient way to compare the five formulations. In Fig. 5.7, the experimental and calculated T_{gl} and T_{gh} values were plotted for 10% sucrose samples. Water plasticizes extruded samples,as exhibited by decreasing Tg with increasing moisture content. Similar results were reported by (Carvalho and Mitchell 2001) in maize and wheat extrudates; (Barrett *et al,.* 1995) in corn extrudates and (Roudaut and Wallecan 2015) in low moisture baked products. Common sugars have a low glass transition temperature compared to biopolymers: i.e. T_g values for dry amorphous sucrose reported in the literature range from 52 to 75 °C (Roe and Labuza 2005), so they usually depress glass transition temperature of biopolymers in sugar-rich foods (Bhandari and Roos 2017, Bhandari and Howes 1999). Water is also considered as a strong plasticizer in food systems because it is the major component responsible for depressing the glass transition temperature of food materials, as water has a very low glass transition temperature of -135 °C. When Gordon-Taylor model was applied to T_{gl} and T_{gh} values, it was "abusively"supposed that the total water content was the same in every phase. As first approach, this assumption allowed the Gordon-Taylor's parameters determination T_{gs} and k values (Table.1) for extruded samples. T_{gs} for both T_{gl} and T_{gh} decreased with increasing sucrose content. The k_s values obtained for extrudates increased with increasing sucrose content. Thus, sucrose seemed to make samples more sensitive to water plasticization. However, this calculation remains a raw estimation because the precise water content of each phase is not exactly known, indeed if according to the isotherms (Fig. 5.1), it is clear that the water content of sucrose-rich phases is lower than the polymer-richer ones, their exact compositions remain unknown.

<u>3.3 Mechanical properties</u>

The changes in mechanical properties in response to different RH exposure were studied as a function of the samples sucrose content. Young's modulus (E_y) is a property commonly used to assess the stiffness of a material. Hydration of cereal-based products is known to lead to plasticization and softening of the starch–protein matrix and thus to alter the strength of the product (Martínez-Navarrete *et al,.* 2004).The Young's modulus curve of extruded samples equilibrated to different a$_w$ followed a sigmoid curve with increasing a$_w$ (Fig. 5.8). Fig. 5.8a shows a peak of E_y at low water activity for extrudates with 20 % sucrose content stored at room temperature just for 2 months; while for samples with various aging times (from few months up to 24 months) E_y shows only a plateau region for low water activities and no maximum in E_y (Fig. 5.8b). The increase of Young modulus in the glassy state when a$_w$ increases is called "anti-plasticization". This effect was already described in literature (Chang *et al,.* 2000), for ultimate stress on crackers (Lewicki *et al,.* 2004), for E_y on extruded corn balls (Mazumder *et al,.* 2007), for deformation force on cheese balls (Harris and Peleg 1996) and for E_y of extruded breads (Fontanet *et al,.* 1997). The increase in rigidity as the water activity increases has been explained by (Harris and Peleg 1996) as a result of partial plasticization of air cell wall material increasing the cohesion and hence the toughness of a product structure. On one hand, at very low water activity, the structure of cellular products collapses rapidly and its destroyed elements offer no resistance to deformation. On the other hand, partial plasticization is accompanied by toughening because moistened structure does not disintegrate so easily (Lewicki *et al,.* 2004). When considering samples at different storage times, E_y did not show any increase with increasing water content: the anti-plasticizing effect was not visible when we introduced aged samples in the set of results.

The samples at low water activity had higher T$_g$ s and were not able to age as fast as glassy samples stored close to their glass transition. So possibly due to the difference of sample densification during storage, an anti-plasticization effect can be seen; when considering long term storage allowing densification for all samples, this effect is no longer visible. (Lourdin *et al,.* 2002) suggested that during aging of the glassy solids, the materials became less compliant with the mechanical relaxation time progressively increasing. The

progressive change in material properties occurred over a timescale similar to the slow densification of the amorphous glasses, characteristic of structural relaxation in the glassy state.

At low water content, E_y increased with increasing sucrose content and there was a positive correlation between E_y and bulk density (0.21-0.42 g/cm³) for sucrose-containing (0-20%) samples, that can explain the hardness of sample with higher sucrose contents. Indeed, (Barrett *et al,.* 1995) worked on corn extrudates containing 0-10 % wt sucrose, and showed that increased sucrose content induced higher density and reduced mean cell size, which resulted in an increase in compressive resistance of dry extrudates.

The onset of E_y decrease was observed at a_w 0.64, 0.47 and 0.43 for extrudates with 0, 10 and 20 % sucrose content respectively; this E_y decrease onset was called "mechanical T_g" (Fig. 5.8). The relationship between E_y and water activity was fitted with a mathematical equation based on the Fermi function (Eq. 5.6). The estimated values of the model constants are reported in Table 1 for each extruded sample under study. The critical water activity, a_{wc} decreased from 0.70 to 0.59 when sample contained more sucrose. The decrease in hardness above a_{wc} is due to increased plasticization by water and sucrose leading to a softening of the matrix. The slope of hardness changes versus water activity increased with the sucrose content increase, showing the higher sensitivity of sucrose containing samples faced with RH changes.

3.4 Physical change–glass transition relationships

The shelf-life and textural properties of food products are closely related to their mechanical and thermal properties. The physical state, water mobility, and water-solid interactions affect storage stability, textural, and functional properties of food (Farroni *et al,.* 2008). DSC results showed heterogeneities of composition in the studied material, characterized by different glass transition temperatures. This also will lead to differences in the water content of the two phases at equilibrium water activity (Tedeschi *et al,.* 2016). (Nicholls *et al,.* 1995) concluded that, for low moisture cereal products, the brittle-ductile transition, and hence the loss of brittle texture, is not necessarily due to changes associated with the glass transition. Therefore, prediction of brittle textures from the determination of T_g alone is not possible and it appears

necessary to study dynamical changes occurring in the glassy state to explain textural or brittle-ductile changes.

Several authors have coupled sorption isotherms data with those of glass transition temperatures, in order to obtain the critical conditions for food storage (Roos 1995, Roos *et al,.* 1998, Karel *et al,.* 1994, Ostrowska-Ligęza *et al,.* 2014). Hence, this stability map allows the calculation of both critical a_w (a_{wc}) and water content (W_c) for extrudates storage. In Fig. 5.9 T_{gl} was used to establish this stability map as the first detected (at low temperature) phenomenon involved in the sample phase transition. The critical water activity, a_{wc} (0.63 and 0.72 for sample with and without sugar for T_{gl}); 0.59 and 0.68 for sample with and without sugar for T_{gh}) and water content, W_c (24.6 and 14.7 % for sample with and without sugar for T_{gl} ; 14.9 and 9.7 % for sample with and without sugar for T_{gh}) were estimated for an ambient temperature of 25 °C. The samples were the most stable at, or below, a_{wc} and W_c at storage temperature (25 °C).

The value of critical water activity and water content for samples containing sucrose are lower than for samples without: these lower values reflect that the sucrose-containing product will go through undesirable changes in textural properties after water sorption in the glassy state, in an easier way than the products without sucrose. W_c decreased from 14.9 to 9.7 % for the 10 % sucrose addition. When stored at a higher temperature, the stability criteria will change to lower values of a_w and water content and the sample will suffer physical transformations such as collapse, stickiness and crispness loss when stored at the critical values determined for 25 °C. Mathematical models for mechanical properties, and sorption isotherm of extruded samples with 0 and 10% sucrose are plotted together in Fig.9a and 9b, with a polynomial curve fitting to visualize the temperature range for glass transition. Water content corresponding to the low glass transition temperature (T_{gl}) equal to 25 °C ranged from 9.7 to14.6 % (for 10% sucrose sample) and from 14.8 to 24.6 % for sample without added sucrose (Fig. 5.9). For both samples at this water content, the Young's modulus showed a sharp decrease due to the softening. For sample at 20% sucrose (data not show), the loss of rigidity corresponded to the rheological changes attributed to the glass transition occurring below 25 °C. The critical water content for Mechanical T_g was the water content at the onset of E_y decrease. It is noticeable that it was lower than the critical water content for T_{gl} for the sample at 0 and 10% sucrose

content. For 20 % sucrose (Fig. 9c), mechanical T_g and T_{gl} are in agreement, probably because the T_g corresponded to the glass transition of sucrose rich-phases. It is important to notice here that the water contents for the "Mechanical T_g" taken as the onset of E_y decrease corresponded to samples which were still in the glassy state, even if considering the lowest visible glass transition T_{gl}. The textural changes could thus be caused by the glass transition of a minor phase, which may not be visible on DSC thermograms (Slade and Levine 1993).

4. Conclusions

In this work, the effect of sucrose addition on the water sorption, glass transition and mechanical properties was investigated. Increasing the sucrose content of extrudates resulted in a significant increase in both RH sensitivity and Young's modulus of dry extruded products and caused a reduction in the glass transition temperature, critical water content and critical water activity of extrudates. The so called anti-plasticizing effect for glassy material that was described for mechanical properties when water content was increased may be correlated to an intermediate state of material aging, leading to a denser material. A detailed analysis of DSC curves supported the idea that multiple endothermic events could be associated with the coexistence of several phases or heterogeneities into extrudates. Sucrose seemed to result in extrudates with higher hardness in the glassy state but lower stability above this temperature with sharper changes in mechanical properties. These results clearly showed the need for complementary techniques to probe the dynamic in the glassy state that could be facilitated in low density zones having lower T_g value and then to manage the stability during storage of this type of dry products. For example, a deeper knowledge of water dynamics using NMR will be carried out.

Acknowledgements

Reference

Andrade, R. & Pérez, C. (2011). Models of sorption isotherms for food: Uses and limitations. *Vitae, Revista de la Faccultad de Quimica Farmaceutica,* **18,** 325-334.

Appelqvist, I. A. M., Cooke, D., Gidley, M. J. & Lane, S. J. (1993). Thermal properties of polysaccharides at low moisture: 1—An endothermic melting process and water-carbohydrate interactions. *Carbohydrate Polymers,* **20,** 291-299.

Arimi, J. M., Duggan, E., O'Sullivan, M., Lyng, J. G. & O'Riordan, E. D. (2010). Effect of water activity on the crispiness of a biscuit (Crackerbread): Mechanical and acoustic evaluation. *Food Research International,* **43,** 1650-1655.

Barrett, A., Kaletunç, G., Rosenburg, S. & Breslauer, K. (1995). Effect of sucrose on the structure, mechanical strength and thermal properties of corn extrudates. *Carbohydrate Polymers,* **26,** 261-269.

Bhandari, B. & Howes, T. (1999). Implication of glass transition for the drying and stability of dried foods. *Journal of Food Engineering,* **40,** 71-79.

Bhandari, B. & Roos, Y. H. (2017). Introduction to Non-Equilibrium States and Glass Transitions—The Fundamentals Applied to Foods Systems. In: Non-Equilibrium States and Glass Transitions in Foods. Pp. xxxiii-l. Woodhead Publishing.

Blond, G. & Simatos, D. (1991). Glass transition of the amorphous phase in frozen aqueous systems. *Thermochimica Acta,* **175,** 239-247.

Bourlieu, C., Guillard, V., Powell, H., Vallès-Pàmies, B., Guilbert, S. & Gontard, N. (2008). Modelling and control of moisture transfers in high, intermediate and low aw composite food. *Food Chemistry,* **106,** 1350-1358.

Carvalho, C. W. P. & Mitchell, J. R. (2001). Effect of Sucrose on Starch Conversion and Glass Transition of Nonexpanded Maize and Wheat Extrudates. *Cereal Chemistry Journal,* **78,** 342-348.

Chang, Y. P., Cheah, P. B. & C. J. Seow, C. (2000). Plasticizing—Antiplasticizing Effects of Water on Physical Properties of Tapioca Starch Films in the Glassy State. **65,** 445-451.

Daly, J. H., Hayward, D., Liggat, J. J. & Mackintosh, A. R. (2004). Ageing and rejuvenation of Biopol™, [poly (3-hydroxybutyrate-co-3-hydroxyvalerate)] copolymers: A dielectric study. *Journal of Materials Science,* **39,** 925-931.

Fabra, M. J., Talens, P., Moraga, G. & Martínez-Navarrete, N. (2009). Sorption isotherm and state diagram of grapefruit as a tool to improve product processing and stability. *Journal of Food Engineering,* **93,** 52-58.

Fan, F. & Roos, Y. H. (2016). Structural relaxations of amorphous lactose and lactose-whey protein mixtures. *Journal of Food Engineering,* **173,** 106-115.

Fan, F. & Roos, Y. H. (2017). Glass Transition-Associated Structural Relaxations and Applications of Relaxation Times in Amorphous Food Solids: a Review. *Food Engineering Reviews,* **9,** 257-270.

Farhat, I. A., Blanshard, J. M. V., Descamps, M. & Mitchell, J. R. (2000). Effect of Sugars on Retrogradation of Waxy Maize Starch-Sugar Extrudates. *Cereal Chemistry Journal,* **77,** 202-208.

Farroni, A. E., Guerrero, S. & Buera, M. P. (2015). Sensorially and Instrumentally Detected Antiplasticizing Effect of Water in Cornflakes. In: Water Stress in Biological, Chemical, Pharmaceutical and Food Systems (edited by GUTIÉRREZ-LÓPEZ, G. F., ALAMILLA-BELTRÁN, L., DEL PILAR BUERA, M., WELTI-CHANES, J., PARADA-ARIAS, E. & BARBOSA-CÁNOVAS, G. V.). Pp. 125-134. New York, NY: Springer New York.

Farroni, A. E., Matiacevich, S. B., Guerrero, S., Alzamora, S. & Buera, M. P. (2010). Thermal Transitions, Mechanical Properties, and Molecular Mobility in Cornflakes as Affected by Water Content. In: Water Properties in Food, Health, Pharmaceutical and Biological Systems: ISOPOW 10. Pp. 583-589. Wiley-Blackwell.

Farroni, A. E., Matiacevich, S. B., Guerrero, S., Alzamora, S. & del Pilar Buera, M. (2008). Multi-Level Approach for the Analysis of Water Effects in Corn Flakes. *Journal of Agricultural and Food Chemistry,* **56,** 6447-6453.

Fayet-Moore, F., McConnell, A., Tuck, K. & Petocz, P. (2017). Breakfast and Breakfast Cereal Choice and Its Impact on Nutrient and Sugar Intakes and Anthropometric Measures among a Nationally Representative Sample of Australian Children and Adolescents. *Nutrients,* **9,** 1045.

Fontanet, I., Davidou, S., Dacremont, C. & Le Meste, M. (1997). Effect of Water on the Mechanical Behaviour of Extruded Flat Bread. *Journal of Cereal Science,* **25,** 303-311.

Gordon, M. & Taylor, J. S. (1952). Ideal copolymers and the second-order transitions of synthetic rubbers. i. non-crystalline copolymers. *Journal of Applied Chemistry,* **2,** 493-500.

Guillard, V., Broyart, B., Bonazzi, C., Guilbert, S. & Gontard, N. (2003). Moisture Diffusivity in Sponge Cake as Related to Porous Structure Evaluation and Moisture Content. *Journal of Food Science,* **68,** 555-562.

Guillard, V., Broyart, B., Guilbert, S., Bonazzi, C. & Gontard, N. (2004). Moisture diffusivity and transfer modelling in dry biscuit. *Journal of Food Engineering,* **64,** 81-87.

Harris, J. L., Schwartz, M. B., Ustjanauskas, A., Ohri-Vachaspati, P. & Brownell, K. D. (2011). Effects of Serving High-Sugar Cereals on Children's Breakfast-Eating Behavior. *Pediatrics,* **127,** 71.

Harris, M. E. G. & Peleg, M. (1996). Patterns of Textural Changes in Brittle Cellular Cereal Foods Caused by Moisture Sorption1. *Cereal Chemistry,* **73,** 225-231.

Hazaveh, P., Mohammadi Nafchi, A. & Abbaspour, H. (2015). The effects of sugars on moisture sorption isotherm and functional properties of cold water fish gelatin films. *International Journal of Biological Macromolecules,* **79,** 370-376.

Ho, C. H. & Vu-Khanh, T. (2003). Effects of time and temperature on physical aging of polycarbonate. *Theoretical and Applied Fracture Mechanics,* **39,** 107-116.

Homer, S., Kelly, M. & Day, L. (2014). Determination of the thermo-mechanical properties in starch and starch/gluten systems at low moisture content – A comparison of DSC and TMA. *Carbohydrate Polymers,* **108,** 1-9.

Hourston, D. J., Song, M., Schafer, F. U., Pollock, H. M. & Hammiche, A. (1999). Modulated-temperature differential scanning calorimetry: 15. Crosslinking in polyurethane–poly(ethyl methacrylate) interpenetrating polymer networks. *Polymer,* **40,** 4769-4775.

Karel, M., Anglea, S., Buera, P., Karmas, R., Levi, G. & Roos, Y. (1994). Stability-related transitions of amorphous foods. *Thermochimica Acta,* **246,** 249-269.

Labuza, T. P. & Hyman, C. R. (1998). Moisture migration and control in multi-domain foods. *Trends in Food Science & Technology,* **9,** 47-55.

Lazou, A. & Krokida, M. (2011). Thermal characterisation of corn–lentil extruded snacks. *Food Chemistry,* **127,** 1625-1633.

Lewicki, P. P., Jakubczyk, E., Marzec, A., Cabral, M. C. & Pereira, P. M. (2004). Effect of water activity on mechanical properties of dry cereal products. **4,** 381-391.

Lourdin, D., Colonna, P., Brownsey, G. J., Noel, T. R. & Ring, S. G. (2002). Structural relaxation and physical ageing of starchy materials. *Carbohydrate Research,* **337,** 827-833.

Martínez-Navarrete, N., Moraga, G., Talens, P. & Chiralt, A. (2004). Water sorption and the plasticization effect in wafers. *International Journal of Food Science & Technology, 39,* 555-562.

Mazumder, P., Roopa, B. S. & Bhattacharya, S. (2007). Textural attributes of a model snack food at different moisture contents. *Journal of Food Engineering, 79,* 511-516.

Mezreb, K., Goullieux, A., Ralainirina, R. & Queneudec, M. (2006). Effect of sucrose on the textural properties of corn and wheat extrudates. *Carbohydrate Polymers, 64,* 1-8.

Nicholls, R. J., Appelqvist, I. A. M., Davies, A. P., Ingman, S. J. & Lillford, P. J. (1995). Glass transitions and the fracture behaviour of gluten and starches within the glassy state. *Journal of Cereal Science, 21,* 25-36.

Ostrowska-Ligęza, E., Jakubczyk, E., Górska, A., Wirkowska, M. & Bryś, J. (2014). The use of moisture sorption isotherms and glass transition temperature to assess the stability of powdered baby formulas. *Journal of Thermal Analysis and Calorimetry, 118,* 911-918.

Pallavi, B. V., Chetana, R., Ravi, R. & Reddy, S. Y. (2015). Moisture sorption curves of fruit and nut cereal bar prepared with sugar and sugar substitutes. *Journal of Food Science and Technology, 52,* 1663-1669.

Palou, E., López-Malo, A. & Argaiz, A. (1997). Effect of temperature on the moisture sorption isotherms of some cookies and corn snacks. *Journal of Food Engineering, 31,* 85-93.

Peleg, M. (1994). A mathematical model of crunchiness/crispness loss in breakfast cereals. *Journal of Texture Studies, 25,* 403-410.

Philipp, C., Oey, I., Silcock, P., Beck, S. M. & Buckow, R. (2017). Impact of protein content on physical and microstructural properties of extruded rice starch-pea protein snacks. *Journal of Food Engineering, 212,* 165-173.

Pittia, P. & Sacchetti, G. (2008). Antiplasticization effect of water in amorphous foods. A review. *Food Chemistry, 106,* 1417-1427.

Pitts, K. F., Favaro, J., Austin, P. & Day, L. (2014). Co-effect of salt and sugar on extrusion processing, rheology, structure and fracture mechanical properties of wheat–corn blend. *Journal of Food Engineering, 127,* 58-66.

Roe, K. D. & Labuza, T. P. (2005). Glass Transition and Crystallization of Amorphous Trehalose-sucrose Mixtures. *International Journal of Food Properties, 8,* 559-574.

Roos, Y. H. (1995). Characterization of food polymers using state diagrams. *Journal of Food Engineering, 24,* 339-360.

Roos, Y. H. (2003). Thermal analysis, state transitions and food quality. *Journal of Thermal Analysis and Calorimetry, 71,* 197-203.

Roos, Y. H. & Drusch, S. (2016). Chapter 6 - Prediction of the physical state. In: Phase Transitions in Foods (Second Edition). Pp. 173-213. San Diego: Academic Press.

Roos, Y. H., Roininen, K., Jouppila, K. & Tuorila, H. (1998). Glass transition and water plasticization effects on crispness of a snack food extrudate. *International Journal of Food Properties, 1,* 163-180.

Roudaut, G. & Champion, D. (2011). Low-Moisture Food: A Physicochemical Approach to Investigate the Origin of Their Physical Instability versus Water or Sucrose. *Food Biophysics, 6,* 313-320.

Roudaut, G., Dacremont, C. & Meste, M. L. (1998). Influence of water on the crispness of cereals-based foods: Acoustic, Mechanical, and sensory studies. *Journal of Texture Studies, 29,* 199-213.

Roudaut, G., Dacremont, C., Pamies, B. V., Mitchell, J. R. & Le Meste, M. (2002). Rehydration of Crispy Cereal Products: A Tentative Explanation of Texture Changes. In: Freshness and Shelf Life of Foods. Pp. 223-234. American Chemical Society.

Roudaut, G. & Wallecan, J. (2015). New insights on the thermal analysis of low moisture composite foods. *Carbohydrate Polymers,* **115,** 10-15.

Sacha, G. A. & Nail, S. L. (2009). Thermal Analysis of Frozen Solutions: Multiple Glass Transitions in Amorphous Systems. *Journal of Pharmaceutical Sciences,* **98,** 3397-3405.

Schmidt, S. J. & Lee, J. W. (2012). Comparison Between Water Vapor Sorption Isotherms Obtained Using The New Dynamic Dewpoint Isotherm Method and those Obtained Using The Standard Saturated Salt Slurry Method. *International Journal of Food Properties,* **15,** 236-248.

Shogren, R. L. (1992). Effect of moisture content on the melting and subsequent physical aging of cornstarch. *Carbohydrate Polymers,* **19,** 83-90.

Simatos, D., Blond, G., Roudaut, G., Champion, D., Perez, J. & Faivre, A. L. (1996). Influence of heating and cooling rates on the glass transition temperature and the fragility parameter of sorbitol and fructose as measured by DSC. *Journal of thermal analysis,* **47,** 1419-1436.

Slade, L. & Levine, H. (1993). The glassy state phenomenon in food molecules*.* Pp. 35-101.

Tedeschi, C., Leuenberger, B. & Ubbink, J. (2016). Amorphous–amorphous phase separation in hydrophobically-modified starch–sucrose blends I. Phase behavior and thermodynamic characterization. *Food Hydrocolloids,* **58,** 75-88.

Tonchev, D. & Kasap, S. O. (2002). Effect of aging on glass transformation measurements by temperature modulated DSC. *Materials Science and Engineering: A,* **328,** 62-66.

Tsami, E., Marinos-Kouris, D. & Maroulis, Z. B. (1990). Water Sorption Isotherms of Raisins, Currants, Figs, Prunes and Apricots. *Journal of Food Science,* **55,** 1594-1597.

Valles Pamies, B., Roudaut, G., Dacremont, C., Le Meste, M. M. & Mitchell, J. R. (2000). Understanding the texture of low moisture cereal products: Mechanical and sensory measurements of crispness. *Journal of the Science of Food and Agriculture,* **80,** 1679-1685.

Wani, S. A. & Kumar, P. (2016). Moisture sorption isotherms and evaluation of quality changes in extruded snacks during storage. *LWT - Food Science and Technology,* **74,** 448-455.

Williams, P. G. (2014). The Benefits of Breakfast Cereal Consumption: A Systematic Review of the Evidence Base. *Advances in Nutrition,* **5,** 636S-673S.

Wungtanagorn, R. & Schmidt, S. J. (2001). Thermodynamic Properties and Kinetics of the Physical Ageing of Amorphous Glucose, Fructose, and Their Mixture. *Journal of Thermal Analysis and Calorimetry,* **65,** 9-35.
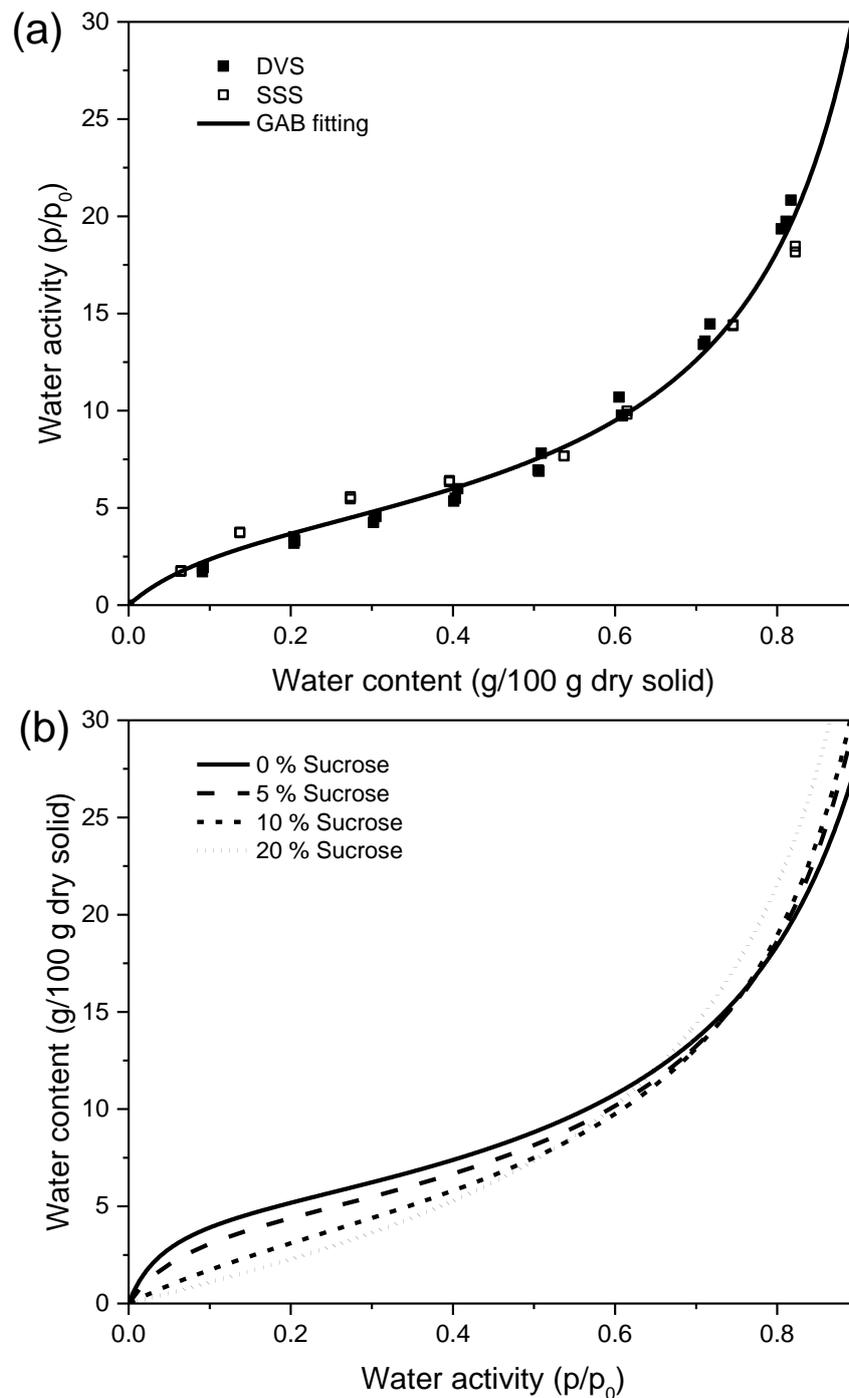
Fig. 5.1 Effect of sucrose content and water processing on adsorption isotherm curve of extrudates breakfast cereal model. Water sorption data obtained by dynamic vapor sorption instrument (DVS) at 25 °C and saturated salt solution method (SSS) at ambient temperature. Line corresponds to the fit with GAB model.
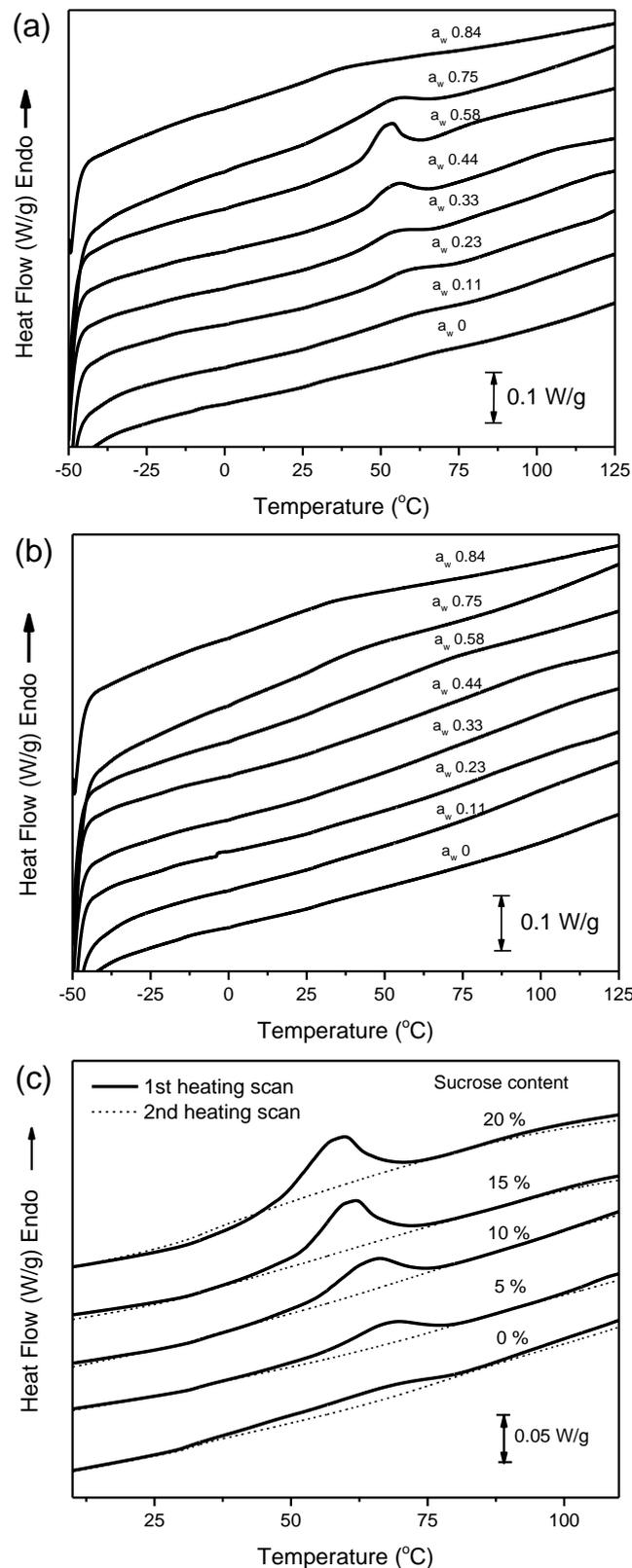
Fig. 5.2 Effect of water content on the DSC thermograms; (a) 1st heating scan and (b) 2nd heating scan at 10°C/min) of extruded sample containing 10 % sucrose content; (c) effect of sucrose content on the DSC thermograms (1st heating scan at 10 °C/min) of extruded products equilibrated at a_w at 0.33
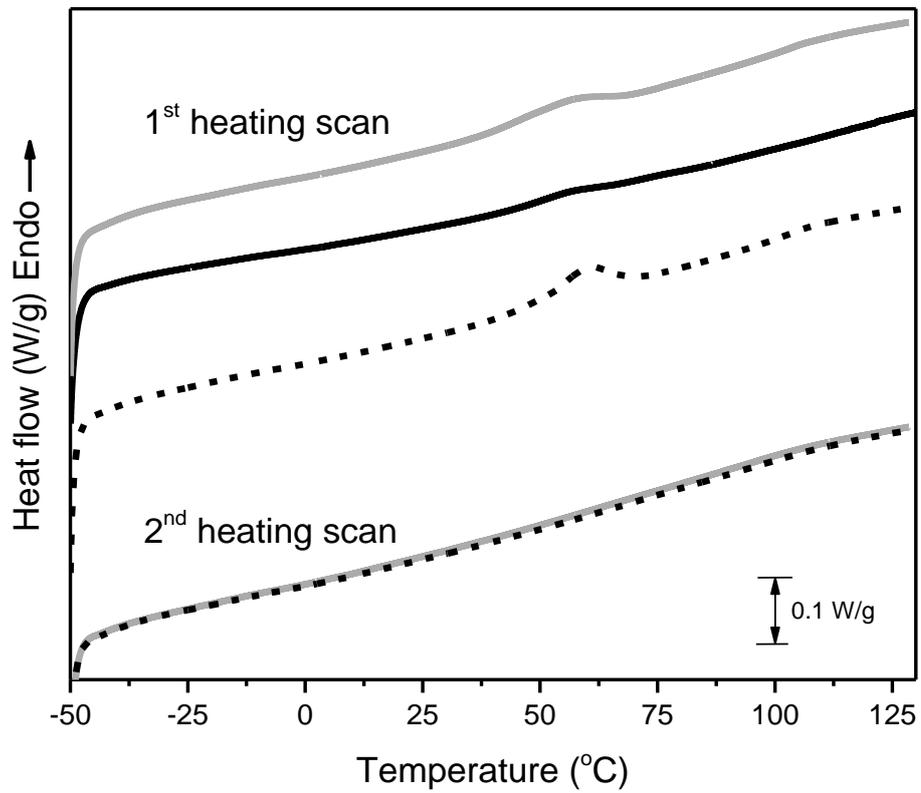
Fig. 5.3 Effect of sample storage history; first and second heating scan DSC thermogram at 10 ºC/min) of extruded sample containing 10 % sucrose stored for 24 months and equilibrated at a_w at 0.33 (▬▬▬), dehydrated at a_w ~ 0 (▬▬) and rehydrated at a_w 0.33 (▬▬).
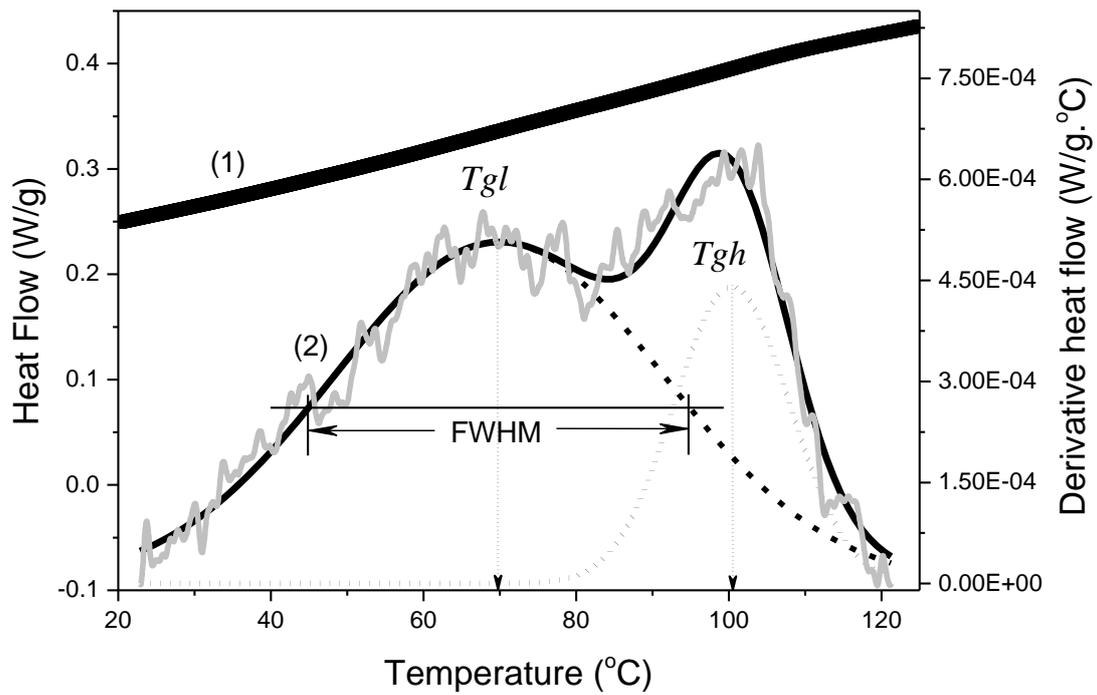
Fig.4 Curve fitting plot of derivative curves of extruded sample: (1,■) heat flow of second heating

scan; (—) experimental data; (····) and (- - -) Gaussian curves corresponding to two glass transition

events; (2,—) summation of Gaussian function.

Fig. 5.4 Curve fitting plot of derivative curves of extruded sample: (1,■) heat flow of second heating scan; (—) experimental data; (••••) and (– – –) Gaussian curves corresponding two glass transition events; (2,—) summation of Gaussian function.
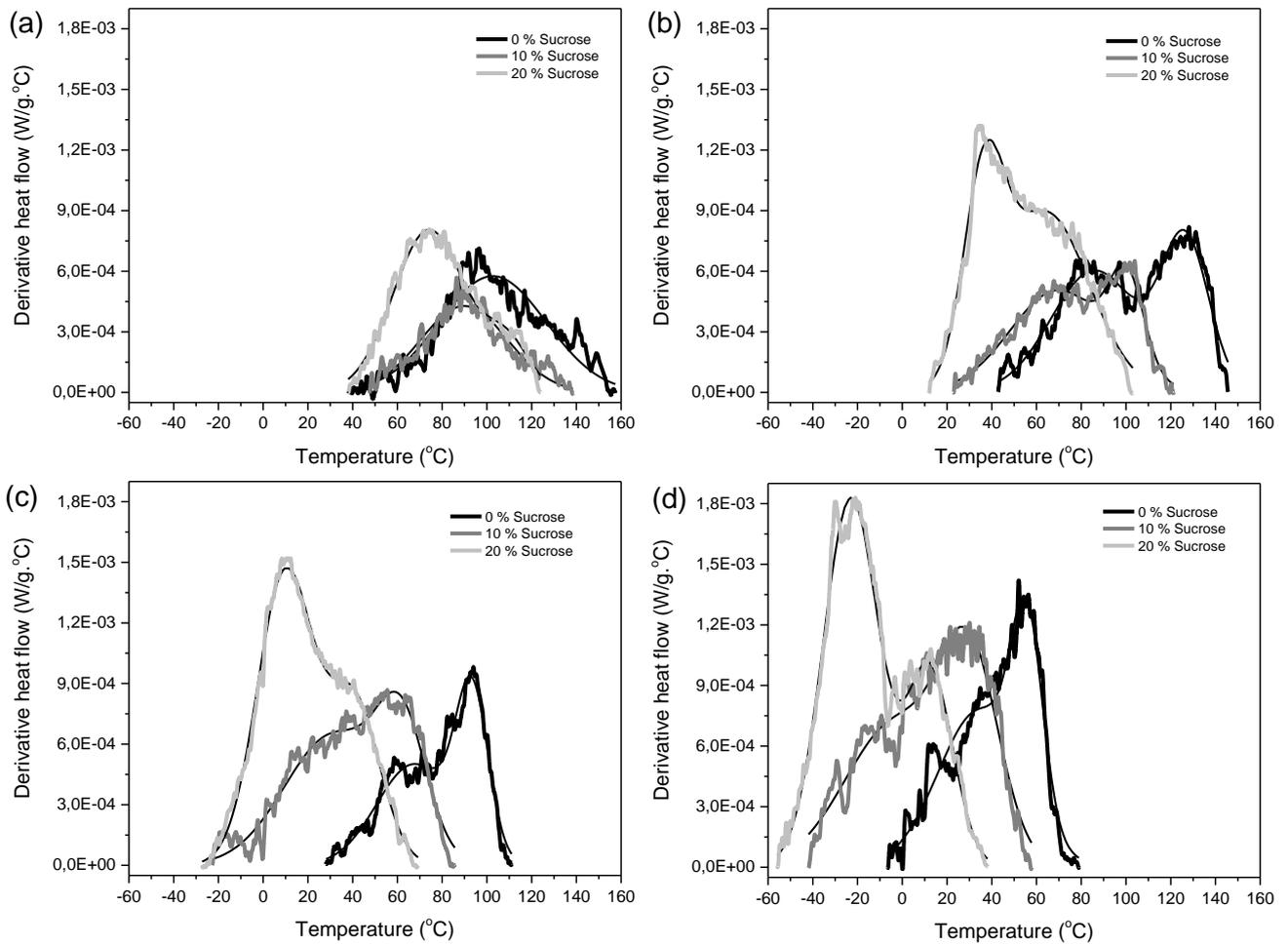
Fig 5.5 Overlay experimental data (solid line) and Gaussian curve (black thin line) of DSC thermogram (2nd heating scan at 10 °C/min) for extruded products containing sucrose 0, 10 and 20 % (db) at a_w 0.23 (a), 0.33 (b), 0.58 (c) and 0.75 (d).
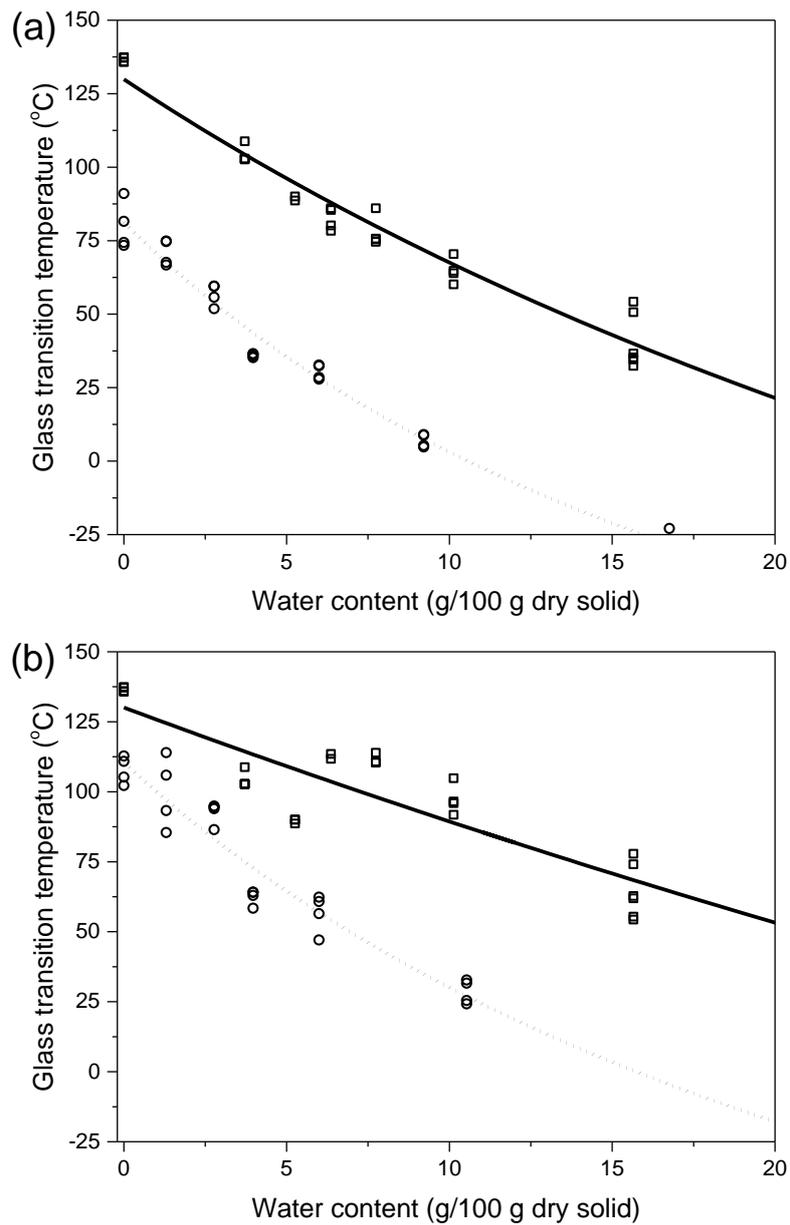
Fig 5.6 Evolution of glass transition temperatures versus water activity for extruded samples with 0 % ($\square$), and 20 % ($\bigcirc$) sucrose content; (a): T_{gl} and (b): T_{gh}. The lines represent Gordon-Taylor fitting for extruded samples with 0% (—) and 20% (••••) sucrose content.
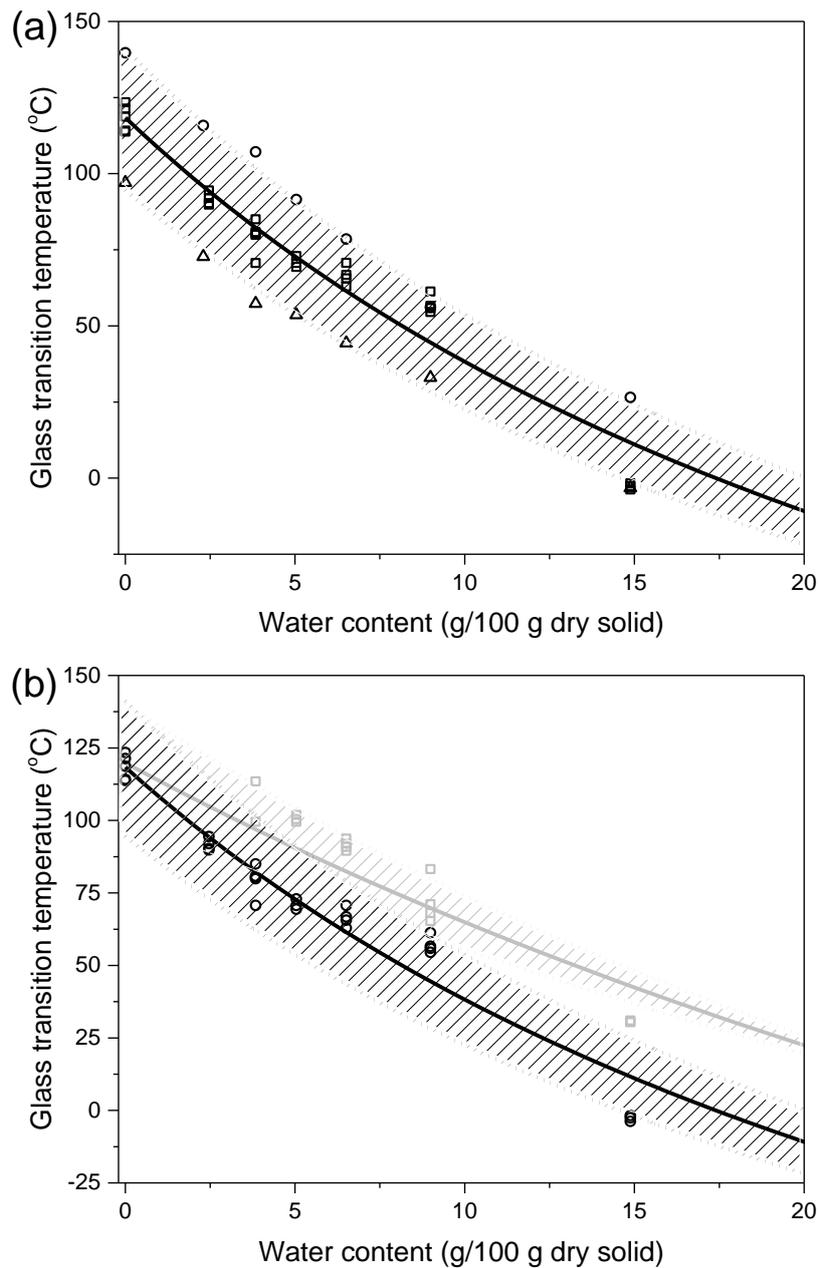
Fig. 5.7 Glass transition temperature for extruded sample with 10% sucrose; T_{gl} (a) and T_{gh} compared with T_{gh} (b). The lines represent T_g fitting with Gordon-Taylor model (━) for Tgl and (━) for T_{gh}. The temperature range calculated from FWHM of Gaussian curve fitting are represented by dot lines and highlighted zones. The symbols represent experimental data for (□) for T_{gl} and ( ) for T_{gh}.
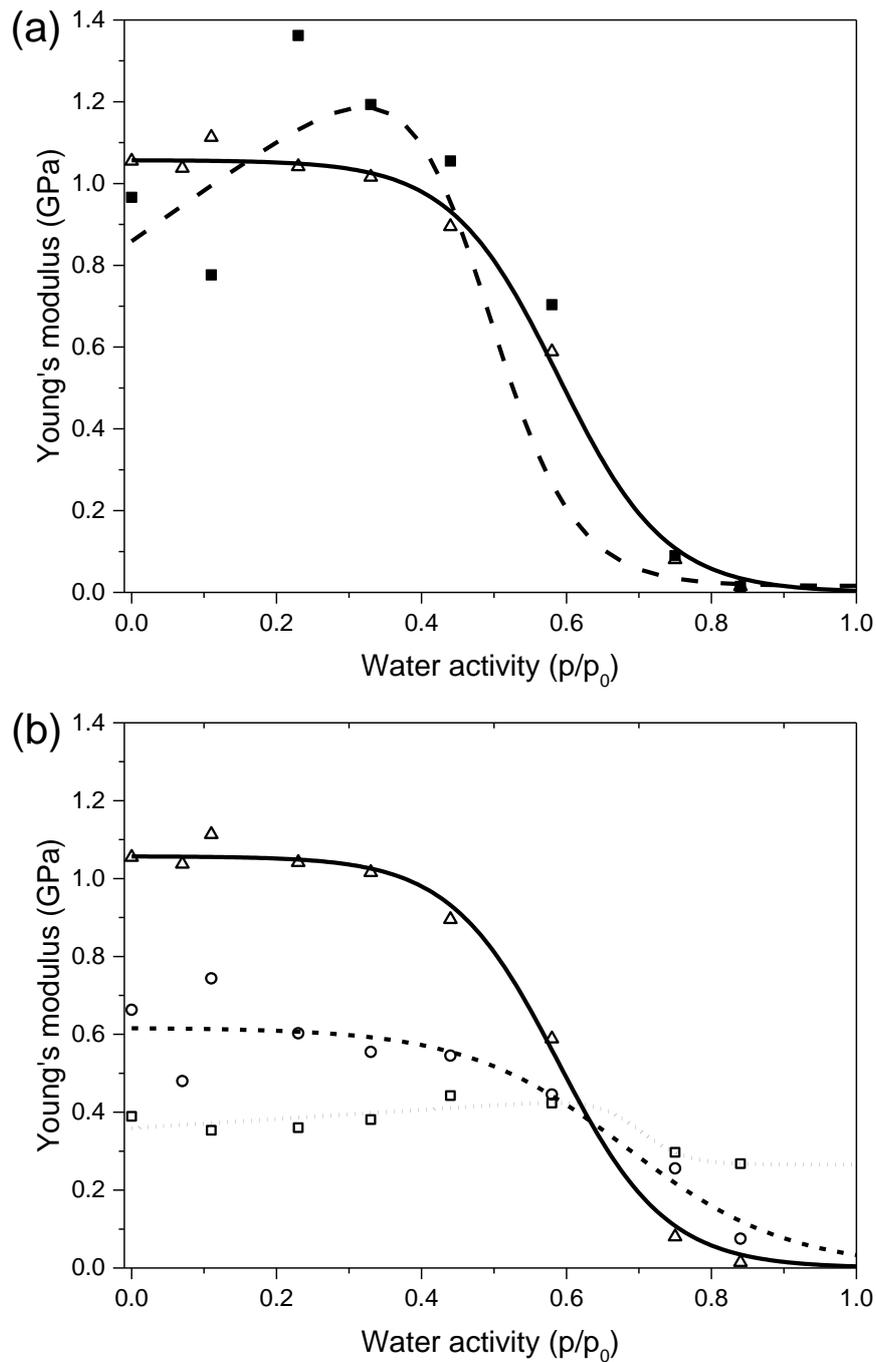
Fig. 5.8 The fit of Fermi function (line) with experimental data (symbol) for extrudates with 20% sucrose content stored for 2 months (—,Δ) and up to 24 months (——,■) after processing (a) and the fitting of average data for sample with 0 (- - -, □), 10 (- - -,o) and 20 (—,Δ) % sucrose content stored for up to 24 months (b). Lines and symbols represented Fermi fitting and experimental data, respectively.
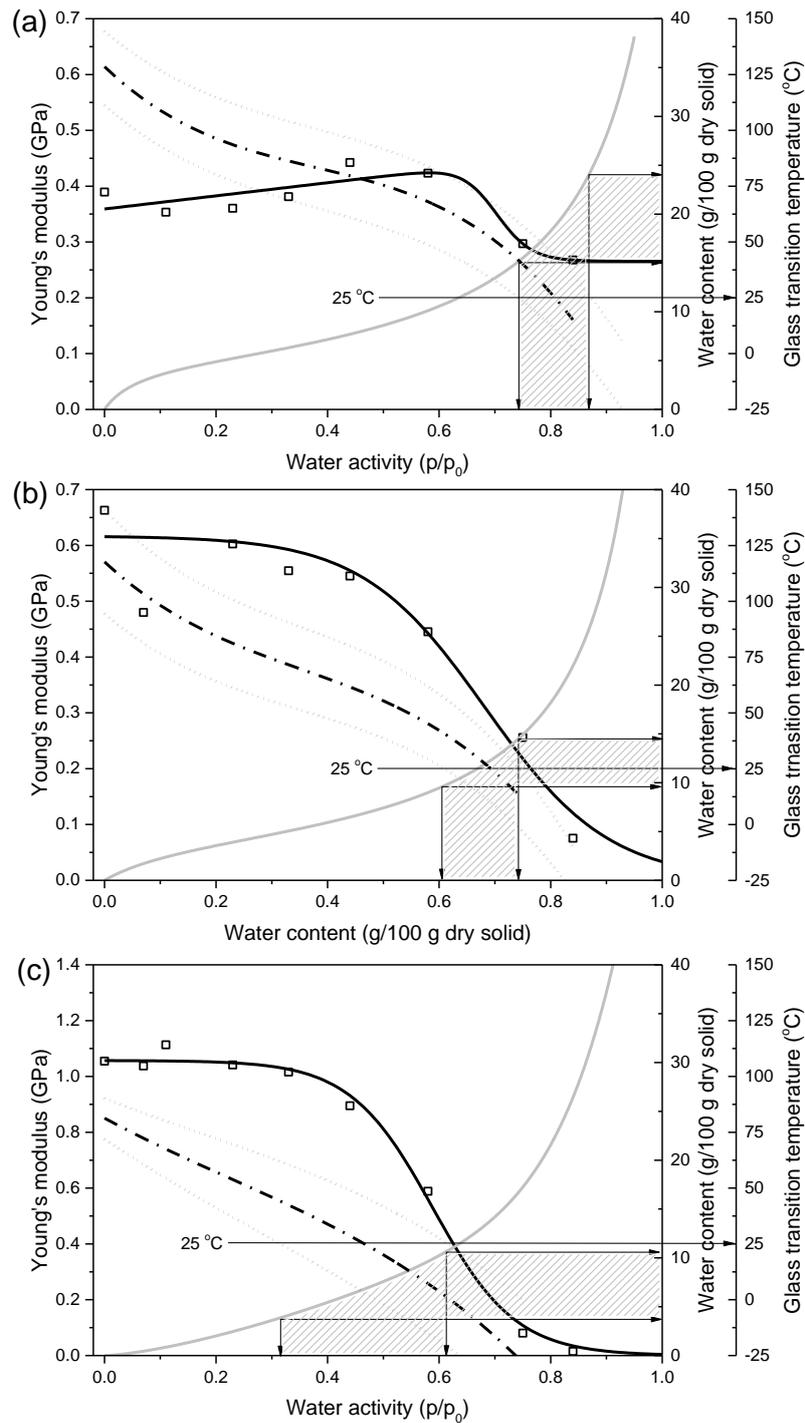
Fig. 5.9 Scheme view of mechanical properties (——) relationship with water activity (——) and low glass transition temperature (Tgl) (—·—) and its range (······) of extruded sample with 0% (a), 10% (b) and 20% (c) sucrose along water activity scale. The zone of critical water content corresponding to glass transition and critical water activity at 25 °C.

Table. 5.1 Fitted values of glass transition data to the Gordon-Taylor equation (**Eq. 5.4**) and fitted values of Young's modulus change caused by hydration to the Fermi equation (**Eq. 5.7**)

Sample	T_{gl}		T_{gh}		Fermi fitted value		
(% Sucrose content)	T_{gs}(°C)	k_s	T_{gs}(°C)	k_s	Y_0(GPa)	a_{wc}	b
0	129.90	2.77	130.10	1.63	0.359	0.70	0.003
10	118.38	4.16	119.83	2.47	0.678	0.64	0.07
15	105.54	5.37	117.56	3.34	-	-	-
20	81.25	5.09	108.65	4.02	1.057	0.59	0.14

Chapter 6:

Study of the impact of sucrose and water content on the water molecular dynamics by nuclear magnetic resonance relaxometry in cereal based-products.

Supuksorn Masavang[a], Philippe Bordart[a], Adam Rachocki[b], Gaëlle Roudaut[a], Dominique Champion[a],*

[a] *Université Bourgogne Franche-Comté, AgroSup Dijon, UMR PAM, 1 Esplanade Erasme, 21000 Dijon, France*

[b] *Institute of Molecular Physics Polish Academy of Sciences, M. Smoluchowskiego 17, 60-179 Poznań, Poland*

*Corresponding author: Dominique Champion
Tel: (+33) 038 0774055
E-mail address: dominique.champion@agrosupdijon.fr

Abstract

Results of preliminary studies concerning proton dynamics within extrudate cereal-based-products are reported. The extrudates, prepared with a twin-screw extruder, are composed of wheat flour, gluten, salt, and sucrose. Low-field nuclear magnetic resonance spectroscopy (LF NMR) at 20 MHz was used to determine relaxation times T_1, T_2 and second moment (M_2) and Fast field Cycling relaxometry (FFC NMR) technique was used to follow the change in relaxation time, T_1 in the 0.01-20 MHz frequency range in samples at different sucrose content (0, 10 and 20%), and humidity (11 - 75% RH). Addition of plasticizer, such as sucrose, caused an increase in magnitude of Solid echo signal, a decrease of T_1 and M_2, while T_2 decreased at low water content (8 %). For FFC NMR, sugar addition clearly modifies the low-frequency part of as a function of Larmor frequencies profile while the high-frequency region is unchanged. The T_1 measured by FFC NMR for extrudates stored at 75% RH showed lower mobility than that of samples stored at 11%RH. T_1 values at 20 MHz determined using both FFC NMR were consistent with the T_1 values measured by LF NMR. These results should contribute to understand and control impact of sucrose and water on the physical properties that govern the gustative qualities of the cereals and also improve their shelf life.

Keywords: Expanded extrudate, Sucrose, Water, FFC MNR, LF NMR, Molecular mobility

1.   Introduction

Dry cereal products are hygroscopic due to chemical composition, porosity and presence of starch in amorphous state and may undergo substantial quality changes associated with water adsorption. Water content correlated with water activity affects crispness, fragility and plasticity of cereal products (Marzec and Lewicki 2006). Extrudates texture changes have been studied as a function of a_w and evidenced an anti-plasticization effect of water (Pittia and Sacchetti 2008), these materials have also shown physical aging (Masavang *et al,.* 2019). Since it was first introduced, the concept of a_w has been regarded as an index of water availability in food systems. A_w measurement is based on the assumption that, in thermal equilibrium, the partial vapor pressure above a product is the same as that of pure water within it. Unfortunately, equilibrium can be considered satisfied only in very dilute food systems (Slade and Levine 1991). Moreover, the limits of the use of this physicochemical parameter describing some structural aspects and phenomena of metastable amorphous food materials are recognized. Such matrices are better explained in terms of water mobility (Slade and Levine 1991). As nuclear magnetic resonance spectroscopy (NMR) reveals information about molecular structure and mobility, it became one of the most powerful non-destructive analytical tools to study water mobility. Wheat cereal products consist of complex multiphasic biopolymer matrices that interact strongly with water, thereby complicating the prediction of food's properties and behavior. These matrices are heterogeneous at the microscopic scale, which affects their macroscale properties (Kovrlija and Rondeau-Mouro 2017). Moreover, most changes in foods, including changes in their composition, structural and mechanical properties, are caused by diffusive processes in one form or another that occur at different scales and include both water and biomolecules. Amongst the latter, starch is one of major components of cereal foods and the properties of starch and interactions with other constituents, particularly with water, are of great interest to the food industry (Delcour *et al,.* 2010). Therefore, studying the mobility of water provides important information in understanding the water dispersion in heterogeneous food system.

Low field-proton NMR (LF NMR) is a one of the most powerful techniques for determining the changes in water mobility, and the dynamic molecular interactions. Relaxation of spins occurs because of the interactions between individual spins and between a spin and its environment. NMR relaxation involves the processes whereby, after absorption of the radiofrequency energy, the excited nuclei (protons) in the sample return to thermal equilibrium through energy release and exchange with the surrounding lattice. NMR signal is commonly analyzed in term of two separate processes, each with their own time constants; spin-lattice (T_1) relaxation time involves a transfer of energy between the spins and the environment, whereas spin-spin relaxation (T_2) time processes are entropic processes that involve the dephasing of nuclear spins. The relaxation process occurs through fluctuations in magnetic field due to random molecular motions, both rotational and translational (Blümich *et al,.* 2009). Due to the different nature of the molecules, their environment and their interactions, the recorded NMR signal is the combination of the contributions of all the nuclei that relax differently. But multi-component signal can also be observed for a single molecule type but localized in various regions (proton compartments) of the sample, or in interaction/exchange with other molecules. This is the case for water molecules in complex samples like foods and more specifically in starch-based matrices (Kovrlija and Rondeau-Mouro 2017). The qualitative and quantitative analyses on the mobility of water interacting with starch or flour have been extensively reported (Leung *et al,.* 1983, Leung *et al,.* 1979, Kim and Cornillon 2001). NMR relaxation is also a convenient method for the continuous monitoring of products during processing up to their final structure (Mortensen *et al,.* 2005, Kovrlija and Rondeau-Mouro 2017, Rondeau-Mouro *et al,.* 2015). Although much research has been conducted on the mobility (dynamic) of starch-water systems, few data are available on their T_1 proton relaxation time. These investigations were mainly performed in low magnetic fields and usually consisted of varying the measurement temperature, the water content or a combination thereof.

The relaxation process perpendicular to the field direction is characterized by transverse relaxation time T_2. Several typical pulse sequences for T_2 studies are used (FID, CPMG, and Solid echo). The CPMG sequence is the standard sequence for measuring the transverse relaxation decay, but

cannot compensate for additional phase spreading of transverse magnetization when investigating solid materials with dipolar couplings such as polymers. To resolve this, the solid echo sequence can be employed where the refocusing pulse is a 90° instead of a 180° rf pulse (Wang and Ramshaw 1972). The benefit of the solid echo sequence is averaging of the homonuclear dipole-dipole interaction between spins pairs, which is largely responsible for the T_2 relaxation of solid materials (Fan *et al,.* 2013).

Fast Field Cycling relaxometry (FFC NMR) is a NMR technique that has been recently proposed for food applications and it might provide additional insight in extrudate molecular dynamics. FFC measures longitudinal relaxation times (T_1), applying a variable magnetic field to the sample to obtain T_1 at different frequencies and, consequently, widening the range of ^1H molecule motions that can be measured (Curti *et al,.* 2011). Nuclear Magnetic Resonance Dispersion (NMRD) profiles ($1/T_1 = R_1$ vs frequency) are particularly valuable to assess the interactions of water molecules with paramagnetic and large-sized macromolecular systems (Baroni *et al,.* 2009a). In particular, the relaxation profile is dominated by the magnetic field dependence of rotationally immobilized protons, dynamically coupled to the spin-lattice relaxation of water protons. The FFC technique has been previously applied to food matrices like mozzarella and Gouda cheese (Godefroy *et al,.* 2003), eggs (Laghi *et al,.* 2005), and balsamic vinegar (Baroni *et al,.* 2009b) to study the water distribution and interaction with the different food components. For low moisture food, the molecular of white bread loaves were characterized by multiple proton NMR techniques (proton FID, T_2, and T_1 relaxation times) over 14 days of storage (Curti *et al,.* 2011). Changes at a molecular level were observed during storage. The results showed a faster decay of proton FIDs and a shift of proton T_2 relaxation time distributions toward shorter times, indicating a proton mobility reduction of the bread matrix with storage time. Multiple T_2 populations were observed and tentatively associated with water-gluten and water-starch domains. Protons T_1 of bread was measured at variable frequencies (FFC NMR) and was found to be strongly dependent on frequency and to decrease in bread during storage, especially at frequencies equal or

lower than to 0.2 MHz. In most cases, the phenomenon under study was better resolved at low frequencies (Guine and Correia 2014).

The main objectives of this work was to understand and interpret the NMR signal measured for cereal based extruded products. This work was undertaken to study the effect of sucrose content in extrudates, focusing the attention on water dynamics and = molecular changes occurring during storage at 11 and 75% RH (Relative Humidity), by means of LF NMR spectroscopy at 20 MHz to determine relaxation time T_1, T_2 and second moment (M_2). More particularly, FFC NMR technique was applied to follow the change in relaxation time T_1 in the 0.01-20 MHz frequency range.

2. Experimental

2.1 Preparation of the extruded samples

Commercial grade wheat flour, wheat starch, gluten and sucrose were supplied by ADM CHAMTOR (Les Sohettes, France). The extrusion of the ingredient blends containing 0, 5, 10, 15 and 20% wt sucrose with wheat flour 53–73% wt, wheat starch 16% wt, gluten 16% wt and sodium chloride 1% wt was carried out in a Clextral BC-45 intermeshing twin-screws extruder with a 1.5 m long barrel using 10% wt initial moisture content (dry basis). The barrel heating zones were at 80 °C, 130 °C and 160 °C (±2 °C). A 6.0 mm circular die was fitted to the end of the barrel and used to produce the cylinder-shaped extrudates. The screw speed was 150 rpm. Feed rates were controlled: the solid feed at 36 kg/hr and water input of 4 L/hr, giving a water content of 19.5–24.5% water content of molten material in barrel depending on blend formulation and ~10% water content in the final extruded samples. After extrusion, samples were dried in oven during 5 min at 150 °C and after cooling, they were hermetically sealed in bag to be kept at ambient temperature.

A series of samples at different water contents have been prepared by controlling the relative humidity (RH) inside the NMR tube. For doing so, glass tubes containing samples were stored over saturated salt solutions in hermetic containers until equilibrium was reached; the tubes were then sealed before the NMR measurement. Because sorption isotherms are known for all studied samples, the results are

given as a function of relative humidities used to equilibrate the water activities in products or as a function of water content.

2.2. NMR measurements

2.2.1 Inversion recovery experiment to determine T_1 (using 180°-τ-90° pulse sequence)

Proton relaxation NMR experiment were performed under standard conditions using a Bruker bench top Minispec model mq20 (Bruker Spectrospin Ltd.) operating with 0.47 T magnetic field, 20 MHz resonance frequency, 40 °C magnet temperature was used, and samples were studied at 25 °C. A piece of sample was sealed in 10-mm diameter NMR glass tube for analysis. Typically 16 scans were accumulated with a recycle delay of 1.5 s, it was chosen to be at least five times T_1. Maximum amplitude values (A) of the longitudinal relaxation curves were recorded at delay time (τ) ranging from 0.08 ms to 3 s. The 90° pulse width was 13 µs. T_1's were accumulated from separate time windows beginning at 0.016 ms for 0.013 ms duration which were called 1st and and beginning at 0.1 ms for the same duration for the 2nd window. The objective of the determination of T_1 in these 2 windows (one more focus on solid part on the sample, and the other corresponding to higher mobility proton population) was to evaluate the homogeneity of the spin-lattice relaxation. The result of each component were fitted to one exponential:

$$A(t) = A_1 e^{(-t/T_1)}$$
Eq. 6.1

with $A(t)$ that represents the NMR signal intensity at time t, T_{1W1} and T_{1W2} corresponds to the spin-lattice relaxation times measured in the time ranges window 1 and 2 respectively. A_1 is proportional to the number of protons in the population. All determinations were performed in duplicate, and results were averaged. Curve fitting and graphical analysis was performed using OriginPro 2017 for Windows (OriginLab, Northampton, USA).

2.2.2 Solid echo relaxation measurement

The spin-spin relaxation time (T_2) of water protons was measured in triplicate for each moisture level. Samples were analyzed at 25 °C with the solid echo pulse sequence by using a Minispec

PC/20 spectrometer (Bruker, Karlsruhe, Germany) working at 20 MHz: 90x-(τ-90y-τ-echo). Solid echo sequence were used to characterize the least mobile proton pools. 128 scans were accumulated with τ-value of 12 μs. The echo was recorded 10 μs after the second pulse. Repetition delay was set to 2 s. to minimize the signal/noise ratio and to prevent signal clipping, the number of scans, as well as the amplification factor, were adjusted according to the moisture content of the analyzed samples. Relaxation curves obtained from the solid echo sequence were analyzed using Eq. 6.2 (OriginPro 2017 for Windows, OriginLab, Northampton, USA). The T_2 for the rigid part is very short and correspond to a highly structured phase; the signals were fitted with model derived of Abragam theory for highly rigid element relaxation (van den Dries *et al,.* 1998) :

$$I(t) = I_1 \, exp\left(-\frac{a^2 t^2}{2}\right)^2 \frac{\sin bt}{bt} + I_2 \, exp\left(\frac{-t}{T_2}\right) + I_0$$
<div align="right">Eq. 6.2</div>

where $I(t)$ is the intensity of the total relaxation signal, t is the time of the relaxation process, a and b is a constant defining the polar-polar interactions in the rigid part, T_2 is the spin-spin relaxation time of the more mobile population, I_1 and I_2 correspond to the amplitude of the rigid and flexible proton populations respectively. The NMR shape with a total $2b$ (s^{-1}), convoluted with a Gaussian line shape with a standard deviation given by the parameter a (s^{-1}). The rigid and mobile proton populations were characterized with their second moment M_2, and transversal relaxation time, T_2, respectively.

The second moment, M_2 (s^{-2}) reflects the strength of dipolar interactions in which the rigid protons are involved (van den Dries *et al,.* 1998); and thus, it inversely correlates to the molecular mobility of the rigid fraction. It is calculated with the following equation:

$$M_2 = a^2 + \frac{1}{3}b^2$$
<div align="right">Eq. 6.3</div>

2.3 FFC relaxometry measurement

Samples were put inside 10-mm-diameter NMR tubes (typical weight of a dry sample is 300 mg). The measurements of the spin-lattice relaxation times (T_1) were performed at the Institute of Molecular Physics, Polish Academy of Science (Poznań, Poland) on a fast field cycling spectrometer (*Stelar*, Italy). This spectrometer allows operating T_1 measurements as a function of the magnetic field

corresponding to proton Larmor frequencies varying from 0.01 to 20 MHz. Proton spins of the system are first polarized in a magnetic field corresponding to a Larmor frequency of 10 MHz, for a duration corresponding to about five times the T_1 estimated at this frequency. The magnetic field is then switched to the measured value of interest for a variable period τ (varying from 3 ms to four times the T_1 estimated at the previous frequency of measurement). Experiments were repeated 16 times to increase the signal-to-noise ratio for each acquisition. The values of the relaxation time (T_1) were computed by fitting the decay curve of the magnetization as a function of τ by an exponential function. The complete dispersion is obtained by repeating this procedure for the 30 different measured field values, ranging from 0.01 to 20 MHz. T_1 profiles were recorded at 25 °C, stabilized by a flow of nitrogen.

Results and discussion

3.1 Spin-Lattice Relaxation (T_1)

The proton longitudinal or spin-lattice relaxation times (T_1) for extruded samples, plotted as a function of sucrose and water content are shown in Fig. 6.1 and 6.2. T_1 was studied in two ranges of times depending on values of delay before amplitude signal record: one corresponding to almost the maximum amplitude (window beginning at 16 µs), and another window beginning at 100 µs to probe only the population with an higher T_2. Whatever the window considered, the relaxation times T1 were fitted with a single exponential for all samples at all humidities and sucrose levels considered (Fig. 6.1 and 6.2). T_1 is decreasing when water content is increased in samples but no effect on the sucrose concentration was detected for samples containing water. For samples with a water content higher than 7.5g/100g dry solid show the same T_1 values whatever the time sampling window; but for lower water contents, two distinct T_1 was calculated: T_{1W1} higher than 125 ms when determined during the first window; and T_{1W2} lower than 100 ms for the second window. These two values for T_1 at low water content could be due to the coexistence of several phases in the samples, showing slightly different viscosities, and these density fluctuations in the material could be not so detectable at higher water content.

Partanen *et al,.* (2004) studied the effect of plasticizer in amylose-glycerol films and they observed that T_1 values decreased by the incorporation of plasticizer into these samples at low water content. Their result suggested that in the glassy state, glycerol may decrease amylose mobility and act as an anti-plasticizer. Both Kou *et al,.* (2000) and Tanner *et al,.* (1991) observed that sorption of water by dry sample caused a decrease in the T_1 of water adsorbed on the biopolymer surface. Given this observation, Kovrlija and Rondeau-Mouro (2017) concluded that moisture content determines the T_1 relaxation path for the starch protons.

3.2 Relaxation time (T_1) measured with FFC NMR

The T_1 values were plotted as a function of Larmor frequency for 0 and 10% sucrose extrudates and stored at 75% RH (Fig. 6.3a) and for extrudates containing 10% sucrose stored at both 11% and 75% RH (Fig. 6.3b). All the curves showed power law dependence of the spin-lattice relaxation rates as a function of the proton Larmor frequency and terminate in a plateau at low frequency range (lower than 0.1 MHz). Sucrose addition in extrudate formulation decreased T_1 values in samples stored at 75% RH (Fig. 6.3a) but the impact is better seen for low Larmor frequency domain than for higher ones. For low frequencies, small amplitude rotational movements could be better probed than at high frequencies. Free water movements in non-homogeneous porous material includes translational motion and rotational motion. The rotational dynamics are much more affected by the confinement: they decay much more slowly (Bakhmutov 2004, Li *et al,.* 2016). The faster the motions are, the lower is the dipolar interaction efficiency, thereby favoring longer T_1 values and shorter relaxation rate (R_1) values. Conversely, slower dynamics can be associated with shorter spin-lattice relaxation times because of stronger nuclear dipolar interactions (Bakhmutov 2004). In hydrated material, Rachocki and Tritt-Goc (2014) suggested that the relaxation may be dominated by the translational diffusion contribution in the low frequency range in more hydrated matrices. In addition, Meier *et al,.* (2013) reported that the low-frequency contribution originates from translational modulations of the intermolecular dipole–dipole interactions, whereas the (larger) high-frequency part reflects the

rotational influence on the intermolecular interaction resulting from the non-central positions of the nuclei in the molecule. As water content was increased, T_1 decreased for extrudate with 10% sucrose (Fig. 6.3b), indicating that molecular mobility decreased. This is in good agreement with the results observed by LF NMR. To go further, T_1 values obtained by LF NMR and FFC NMR were compared (Table 6.3), and they are in the same order of magnitude whatever the two equipments used.

3.3 Spin-Spin relaxation measurement

3.3.1 NMR signal

To investigate low spin-spin relaxation times, the solid echo sequence are used, being specific to characterize the proton pools associated with the rigid matrix (Fig. 6.4). Spectrum fitting is described by two components (Eq. 6.2): each ascribed to one pool of protons; the first one corresponds to the rigid population defined by M_2 (Eq. 6.3) and the second pool with longer relaxation time (mobile population). The acquired solid echo signal exhibited for all samples a damped sinusoidal or beat pattern at approximately 0.05 ms (Fig. 6.4), reflecting strong dipolar interactions between the protons of the rigid component (Roudaut *et al,.* 2009).

This damped sinusoidal or beat pattern has also been depicted for FID signal in glassy oligosaccharides such as maltose (van den Dries *et al,.* 1998, Derbyshire *et al,.* 2004), maltodextrins with different dextrose equivalent (Grattard *et al,.* 2002), film of arabinoxylans extracted from wheat flour (Rondeau-Mouro *et al,.* 2011) or starch (Partanen *et al,.* 2004, Roudaut *et al,.* 2009). The sinusoidal pattern became less pronounced as the water and sucrose content increased (Fig. 6.4). We interpreted this observation as a decrease of strength of dipolar interactions in the sugar-water (van den Dries *et al,.* 2000). Partanen *et al.* (2004) in amylose-glycerol films, suggested that beat pattern reflects the increase in molecular mobility of amylose through plasticization by water. They also pointed that the beat was observed even at the highest plasticization level (30% glycerol, 95% RH), indicating that the mobility of a significant fraction of amylose protons, most probably those involved in ordered regions, is not significantly increased by water and glycerol plasticization. In the present

study, the sinusoidal pattern remained very pronounced when sucrose content decreases at low relative humidity (Fig. 6.4a and b). However, this pattern became less pronounced with sucrose increase at high relative humidity. Sucrose seemed to induce dipolar interactions in the biopolymer-sucrose matrix at low water content, while an increase in water content showed the opposite effect. Roudaut *et al,.* (2009) suggested that increasing the sample water content may cause a decrease of proton density (which depends on both number and strength of dipolar interactions) and thus a decrease of dipolar interactions. Solid echo curves were fitted with Eq. 6.2 to obtain quantitative information about the relaxation time and percentage of protons belonging to the most rigid and most mobile proton populations.

3.3.2 Second moment (M_2)

M_2 increase with sucrose content (Fig. 6.5) because sucrose molecules give more dipolar interactions with others molecules in the mix or even with other sucrose molecules in its close environment. For the various extruded samples stored at different RH, second moments M_2 diminished as the moisture were increased which indicated weaker proton dipolar strength which in turn has been attributed to an increase in the anisotropic mobility and/or average distances of the polysaccharide protons (van den Dries *et al,.* 2000, Rondeau-Mouro *et al,.* 2011, Ying *et al,.* 2011). Moreover, Partanen *et al,.* (2004) explained that water has higher proton densities than amylose. Therefore, increasing water content yields increases overall proton density. Thus the decrease in the second moment could be related to the plasticization of starch macromolecules resulting in increasing molecular mobility. M_2 was much higher in the sucrose-containing samples than in the sucrose free ones, for a given water content. This suggested a sucrose-induced reinforcement in dipolar interactions between the protons of the rigid component. Moreover, sucrose seemed to decrease the sensitivity to water effect because the slope of M_2 as a function of water content is lower with 20% sucrose. Such a reinforcement of interactions has previously been suggested for glassy starch based-product (Roudaut *et al,.* 2009).

3.3.3 Spin-spin relaxation time, T_2

A_1 and A_2 are signal amplitudes of respectively, the rigid and mobile proton populations and should be described with respect to the proton density or number of protons of the two popilations in the extrudates (Farhat *et al,.* 1996). As the water content increased, all samples displayed the proportional number of proton for rigid component decreased, while that of mobile component increased (Table. 6.1) which was consistent with a greater polymer segmental mobility induced by plasticization by water. At higher water content, the rate of proton exchange between water and starch hydroxyls groups became important on the time scales of the NMR relaxation measurement (Farhat *et al,.* 1996). The increasingly effective exchange is demonstrated by a decrease in the proportional number of A_1 and an increase in proportional number of A_2: the higher sucrose content, the larger the changes of the rigid component amplitude. At low water content, a proportional number of rigid component (A_1) increased, while A_2 decreased as sucrose content increased, the inverse effect was observed for extrudates stored at high % RH. This suggests that sucrose contributed to the NMR signal, resulting from sucrose-biopolymer interaction at low water content. At high water content, the entire sucrose content was hydrated in the aqueous phase at approximately of 20% moisture content (corresponding to 75% RH). T_2's (corresponding to the mobile population) for all sample decreased with increasing water content (Fig. 5) up to 5.5 g/ 100 g dry solid (~45% RH) and then a T_2 minimum value was observed. This T_2 minimas were shifted to higher water content with increasing sucrose content. Ablett *et al,.* (1978) observed the T_2 minima as a function of temperature for agarose and they explained that the minimum in the observed T_2 value involved an increasingly effective exchanges of water protons with exchangeable protons (mainly with hydroxyl groups) of macromolecules or a more rigid proton species.

The sucrose effect on mobility in extrudates seemed similar to the mechanical properties of the material: the sucrose addition depressed the calorimetric glass transition of the starch material but induced a decrease in mobility of the glassy matrix. Roudaut *et al,.* (2009) showed similar evolution of T_2 for starch-sucrose system above 6% of water, the T_2 values were affected by the sample

composition: the mobile protons of starch alone samples were more mobile than the ones of starch-sucrose blends. Thus, sucrose reduced both the rigid and mobile protons mobility by reinforcement of the dipolar interactions strength. The minimum observed on T_2 versus hydration for all samples could relate to both a mobility change and /or consist in a protons displacement from the rigid population to mobile population: the most mobile protons of the 1st population shifting towards the 2nd population would thus reduce the average mobility of 2nd population (Roudaut *et al,.* 2009). T_2 values were also detected by extrapolation of the T_1 behavior close to zero frequency for all studied samples and these observations are consistent with the results of the LF NMR measurement (Table 6.2). The mobile population represents the lower amplitude population in the water content range of samples but seems to be the one is detected with the T_1 measurements, probably because the spin-lattice relaxation is only possible in these areas of the sample.

4. Conclusion

The roles of water and sucrose in extruded products were investigated by monitoring proton mobility using both LF and FFC NMRs. The spin-lattice parameter (T_1) decreased with addition of plasticizer. Water appears as a key parameter in the control of molecular mobiliy in the extrudates. Solid echo signal showed two T_2 populations: "rigid" and "mobile" populations. T_2 depended also on water content but showed a minimum probably indicating the exchanges of water protons with exchangable protons of the other molecules in the matrix. For higher water content, T_2 increased with water content, while the impact of sucrose content was not significant at low water content. The second moment M_2 was found to be sensitive to the relaxations of sucrose. The T_1 frequency dependency showed a decrease in relaxation rate as sucrose and water content increased. For samples with different sucrose content, only low Larmor frequencies allowed to distinguish the samples, reflecting sucrose may change the ability of rotation/low amplitude translational mobility, but have no impact on higher frequency movements at the the proton scale. T_1 for extrudates stored at 75% RH were higher than that of samples stored at 11%, meaning that higher water content induced lower

mobility in this range of water content. These results suggest that the study of molecular properties in extrudates at different frequencies by mean of NMR FFC techniques might be useful in monitoring molecular dynamics in extruded product and possibly should open prospects for a more fundamental study of heterogeneity and physical aging of complex biopolymer systems.

References

Ablett, S., Lillford, P. J., Baghdadi, S. M. A. & Derbyshire, W. (1978). Nuclear magnetic resonance investigations of polysaccharide films, sols, and gels: I. Agarose. *Journal of Colloid and Interface Science,* **67,** 355-377.

Bakhmutov, V. I. (2004). Practice NMR Relaxation for Chemists. Jhon Wiley & Sons Ltd., Chichester, UK.

Baroni, S., Bubici, S., Ferrante, G. & Aime, S. (2009a). Applications of field cycling relaxometry to food characterization. *Magnetic Resonance in Food Science: Challenges in a Changing World,* 65-72.

Baroni, S., Consonni, R., Ferrante, G. & Aime, S. (2009b). Relaxometric studies for food characterization: The case of balsamic and traditional balsamic vinegars. *Journal of Agricultural and Food Chemistry,* **57,** 3028-3032.

Blümich, B., Casanova, F. & Appelt, S. (2009). NMR at low magnetic fields. *Chemical Physics Letters,* **477,** 231-240.

Curti, E., Bubici, S., Carini, E., Baroni, S. & Vittadini, E. (2011). Water molecular dynamics during bread staling by Nuclear Magnetic Resonance. *LWT - Food Science and Technology,* **44,** 854-859.

Delcour, J. A., Bruneel, C., Derde, L. J., Gomand, S. V., Pareyt, B., Putseys, J. A., Wilderjans, E. & Lamberts, L. (2010). Fate of starch in food processing: From raw materials to final food products. *Annual Review of Food Science and Technology,* **1,** 87-111.

Derbyshire, W., van den Bosch, M., van Dusschoten, D., MacNaughtan, W., Farhat, I. A., Hemminga, M. A. & Mitchell, J. R. (2004). Fitting of the beat pattern observed in NMR free-induction decay signals of concentrated carbohydrate–water solutions. *Journal of Magnetic Resonance,* **168,** 278-283.

Fan, D., Ma, S., Wang, L., Zhao, H., Zhao, J., Zhang, H. & Chen, W. (2013). 1H NMR studies of starch–water interactions during microwave heating. *Carbohydrate Polymers,* **97,** 406-412.

Farhat, I. A., Mitchell, J. R., Blanshard, J. M. V. & Derbyshire, W. (1996). A pulsed 1H NMR study of the hydration properties of extruded maize-sucrose mixtures. *Carbohydrate Polymers,* **30,** 219-227.

Godefroy, S., Korb, J.-P., Creamer, L. K., Watkinson, P. J. & Callaghan, P. T. (2003). Probing protein hydration and aging of food materials by the magnetic field dependence of proton spin-lattice relaxation times. *Journal of Colloid and Interface Science,* **267,** 337-342.

Grattard, N., Salaün, F., Champion, D., Roudaut, G. & LeMeste, M. (2002). Influence of physical state and molecular mobility of freeze-dried maltodextrin matrices on the oxidation rate of encapsulated lipids. *Journal of Food Science,* **67,** 3002-3010.

Guine, R. d. P. F. & Correia, P. M. d. R. (2014). Engineering Aspects of Cereal and Cereal-Based Products. New York, CRC Press.

Kim, Y.-R. & Cornillon, P. (2001). Effects of temperature and mixing time on molecular mobility in wheat Dough. *LWT - Food Science and Technology,* **34,** 417-423.

Kou, Y., Dickinson, L. C. & Chinachoti, P. (2000). Mobility Characterization of Waxy Corn Starch Using Wide-Line 1H Nuclear Magnetic Resonance. *Journal of Agricultural and Food Chemistry,* **48,** 5489-5495.

Kovrlija, R. & Rondeau-Mouro, C. (2017). Multi-scale NMR and MRI approaches to characterize starchy products. *Food Chemistry,* **236,** 2-14.

Laghi, L., Cremonini, M. A., Placucci, G., Sykora, S., Wright, K. & Hills, B. (2005). A proton NMR relaxation study of hen egg quality. *Magnetic Resonance Imaging,* **23,** 501-510.

Leung, H. K., Magnuson, J. A. & Bruinsma, B. L. (1979). Pulsed nuclear magnetic resonance study of water mobility in flour doughs. *Journal of Food Science,* **44,** 1408-1411.

Leung, H. K., Magnuson, J. A. & Bruinsma, B. L. (1983). Water binding of wheat flour doughs and breads as studied by deuteron relaxation. *Journal of Food Science,* **48,** 95-99.

Li, X., Wang, X. & Zhang, M. (2016). Molecular dynamics of water in wood studied by fast field cycling nuclear magnetic resonance relaxometry. *BioResources,* **11,** 1882-1891.

Marzec, A. & Lewicki, P. P. (2006). Antiplasticization of cereal-based products by water. Part I. Extruded flat bread. *Journal of Food Engineering,* **73,** 1-8.

Masavang, S., Roudaut, G. & Champion, D. (2019). Identification of complex glass transition phenomena by DSC in expanded cereal-based food extrudates: Impact of plasticization by water and sucrose. *Journal of Food Engineering,* **245,** 43-52.

Meier, R., Kruk, D. & Rössler, E. A. (2013). Intermolecular Spin Relaxation and Translation Diffusion in Liquids and Polymer Melts: Insight from Field-Cycling 1H NMR Relaxometry. *ChemPhysChem,* **14,** 3071-3081.

Mortensen, M., Thybo, A. K., Bertram, H. C., Andersen, H. J. & Engelsen, S. B. (2005). Cooking effects on water distribution in potatoes using nuclear magnetic resonance relaxation. *Journal of Agricultural and Food Chemistry,* **53,** 5976-5981.

Partanen, R., Marie, V., MacNaughtan, W., Forssell, P. & Farhat, I. (2004). 1H NMR study of amylose films plasticised by glycerol and water. *Carbohydrate Polymers,* **56,** 147-155.

Pittia, P. & Sacchetti, G. (2008). Antiplasticization effect of water in amorphous foods. A review. *Food Chemistry,* **106,** 1417-1427.

Rachocki, A. & Tritt-Goc, J. (2014). Novel application of NMR relaxometry in studies of diffusion in virgin rape oil. *Food Chemistry,* **152,** 94-99.

Rondeau-Mouro, C., Cambert, M., Kovrlija, R., Musse, M., Lucas, T. & Mariette, F. (2015). Temperature-associated proton dynamics in wheat starch-based model systems and wheat flour dough evaluated by NMR. *Food and Bioprocess Technology,* **8,** 777-790.

Rondeau-Mouro, C., Ying, R., Ruellet, J. & Saulnier, L. (2011). Structure and organization within films of arabinoxylans extracted from wheat flour as revealed by various NMR spectroscopic methods. *Magnetic Resonance in Chemistry,* **49,** S85-S92.

Roudaut, G., Farhat, I., Poirier-Brulez, F. & Champion, D. (2009). Influence of water, temperature and sucrose on dynamics in glassy starch-based products studied by low field 1H NMR. *Carbohydrate Polymers,* **77,** 489-495.

Slade, L. & Levine, H. (1991). Beyond water activity: Recent advances based on an alternative approach to the assessment of food quality and safety. *Critical Reviews in Food Science and Nutrition,* **30,** 115-360.

Tanner, S. F., Hills, B. P. & Parker, R. (1991). Interactions of sorbed water with starch studied using proton nuclear magnetic resonance spectroscopy. *Journal of the Chemical Society, Faraday Transactions,* **87,** 2613-2621.

van den Dries, I. J., van Dusschoten, D. & Hemminga, M. A. (1998). Mobility in maltose–water glasses studied with 1H NMR. *The Journal of Physical Chemistry B,* **102,** 10483-10489.

van den Dries, I. J., van Dusschoten, D., Hemminga, M. A. & van der Linden, E. (2000). Effects of water content and molecular weight on spin probe and water wobility in malto-oligomer Glasses. *The Journal of Physical Chemistry B,* **104,** 10126-10132.

Wang, C. H. & Ramshaw, J. D. (1972). Decay of multiple spin echoes in dipolar solids. *Physical Review B,* **6,** 3253-3262.

Ying, R., Ruellet, J. & Rondeau-Mouro, C. (2011). Time domain 1H-NMR of arabinoxylans and 1 β-Glucans films, models of a lamellar organisation in endosperm cell walls of cereal grains. In: Magnetic Resonance in Food Science: An Exciting Future. Pp. 105-113. The Royal Society of Chemistry.
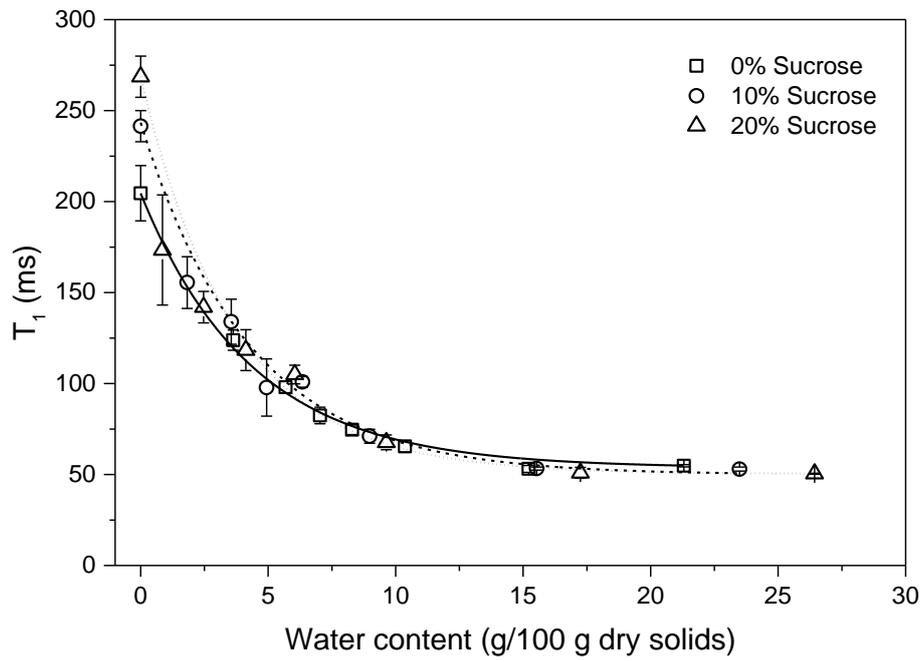
Fig. 6.1 Spin-lattice relaxation time constant (T_1) at delay sampling window 0.016 ms for extrudates contained 0, 10, and 20% sucrose as a function of water content obtained by using single exponential fitting.
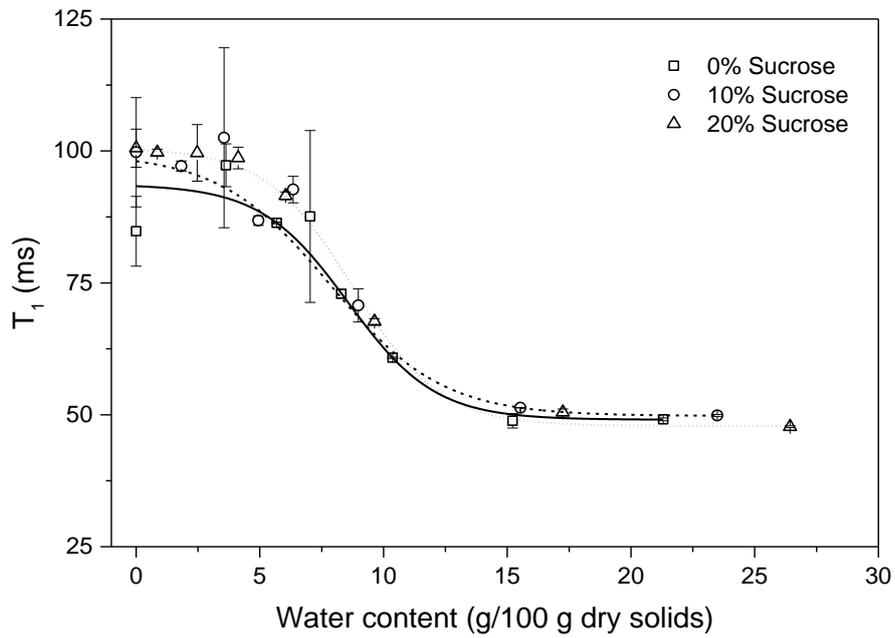
Fig. 6.2 Spin-lattice relaxation time constant (T_1) at delay sampling window 0.1 ms for extrudates contained 0, 10, and 20% sucrose as a function of water content obtained by using single exponential fitting.
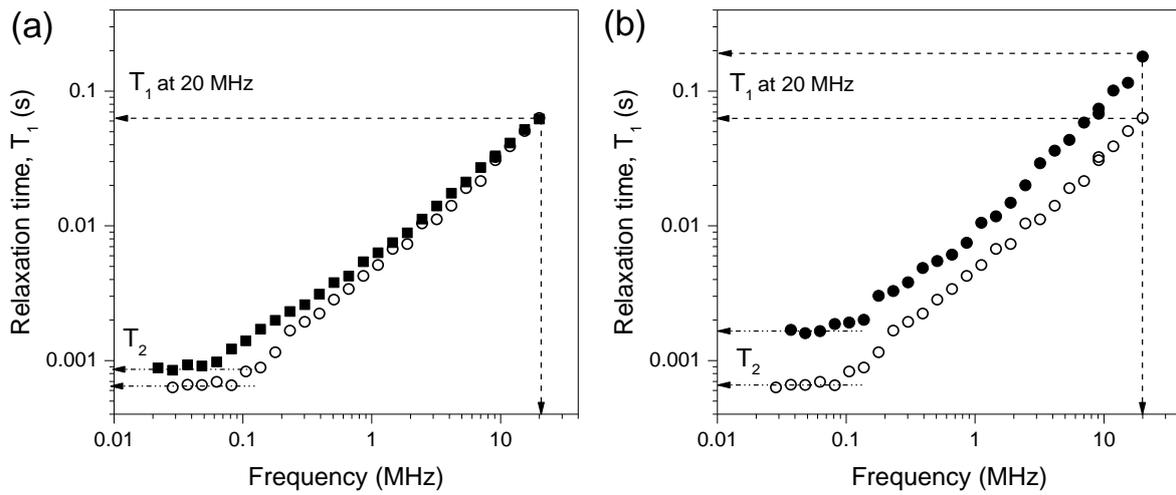
Fig. 6.3 Proton spin-lattice relaxation dispersion (T_1) as a function of frequency: (a) extruded sample contained 0 (■) and 10 (○) % sucrose and stored at 75% relative humidity; (b) extruded sample contained 10% sucrose and stored at 11 (●) and 75% (○) relative humidity.
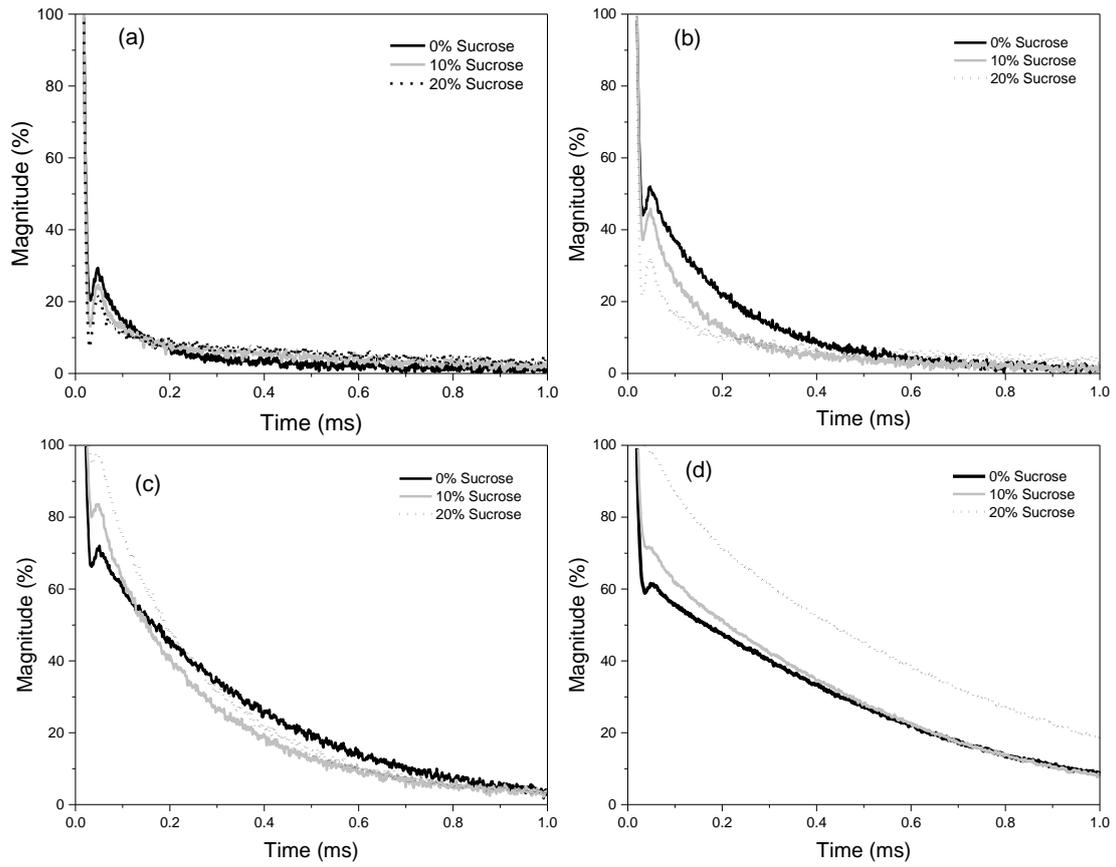
Fig. 6.4 Examples of spectra collection by the Solid echo sequence for extruded samples contained 0, 10, and 20% sucrose content and stored at 11% (a), 32% (b), 58% (c) and 75% (d) relative humidity.
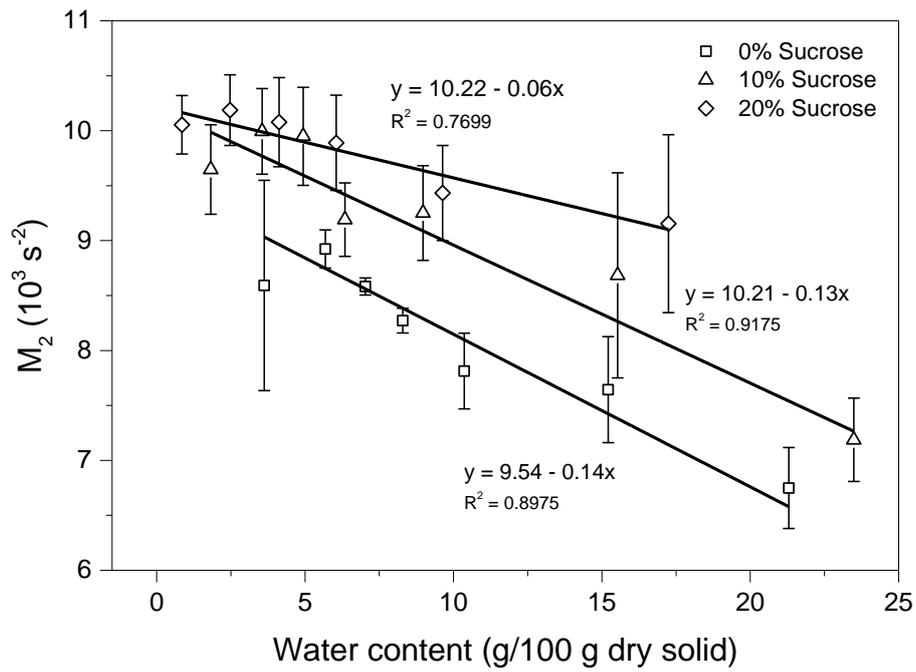
Fig. 6.5 Second moment (M_2) calculating by Eq. 6.3 for extrudates contained 0 (□), 10 (△), and 20 (◇) % sucrose as a function of water content at 25 °C.
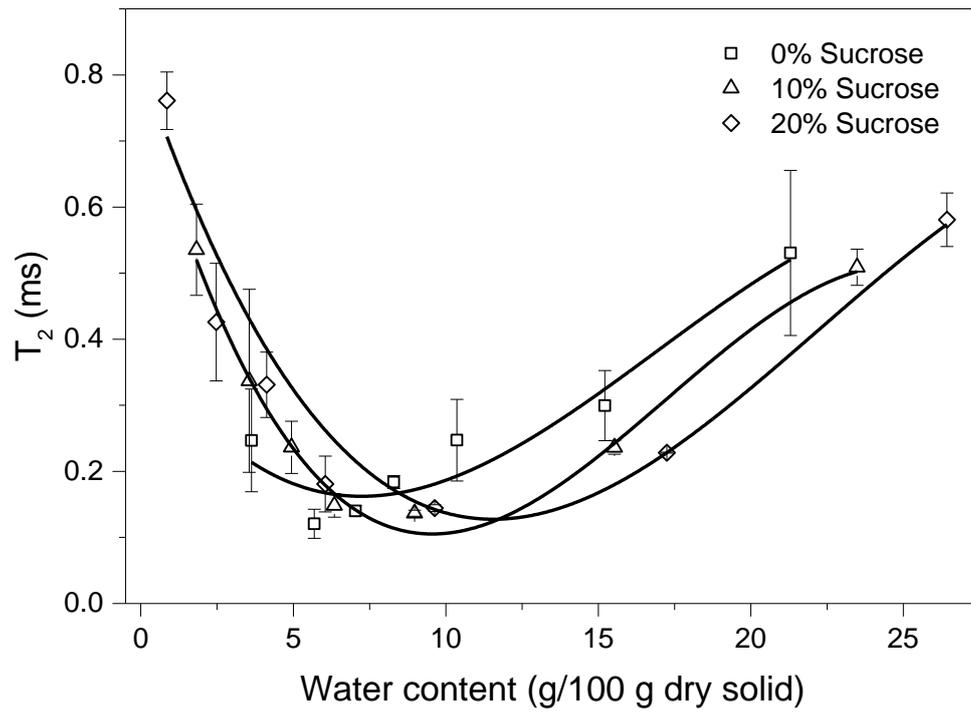
Fig. 6.6 Spin-spin relaxation time constant (T_2) for extrudates with 0, 10, and 20% sucrose content: fitting with the combination of Abragam, Gaussian and exponential functions (Eq. 6.2) as a function of water content.

Table. 6.1. The combination of Abragam, Gaussian and exponential functions fitted values for Solid echo signal of extrudates with various sucrose content and stored at 11, 32, 58 and 75% relative humidity.

| Relative humidity (%)	Sucrose content (%)	Proportional number of proton for rigid component (A_1) (%)	Proportional number of proton for mobile component (A_2) (%)	T_2 (ms)	a (ms^{-1})	b (ms^{-1})	M_2 ($10^3.s^{-2}$)
11	0	91.00	9.00	0.15	65.01	115.57	8.68
	5	95.56	4.44	0.32	74.33	106.98	9.34
	10	96.23	3.77	0.42	72.24	111.11	9.33
	15	96.41	3.59	0.55	65.82	125.26	9.56
	20	96.80	3.20	0.56	67.53	123.08	9.61
32	0	83.44	16.56	0.19	59.64	117.82	8.18
	5	87.27	12.73	0.16	66.87	113.75	8.78
	10	90.48	9.52	0.16	65.67	114.92	8.72
	15	92.09	7.91	0.18	68.48	112.60	8.92
	20	93.93	6.07	0.21	74.68	107.37	9.42
58	0	77.50	22.50	0.26	61.34	111.85	7.93
	5	73.69	26.31	0.35	56.18	115.14	7.58
	10	78.73	21.27	0.23	59.74	113.54	7.87
	15	79.16	20.84	0.22	62.63	110.50	7.99
	20	80.37	19.63	0.23	70.37	102.51	8.45
75	0	65.43	34.57	0.66	51.38	108.39	6.56
	5	66.37	33.63	0.51	55.12	108.28	6.95
	10	66.08	33.92	0.52	61.92	98.57	7.07
	15	63.37	36.63	0.47	65.44	110.50	7.94
	20	50.02	50.98	0.56	34.74	155.87	9.30

Table. 6.2. Relaxation time, T_1 at 20 HMz and T_2 extracted from the plot of T_1 versus Larmor frequencies obtaining from FFC NMR (Fig. 6.6).

Sucrose content (%)	Relative humidity (%)	LF NMR (20 MHz) T_1 (1st window) (ms)	FFC NMR T_1 (ms) (20 MHz)	T_2 (ms) ($\rightarrow$ 0 Hz)	T_2 (ms) (20 MHz)
0	11	120.79	-	-	97.29
0	75	52.64	61.74	0.87	48.86
10	11	148.65	189.79	1.66	97.13
10	75	52.85	61.74	0.65	51.34

Chapter 7:

Conclusions and perspectives

Discussion

Extruded products exist in disordered non-equilibrium amorphous states and their dynamics are particularly important for the stability of systems with long-term shelf-life requirements. The physical state, water mobility, and water-solid interactions affect storage stability, textural, and functional properties of food. The objectives of this work were to evaluate how the presence of sucrose and water content affects physico-chemical properties. The physical stability of these materials were monitored at different molecular scales such as macroscopic, mesoscopic and molecular scales (Fig 7.1). Sugar and water content significantly impacted on extrudate properties and showed both synergistic and antagonistic effects. To study product stability, the combination of techniques provided a better understanding on this issue.
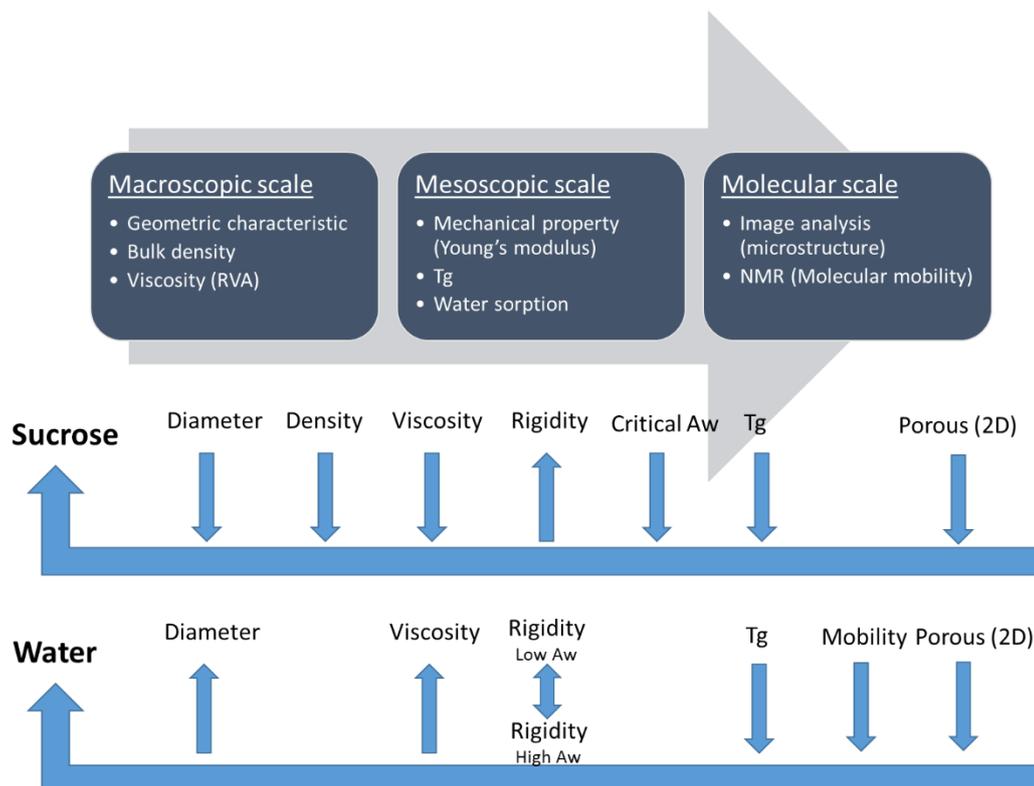

Fig. 7.1 The effect of sucrose and water content on physico-chemical properties of extrudate through an insight at different scales.

In this work, we attempted to relate the water uptake and sucrose content to the thermal events occurring at glass transition temperatures and product stability in extruded cereal-based products and to determine the relationship between the temperature of these events and textural properties observed by mechanical analysis. The studies provide a general view of the samples' stability versus moisture taking into account : thermal phase behavior, and mechanical behavior in material containing several types of biopolymers and several plasticizers. More specifically, an alternative technique for the determination of multiple glass transitions in composite food, (the analysis of the DSC heat flow derivative, by applying the two Gaussian functions) ghas proved useful. These approaches provided some insight into the dependency of observations on the sugar and water content. However, this is not easily achievable because the partitioning of water in multicomponent systems depends on the overall water content, but also on its distribution between the components of food products. In such complex phase separating systems water content cannot be kept constant and, subsequently, the availability of water to plasticize the components of each phase is not directly controlled. The roles of water and sugar in plasticizing biopolymers may therefore be more complex than is often considered when single phase behaviour is assumed. Although it might be expected that small molecules such as sugars would form homogeneous mixtures with biopolymers, there is clear experimental evidence that there is a considerable degree of heterogeneity in the biopolymer-sugar systems of the extruded products assessed in this study. The effect of the heterogeneity of the blends on their thermal properties was studied using DSC. The thermal properties of these products reflected their heterogeneous character with the appearance of multiple transitions in their DSC thermogram. Two main transitions were identified and assigned, in order of increasing temperature, the glass-transition of sucrose-rich phase (Tgl) and to the glass-transition of biopolymer-rich phase (Tgh). The results suggested that a fraction of sugar might plasticizes the biopolymer in a biopolymer-rich phase. The possible phase segregation appeared to be more related to the water content of the sample than to the sucrose concentration. However, to be visible on the DSC derivative, this phase separation required dynamics that could only be reached when the water content was sufficiently high. The

overlapping of the transition peaks suggests a non-unique composition for phases and distributions of microenvironments, i.e. heterogeneities. The presence of two phases leads to a dynamic compositional behavior with respect to water transfer and plasticization, the sucrose-rich phase becoming ergodic at a temperature slightly above the glass transition temperature and the water content of the phase being governed by the mixing entropy of the phase. Thus, sucrose seemed to make samples more sensitive to water plasticization. However, this calculation remains a raw estimation because the precise water content of each phase is not exactly known. iIndeed according to the isotherms, it is clear that the water content of sucrose-rich phases is lower than the polymer-richer ones, but their exact compositions remain unknown. It is suggested that this leads to a transfer of water from the biopolymer-rich phase to the sucrose-rich phase, reflecting in a significant increase of the intensity of derivative heat flow peak of the biopolymer-rich phase and a decrease of that of the sucrose-rich phase as water content increases.

Gordon-Taylor models were derived based on the assumptions that the matrix components are miscible at the molecular level and that the properties of the matrix components are additive in terms of the volume fractions they occupy of the overall matrix. In particular the latter assumption is likely to be invalid for carbohydrate-water systems. Whilst the water activity of the blends is constant, the water content of the individual phases may vary considerably. When considering samples at different storage times, the results did not show any increase with increasing water content: the anti-plasticizing effect was not visible when we introduced aged samples in the set of results. During aging of the glassy solids, the materials became less compliant with the mechanical relaxation times progressively increasing. The change in material properties occurred over a timescale similar to the slow densification of the amorphous glasses, characteristic of structural relaxation in the glassy state. Therefore, prediction of brittle textures from the determination of Tg alone is not possible and it appears necessary to study dynamic changes occurring in the glassy state to explain textural or brittle-ductile changes. Coupling of sorption isotherm data with glass transition temperatures and mechanical properties as a function of water content were examined, in order to obtain the critical conditions for

food storage. For low moisture cereal products, the relationship between water plasticization and mechanical properties is likely to apply generally, but it should be remembered that the brittle-ductile transitions do not necessarily change in unison as food undergoes a glass transition due to the effects of phase separation and their separate physical aging on the mechanical properties of amorphous components as shown in DSC and NMR experiments. It is important to notice here that water contents for the Young's modulus taken at the onset of a decrease corresponded to samples which were still in the glassy state, even if considering the lowest visible glass transition, which may not always be observed on DSC thermograms.

Studying the properties of water and its distribution in low moisture food systems can be very challenging. Indeed very heterogeneous areas of the food can be created that greatly affect the structure and texture of final product. Understanding moisture uptake and water migration in such systems should help in designing better processes to control the behavior of water during storage. In this work, NMR techniques have been used to determine how water interacts in such systems depending on sucrose content and storage humidity. The characteristic changes in relaxation time constants observed by LF MNR technique were attributed to the segmental motion of polymers varying in different physical states. Therefore, a deeper knowledge of water dynamics using NMR was carried out. The T_1 experiment presented only one T_1 depending on the delay sampling time that it was not expected. It seems water is apparently incorporated into the biopolymer matrix and contributes to mainly the solid signal. The solid echo signal were described by two components: each ascribed to one pool of protons: the first one with a short relaxation time (rigid population) and the second with longer relaxation time (mobile population). The fitting by combination functions of Abragam-Gaussian and Exponential showed motional heterogeneity in extruded products as the proportional of more rigid and mobile protons in extrudates were different. A T_2 minima was observed as a function of moisture content. ,which we interpret as an exchange of water protons with exchangeable protons on the macromolecules. The phase separations is confirmed by LF NMR, which furthermore shows that the dynamics in the extrudates contained sucrose up to 20% wt are characterized by a rigid phase and a

mobile phase; the fraction of the mobile phase increasing when the sucrose-rich phase passes through the glass transition. It is unclear why such behavior would occur. It may be related to phase separations or redistribution of the internal interactions throughout the cereal.

Textural properties of extrudates are strongly impacted by the addition of sugar. Hardness of extruded products obtained from different recipes follows a general trend linked to porosity; the higher the porosity, the higher the aeration of the products, the lower the hardness. Additionally studies considered the use of neutron imaging technique for the structure analysis of porous cereal products. The relationship between porous structure of extruded starchy products and their mechanical properties, showed that for the same relative density, lower mechanical moduliwere obtained for products displaying a wide range of pore size and wall thickness. Since relative density is key for mechanical properties, the internal microstructure of porous extruded cereals has also an impact.

We suggest that when the sucrose-rich phase is in the rubbery state at 25 $^{\circ}$C post aw equilibration, there is a migration of water and/or sucrose from the biopolymer-rich phase to the sucrose-rich phase resulting in the inverse point on sorption isotherm curve, due to the loss of plasticizer from the polymer phase. From a situation of dynamic water equilibrium between the two phases, we propse the net migration of water from the biopolymer-rich phase to the sucrose-rich phase as water is added. Furthermore, the apparent monolayer values show a tendency to decrease with an increase in sucrose content. The degree of hydrogen bonding between polymers is reduced with increasing sugar, thereby decreasing the availability of active sites for water binding and thus, the mono-layer moisture content.

This work clearly showed that the composition of extruded materials can be manipulated to control water sorption and plasticization properties and, thereby, mechanical properties. These properties are often related to glass transition and effect on rigidity. Among the structural differences observed at various scales between extruded products, these results clearly present the need for

complementary techniques to probe the dynamic and architecture in the glassy state for heterogeneous food systems. This can be modulated to manage the stability during storage of this type of dry products.

Conclusions and perspectives

A number of breakfast cereals and cereal-based snack foods have a characteristic, porous, crispy texture. The materials have a low water content which provides microbialstability and retention of desired textural properties. The objective of our study was to relate the extrusion parameters to; structural characteristics such as density, expansion, viscosity, water absorption, water solubility and cell size distribution); physicochemical properties (glass transition, sorption isotherm, mechanical properties, water mobility) and microstructure of extrudates. Such correlation would assist development of extruded products, and provide explanation of mechanisms of behaviour.The effects of sucrose addition and water content on such properties were investigated, since when products are improved nutritionally by reduction sucrose, this approach can be used to obtain the targeted properties, including product stability. Food product structure, studied at different length scales, is key to understanding the link between processing conditions and final product properties. The relationships is described in Fig. 7.2.
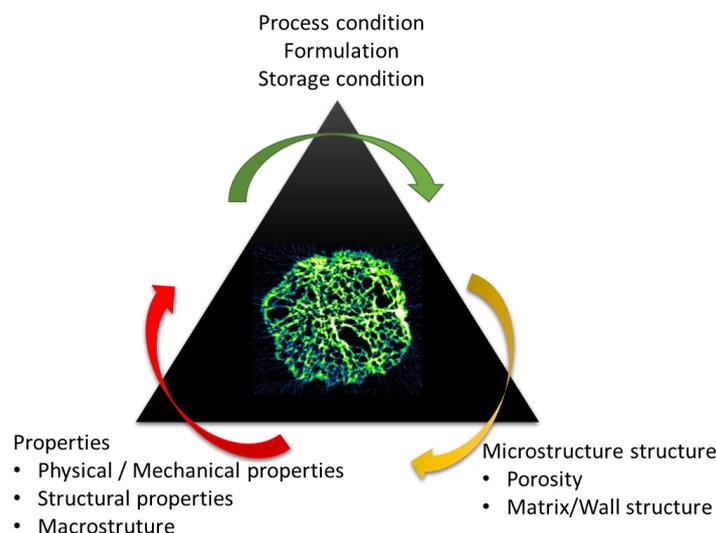

Fig. 7.2 Approach used to study the relationships of process extrusion, extrudate's properties and product microstructure.

Moisture migration in heterogeneous food systems can lead to both physical and chemical changes that reduce the shelf life of the food. The transfer of moisture is controlled by both thermodynamics (The direction of change, relating to water sorption isotherms) and dynamics (The rate of change, relating to diffusion rates of water and biopolymer substrates). Knowledge of these factors leads to several principles that can be used to reduce the rate of transfer of moisture, enhancing stability. Two different behaviors, depending of water activity (a_w), were detected for all the extrudates when sucrose was present. For high aw, the presence of sucrose in the polymer increased the water sorption. This result follows the idea of sucrose acting both as plasticizer increasing the molecular mobility of the system and as a hygroscopic compound contributing to the hydration of the system. This behavior was accurately represented by GAB model where the *k* constant increased in the presence of sucrose suggestion an increase in the heat sorption (binding energy in the multilayer domain) at high RHs. For low aw, the presence of sucrose decreased the water content. This result can be related to the obtained monolayer value m0 from GAB models, which decreased when sucrose content increased. Theoretically the decrease in this parameter suggests less sorption sites available for water molecules. The reduction in these sorption sites could be related to sucrose-biopolymer interactions which are favored over that of sucrose-water.

Since the mechanism of moisture uptake is related to both the water movement within the cereal and the ability of the cereal to hydrate, the kinetics of hydration and the textural changes of these products were studied in order to examine the influence of the sucrose and water content on the product quality. Water migration kinetics were studied by applying kinetic data, including first-order and second order exponential rate models. Second order exponential decay equations exhibited the best fit for the kinetic studies. The kinetic decay times show the water migration has two rate processes. The first showed that the initial water uptake was at an almost constant rate and could be adsorption phenomena at the surface. The second showedan increase with higher water content. This behavior may be related to the decrease of extrudates porosity leading to increased capillary flow as moisture content increases. Further application of imaging techniques could establish these models

The rates increased when the concentration of sucrose increased which indicates that there is diffusion process controlled by the sucrose level. Further studies including multi-cycle sorption isotherms and X-ray diffraction proved that the structure collapse occurred without sugar crystallization during storage. This proved that the change in water mass transfer could related to physical state, of the glass.

Physical state was studied by differential scanning calorimetry (DSC). After removal of the so called stress relaxation peak,multiple glass transition are resolved by modeling the DSC thermograms across a wide temperature range using Gaussian function. DSC thermograms for extrudates at a_w lower than 0.11 appears to be a single, wide transition. At higher values of aw, two separate glass transitions became clearly visible. A detailed analysis of the differential heat flow curves demonstrates that a single transition cannot explain the results, and we propose that a significant degree of phase separation occurs in amorphous blends of extrudate, as indicated by the presence of these multiple distinct glass transitions. We proposethat one of the phases is enriched in biopolymer and the other is enriched in sucrose. Physical hardening occurred in glasses upon hydration in extrudates. The use of supplemented state diagrams helped to understand the occurrence of those changes, the conditions prevailing in each stage, and the physical state of the sample. Material characterization using various techniques, determination of effects of phase separation on extrudate structure, textural properties, as well as the significance of molecular mobility below T_g on food storage stability, should be given particular attention in further studies of phase transitions and structure of food matrices. Our results indicate that many matrices of relevance to extrudates show significant the matrix heterogeneity, most likely originating in phase separation. It is important to point out whilst the water activity of the blends is constant, the water content of the individual phases may vary considerably andt may have a major impact on stability and performance.

Most models fit the plasticization of carbohydrates by water fairly well. Here, we use the Gordon–Taylor (GT) equation for a binary blend of a carbohydrate and water to model the dependence of T_g on water content in extrudates. T_{gl} decreases with water content for all extruded samples, as

expected for materials that are plasticized by water. where there are more than 2 expected T_gs , the glass transition temperatures of the various phases, the theoretical weight fractions of sugar and "flour" present in each phase for all a_w's were fitted using the Couchman–Karasz relation for a ternary polymer/sugar/water system.

Sorption behavior can be related to the glass transition temperature by at least two models: (i) by a change in molecular diffusion mechanisms; (ii) by a change in the particle geometry. The finding discussed above do not entirely agree with eithermodel. It was clearly showed that the capacity of sucrose to influence water sorption in starches was highly dependent on the relative humidity (RH). Similarly, the effect of sugar on water activity (a_w) of these systems also increased or decreases depending on the surrounding RH. Kinetic time constants of water mass transfer in the studied extrudates increased in the presence of sucrose only up to certain a_w, after which a decrease was detected. This point was identified as the mixture T_g where particle geometrical integrity changed as reflected by the Young's modulus (Fig. 7.3).
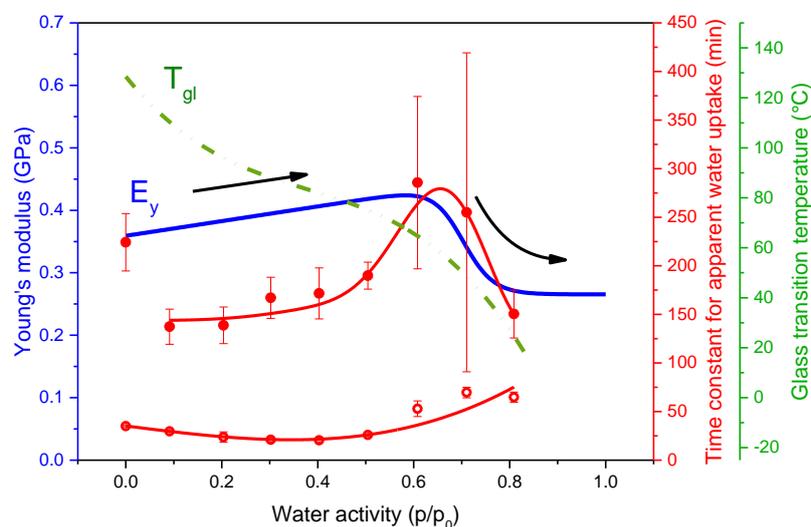

Fig. 7.3 State diagram established including with low glass transition temperature (green dash line), Young's modulus (blue solid line), fast (O, red solid line) and slow (●, red solid line) kinetic time constant for water migration as a function of water activity.

It seems clearly that adding sucrose increased the extent of hardening of extrudates over time as shown by the higher apparent modulus in force deformation curve (Fig. 7.4). Increasing the sucrose

content of extrudates resulted in a significant increase in both RH sensitivity and Young's modulus of dry extruded products and caused a reduction in the glass transition temperature, critical water content and critical water activity of extrudates. For the lower moisture content, the increase in Young's modulus seems to be related to the so-called "physical aging" where structural relaxation and subsequent densification occur. Although, its seems unlikely that sucrose may have an effect on the relaxation kinetics by molecular interactions with the starch, it is possible that its plasticizing effect could have T_g. Comparison of Young's modulus between fresh extrudate (after processing), aged-sample and rejuvenated samples could be done in order to have a better understanding on the anti-plasticizing effect on mechanical properties at low content. The prospered rejuvenation method also could be considered.
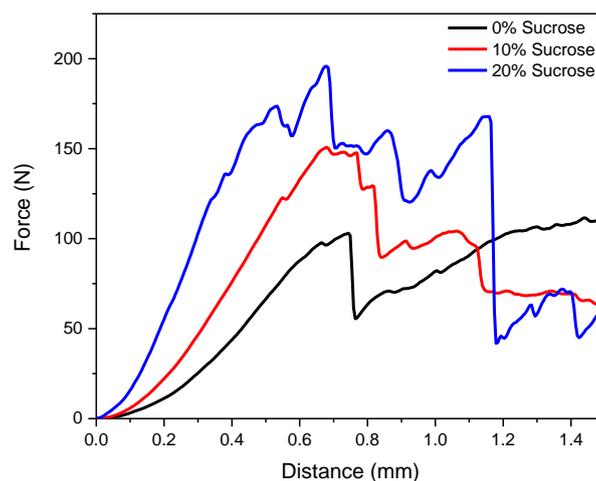

Fig. 7.4 Force-distance deformation curves during compression of extrudates contained 0, 10, and 20% sucrose.

Studies on extrudates with different aged products detected a significant INCREASE??? in the Apparent modulus of these materials during storage (Fig. 7.5), probably because the structure of extrudate reorganized due to redistribution of water and increased chemical crosslinking in samples. A futher experiment was designed to de-age sample a sample p[reviously stored for several years by heating at 80 °C for 1 hour over $MgCl_2$ saturated salt solution in closed container to avoid dehydration. This should remove the endothermic peak (or enthalpic relaxation peaks) seen on first heating scan

obtained by differential scan calorimetry (DSC). De-aged sample showed less rigidity, which may reflect the change in water distribution, which changes the modulusf glassy material. This data does not agreed with the proposed hypothesis, which attributed this change in texture to reassociation of the amorphous structure of the starch component as confirmed by DSC. Another factor that could have contributed to the change in rigidity in one of the products evaluated was a slight change in the moisture content or moisture distribution in the extrudate structure during storage. Aging studies at different T_g or storage temperatures are needed to test this hypothesis further.
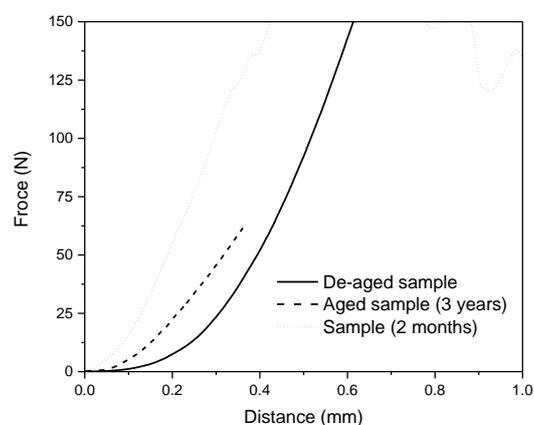

Fig. 7.5 Force-distance deformation curves during compression of extrudates contained 10 sucrose and stored at 32% relative humidity.

Effect of formulation on process parameters

The properties of extrudates depend on sucrose content in blend and feed water during extrusion. Increasing the sucrose and feed water contents which replace higher molecular weight starch, decreased the SME input, die pressure, product diameter, expansion index, specific length, hence reduced starch degradation. However, the bulk density increased as the sucrose content increased for samples extruded at 10% feed water, while no obvious difference was shown for samples extruded at 15% feed water . The SME, expansion ratio, cold and hot paste viscosities of extrudates decreased with increasing sucrose content. Higher feed water contents decreased the melt viscosity, and then the expansion ratio of the extrudates, resulting in a higher density. HPSEC showed that both amylopectin and amylose macromolecules were fragmented during extrusion, resulting in reductions in the relative percentages of amylopectin. Our results demonstrated that specific mechanical energy

plays a critical role in the degradation of starch in wheat flour in a twin-screw extruder. It was also shown that sucrose content and feed water acted as plasticizers and impacted molecular size distribution of extrudates. This knowledge can help manufacturers to better control process conditions within an extruder to yield products with predictable and consistent characteristics.

The attributes of extrusion cooked, expanded breakfast cereals are based on mechanical properties which are mainly influenced by bulk expansion and porosity. Porosity can be determined by size distribution and cell wall thickness. Non-destructive methods for characterization of these properties are necessary. Neutron tomography deliver information in 2D and 3D, which is required for a comprehensive analysis of the geometrical aspects of extruded products. Consequently, some preliminary trials have already been conducted, the image acquisition parameters such as acquisition time, rotation angle, the distance of the camera, the position of the sample on the rotating stand), as well as image segmentation methods (manual thresholding, histogram thresholding) played the important roles on the image analysis and quantitative data (Fig. 7.5). The images clearly indicate that the objective of reducing sucrose content and increasing relative humidity clearly decreased the porosity of for extrudates. This is because both could probably be related to the reduce expansion and pore size of extrudate structure reduced as sucrose and water content increased. This work shows the real potential of neutron imaging technique for quantitatively assessing porous starch extrudates during storage and provided useful data by which to characterize extrudate structure. However, the quality of data quantitative analysis still need to be improved. Further experiments need to probe the water distribution changes in porous structure during storage by mean of neutron imaging technique. 3D image analyses of high-quality processed images can also be used in the food industry as a reliable and accurate measure of heterogeneous food structure, which can be further used to understand the relationship between physicochemical properties of porous solid foods and food morphology.
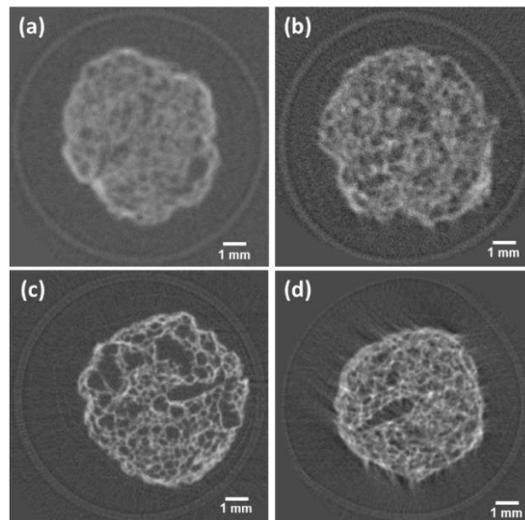
Fig. 7.6 reconstruction 2-D images performed with different acquisition parameters (rotation angle and exposing time): (a) 1.5 °, 60 s; (b) 1.5 °, 120 s; (c) 1.0 °, 120 s; (d) 1.0 °, 120 s (sample was not at the at rotating stand).

Differential scanning calorimetry displayedmultiple glass transitions revealing heterogeneities that could be associated with either a polymer-rich phase and/or a plasticizer (sugar)-rich phase. 3D image obtained by neutron imaging technique, reveals different attenuations of the neutron beam by protons, and may be detecting different water dispersion in different zones within product structure. ifextrudates stored at the same water activity, present different in the zones inside the materials with distinct water content, they may be directly imaged by this technique.

We applied the low field NMR and ^{1}H FFC NMR to study the water mobility in extrudate matrix under different sucrose content and relative humidity for storage. The typical relaxation features that we observed for frequency dependence of the proton spin-lattice relaxation rates have been interpreted. This work showed the potential of NMR to probe molecular mobility in low moisture complex food products. The results of the work give a basis for going further with NMR experiments for this kind of materials. In particular, the roles of water and sucrose in plasticizing in extruded products were investigated by monitoring proton mobility using ^{1}H NMR and ^{1}H FFC NMR. The ^{1}H NMR T_1, and T_2 values were obtained using the inversion-recovery pulse sequence, the Solid echo sequence and , FID, respectively. The spin-lattice parameter (T_1) decreased by addition of plasticizer. Solid echo signals shows two T_2 populations: "rigid" and "mobile" populations. T_2 of the mobile process depends

on water content but shows a minimum probably indicating the onset of fast exchange between the

rigid population on the mobile one. The second moment M_2 was found to be sensitive with regard to

the sucrose levels. T_1 obtained by FFC NMR showed a decrease as sucrose and water content increased,

indicating the lower mobilities. T_1 obtained by the fitting procedure used here represented only the

proton of the solid population. However, by applying the proper experimental parameters, and by

performing an appropriate fit to the decay curve (bi-exponential fit), it would be possible to study

differences in water mobility in both rigid and mobile population protons. T_1 and T_2 measured by using

FFC NMR are consistent with the values obtained from LF NMR. These results suggest that the study

of molecular properties in extrudates at different frequencies by mean of ^{1}H NMR FFC techniques

might useful in monitoring molecular dynamics in extruded product and possibly lead to a more

complete understanding of heterogeneity and physical aging of complex biopolymer system.

Although, a better understanding of the functionally of sucrose in starch based-systems was

obtained from the presented work, further study on these systems is requred. An important variable

not covered was the effect of temperature on the sorption and mechanical properties as well as on

the water diffusion kinetic during storage. This would compliment the information related to the

effects relative humidities during storage. Both factors could contribute to the development of more

accurate predictive models.

Additionally, sorption isotherm showed results consistent with a model in whichthe water content of

sucrose-rich phases is lower that the polymer richer ones, their exact compositions remain unknown.

These results clearly showed the need for complementary techniques to probe the precise water

content of each phase, including consideration of the phase behaviour of complex systems and thus

the properties of their individual phases. This is vital to obtain a better understanding of the physical

stability of the products.

The results also show the potential of neutron imaging technique as a tool for evaluting microstructure

of extruded cereal based-products, examining the microstructure which correlates with hydration

properties and the changes in porous structure (i.e. pore size and pore wall thickness) and geometric

changes of extrudates (i.e. swelling and collapsing) occurring in the cereals upon hydration. Image processing will need to be improved to achieve resolution for image segmentation and image processing ^{1}H NMR is also of valuein examining the dynamics in the glassy state of complex starch based-products. The result suggested that ^{1}H NMR FFC technique might open an additional window in monitoring molecular dynamics in extrudates, leading to the full understanding of the physico-chemical change phenomenon.